VOLUME: 18 NO: 1 YEAR: 2021

Indexed in PMC and Web of Science
ULAKBİM / TR Dizin, Scopus

ISSN: 1304-530X

TURKISH JOURNAL OF PHARMACEUTICAL SCIENCES

An Official Journal of the Turkish Pharmacists' Association, Academy of Pharmacy

TURKISH
JOURNAL OF PHARMACEUTICAL SCIENCES

TURKISH
JOURNAL OF PHARMACEUTICAL SCIENCES

TURKISH JOURNAL OF PHARMACEUTICAL SCIENCES

AIMS AND SCOPE

The Turkish Journal of Pharmaceutical Sciences is the only scientific periodical publication of the Turkish Pharmacists' Association and has been published since April 2004.
Turkish Journal of Pharmaceutical Sciences journal is regularly published 6 times in a year (February, April, June, August, October, December). The issuing body of the journal is Galenos Yayinevi/Publishing House level.
The aim of Turkish Journal of Pharmaceutical Sciences is to publish original research papers of the highest scientific and clinical value at an international level. The target audience includes specialists and professionals in all fields of pharmaceutical sciences.
The editorial policies are based on the "Recommendations for the Conduct, Reporting, Editing, and Publication of Scholarly Work in Medical Journals (ICMJE Recommendations)" by the International Committee of Medical Journal Editors (2013, archived at http://www.icmje.org/) rules.

Editorial Independence

Turkish Journal of Pharmaceutical Sciences is an independent journal with independent editors and principles and has no commerical relationship with the commercial product, drug or pharmaceutical company regarding decisions and review processes upon articles.

ABSTRACTED/INDEXED IN

PubMed Central
Web of Science-Emerging Sources Citation Index (ESCI)
SCOPUS SJR
TÜBİTAK/ULAKBİM TR Dizin
Directory of Open Access Journals (DOAJ)
ProQuest
Chemical Abstracts Service (CAS)
EBSCO
EMBASE
GALE
Index Copernicus
Analytical Abstracts
International Pharmaceutical Abstracts (IPA)
Medicinal & Aromatic Plants Abstracts (MAPA)
British Library
CSIR INDIA
GOALI
Hinari
OARE
ARDI
AGORA
Türkiye Atıf Dizini
Türk Medline
UDL-EDGE
J- Gate
Idealonline
ROOTINDEXING
CABI

OPEN ACCESS POLICY

This journal provides immediate open access to its content on the principle that making research freely available to the public supports a greater global exchange of knowledge.
Open Access Policy is based on the rules of the Budapest Open Access Initiative (BOAI) http://www.budapestopenaccessinitiative.org/. By "open access" to peer-reviewed research literature, we mean its free availability on the public internet, permitting any users to read, download, copy, distribute, print, search, or link to the full texts of these articles, crawl them for indexing, pass them as data to software, or use them for any other lawful purpose, without financial, legal, or technical barriers other than those inseparable from gaining access to the internet itself. The only constraint on reproduction and distribution, and the only role for copyright in this domain, should be to give authors control over the integrity of their work and the right to be properly acknowledged and cited.

CORRESPONDENCE ADDRESS

All correspondence should be directed to the Turkish Journal of Pharmaceutical Sciences editorial board;

Post Address: Turkish Pharmacists' Association, Mustafa Kemal Mah 2147.Sok No:3 06510 Çankaya/Ankara, TURKEY
Phone: +90 (312) 409 81 00
Fax: +90 (312) 409 81 09
Web Page: http://turkjps.org
E-mail: teb@teb.org.tr

PERMISSIONS

Requests for permission to reproduce published material should be sent to the publisher.
Publisher: Erkan Mor
Adress: Molla Gürani Mah. Kaçamak Sok. 21/1 Fındıkzade, Fatih, Istanbul, Turkey
Telephone: +90 212 621 99 25
Fax: +90 212 621 99 27
Web page: http://www.galenos.com.tr/en
E-mail: info@galenos.com.tr

ISSUING BODY CORRESPONDING ADDRESS

Issuing Body : Galenos Yayınevi
Address: Molla Gürani Mah. Kaçamak Sk. No: 21/1, 34093 İstanbul, Turkey
Phone: +90 212 621 99 25 Fax: +90 212 621 99 27
E-mail: info@galenos.com.tr

MATERIAL DISCLAIMER

The author(s) is (are) responsible for the articles published in the JOURNAL.
The editor, editorial board and publisher do not accept any responsibility for the articles.

galenos yayınevi

Galenos Publishing House
Owner and Publisher
Derya Mor
Erkan Mor
Publication Coordinator
Burak Sever
Web Coordinators
Fuat Hocalar
Turgay Akpınar
Graphics Department
Ayda Alaca
Çiğdem Birinci
Gülşah Özgül
Finance Coordinator
Sevinç Çakmak

Project Coordinators
Aysel Balta
Duygu Yıldırm
Gamze Aksoy
Gülay Akın
Hatice Sever
Melike Eren
Meltem Acar
Özlem Çelik
Pınar Akpınar
Rabia Palazoğlu
Research&Development
Mert Can Köse
Digital Marketing Specialist
Seher Altundemir

Publisher Contact
Address: Molla Gürani Mah. Kaçamak Sk. No: 21/1
34093 İstanbul, Turkey
Phone: +90 (212) 621 99 25 **Fax:** +90 (212) 621 99 27
E-mail: info@galenos.com.tr/yayin@galenos.com.tr
Web: www.galenos.com.tr | Publisher Certificate Number: 14521

Printing at: Üniform Basım San. ve Turizm Ltd. Şti.
Matbaacılar Sanayi Sitesi 1. Cad. No: 114 34204 Bağcılar, İstanbul, Turkey
Phone: +90 (212) 429 10 00 **Certificate Number:** 42419
Printing Date: February 2021
ISSN: 1304-530X
International scientific journal published quarterly.

TURKISH
JOURNAL OF PHARMACEUTICAL SCIENCES

INSTRUCTIONS TO AUTHORS

Turkish Journal of Pharmaceutical Sciences journal is published 6 times (February, April, June, August, October, December) per year and publishes the following articles:

• Research articles

• Reviews (only upon the request or consent of the Editorial Board)

• Preliminary results/Short communications/Technical notes/Letters to the Editor in every field of pharmaceutical sciences.

The publication language of the journal is English.

The Turkish Journal of Pharmaceutical Sciences does not charge any article submission or processing charges.

A manuscript will be considered only with the understanding that it is an original contribution that has not been published elsewhere.

The Journal should be abbreviated as "Turk J Pharm Sci" when referenced.

The scientific and ethical liability of the manuscripts belongs to the authors and the copyright of the manuscripts belongs to the Journal. Authors are responsible for the contents of the manuscript and accuracy of the references. All manuscripts submitted for publication must be accompanied by the Copyright Transfer Form [copyright transfer]. Once this form, signed by all the authors, has been submitted, it is understood that neither the manuscript nor the data it contains have been submitted elsewhere or previously published and authors declare the statement of scientific contributions and responsibilities of all authors.

Experimental, clinical and drug studies requiring approval by an ethics committee must be submitted to the JOURNAL with an ethics committee approval report including approval number confirming that the study was conducted in accordance with international agreements and the Declaration of Helsinki (revised 2013) (http://www.wma.net/en/30publications/10policies/b3/). The approval of the ethics committee and the fact that informed consent was given by the patients should be indicated in the Materials and Methods section. In experimental animal studies, the authors should indicate that the procedures followed were in accordance with animal rights as per the Guide for the Care and Use of Laboratory Animals (http://oacu.od.nih.gov/regs/guide/guide.pdf) and they should obtain animal ethics committee approval.

Authors must provide disclosure/acknowledgment of financial or material support, if any was received, for the current study.

If the article includes any direct or indirect commercial links or if any institution provided material support to the study, authors must state in the cover letter that they have no relationship with the commercial product, drug, pharmaceutical company, etc. concerned; or specify the type of relationship (consultant, other agreements), if any.

Authors must provide a statement on the absence of conflicts of interest among the authors and provide authorship contributions.

All manuscripts submitted to the journal are screened for plagiarism using the 'iThenticate' software. Results indicating plagiarism may result in manuscripts being returned or rejected.

The Review Process

This is an independent international journal based on double-blind peer-review principles. The manuscript is assigned to the Editor-in-Chief, who reviews the manuscript and makes an initial decision based on manuscript quality and editorial priorities. Manuscripts that pass initial evaluation are sent for external peer review, and the Editor-in-Chief assigns an Associate Editor. The Associate Editor sends the manuscript to at least two reviewers (internal and/or external reviewers). The Associate Editor recommends a decision based on the reviewers' recommendations and returns the manuscript to the Editor-in-Chief. The Editor-in-Chief makes a final decision based on editorial priorities, manuscript quality, and reviewer recommendations. If there are any conflicting recommendations from reviewers, the Editor-in-Chief can assign a new reviewer.

The scientific board guiding the selection of the papers to be published in the Journal consists of elected experts of the Journal and if necessary, selected from national and international authorities. The Editor-in-Chief, Associate Editors may make minor corrections to accepted manuscripts that do not change the main text of the paper.

In case of any suspicion or claim regarding scientific shortcomings or ethical infringement, the Journal reserves the right to submit the manuscript to the supporting institutions or other authorities for investigation. The Journal accepts the responsibility of initiating action but does not undertake any responsibility for an actual investigation or any power of decision.

The Editorial Policies and General Guidelines for manuscript preparation specified below are based on "Recommendations for the Conduct, Reporting, Editing, and Publication of Scholarly Work in Medical Journals (ICMJE Recommendations)" by the International Committee of Medical Journal Editors (2013, archived at http://www.icmje.org/).

Preparation of research articles, systematic reviews and meta-analyses must comply with study design guidelines:

CONSORT statement for randomized controlled trials (Moher D, Schultz KF, Altman D, for the CONSORT Group. The CONSORT statement revised recommendations for improving the quality of reports of parallel group randomized trials. JAMA 2001; 285: 1987-91) (http://www.consort-statement.org/);

PRISMA statement of preferred reporting items for systematic reviews and meta-analyses (Moher D, Liberati A, Tetzlaff J, Altman DG, The PRISMA Group. Preferred Reporting Items for Systematic Reviews and Meta-Analyses: The PRISMA Statement. PLoS Med 2009; 6(7): e1000097.) (http://www.prisma-statement.org/);

STARD checklist for the reporting of studies of diagnostic accuracy (Bossuyt PM, Reitsma JB, Bruns DE, Gatsonis CA, Glasziou PP, Irwig LM, et al., for the STARD Group. Towards complete and accurate reporting of studies of diagnostic accuracy: the STARD initiative. Ann Intern Med 2003;138:40-4.) (http://www.stard-statement.org/);

STROBE statement, a checklist of items that should be included in reports of observational studies (http://www.strobe-statement.org/);

MOOSE guidelines for meta-analysis and systemic reviews of observational studies (Stroup DF, Berlin JA, Morton SC, et al. Meta-analysis of observational studies in epidemiology: a proposal for reporting Meta-analysis of observational Studies in Epidemiology (MOOSE) group. JAMA 2000; 283: 2008-12).

GENERAL GUIDELINES

Manuscripts can only be submitted electronically through the Journal Agent website (http://journalagent.com/tjps/) after creating an account. This system allows online submission and review.

TURKISH
JOURNAL OF PHARMACEUTICAL SCIENCES

INSTRUCTIONS TO AUTHORS

Format: Manuscripts should be prepared using Microsoft Word, size A4 with 2.5 cm margins on all sides, 12 pt Arial font and 1.5 line spacing.

Abbreviations: Abbreviations should be defined at first mention and used consistently thereafter. Internationally accepted abbreviations should be used; refer to scientific writing guides as necessary.

Cover letter: The cover letter should include statements about manuscript type, single-Journal submission affirmation, conflict of interest statement, sources of outside funding, equipment (if applicable), for original research articles.

ETHICS COMMITTEE APPROVAL

The editorial board and our reviewers systematically ask for ethics committee approval from every research manuscript submitted to the Turkish Journal of Pharmaceutical Sciences. If a submitted manuscript does not have ethical approval, which is necessary for every human or animal experiment as stated in international ethical guidelines, it must be rejected on the first evaluation.

Research involving animals should be conducted with the same rigor as research in humans; the Turkish Journal of Pharmaceutical Sciences asks original approval document to show implements the 3Rs principles. If a study does not have ethics committee approval or authors claim that their study does not need approval, the study is consulted to and evaluated by the editorial board for approval.

SIMILARITY

The Turkish Journal of Pharmaceutical Sciences is routinely looking for similarity index score from every manuscript submitted before evaluation by the editorial board and reviewers. The journal uses iThenticate plagiarism checker software to verify the originality of written work. There is no acceptable similarity index; but, exceptions are made for similarities less than 15 %.

REFERENCES

Authors are solely responsible for the accuracy of all references.

In-text citations: References should be indicated as a superscript immediately after the period/full stop of the relevant sentence. If the author(s) of a reference is/are indicated at the beginning of the sentence, this reference should be written as a superscript immediately after the author's name. If relevant research has been conducted in Turkey or by Turkish investigators, these studies should be given priority while citing the literature.

Presentations presented in congresses, unpublished manuscripts, theses, Internet addresses, and personal interviews or experiences should not be indicated as references. If such references are used, they should be indicated in parentheses at the end of the relevant sentence in the text, without reference number and written in full, in order to clarify their nature.

References section: References should be numbered consecutively in the order in which they are first mentioned in the text. All authors should be listed regardless of number. The titles of Journals should be abbreviated according to the style used in the Index Medicus.

Reference Format

Journal: Last name(s) of the author(s) and initials, article title, publication title and its original abbreviation, publication date, volume, the inclusive page numbers. Example: Collin JR, Rathbun JE. Involutional entropion: a review with evaluation of a procedure. Arch Ophthalmol. 1978;96:1058-1064.

Book: Last name(s) of the author(s) and initials, book title, edition, place of publication, date of publication and inclusive page numbers of the extract cited.

Example: Herbert L. The Infectious Diseases (1st ed). Philadelphia; Mosby Harcourt; 1999:11;1-8.

Book Chapter: Last name(s) of the author(s) and initials, chapter title, book editors, book title, edition, place of publication, date of publication and inclusive page numbers of the cited piece.

Example: O'Brien TP, Green WR. Periocular Infections. In: Feigin RD, Cherry JD, eds. Textbook of Pediatric Infectious Diseases (4th ed). Philadelphia; W.B. Saunders Company;1998:1273-1278.

Books in which the editor and author are the same person: Last name(s) of the author(s) and initials, chapter title, book editors, book title, edition, place of publication, date of publication and inclusive page numbers of the cited piece. Example: Solcia E, Capella C, Kloppel G. Tumors of the exocrine pancreas. In: Solcia E, Capella C, Kloppel G, eds. Tumors of the Pancreas. 2nd ed. Washington: Armed Forces Institute of Pathology; 1997:145-210.

TABLES, GRAPHICS, FIGURES, AND IMAGES

All visual materials together with their legends should be located on separate pages that follow the main text.

Images: Images (pictures) should be numbered and include a brief title. Permission to reproduce pictures that were published elsewhere must be included. All pictures should be of the highest quality possible, in

JPEG format, and at a minimum resolution of 300 dpi.

Tables, Graphics, Figures: All tables, graphics or figures should be enumerated according to their sequence within the text and a brief descriptive caption should be written. Any abbreviations used should be defined in the accompanying legend. Tables in particular should be explanatory and facilitate readers' understanding of the manuscript, and should not repeat data presented in the main text.

MANUSCRIPT TYPES

Original Articles

Clinical research should comprise clinical observation, new techniques or laboratories studies. Original research articles should include title, structured abstract, key words relevant to the content of the article, introduction, materials and methods, results, discussion, study limitations, conclusion references, tables/figures/images and acknowledgement sections. Title, abstract and key words should be written in both Turkish and English. The manuscript should be formatted in accordance with the above-mentioned guidelines and should not exceed 16 A4 pages.

Title Page: This page should include the title of the manuscript, short title, name(s) of the authors and author information. The following descriptions should be stated in the given order:

TURKISH
JOURNAL OF PHARMACEUTICAL SCIENCES

INSTRUCTIONS TO AUTHORS

1. Title of the manuscript (Turkish and English), as concise and explanatory as possible, including no abbreviations, up to 135 characters

2. Short title (Turkish and English), up to 60 characters

3. Name(s) and surname(s) of the author(s) (without abbreviations and academic titles) and affiliations

4. Name, address, e-mail, phone and fax number of the corresponding author

5. The place and date of scientific meeting in which the manuscript was presented and its abstract published in the abstract book, if applicable

Abstract: A summary of the manuscript should be written in both Turkish and English. References should not be cited in the abstract. Use of abbreviations should be avoided as much as possible; if any abbreviations are used, they must be taken into consideration independently of the abbreviations used in the text. For original articles, the structured abstract should include the following sub-headings:

Objectives: The aim of the study should be clearly stated.

Materials and Methods: The study and standard criteria used should be defined; it should also be indicated whether the study is randomized or not, whether it is retrospective or prospective, and the statistical methods applied should be indicated, if applicable.

Results: The detailed results of the study should be given and the statistical significance level should be indicated.

Conclusion: Should summarize the results of the study, the clinical applicability of the results should be defined, and the favorable and unfavorable aspects should be declared.

Keywords: A list of minimum 3, but no more than 5 key words must follow the abstract. Key words in English should be consistent with "Medical Subject Headings (MESH)" (www.nlm.nih.gov/mesh/MBrowser.html). Turkish key words should be direct translations of the terms in MESH.

Original research articles should have the following sections:

Introduction: Should consist of a brief explanation of the topic and indicate the objective of the study, supported by information from the literature.

Materials and Methods: The study plan should be clearly described, indicating whether the study is randomized or not, whether it is retrospective or prospective, the number of trials, the characteristics, and the statistical methods used.

Results: The results of the study should be stated, with tables/figures given in numerical order; the results should be evaluated according to the statistical analysis methods applied. See General Guidelines for details about the preparation of visual material.

Discussion: The study results should be discussed in terms of their favorable and unfavorable aspects and they should be compared with the literature. The conclusion of the study should be highlighted.

Study Limitations: Limitations of the study should be discussed. In addition, an evaluation of the implications of the obtained findings/results for future research should be outlined.

Conclusion: The conclusion of the study should be highlighted.

Acknowledgements: Any technical or financial support or editorial contributions (statistical analysis, English/Turkish evaluation) towards the study should appear at the end of the article.

References: Authors are responsible for the accuracy of the references. See General Guidelines for details about the usage and formatting required.

Review Articles

Review articles can address any aspect of clinical or laboratory pharmaceuticals. Review articles must provide critical analyses of contemporary evidence and provide directions of or future research. Most review articles are commissioned, but other review submissions are also welcome. Before sending a review, discussion with the editor is recommended.

Reviews articles analyze topics in depth, independently and objectively. The first chapter should include the title in Turkish and English, an unstructured summary and key words. Source of all citations should be indicated. The entire text should not exceed 25 pages (A4, formatted as specified above).

TURKISH
JOURNAL OF PHARMACEUTICAL SCIENCES

CONTENTS

TURKISH
JOURNAL OF PHARMACEUTICAL SCIENCES

CONTENTS

PUBLICATION NAME	Turkish Journal of Pharmaceutical Sciences
TYPE OF PUBLICATION	Vernacular Publication
PERIOD AND LANGUAGE	Bimonthly-English
OWNER	Erdoğan ÇOLAK on behalf of the Turkish Pharmacists' Association
EDITOR-IN-CHIEF	Prof.Terken BAYDAR, Ph.D.
ADDRESS OF PUBLICATION	Turkish Pharmacists' Association, Mustafa Kemal Mah 2147.Sok No:3 06510 Çankaya/ Ankara, TURKEY

TURKISH
JOURNAL OF PHARMACEUTICAL
SCIENCES

Volume: 18, No: 1, Year: 2021

CONTENTS

Turk J Pharm Sci 2021;18(1):1-2
DOI: 10.4274/tjps.galenos.2020.88864

LETTER TO EDITOR

Drug-drug Interactions of Antithrombotic Medications During Treatment of COVID-19

COVID-19 Tedavi Sürecinde Antitrombotik İlaçların İlaç-ilaç Etkileşimleri

Oğuzhan FIRAT*, Burcu KELLECİ ÇAKIR, Kutay DEMİRKAN

Hacettepe University Faculty of Pharmacy, Department of Clinical Pharmacy, Ankara, Turkey

Key words: COVID-19, antithrombotics, drug-drug interactions

Anahtar kelimeler: COVID-19, antitrombotik ilaçlar, ilaç-ilaç etkileşimleri

Dear Editor,

Coronavirus Disease-2019 (COVID-19), as an outbreak, is associated with high morbidity and mortality.[1] Since it affects the elderly more than other age groups, intensive care requirement and the risk of cardiovascular diseases and stroke become important due to the wide usage of antithrombotic medication. As a result of potential drug-drug interactions, these high-risk medications may cause gastrointestinal bleeding.[2] We believe that identifiying drug-drug interactions between COVID-19 and antithrombotic medications, which are commonly used in patients in the intensive care unit who suffer from cardiovascular diseases or stroke, is beneficial to ensure appropriate and safe treatment.

Hydroxychloroquine, a first-line treatment option for COVID-19, has a few drug interactions with antithrombotics. Although hydroxychloroquine does not have any drug-drug interaction with other antithrombotics (such as heparin, enoxaparin, aspirin, clopidogrel, and warfarin), it can increase the blood levels of apixaban (low risk), dabigatran (moderate risk), edoxaban (moderate risk), and rivaroxaban (low risk).[3]

Lopinavir/ritonavir (LPV/r) combination and strong inhibitors of cytochrome P450-3A4 and P-glycoprotein may enhance the blood levels of apixaban (high risk), edoxaban (moderate risk), rivaroxaban (high risk), and ticagrelor (high risk). During concomitant use with LPV/r, it is recommended to adjust the dose of apixaban to 2.5 mg twice daily. Additionally, concurrent use of LPV/r may decrease the serum concentrations of clopidogrel (high risk), dabigatran (moderate risk), dipyridamole (moderate risk), and warfarin (moderate risk). If possible, switching to prasugrel is recommended for patients using clopidogrel with LPV/r.[3]

Concurrent use of oseltamivir and warfarin (low risk) can lead to increased serum concentration of warfarin; however, this interaction does not require any intervention except monitoring the international normalized ratio. Additionally, clopidogrel (moderate risk) may decrease the serum concentrations of active metabolites of oseltamivir.[4]

In some countires, the use of azithromycin in combination with hydroxychloroquine is the most common approach among treatment options of COVID-19. In case of concomitant use of azithromycin during venous thromboembolism treatment with edoxaban, the serum concentration of edoxaban may significantly increase, which leads to the risk of exceeding its maximum daily dose (30 mg). The use of azithromycin with apixaban (minor risk), rivaroxaban (low risk), dabigatran (moderate risk), or warfarin (moderate risk) may enhance the serum concentration of these antithrombotic drugs.[5]

In terms of interaction with antithrombotics, because of limited data available at the moment, favipiravir seems to be the safest option among other medications used in COVID-19 treatment. The interaction of favipiravir with antithrombotic drugs has not been reported.[3]

*Correspondence: ogzhnfrt@gmail.com, Phone: +90 541 489 42 06 ORCID-ID: orcid.org/0000-0002-8726-8530
Received: 14.09.2020, Accepted: 22.09.2020

During COVID-19 treatment, concomitant use of high-risk medications such as antithrombotics should be assessed carefully for drug-drug interactions to avoid any negative outcomes in the treatment process.

Conflicts of interest: No conflict of interest was declared by the authors. The authors alone are responsible for the content and writing of the paper.

REFERENCES

1. Aggarwal G, Lippi G, Michael Henry B. Cerebrovascular disease is associated with an increased disease severity in patients with Coronavirus Disease 2019 (COVID-19): A pooled analysis of published literature. Int J Stroke. 2020;15:385-389.
2. Delaney JA, Opatrny L, Brophy JM, Suissa S. Drug drug interactions between antithrombotic medications and the risk of gastrointestinal bleeding. CMAJ. 2007;177:347-351.
3. Interactions with Experimental COVID-19 Therapies, Liverpool Drug Interaction Group, 2020. (Accessed March 13, 2020 at https://www.covid19-druginteractions.org/)
4. Drugs.com [Internet]. Oseltamivir Drug Interactions from Drugs.com; c1996-2020 [Updated: 10 April 2020; Cited: 27 April 2020]. Available from: https://www.drugs.com/drug-interactions/oseltamivir.html
5. Azithromycin. In: Lexi-drugs online [database on the Internet]. Hudson (OH): Lexicomp, Inc.; 2020 [accessed 27 April 2020]. Available from: https://www.uptodate.com/contents/azithromycin-systemic-drug-information?search=azithromycin&source=panel_search_result&selectedTitle=1~145&usage_type=panel&display_rank=1

Turk J Pharm Sci 2021;18(1):3-9
DOI: 10.4274/tjps.galenos.2019.30316

ORIGINAL ARTICLE

Evaluation of Nootropic Activity of *Limonia acidissima* Against Scopolamine-induced Amnesia in Rats

Limonia acidissima'nın Sıçanlarda Skopolamin ile İndüklenen Amneziye Karşı Nootropik Aktivitesinin Değerlendirilmesi

Kailas K MALI[1]*, Guruprasad V SUTAR[2], Remeth J DIAS[3], Omkar A DEVADE[1]

[1]Adarsh College of Pharmacy, Department of Pharmacology, Vita, Maharashtra, India
[2]Annasaheb Dange College of B-Pharmacy, Department of Pharmacology, Astha, Maharashtra, India
[3]Government College of Pharmacy, Karad, Maharashtra, India

ABSTRACT

Objectives: The present study aimed to evaluate the nootropic activity of *Limonia acidissima* in rats.

Materials and Methods: Methanolic extract of *Limonia acidissima* was used to evaluate nootropic activity, piracetam (200 mg/kg, i.p.) was used as a standard, and scopolamine (1 mg/kg, i.p.) was used to induce amnesia. The effect of drugs on learning and memory in rats was evaluated by using the Y-maze task and elevated plus maze on scopolamine-induced amnesia models. Locomotor activity was performed using an actophotometer. Also, levels of acetylcholinestrease, including histopathological examination of rat brains, were assessed.

Results: Methanolic extract of *Limonia acidissima* showed increased alteration of the behavior response and percentage spontaneous alteration with the Y-maze task. In the elevated plus maze scopolamine-induced amnesia model, methanolic extract of *Limonia acidissima* showed a decrease in transfer latency, which is indicative of cognition improvement. Methanolic extract increased locomotor activity in rats and decreased the levels of acetylcholinestrease enzyme significantly. A histopathological study with both low and high doses of extract showed effective regenerative scores as compared to normal control, negative control and standard treatment.

Conclusion: The results suggested that the administration of methanolic extract of *Limonia acidissima* enhances learning and memory in different experimental models. The histopathological study revealed the neuroprotective property of the extract. The study indicates that the extract may be used in the treatment of Alzheimer's disease.

Key words: Nootropic activity, *Limonia acidissima*, Alzheimer's disease, piracetam, scopolamine

ÖZ

Amaç: Bu çalışmada, sıçanlarda *Limonia acidissima*'nın nootropik aktivitesinin değerlendirilmesi amaçlanmıştır.

Gereç ve Yöntemler: Nootropik aktiviteyi değerlendirmek için *Limonia acidissima*'nın metanol ekstresi, standart olarak pirasetam (200 mg/kg, i.p.) ve amneziyi indüklemek için skopolamin (1 mg/kg, i.p.) kullanıldı. İlaçların sıçanlarda öğrenme ve hafıza üzerindeki etkisi, skopolamin ile indüklenen amnezi modelinde Y-labirent testi ve yükseltilmiş artı labirent testi kullanılarak değerlendirildi. Lokomotor aktivite, bir aktofotometre kullanılarak gerçekleştirildi. Ayrıca, sıçan beyinlerinin asetilkolinestreaz aktivitesinin değerlendirilmesi de dahil olmak üzere histopatolojik incelemesi yapıldı.

Bulgular: Y-labirent testi ile *Limonia acidissima*'nın metanol ekstresinin davranış tepkisinde ve yüzde spontan değişikliklerde artışa neden olduğu gösterildi. Skopolamin ile indüklenen amnezi modelinin kullanıldığı yükseltilmiş artı labirent testinde, *Limonia acidissima*'nın metanol ekstresinin, biliş gelişiminin göstergesi olan transfer gecikmesinde bir azalmaya yol açtığı gösterildi. Metanol ekstresi, sıçanlarda lokomotor aktiviteyi artırdı ve asetilkolinestreaz enzim aktivitesini önemli ölçüde düşürdü. Hem düşük hem de yüksek dozda ekstreyle yapılan histopatolojik çalışmada, normal kontrol, negatif kontrol ve standart tedaviye kıyasla efektif rejeneratif skorlar elde edildi.

Sonuç: Sonuçlar, *Limonia acidissima*'nın metanol ekstresinin uygulanmasının farklı deneysel modellerde öğrenmeyi ve hafızayı geliştirdiğini göstermiştir. Histopatolojik çalışma, ekstrenin nöroprotektif özellikte olduğunu ve ekstrenin Alzheimer hastalığının tedavisinde kullanılabileceğini göstermiştir.

Anahtar kelimeler: Nootropik aktivite, *Limonia acidissima*, Alzheimer hastalığı, pirasetam, skopolamin

*Correspondence: malikailas@gmail.com, Phone: +09552527353 ORCID-ID: orcid.org/0000-0002-1789-3592
Received: 13.12.2018, Accepted: 21.03.2019

INTRODUCTION

According to the World Health Organization, approximately 450 million people suffer from a mental or behavioral disorder.[1] Dementia (age-related mental disorder) is a characteristic symptom of Alzheimer's disease (AD).[2-4] AD is a progressive, neurodegenerative, and cerebrovascular disease.[2,5] It destroys cells in the brain, causing problems with memory, unusual behavior[6], difficulty thinking, personality changes,[7] and ultimately death.[8-10] AD is characterized by the loss of neuronal cells and is primarily linked to neurofibrillary tangles and neuritic plaques.[7,11] The cholinergic system in the brain plays an important role in learning and memory,[12] which involves acetylcholine (Ach).[13] Dementia is produced due to reduction of Ach in the brains of patients with AD.[7] In rodents and human beings, drugs like scopolamine impair learning and memory.[4,13] Memory loss, amnesia, dementia, anxiety, schizophrenia, and AD may be produced due to certain conditions like age, stress, and emotion.[14,15]

There are a few nootropic medicines used in the treatment of AD, called nootropic drugs, belonging to the class of psychotropic agents.[16] The term nootropic was coined by Giurgea in 1972, from the Greek noon (mind) and tropos (turn).[17] Nootropics are also referred to as smart drugs, as they improve mental functions such as memory, increase blood circulation to the brain, and improve the oxygen supply to the brain.[18] Synthetic medicines like tacrine, dopnezil,[19] aniracetam, piracetam, and rivastigmine are used for the treatment of cognitive dysfunction and memory loss associated with AD.[20] However, these drugs pose some adverse effects and bioavailability issues.[21] To overcome these problems, researchers are seeking herbal formulations that can overcome the adverse effects of synthetic drugs.

Many herbs have been studied extensively and reported to have memory-enhancing properties.[22] The plant *Limonia acidissima* is a herbal drug used in Ayurvedic systems of medicine.[23] It is also used in a variety of conditions for its antimicrobial, hepatoprotective, antidiarrhoeal, anticancer, diuretic, hepatoprotective, antispermatogenic, antioxidant, antidiabetic, and wound-healing activities.[24,25]

The present study seeks to determine whether the methanolic extract of leaves and fruit pulp of *Limonia acidissima* shows nootropic activity in an animal model.

MATERIALS AND METHODS

Experimental animals

Wistar rats of either sex weighing between 150 and 200 g were used for the present study. They were housed under standard laboratory conditions (temperature 25°C±1°C), relative humidity 55%±5% and 12.00:12.00 h dark: light cycle) with a standard pellet diet and water ad libitum.

The experiment was conducted as per the standard procedure prescribed by CPCSEA, India. The study protocol was approved by the Ethical Committee of IAEC of Yashoda Technical Campus, Satara (YSPM/YTC/PHARMA/20/2017).

Drugs and chemicals

Piracetam (Dr. Reddy's, India), scopolamine hydrobromide (APP Pharmaceuticals, India), and normal saline were used for the study. All other reagents and chemicals were of analytical grade and procured from Loba Chemie, Mumbai, India.

Plant material and preparation of extracts

Plant material was collected from Phaltan, identified, and authenticated by the Department of Botany, Yashwantrao Chavan Institute of Science, Satara, Maharashtra, India. A voucher specimen (no: 57) of plant material was kept in the Department of Pharmacognosy, Yashoda Technical Campus, Satara. The fully ripe fruits and leaves of the plant were dried in the shade for 1 week. Then, fruits were cracked open, and the rind, seed, and pulp were separated and shade dried with the leaves at room temperature for more than 2 weeks. After drying, the rind, pulp, and seeds were ground separately into a coarse powder, and the leaves was also separately ground into a coarse powder for further extraction. The coarsely powdered material was extracted with methanol by using the Soxhlet extraction method for 4 days at 45°C, at a ratio of 1:1:1 (seeds, pulp, and leaves). The obtained extract was filtered and concentrated (yield 8.8%).

Preliminary phytochemical investigation

The methanolic extract was subjected to phytochemical tests for alkaloids, flavonoids, glycosides, saponins, carbohydrates, and tannins.[26]

Acute toxicity study

An acute toxicity study was performed according to OECD guideline 423. Six swiss albino female mice, weighing in the range of 20-25 g, were administered the test solution at a dose of 2.000 mg/kg. After administration of the test formulation at intervals of 30 min, 1 h, 2 h, 4 h, 24 h, 48 h, and 72 h up to a period of 14 days, mice were observed for clinical signs, gross behavioral changes, and mortality.[27]

Behavioral study

Rats were trained for the behavioral study by conducting 1 week of training during which they did not receive any plant extract or drug. The completely trained rats were selected for the study. An experiment was carried out in the light period between 8.00 am and 03:00 pm in a sound- proof room.

Y-maze task

Five groups of animals were formed, each group comprising six animals as follows. Group 1: Control group (normal saline), group 2: Negative group (scopolamine 1 mg/kg i.p), group 3: Standard treatment (piracetam 200 mg/kg i.p. + scopolamine 1 mg/kg i.p.), group 4: Low dose of extract + scopolamine (200 mg/kg p.o + 1 mg/kg i.p.), group 5: High dose of extract + scopolamine (400 mg/kg p.o + 1 mg/kg i.p.).

The Y-maze task is a simple method to evaluate memory-enhancing activity in laboratory animals. It is generally used to check behavioral patterns in animals. The wooden Y-maze was used for the study. It consists of three arms with an angle of 120° between each of the two arms. Each arm was 8 cm wide,

30 cm long, and 15 cm deep. The arms were designated as the start arm (A), novel arm with food stimuli (B), and other arm (C).[28] In the first trial, the rat was placed just inside the arm and allowed to move freely through the apparatus for 5-10 min. In the second trial, the rat was placed in the maze and explored arms A, B, and C, systematically entering each arm. The ability to alternate requires that the rat know which arm they have already visited. A total of 13 entries were recorded for each rat visually, and finally, the percentage of spontaneous alteration was calculated by using the following formula:[29,30]

$$\text{Percentage alteration} = \frac{\text{Number of positive entries}}{\text{(Total number of arm entries - 2)}} \times 100$$

Scopolamine-induced amnesia in rats

Animals were grouped as per the Y-maze task. All animals were treated for 14 days, and at the end of the treatment period, all the extract-treated animals were subjected to scopolamine (1 mg/kg i.p.) 60 minutes after administration of extract, except the first group, which served as a vehicle control.

In this method, scopolamine is used as an inducer of memory impairments in rats, which is calculated by using the elevated plus maze (EPM) apparatus. The EPM is made up of wooden material. It consists of two arms, a closed arm and an open arm. In the EPM task, transfer latency was recorded. The rat was placed in the arm and allowed to explore the maze for 1 min. If the rat was not transferred into the other arm within 90 sec, it was gently pushed into the other arm, and the transfer latency was considered as 90 sec. All groups of animals were treated for 14 days, and at the end of the treatment, transfer latency was recorded and served as the parameter transfer latency on the 14th day (acquisition day) and 15th day (retention day).[31]

Locomotor activity

Animals were grouped as per the Y-maze task. Before the test, all rats were fasted for 4 h and treated as per the grouping. One hour after treatment, each rat was placed individually in an actophotometer for a period of 10 minutes, and locomoter activity was scored. The difference in locomotor activity of all groups was recorded.[6,32]

Estimation of acetylcholinestrease enzyme

Animals were grouped as per the Y-maze task. All rats were treated as per the groups with saline, scopolamine, piracetam, and extract. After 60 minutes of treatment, rats were decapitated, and the brains were removed quickly and stored in ice-cold saline. The frontal cortex, hippocampus, and septum were quickly dissected out on a petri dish chilled on crushed ice. The tissues were weighed and homogenized in 0.05 M phosphate buffer (pH 7.2). The homogenate (0.4 mL) was added to a test tube containing 2.6 mL phosphate buffer and 100 µL of 5,5-dithiobisnitrobenzoic acid and mixed. The absorbance of the resulting mixture was measured at 412 nm using a spectrophotometer. The stable value of absorbance was recorded. Then, acetylthiocholine iodide (20 µL) was added, and the change in absorbance per minute was determined. The mean change in absorbance was considered for calculation using the following formula, and acetylcholinestrease activity was measured as µM/L/min/g of tissue.[33]

$R = (\delta \text{ OD volume of assay} / E) \times \text{mg of protein}$

Where R is the rate of enzyme activity in "n" mole of Ach iodide hydrolyzed per minute per mg of protein, δ OD is the change in absorbance per minute, and E is the extinction coefficient (1.36×10^4 $M^{-1}cm^{-1}$).[34]

Brain histopathology

After the treatment and behavioral studies, two animals from each group were sacrificed by excessive CO_2 anesthesia, and the brains were isolated and kept in 10% formaldehyde solution. The brain was stained with crestyl violet, and the cerebellum and basal ganglia were studied under a light microscope.[35]

Statistical analysis

The statistical analysis was carried out by using GraphPad Prism software version 5.0, and the results were compared by One-Way ANOVA followed by Tukey's multiple comparison test. A p value less than 0.05 was considered as statistically significant.

RESULTS

Preliminary phytochemical investigation

The results of preliminary phytochemical screening of methanolic extract of *Limonia acidissima* are given in Table 1. The *Limonia acidissima* extract gave positive results for alkaloids, flavonoids, carbohydrates, glycosides, and saponin. Proteins, steroids, and phenols were absent.

Acute toxicity test

As female mice are more sensitive to drugs than males, female mice were used in the acute oral toxicity study as per OECD guideline 423. Methanolic extract of *Limonia acidissima* did not showed any toxic effects up to 2.000 mg/kg oral dose. Central nervous system (CNS) stimulation parameters such as hyperactivity, irritability, tremors, and convulsions were found to be negative in mice. CNS depressant parameters such as hypoactivity, narcosis, and ataxia were found to be negative in mice.

Table 1. Phytochemical analysis of *Limonia acidissima* extract

Serial number	Phytochemical test	Result
1	Test for alkaloids	+ Ve
2	Test flavonoids	+ Ve
3	Test for carbohydrates	+ Ve
4	Test for glycosides	+ Ve
5	Test for saponin	+ Ve
6	Test for proteins	- Ve
7	Test for steroids	- Ve
8	Test for phenols	- Ve

+ Ve: Indicates the presence of compounds, - Ve: Indicates the absence of compounds

Y-maze task

The Y-maze model proved to be a sensitive measure of spatial recognition memory. The effect on alteration behavior was studied on the parameter % alteration (Table 2). The negative control group showed a significant ($p<0.001$) decrease in the alternation of behavior when compared with the normal control. The results of the standard treatment groups showed a significant ($p<0.001$) increase in the alternation of behavior with respect to methanolic extract of *Limonia acidissima* 400 mg/kg.

Scopolamine-induced amnesia in rats

Scopolamine-induced amnesia in a rat model was carried out by using the EPM. The scopolamine-treated group showed a significant ($p<0.001$) increase in transfer latency and memory retention on the 14th acquisition and 15th retention days when compared with the normal control, standard treatment, and high-dose extract groups, respectively. The piracetam standard treatment group, when compared with methanolic extract of *Limonia acidissima* at a dose of 200 mg/kg, showed a significant ($p<0.01$) decrease in transfer latency and memory retention on the 14th acquisition day and 15th retention day, respectively. The result is given in Table 2.

Locomotor activity

Locomotor activity in rats was assessed using an actopotometer. The methanolic extract of *Limonia acidissima* showed nootropic activity by increasing locomotor activity (Table 3). The negative group showed a decrease in locomotor activity as compared with the normal control, while the extract-treated groups showed significantly ($p<0.001$) increased locomotor activity as compared with negative control group.

Estimation of acetyl cholinesterase (AChE) enzyme

The results for levels of AChE are given in Table 3. In the normal control, the level of AChE was very low, while in the negative control it was found to be high. In the case of the piracetam-treated group, the level of AChE was significantly reduced as compared with the negative control group. The methanoloc extract of *Limonia acidissima* (200 and 400 mg/kg) significantly ($p<0.001$) lowered AChE activity as compared with the negative control. The significant decrease in the level of AChE indicated that *Limonia acidissima* is a potential anti cholinesterase agent and possesses nootropic activity.

Histopathological analysis of scopolamine-induced amnesia in rats

The results of histopathological analysis are given in Figure 1 and Table 4. Figure 1A shows the histopathological section of normal control rat showed neuronal degeneration without vascular degeneration and gliosis, while the negative control group (Figure 1B) showed vascular degeneration, neuronal degeneration, and gliosis. In the case of the standard treatment group (Figure 1C), low-dose group (Figure 1D) and high-dose group (Figure 1E), vascular degeneration, neuronal degeneration, and gliosis were found to be lower as compared with the negative control group. Group 2, treated with scopolamine, showed maximum pathological changes as compared with the rest of the groups. Both a low dose and a high dose of methanolic extract of *Limonia acidissima* showed good regenerative scores as compared with the normal control, negative control and standard treatment.

Table 2. Effect of methanolic extract on alteration behavior and transfer latency in rats

Group	Treatment	Alterations (%)	Acquisition day 14 (sec)	Retention day 15 (sec)
1	Normal control: (Normal saline, p.o.)	66.31±2.45	41.00±1.67	38.33±1.22
2	Negative control: Scopolamine (1 mg/kg, p.o.)	35.80±3.19$^{c\#}$	74.14±3.37$^{c\#}$	71.50±3.50$^{c\#}$
3	Standard treatment: Piracetam (200 mg/kg, i.p.) + scopolamine (1 mg/kg, i.p.)	80.50±3.61$^{a\#c\dagger}$	25.67±1.22$^{c\#c\dagger}$	21.33±1.22$^{c\#c\dagger}$
4	Low dose of extract (100 mg/kg, p.o.) + scopolamine (1 mg/kg i.p.)	46.45±2.71$^{c\#c\dagger\dagger}$	34.83±1.24$^{c\dagger a\dagger\dagger}$	31.50±1.35$^{c\dagger a\dagger\dagger}$
5	High dose of extract (400 mg/kg, p.o.) + scopolamine (1 mg/kg, i.p.)	70.27±2.29^{c†}	27.50±1.17$^{c\#c\dagger}$	23.67±1.17$^{c\#c\dagger}$

Values represent mean ± standard error of the mean; n=6, analysis was performed using One-Way ANOVA followed by Tukey's multiple comparison test, p value less than 0.05 was considered as statistically significant. ^{a}: $p<0.05$, ^{b}: $p<0.01$, ^{c}: $p<0.001$, $^{\#}$: Data compared with normal control, †: Data compared with negative control, ††: Data compared with standard treatment

Table 3. Effect of methanolic extract on locomotor activity and brain acetylcholinesterase levels in rats

Group	Treatment	After treatment	AChE (μM/L/min/mg Protein)
1	Normal control: (Normal saline, p.o.)	562±30.12	13.03±1.55
2	Negative control: Scopolamine (1 mg/kg, p.o.)	251.2 42.6$^{c\#}$	24.09±1.56$^{c\#}$
3	Standard treatment: Piracetam (200 mg/kg, i.p.) + scopolamine (1 mg/kg, i.p.)	515±52.65^{c†}	15.52±1.13^{c†}
4	Low dose of extract (100 mg/kg, p.o.) + scopolamine (1 mg/kg i.p.)	324.5±48.5$^{c\#c\dagger\dagger}$	20.97±1.20$^{c\#c\dagger\dagger}$
5	High dose of extract (400 mg/kg, p.o.) + scopolamine (1 mg/kg, i.p.)	451.3±48.18$^{b\#c\dagger}$	18.00±1.19$^{c\#c\dagger}$

Values represent mean ± standard error of the mean, n=6, analysis was performed using One-Way ANOVA followed by Tukey's multiple comparison test, p value less than 0.05 was considered as statistically significant. ^{a}: $p<0.05$, ^{b}: $p<0.01$, ^{c}: $p<0.001$, $^{\#}$: Data compared with normal control, †: Data compared with negative control, ††: Data compared with standard treatment, AChE: Acetyl cholinesterase

DISCUSSION

The number of patients suffering from AD is rising steadily day by day all over the world.[36] AD is characterized by degenerative changes in the brain resulting in memory loss.[37,38] The main cause of AD is death of cholinergic neurons in the basal forebrain area, which results in a deficit of Ach.[36] Scopolamine is an antimuscarnic agent; after administration, it produces memory deficit.[39] Scopolamine-induced memory loss is a well-reported animal model for screening anti amnestic molecules.[40] It is a non-selective muscarinic receptor antagonist that competitively inhibits muscarinic receptors for Ach and reduces the level of Ach. Furthermore, it causes impairment of learning acquisition short-term memory as it produces depression of the cerebral cortex, especially in the motor areas.[41]

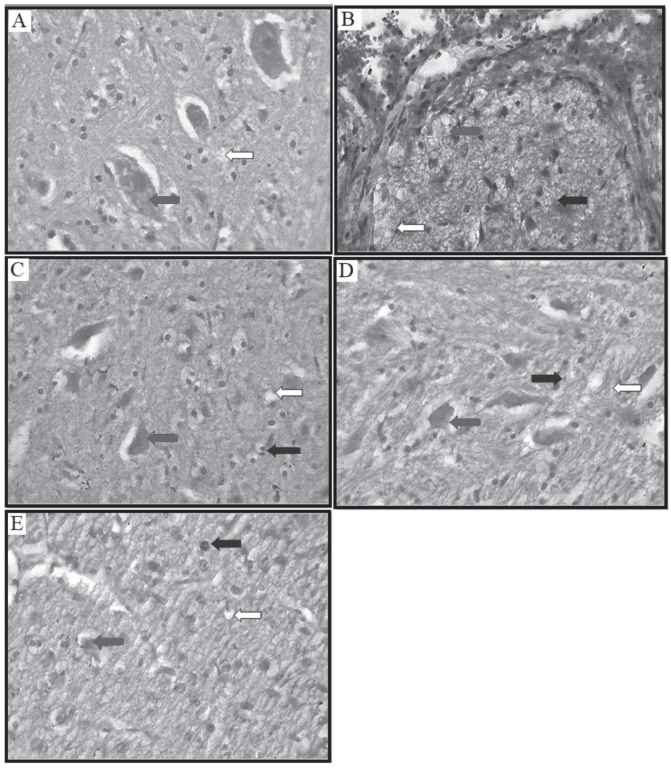

Figure 1. Histopathological observation of brain tissues in scopolamine-induced amnesia in rats

A) Normal control: Section showing only stress amount of neuronal degeneration (grey arrow). B) Negative control: Section showing vascular degeneration (white arrow), neuronal degeneration (grey arrow) and glial cell infiltration (black arrow). C) Standard treatment: Section showing vascular degeneration (white arrow), neuronal degeneration (grey arrow) glial cell infiltration (black arrow) less as compared with negative control. D) Low dose of extract: Section showing vascular degeneration (white arrow), neuronal degeneration (grey arrow) glial cell infiltration (black arrow) less as compared with negative control. E) High dose of extract: Section showing vascular degeneration (white arrow), neuronal degeneration (grey arrow) glial cell infiltration (black arrow) less as compared with negative control

Piracetam is a standard drug used to treat amnesia, dementia, and other health problems like brain stroke, AD, vascular dementia, DLB, and Huntington's disease. Piracetam has the ability to bind to receptors and increases Ach levels in the brain. It acts on cholinergic receptors and increases the synthesis of Ach. It increases oxygen supply to the brain. It has a positive therapeutic effect which is useful in clotting, coagulation, and thrombotic disorders. It also acts as an antioxidant/neurotonic. It also enhances the number of Ach receptors; thus, it might be effective at enhancing learning and memory.[42]

In this study, we investigated the effect of methanolic extract of *Limonia acidissima* on spatial memory and neurodegeneration in an animal model of AD. The results clearly demonstrated that spatial memory and neurodegeneration were significantly improved by *Limonia acidissima*.

Methanolic extract of *Limonia acidissima* at doses of 200 mg/kg and 400 mg/kg was administered orally for 7 days and improved learning and memory significantly in rats in the Y-maze task. When the negative control group was compared with the standard treatment and extract groups, both standard and extract-treated groups showed a significant ($p<0.001$) increase in percentage alteration behavior.

In the EPM model, methanolic extract of *Limonia acidissima* possessed nootropic activity on scopolamine-induced amnesia. The extract-treated group showed a significant decrease in transfer latency and memory retention with $p<0.001$ when compared with the negative and standard group at the 14th acquisition and 15th retention day of the study, which is an indicative of cognition improvement.

Locomotor activity in patients suffering from AD is absent. The actophometer is the model used to observe the locomotor behavior of animals. So, in the present study the actophometer model was used to know about the locomotor activity of animals treated with methanolic extracts. The methanolic extract of *Limonia acidissima* passes nootropic activity by increasing locomotor activity. The significant ($p<0.001$) locomotor activity was observed in rats treated with low-dose and high-dose treated groups.

Table 4. Histopathology of the brain tissues in scopolamine-induced amnesia in rats

Group	Vacuolar degeneration	Neuronal degeneration	Gliosis
Normal control: (Normal saline, p.o.)	0	+	0
Negative control: Scopolamine (1 mg/kg, p.o.)	+++	+++	++
Standard treatment: Piracetam (200 mg/kg, i.p.) + scopolamine (1 mg/kg, i.p.)	++	++	+
Low dose of extract (100 mg/kg, p.o.) + scopolamine (1 mg/kg i.p.)	++	++	+
High dose of extract (400 mg/kg, p.o.) + scopolamine (1 mg/kg, i.p.)	+	++	+

No abnormality detected (0), damage/active changes up to less than 25% (+), damage/active changes up to less than 50% (++), damage/active changes up to less 75% (+++), damage/active changes up to more than 75 (++++)

Ach is considered as a major neurotransmitter involved the regulation of cognitive functions.[31] Changes in the cholinergic system lead to impairment in learning, memory, and behavior in patients with dementia. In the present study, *Limonia acidissima* inhibited acetylcholinestrease, thereby elevating the Ach concentration in the brain. The findings suggested a possible neuroprotective role of *Limonia acidissima*. Thus, it seems that *Limonia acidissima* may prove to be useful in the treatment of AD. However, further investigations are necessary to support these results.

The histopathological study also showed that both a low dose and a high dose of methanolic extract of *Limonia acidissima* showed good regenerative scores as compared with other group, which is good indicator of the neuro-protective property with the potential to treat AD.

In a few studies, the use of antiinflammatory drugs showed a reduction in symptoms of AD.[43] Epidemiological studies also confirmed the suitability of non-steroidal antiinflammatory drugs to reduce the incidence of AD.[44] *Limonia acidissima* has been reported to produce antiinflammatory action in rodents.[45] This antiinflammatory property of *Limonia acidissima* will likely help in the treatment Alzheimer's patients.

CONCLUSION

The present study suggests that methanolic extract of *Limonia acidissima* provided significant protection against AD. The methanolic extract of *Limonia acidissima* increased locomotor activity in rats and inhibited acetylcholinestrease, thereby elevating the Ach concentration in the brain. The histopathology of the brain also showed a good regenerative score; therefore, methanolic extract of *Limonia acidissima* can be used in the management of AD. An extensive study along these lines is required in the future to support the methanolic extract of *Limonia acidissima* as a novel and natural nootropic/memory-enhancing agent.

ACKNOWLEDGMENTS

The authors are thankful to the Founder President, Prof. Dasharath Sagare, YSPM's Yashoda Technical Campus, Satara for providing the laboratory facilities. Authors are also thankful to Dr. D.S. Suryawanshi, Omega Laboratory, Lonand for providing facility of histopathology study.

Conflicts of interest: No conflict of interest was declared by the authors. The authors alone are responsible for the content and writing of the paper.

REFERENCES

1. Gupta R, Singh HK. Nootropic potential of Alternanthera sessilis and Clerodendrum infortunatum leaves on mice. Asian Pacific J Trop Dis. 2012;2(Suppl1)465-470.
2. Shivakumar L, ST Gouda, Rao NV, Shalam, Richa V. Evaluation of nootropic activity of polyherbal formulation Sr-105. Int Res J Pharm. 2011;2:101-107.
3. Ansari OA, Tripathi JS, Ansari S. Evidence based anti-dementing activity of Saraswata ghrita "a nootropic compound from Ayurveda. Int J Pharm Sci Res. 2013;4:4194-4202.
4. Kumar KA, Kumar MS, Babu AN, Tony DE. Evaluation of nootropic activity of leaf extract of typha angustata. Int J Preclin Pharm Res. 2014;5:57-60.
5. Parle M, Dhingra D, Kulkarni SK. Memory-strengthening activity of Glycyrrhiza glabra in exteroceptive and interoceptive behavioral models. J Med Food. 2004;7:462-466.
6. Joshi H, Parle M. Nootropic activity of calyces of Hibiscus sabdariffa Linn. Iran J Pharmacol Ther. 2006;5:15-20.
7. Kulkarni PD, Ghaisas MM, Chivate ND, Sankpal PS. Memory enhancing activity of cissampelos pariera in mice. Int J Pharm Pharm Sci. 2011;3:206-211.
8. Kaur K, Kaur R, Kaur M. Recent advances in alzheimer's disease: causes and treatment. Int J Pharm Pharm Sci. 2016;8:8-15.
9. Gupta A, Hemraj, Jalhan S, Jindal A, Upmanyu N. Various animal models to check learning and memory - A review. Int J Pharm Pharm Sci. 2012;4:91-95.
10. Naylor MD, Karlawish JH, Arnold SE, Khachaturian AS, Khachaturian ZS, Lee VM, Baumgart M, Banerjee S, Beck C, Blennow K, Brookmeyer R, Brunden KR, Buckwalter KC, Comer M, Covinsky K, Feinberg LF, Frisoni G, Green C, Guimaraes RM, Gwyther LP, Hefti FF, Hutton M, Kawas C, Kent DM, Kuller L, Langa KM, Mahley RW, Maslow K, Masters CL, Meier DE, Neumann PJ, Paul SM, Petersen RC, Sager MA, Sano M, Schenk D, Soares H, Sperling RA, Stahl SM, van Deerlin V, Stern Y, Weir D, Wolk DA, Trojanowski JQ. Advancing Alzheimer's disease diagnosis, treatment, and care: Recommendations from the Ware Invitational Summit. Alzheimers Dement. 2012;8:445-452.
11. Kwon SH, Lee HK, Kim JA, Hong SI, Kim HC, Jo TH, Park YI, Lee CK, Kim YB, Lee SY, Jang CG. Neuroprotective effects of chlorogenic acid on scopolamine-induced amnesia via anti-acetylcholinesterase and anti-oxidative activities in mice. Eur J Pharmacol. 2010;649:210-217.
12. Nabeshima T. Behavioral aspects of cholinergic transmission: role of basal forebrain cholinergic system in learning and memory. Prog Brain Res. 1993;98:405-411.
13. Khakpai F, Nasehi M, Haeri-Rohani A, Eidi A, Zarrindast MR. Scopolamine induced memory impairment; possible involvement of NMDA receptor mechanisms of dorsal hippocampus and/or septum. Behav Brain Res. 2012;231:1-10.
14. Une HD, Ejaj MA, Tarde VA. Nootropic Activity of Saponins obtained from Tinospora Cordifolia Stem in Scopolamine induced Amnesia. Int J Pharma Res Rev. 2014;3:28-35.
15. Pal A, Jena M, Mishra S. Nootropic Activity of Zingiber Officinale in Albino Mice : A Behavioral and Neurochemical Approach. Res J Pharm, Biol Chem Sci. 2013;4:1129-1138.
16. Chintawar SD, Somani RS, Kasture VS, Kasture SB. Nootropic activity of Albizzia lebbeck in mice. Ethnopharmacol. 2002;81:299-305.
17. Gouliaev AH, Senning A. Piracetam and other structurally related nootropics. Brain Res Brain Res Rev. 1994;19:180-222.
18. Mali AA, Shenoy PA, Bhandawane DD, Nipate SS, Chaudhari PD. Screening of Nootropics: An overview of preclinical evaluation techniques. Int J Pharm. 2012;2:159-180.
19. Gibbs RB, Mauk R, Nelson D, Johnson DA. Donepezil treatment restores the ability of estradiol to enhance cognitive performance in aged rats:

Evidence for the cholinergic basis of the critical period hypothesis. Horm Behav. 2009;56:73-83.

20. Winnicka K, Tomasiak M, Bielawska A. Piracetam - an old drug with novel properties? Acta Pol Pharm. 2005;62:405-409.
21. Mukherjee PK, Kumar V, Mal M, Houghton PJ. Acetylcholinesterase inhibitors from plants. Phytomedicine. 2007;14:289-300.
22. Dwivedi P, Singh R, Malik MT jawaid T. A traditional approach to herbal nootropic agents: an overview. Int J Pharm Sci Res. 2012;3:630-636.
23. Dhanapal R, Vijaya Ratna J, Sarathchandran I, Gupta M. Reversible antispermatogenic and antisteroidogenic activities of Feronia limonia fruit pulp in adult male rats. Asian Pac J Trop Biomed. 2012;2:684-690.
24. Vijayvargia P, Vijayvergia R. A review on *Limonia acidissima* l.: Multipotential medicinal plant. Int J Pharm Sci Rev Res. 2014;28:191-195.
25. Priya Darsini DT, Maheshu V, Vishnupriya M, Nishaa S, Sasikumar JM. Antioxidant potential and amino acid analysis of underutilized tropical fruit *Limonia acidissima* L. Free Radicals Antioxidants. 2013;3:S62-69.
26. Kokate CK. Practical Pharmacognosy. 4th ed. New Delhi: Vallabh Prakashan; 1999.
27. OECD Guidelines for Testing Chemicals. Guideline 423 Acute Oral Toxicity. 2001. page 1-14.
28. Saxena V, Ahmad H, Gupta R. Memory enhancing effects of Ficus carica leaves in hexane extract on interoceptive behavioral models. Asian J Pharm Clin Res. 2013;6(Suppl.3):109-113.
29. Kumar MN. Evaluation of Nootropic Activity in Mice. An Int Q J Biol life Sci. 2016;1:45-54.
30. Sudeepthi NL, Eswar K, Pradesh A. Nootropic activity of acetone extract of curcuma amada using Y-maze and elevated plus maze. J Pharm Mol Biol. 2013;1:51-66.
31. Sujith K, Darwin CR, Sathish, Suba V. Memory-enhancing activity of Anacyclus pyrethrum in albino Wistar rats. Asian Pacific J Trop Dis. 2012;2:307-311.
32. Vyawahare NS, Ambikar DB. Evaluation of neuropharmacological activity of hydroalcoholic extract of fruits of trapa bispinosa in laboratory animals. Int J Pharm Pharm Sci. 2010;2(Suppl 2):32-35.
33. Varma RK, Singh L, Garg VK, Yadav P, Singh VK. Nootropic effect of Vigna Mungo (L.) hpper seeds extract in scopalamine induced amnesic rats. World J Pharm Pharm Sci. 2016;5:1176-1192.
34. Anantha Lakshmi J, Satyavati D. A study on nootropic activity of methanolic extract of Brassica oleraceae var. Caulorapa bulb in rodents. Asian J Pharm Clin Res. 2015;3:107-115.
35. Hafez HS, Ghareeb DA, Saleh SR, Abady MM, El Demellawy MA, Hussien H, Abdel-Monem N. Neuroprotective effect of ipriflavone against scopolamine-induced memory impairment in rats. Psychopharmacology (Berl). 2017;234:3037-3053.
36. Chonpathompikunlert P, Wattanathorn J, Muchimapura S. Piperine, the main alkaloid of Thai black pepper, protects against neurodegeneration and cognitive impairment in animal model of cognitive deficit like condition of Alzheimer's disease. Food Chem Toxicol. 2010;48:798-802.
37. Sheikh RA, Turaskar A, More S, Irene PR, Nathani MN. Study on nootropic activity of alcoholic extracts of flower of Securinega leucopyrus (AEFSL) in mice. Der Pharm Lett. 2014;6:67-71.
38. Ahmed T, Gilani AH. Inhibitory effect of curcuminoids on acetylcholinesterase activity and attenuation of scopolamine-induced amnesia may explain medicinal use of turmeric in Alzheimer's disease. Pharmacol Biochem Behav. 2009;91:554-559.
39. Higashida A, Ogawa N. Differences in the acquisition process and the effect of scopolamine on radial maze performance in three strains of rats. Pharmacol Biochem Behav. 1987;27:483-489.
40. Hanumanthachar J, Navneet K, Jyotibala C. Evaluation of Nootropic Effect of Argyreia speciosa in Mice. J Heal Sci. 2007;53:382-388.
41. Izquierdo I. Mechanism of action of scopolamine as an amnestic. Trends Pharmacol Sci. 1989;10:175-177.
42. Khare P, Rituparna P, Pranit S, Noorpur K, Yadav G. Recent Advances on Piracetam. Adv Biol Res. 2016;10:264-270.
43. Rao SK, Andrade C, Reddy K, Madappa KN, Thyagarajan S, Chandra S. Memory protective effect of indomethacin against electroconvulsive shock-induced retrograde amnesia in rats. Biol Psychiatry. 2002;51:770-773.
44. Breitner JC. The role of anti-inflammatory drugs in the prevention and treatment of alzheimer's disease. Annu Rev Med. 1996;47:401-411.
45. Khare S, Khare P, Jain SK. Anti-Inflammatory Activity of Ethanolic Extract of Feronia *Limonia* (L .) Leaves. World J Pharm Pharm Sci. 2014;3:870-876.

Turk J Pharm Sci 2021;18(1):10-16
DOI: 10.4274/tjps.galenos.2019.59320

ORIGINAL ARTICLE

Antibacterial, Antifungal, and Antioxidant Activity of *Cleome coluteoides*: An *In Vitro* Comparative Study Between Leaves, Stems, and Flowers

Cleome coluteoides Boiss Antibakteriyel, Antifungal ve Antioksidan Aktiviteleri: Yaprak, Çiçek ve Kök Ekstrelerinin *İn Vitro* Karşılaştırmalı Çalışması

Parastoo ZARGHAMI MOGHADDAM[1], Ameneh MOHAMMADI[1], Paiman ALESHEIKH[1], Peyman FEYZI[1], Ali HAGHBIN[1], Samaneh MOLLAZADEH[1], Zahra SABETI[2], Ailar NAKHLBAND[1], Jamal KASAIAN[1]*

[1]North Khorasan University of Medical Sciences, Natural Products and Medicinal Plants Research Center, Bojnurd, Iran
[2]Mashhad University of Medical Sciences School of Pharmacy, Department of Microbiology and Virology, Mashhad, Iran

ABSTRACT

Objectives: *Cleome coluteoides*, which belongs to the Capparidaceae family, and has been used in folk medicine for a long time. Our research aims to measure the antioxidant, antibacterial, and antifungal activities of *C. coluteoides*.

Materials and Methods: Various solvents, such as ethyl acetate, methanol, and dichloromethane, were used to extract different plant parts. Antibacterial and antifungal activities were assayed by disk and well diffusion methods, and the antioxidant activity was screened by 2,2-diphenyl-1-picrylhydrazyl (DPPH) and ferric reducing ability of plasma methods.

Results: Results showed that Gram-negative bacteria and fungus were resistant to various plant extracts. Against all Gram-positive bacteria tested, *C. coluteoides*' flower extract had the highest inhibition effects. Also, the most sensitive bacterium was *Bacillus cereus*, which had an 18-mm inhibition zone. Due to the solvent's physical and chemical properties, different *C. coluteoides* extracts exhibited various antioxidant activities in the antioxidant activity assay. To some extent, methanol extract of leaves showed the highest DPPH radical scavenging activity at various concentrations that ranged from 5 to 160 mg.mL^{-1}. The methanol extract of flower was observed to have the highest level of phenolics among all tested extracts.

Conclusion: This study demonstrates that different extracts from various *C. coluteoides* parts are different in their properties, therefore, a proper solvent should be used to extract maximum amounts of antioxidant and antibacterial components from a typical plant material.

Key words: *Cleome coluteoides*, antibacterial, antifungal, antioxidant

ÖZ

Amaç: *Cleome coluteoides*, Capparidaceae familyasına aittir ve uzun süredir geleneksel tıpta kullanılmaktadır. Çalışma *C.coluteoides*'in antioksidan, antibakteriyal ve antifungal aktivitesini ölçmeyi amaçlamıştır.

Gereç ve Yöntemler: Bitkinin farklı kısımları etil asetat, metanol ve diklorometan gibi çeşitli çözücüler ile ekstre edildi. Antibakteriyel ve antifungal aktiviteler disk ve kuyu difüzyon yöntemleriyle, antioksidan aktivite ise 2,2-difenil-1-pikrilhidrazil (DPPH) ve ferrik indirgeme kabiliyeti ile belirlendi.

Bulgular: Sonuçlar, Gram-negatif bakteri ve mantarların yukarıda bahsi geçen çeşitli bitki ekstrelerine karşı dayanıklı olduğunu gösterdi. *C. coluteoides*'in çiçek ekstresi, test edilen Gram-pozitif bakterilerin tümüne karşı en yüksek inhibitör etkiye sahipti. Ayrıca, *Bacillus cereus*, 18-mm inhibitör zonuyla en hassas bakteridir. Antioksidan aktivite analizinde, farklı *C. coluteoides* ekstreleri, solvanların fiziksel ve kimyasal özelliklerinden dolayı çeşitli antioksidan aktiviteler göstermişlerdir. Bir şekilde, yaprakların metanol ekstresi, 5-160 mg.mL^{-1} arasında değişen konsantrasyonlarda en yüksek DPPH serbest radikal süpürücü aktivite göstermiştir. Test edilen ekstreler arasında çiçeklerin metanol ekstresinin en yüksek fenolik içeriğe sahip olduğu bulundu.

Sonuç: Bu çalışma, *C. coluteoides*'in çeşitli kısımlarının özelliklerinin farklı özelliklere sahip olduğunu göstermektedir, bu nedenle bir bitki materyalinin optimize edilmiş antioksidan ve antibakteriyel aktiviteleri için uygun bir çözücü bulmak hayati öneme sahiptir.

Anahtar kelimeler: *Cleome coluteoides*, antibakteriyel, antifungal, antioksidan

***Correspondence:** kasaianj1@gmail.com, **Phone:** +09858-31513017 **ORCID-ID:** orcid.org/0000-0002-5661-5106
Received: 08.06.2019, **Accepted:** 24.10.2019

INTRODUCTION

Free radicals are unstable and highly reactive atoms/groups with unpaired electrons, which can cause membrane damage, heart complications, aging, and cancer. To protect damages caused by free radicals, antioxidants can be used.[1] The stability of drugs, foods, and nutrients and increase antiinflammatory, antiallergic, and anticancer potential of the human body can be efficiently improved by natural antioxidants. Plants with high phenolic contents, on the other hand, are a good source of powerful antioxidants.[2] One of the most serious public health problems is microbial resistance to antibiotics, especially in developing countries where infectious diseases are a major cause of human mortality.[3] Thus, there is great interest in finding new compounds derived from medicinal plants. Brought to light by recent studies, organic herbs contain secondary metabolites that make them good candidates for traditional or native remedies, especially as antimicrobial and antifungal agents.[4] Recent investigations have proved that pathogenic microbes can be controlled via medicinal plants-based drugs.[5] Accordingly, examining different medicinal plant extracts and constituents is essential for their antibacterial activity.

Cleome L. belongs to Capparidaceae family, and is a large genus with 200 species worldwide. Because of its ethnomedicinal properties, including anthelmintic, carminative, anticonvulsant, antidiarrheal, antimicrobial, and wound-healing effects, this genus has been used in folk medicine for a long time.[6] Some species in this genus, such as *Cleome arabica* L, *Cleome viscosa* Linn, *Cleome droserifolia* (Forssk.), *Cleome* enrichment, *Cleome rutidosperma* DC, *Cleome gynandra* L, possesses antipyretic and antidiarrheal properties, and have been used as traditional medicine in treatment of scabies, inflammation, rheumatic pains, blood problems, uterine complaints, malaria, counteract diabetic hyperglycemia, treat paralysis, anthelmintic problems, epilepsy, convulsions, spasm, pain, and skin disease.[7-11] Different parts of *Cleome* genus like leaves, roots, and seeds are used as stimulant, antiscorbutic, anthelmintic, rubefacient, vesicant, and carminative factors according to the mentioned traditional applications.[12] Phytochemical screening studies of the *Cleome* genus found phenolic compounds, alkaloids, terpenoids, flavonoids, fatty acids, coumarino-lignan, and rich source of nutrients, especially vitamins A and C, protein, gallotannins, saponins, iridoid, hexacosanol, and kaempferol.[7,13-17] Therefore, a promising approach is to find natural antibacterial, antifungal, and antioxidant agents with similar therapeutic effect that is safer and healthier.[18] To date, the chemical composition and pharmacological effects of various species of *Cleome* have been reported. However, to our knowledge, *Cleome coluteoides*' chemical components and extracts-related activities have not been shown. The focus of this study is on the antioxidant, antibacterial, and antifungal activities of various extracts of *C. coluteoides.*

MATERIALS AND METHODS

Folin-Ciocalteau reagent (F9252, Sigma-Aldrich), gallic acid (91215, Fluka), aluminum chloride (563919, anhydrous powder, 99.999%, Sigma-Aldrich), 2,2-diphenyl-1-picrylhydrazyl (257621, Sigma-Aldrich), 2,4,6-tripyridyl-s-triazine (T1253 for spectrophotometric, ≥98%, Sigma), butylated hydroxy toluene (BHT) (W218405 ≤99, Sigma-Aldrich), Na_2CO_3 (451614, anhydrous powder, 99.999%, Sigma-Aldrich), $FeSO_4.7H_2O$ (21542, ≥99.0%, Sigma-Aldrich) were used in this study.

In June 2017, the stems, flowers, and leaves of *C. coluteoides* were collected from the Roein region of the North Khorasan Province of Iran. The voucher specimen (MP.1247) was authenticated by botanist and it has been deposited at the Herbarium of Natural Products and Medicinal Plants Research Center in North Khorasan University of Medical Sciences. From Pasteur Institute of Iran, bacterial and fungal strains were procured.

Extracts preparation

Various solvents, such as ethyl acetate, methanol, and dichloromethane, were used to separately extract powdered stems, flowers, and leaves of *C. coluteoides* by maceration method for 24 h at room temperature. To yield crude extracts, they were filtered through a paper filter and the solvent was evaporated under a vacuum at 45°C.

Microorganisms

Escherichia coli (ATCC 8739), *Bacillus cereus* (PTCC 1247), and *Staphylococcus aureus* (ATCC 6538) were the microorganisms used for antimicrobial activities screening, whereas *Fusarium solani* (PTCC 5284) and *Candida albicans* (ATCC 10231) were applied for antifungal tests. Disk and well diffusion methods (CLSI 2012 standard) were used in this study for the antimicrobial activity assay.

Well diffusion method

Punched into the agar plates were 6-mm diameter wells with Mueller-Hinton agar (MHA) for bacterial and Soybean Casein Agar [(SCA) or Tryptic Soy Agar)] for fungal strains. On the plates' surface, a density of $1.5x10^8$ microorganism cells had been spread. Next, added into the wells were 50 µL plant extracts (100 $mg.mL^{-1}$). Incubation lengths were 16-20 h at 37°C for bacteria and 36-48 h at 32°C for fungi; inhibition zones (mm) were then measured.[19]

Disk-diffusion method

The discs (6 mm diameter) contained plant extracts (100 $mg.mL^{-1}$) were placed on the plates containing MHA for bacterial and SCA for fungal strains with $1.5x10^8$ microorganism cells. Incubation lengths for bacteria and fungi were 16-20 h at 37°C and 36-48 h at 32°C, respectively. By measuring the zone of inhibition zones surrounding the disks, antimicrobial activity was evaluated. Gentamycin and nystatin were used as a positive control and dimethyl sulfoxide as a negative control.[20]

Antioxidant activity evaluation

Free radical scavenging activity assay

1,1-diphenyl-2-picrylhydrazyl (DPPH) was used to assess the free radical scavenging activity. To do so, in a 96-well microplate, 100 µL of each extract (5-160 mg/mL) was incubated with 200 µL

DPPH (300 µM) at 37°C for 30 min. After that, an enzyme-linked immunosorbent assay (ELISA) microplate reader (BioTek) was used to measure absorption at 490 nm. MeOH and BHT were used as blank and positive controls, respectively. Free radical inhibition of DPPH was calculated as follows:

% inhibition: $(A_{blank} - A_{sample}/A_{blank}) \times 100$,

where A_{blank} is the absorbance of the blank group and A_{sample} is the absorbance of each extract.[21]

Ferric reducing antioxidant power assay

As a standard, ferrous sulfate (10-100 mM $FeSO_4 \cdot 7H_2O$) was used. The ferric reducing antioxidant power (FRAP) reagent (3 mL) was added 100 µL of each extract (50 mg/mL), and was incubated in a water bath for 10 min at 37°C. By using the ELISA microplate reader, the absorbance was measured at 600 nm after incubation. All tests were performed in triplicates. The results were presented as means ± standard deviation (SD), and FRAP values were expressed as mmol Fe (2) per gram of extract.[22]

Determination of total phenolic content

In 96-well plates, 10 µL of each extract was added to 100 µL of Folin-Ciocalteu's phenol reagent (0.2 N). After 3 min, added to the mixture was 90 µL of saturated sodium carbonate solution and was incubated at room temperature for 1 h. The samples were measured at 630 nm. Gallic acid (concentration range 3.25 to 500 mg/mL^{-1}) was used to calculate the total phenolic content by standard curve. Results were expressed as microgram gallic acid equivalent (GAE) per milligram dry weight (DW) (µg GAE/mg DW).[21,22]

Statistical analysis

For each experimental point, data were expressed as mean ± SD for at least three independent determinations in triplicate. GraphPad Prism version 5.01 software was used to calculate the IC_{50} values in DPPH test.

RESULTS

Different extracts from various parts of *C. coluteoides*, as expected, represented different extractable yield amounts. Extracts are expressed as follows: Dichloromethane extract of leaves (DEL); methanol extract of leaves (MEL); ethyl acetate extract of leaves (EEL); dichloromethane extract of flower (DEF); methanol extract of flower (MEF); ethyl acetate extract of flower (EEF); dichloromethane extract of stem (DES); methanol extract of stem (MES); and ethyl acetate extract of stem (EES). MEF obtained the highest yield (9.63%) and the lowest ones were from DES and EES. Altogether, to get more yields from various parts of the plant, the methanol solvent system could be more efficient (Figure 1). Disc/well diffusion methods were used to test the antibacterial and antifungal activities of dried extracts (ethyl acetate, methanol, and dichloromethane extracts) of stems, flowers, and leaves were tested for antibacterial and antifungal activities, and their results are shown in Table 1. In both methods, the diameter of inhibitory zones for Gram-negative bacteria and fungus was 6.0 mm, and all microorganisms were resistant to various plant extracts. Therefore, well and disk-diffusion method results were similar. Against all the tested microorganisms, flower extract of *C. coluteoides* had the highest inhibition effects; however, its activity was markedly lower than gentamicin in bacteria. In the disk-diffusion method, *B. cereus* was the more sensitive bacteria with an inhibition zone of 18 mm.

Table 2 presents the free radical scavenging activities of various extracts. It should be mentioned that a lower IC_{50} value indicates a higher antioxidant activity. Tests by DPPH radical scavenging activity showed that MEL exhibited remarkable antioxidant activities (19.54±0.21 mg/mL). All the plant parts' IC_{50} were higher than standard BHT, which was 0.15 mg/mL. In Figure 2, the test samples' DPPH radical scavenging activity rapidly increased from 5 to 160 mg/mL in a dose-dependent manner. Findings indicated that dichloromethane extracts possessed the lowest antioxidant activity. Table 3 displays the total phenolic compound contents, which are expressed in mg EAG/g. Total phenolic compounds extracted from the samples significantly varied from each other. Methanol extracts showed higher phenolic contents than the others, followed by ethyl acetate and dichloromethane extracts.

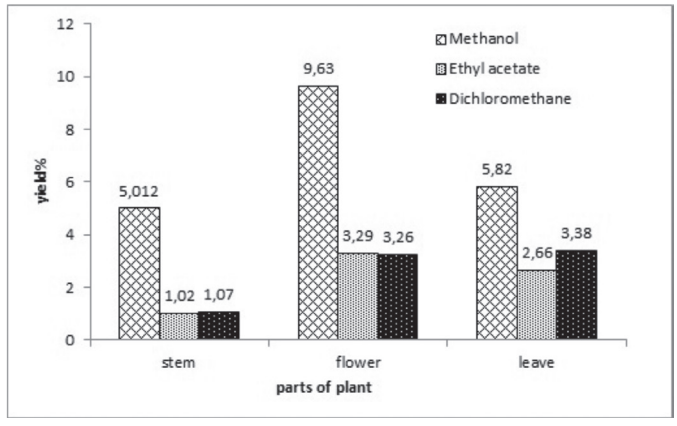

Figure 1. Extraction yields of different extracts from various parts of *Cleome coluteoides*

DISCUSSION

By extracting different parts of *C. coluteoides*, including leaves, flowers, and stems, with various types of solvent (methanol, dichloromethane, and ethyl acetate), plant parts were screened for antioxidant and antibacterial activities. Variation in the extract yields of the plant may be due to the various chemical natures of the compounds available in the leaves, barks and seeds may be the cause in the extract yield variation of the plant; polarity, solubility, concentration, pH, temperature, and nature of the extraction solvents also affects the extraction yields.[23] Hence, for the extraction of maximum amounts of potent antioxidant components from typical plant materials, a proper solvent system must be used.[24] On the one hand, secondary metabolites are produced by medicinal plants, which are responsible for their therapeutic properties. Moreover, environmental factors like geographical locations and plant

Table 1. Antifungal and antibacterial activities of dried extracts of *C. coluteoides* in disk and well diffusion method

Sample	Microorganism[a]						
	Bacillus cereus		*Staphylococcus aureus*		*Escherichia coli*	*Candida albicans*	*Fusarium solani*
	Disc	Well	Disc	Well	Disc and well	Disc and well	Disc and well
MES[b]	8.3±0.57	9.0±0.24	9.3±0.63	10.3±0.12	-[c]	-	-
MEF	10.0±0.14	10.0±0.28	10.3±0.74	11.3±0.37	-	-	-
MEL	14.3±0.24	10.0±0.47	12.0±0.52	6.0±0.35	-	-	-
EEF	18.0±0.89	15.0±0.16	6.0±0.41	6.0±0.21	-	-	-
EEL	15.3±0.43	11.0±0.38	11.3±0.14	11.6±0.26	-	-	-
DEF	15.0±0.16	11.6±0.37	6.0±0.21	6.0±0.14	-	-	-
DEL	16.3±0.35	11.3±0.41	6.0±0.16	10.0±0.12	-	-	-
Gentamycin	30.3±0.19	32.3±1.15	31.3±0.21	40.0±0.23	29.6±0.15	-	-
Nystatin	-		-		-	25.0±0.25	26±0.14

[a]: Antibacterial and antifungal activities of extract were evaluated by the presence or absence of inhibition zone based on zone diameters (mm), [b]: DEL: Dichloromethane extract of leaves, MEL: Methanol extract of leaves, EEL: Ethyl acetate extract of leaves, DEF: Dichloromethane extract of flower, MEF: Methanol extract of flower, EEF: Ethyl acetate extract of flower, DES: Dichloromethane extract of stem, MES: Methanol extract of stem, EES: Ethyl acetate extract of stem, [c]: Non-effective

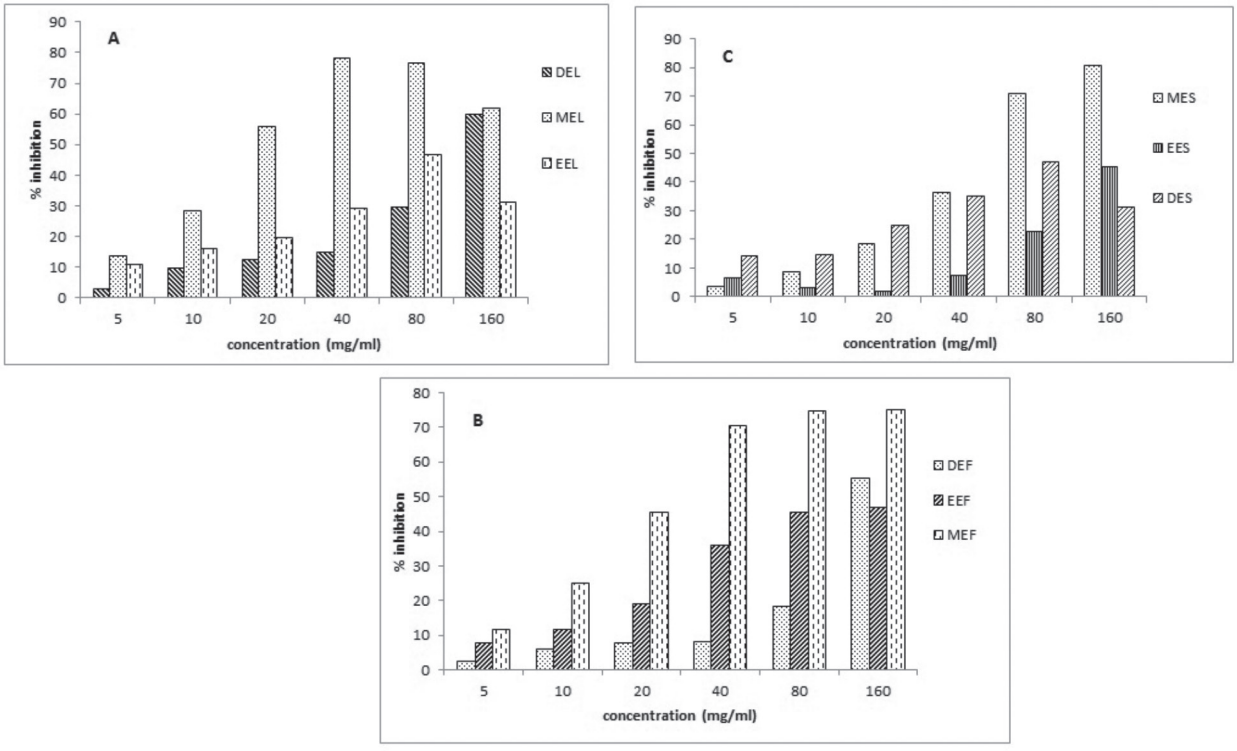

Figure 2. Radical scavenging activities of various extracts from different parts of *Cleome coluteoides*. (A) Leaves parts: DEL, dichloromethane extract; MEL, methanol extract; EEL, ethyl acetate extract. (B) flower parts: DEF, dichloromethane extract; MEF, methanol extract; EEF, ethyl acetate. (C) stem parts: DES, dichloromethane extract; MES, methanol extract; EES, ethyl acetate extract

origin affect the quality and quantity of these molecules and, conversely, their activities.[25] *C. coluteoides* extracts were found to be inactive against tested bacterial and fungal strains in the present study. In return, Gram-positive bacterial strains dedicated better resistance to the extracts. Antimicrobial functions of medicinal plants are reported from several parts of the world. Today, the World Health Organization has approved the use of herbs or their active ingredients in the traditional way.[26] As evidenced, methanol extract of *C. viscosa* exhibited the highest and significant antibacterial activity against seven bacterial strains.[27] Subsequently, ethanolic extract of *Cleome ciliata* had inhibitory effects against *S. aureus* and *Pseudomonas aeruginosa*; the tannin fraction was active only against *S. aureus*.[28] Antimicrobial test of *C. viscosa*'s methanolic extract displayed moderate sensitivity to the Gram-positive and Gram-negative bacteria. *Shigella sonnie* was recorded to

Table 2. Free radical scavenging activity and FRAP of different extracts from various parts of *Cleome coluteoides*[a]

Sample	FRAP (mmol Fe^{2}+/g extract)	DPPH IC_{50} (mg/mL)
MES[b]	-[c]	49.35±0.25
MEF	68.24±0.12	24.02±2.02
MEL	90.98±0.12	19.54±2.41
EES	59.44±0.18	58.45±3.48
EEF	81.03±0.19	157.25±1.49
EEL	-	159.33±1.64
DES	61.68±0.45	99.05±5.17
DEF	-	424.02±0.25
DEL	-	169.90±2.66
BHT[d]	14.32±0.58	0.40±0.03

[a]: Data are expressed as mean ± standard deviation, (n=3), [b]: DEL: Dichloromethane extract of leaves, MEL: Methanol extract of leaves, EEL: Ethyl acetate extract of leaves, DEF: Dichloromethane extract of flower, MEF: Methanol extract of flower, EEF: Ethyl acetate extract of flower, DES: Dichloromethane extract of stem, MES: Methanol extract of stem, EES: Ethyl acetate extract of stem, [c]: Non-effective, [d]: Positive control, FRAP: Ferric reducing antioxidant power, BHT: Butylated hydroxy toluene, DPPH: 1,1-diphenyl-2-picrylhydrazyl

Table 3. Total polyphenolics contents of different extracts from various parts of *Cleome coluteoides*[a]

Sample	Total polyphenols (mg GAE/g extract)
MES	14.81±0.15
MEF	24.58±0.35
MEL	23.27±0.14
EES	14.17±0.72
EEF	18.97±0.61
EEL	17.58±0.89
DES	5.24±0.57
DEF	15.87±0.45
DEL	5.66±0.36

[a]: Data are expressed as mean ± standard deviation, (n=3), DEL: Dichloromethane extract of leaves, MEL: Methanol extract of leaves, EEL: Ethyl acetate extract of leaves, DEF: Dichloromethane extract of flower, MEF: Methanol extract of flower, EEF: Ethyl acetate extract of flower, DES: Dichloromethane extract of stem, MES: Methanol extract of stem, EES: Ethyl acetate extract of stem, GAE: Gallic acid equivalent

have the highest inhibition zone (16.34 mm).[15] *C. viscosa*'s crude extracts presented antibacterial potency against *P. aeruginosa*.[5] Alkaloids and tannins were reported by other researchers to be present in *C. viscosa*, and are associated with antibacterial activity.[5]

DPPH and FRAP tests were the two methods used to evaluate the extracts' antioxidant activity. The antioxidants' potential to naturalize free radicals through reduction mechanisms are assessed by DPPH, which discolorates stable free radical DPPH of violet color to yellow.[29] DPPH scavengers is well known to have a wide range of biological functions such as lipid peroxidation inhibitory action and radioprotective.[30] There is a line of evidence that show that plants' antioxidant and pharmacological properties are usually associated with the presence of phenolic compounds and as electron donor agents.[31] In this study, a flower extracts' strong antioxidant activity is probably due to its phenolic contents.[21] Similarly, *C. gynandra*'s butanol fractions demonstrated remarkable anti-FRAP, -ABTS, and -DPPH activities. Moreover, *C. gynandra*'s best phenolic content was obtained with n-butanol fraction.[16] Soluble and stable iron complex, which can easily be excreted from the body, can be formed by phenolic and antioxidant compounds.[32] Table 2 summarizes the extracts' ferrous chelating activities (known as an important antioxidant mechanism). According to the results, methanol extract had greater chelating action because of its higher phenol contents. As indicated in Table 3, the total phenolic contents of various *C. coluteoides* extracts ranged from 5.24±0.57 to 24.58±0.35 mg GAE/100 g DW, and the highest content was found in MEF (24.58±0.35 g GAE/g DW). Furthermore, phenolic compounds were found in the following order: MEF › MEL › EEF › EEL › DEF › MES › EES › DEL › DES. Collectively, the phenolic contents in each sample were in agreement with the findings of DPPH. In keeping with our results, plant phenolics act as reducing agents and antioxidants through their hydroxyl groups' hydrogen-donating property.[33] Hence, antioxidant activity observed in this study could be explained by polyphenol contents. Thus, it can be concluded that the best solvent for *C. coluteoides*' antioxidant activity extraction was the methanol solvent. Our phenolic results of different plant parts reported greater amounts phenolics in the leaves than in the stem parts, which is in agreement with previous investigations.[34] A larger amount of phenolic and flavonoid in plant leaves might be the result of photosynthesis in this section.[35] Consistently, the highest amounts of total phenols in stem extracts of *C. gynandra* L. are determined in its aqueous extract.[36] The varied scavenging activity in different plant parts could be attributed to the presence of bioactive compounds such as phenolics, flavonoids, and tannins.[37] Previously, a strong correlation was observed between a plant extracts' radical scavenging power and total phenolic and flavonoid content.[24] The present results provided evidence that most extracts with high phenolic content exhibited greater potency to scavenge free radicals. Nevertheless, some extracts with less phenolic amounts depicted appreciable activity, which suggests that the presence of other secondary metabolites (carotenoids, volatile oils, and vitamins) may also contribute to the scavenging capacity.[38] Accordingly, in the current study MES had fewer phenolic amount than flowers, however, it exhibited greater antioxidant activity.[39,40] In general, our antioxidant and antibacterial activity results are consistent with other *Cleome* species-related studies mentioned earlier.[16]

CONCLUSION

This study demonstrates that different extracts from various parts of *C. coluteoides* have different antioxidant and antimicrobial effects. As indicated in the results, MEL possessed the highest antioxidant properties and EEF had the highest antimicrobial activities, which are probably correlated with total phenolics.

To characterize the antioxidant and antibacterial agents, phytochemical analysis on *C. coluteoides*' phytochemical should be conducted. This work demonstrates that extracting various parts of the plants with different solvents have variable antioxidant and antibacterial activities. To our knowledge, the antioxidant and antibacterial value of *C. coluteoides* were first revealed in this report.

ACKNOWLEDGMENTS

This study was financially supported by North Khorasan University of Medical Sciences, Bojnurd, Iran.

Conflicts of interest: No conflict of interest was declared by the authors. The authors alone are responsible for the content and writing of the paper.

REFERENCES

1. Venkatesh B, Dorai A. Antibacterial and antioxidant potential of white and pink nelumbo nucifera gaertn flowers. International Conference on Bioscience, Biochemistry and Bioinformatics. 2011;5:213-217.
2. Akyuz E, Şahin H, Islamoglu F, Kolayli S, Sandra P. Evaluation of phenolic compounds in tilia rubra subsp. caucasica by HPLC-UV and HPLC-UV-MS/MS. Int J Food Prop. 2014;17:331-343.
3. da Silva AP, Nascimento da Silva LC, Martins da Fonseca CS, de Araújo JM, Correia MT, Cavalcanti Mda S, Lima VL. Antimicrobial activity and phytochemical analysis of organic extracts from *Cleome spinosa* jaqc. Front Microbiol. 2016;7:1-10.
4. Oussalah M, Caillet S, Saucier L, Lacroix M. Inhibitory effects of selected plant essential oils on the growth of four pathogenic bacteria: E. coli O157:H7, *Salmonella Typhimurium*, *Staphylococcus aureus* and *Listeria monocytogenes*. Food Control. 2007;18:414-420.
5. Donkor AM, Gumah Bugri KM, Akugbire Atindaana E. Evaluation of Antibacterial Potentiation of Crude Extracts of *Phyllanthus amarus*, *Tamarindus indica* and *Cleome viscosa* and Their Formulation. Int J Plant Res. 2014;4:23-28.
6. Muhaidat R, Al-Qudah MA, Samir O, Jacob JH, Hussein E, Al-Tarawneh IN, Bsoul E, Abu Orabi ST. Phytochemical investigation and *in vitro* antibacterial activity of essential oils from *Cleome droserifolia* (Forssk.) *Delile* and *C. trinervia Fresen*. (Cleomaceae). S Afr J Bot. 2015;99:21-28.
7. Ladhari A, Omezzine F, DellaGreca M, Zarrelli A, Zuppolini S, Haouala R. Phytotoxic activity of *Cleome arabica* L. and its principal discovered active compounds. S Afr J Bot. 2013;88:341-351.
8. Motaal AA, Ezzat SM, Haddad PS. Determination of bioactive markers in *Cleome droserifolia* using cell-based bioassays for antidiabetic activity and isolation of two novel active compounds. Phytomedicine. 2011;19:38-41.
9. Shanmuganathan T, Karthikeyan AVP. Free radical scavenging activity of aqueous and ethanolic extracts of wild and L-arginine treated *Cleome gynandra L*. Int J Pharm Sci Res. 2014;5:346-349.
10. Parimaladevi B, Boominathan R, Mandal SC. Studies on analgesic activity of *Cleome viscosa* in mice. Fitoterapia. 2003;74:262-266.
11. Ding HY, Wu PS, Wu MJ. *Cleome rutidosperma* and *Euphorbia thymifolia* Suppress Inflammatory Response via Upregulation of Phase II Enzymes and Modulation of NF-κB and JNK Activation in LPS-Stimulated BV2 Microglia. Int J Mol Sci. 2016;17:1420.
12. Bose A, Mondal S, Gupta JK, Ghosh T, Si S, Debbhuti D. A study on antimicrobial activity of *Cleome rutidosperma* DC. Journal of Natural Remedies. 2007;7:132-134.
13. Abdel-Monem AR. A new alkaloid and a new diterpene from *Cleome paradoxa* B.Br. (Cleomaceae). Nat Prod Res. 2012;26:264-269.
14. Jordheim M, Andersen ØM, Nozzolillo C, Amiguet VT. Acylated anthocyanins in inflorescence of spider flower (*Cleome hassleriana*). Phytochemistry. 2009;70:740-745.
15. Bose U, Bala V, Nath Ghosh T, Gunasekaran K, Ayedur Rahman A. Antinociceptive, cytotoxic and antibacterial activities of *Cleome viscosa* leaves. Rev Bras Farmacogn. 2011;21:165-169.
16. Meda NTR, Bangou MJ, Bakasso S, Millogo-Rasolodimby J, Nacoulma OG. Antioxidant activity of phenolic and flavonoid fractions of *Cleome gynandra* and *Maerua angolensis* of Burkina Faso. J Appl Pharm Sci. 2013;3:36-42.
17. Singh H, Mishra A, Kumar Mishra A. *Cleome viscosa* Linn (Capparaceae): A Review. Pharmacogn J. 2015;7:326-329.
18. Sridhar KR, Rajeev B. Lotus - A potential nutraceutical source. J Agri Tech. 2007;3:143-155.
19. Baskaran C, Ratha bai V, Velu S, Kumaran K. The efficacy of Carica papaya leaf extract on some bacterial and a fungal strain by well diffusion method. Asian Pac J Trop Dis. 2012;2:658-662.
20. Kamali M, Khosroyar S, Mohammadi A. Antibacterial activity of various extracts from Dracocephalum kotschyi against food pathogenic microorganisms. Int J PharmTech Res. 2015;8:158-163.
21. Kamali H, Ahmadzadeh Sani T, Mohammadi A, Alesheikh P, Khodaverdi E, Hadizadeh F. A comparison between pressurized hot water and pressurized liquid extraction for optimizing phenolic and antioxidants capacity of the wooden layer between of walnut seed. J Supercrit Fluid. 2018;133:535-541.
22. Eslami A, Roghani K, Mohammadi A. *In vitro* antioxidant potential of *polygonum convolvulus* extracts. Plant Archives. 2017;17:267-270.
23. Roselló-Soto E, Martí-Quijal FJ, Cilla A, Munekata PES, Lorenzo JM, Remize F, Barba FJ. Influence of Temperature, Solvent and pH on the Selective Extraction of Phenolic Compounds from Tiger Nuts by-Products: Triple-TOF-LC-MS-MS Characterization. Molecules. 2019;24:797-810.
24. Namvar K, Mohammadi A, Ataei Salehi E, Feyzi P. Evaluation of Solvent Effect (Methanol: Water Mixture) on the Phenolic Content and Antioxidant Activities of *Stachys turcomanica Trautv*. J Pharm Sci. 2017;23:244-248.
25. Ullah N, Khurram M, Usman Amin M, Khan TA, Umar Khayyam S, Khan FA, Najeeb U, Ullah S. Impact of geographical locations on Mentha spicata antibacterial activities. J Med Plants Res. 2012;6:1201-1206.
26. Bhalodia NR, Shukla VJ. Antibacterial and antifungal activities from leaf extracts of *Cassia fistula* l.: An ethnomedicinal plant. J Adv Pharm Technol Res. 2011;2:104-109.
27. Saradha JK, Rao BS. 2010. *In vitro* antibacterial activity of *Cleo me viscosa* Linn. Int J Pharm Sci. 2011;1:71-78.
28. Umerie SC, Okorie NH, Ezea SC, Okpalaononuju AN. Antibacterial screening and phytochemical analysis of *Cleome ciliate* (capparidaceae) leaves. Int J Curr Res Rev. 2012;4:1-10.
29. Brand-Williams W, Cuvelier ME, Berset C. Use of a free-radical method to evaluate antioxidant activity. Food Sci Technol. 1995;28:25-30.

30. Rahman MM, Islam MB, Biswas M, Khurshid Alam AHM. *In vitro* antioxidant and free radical scavenging activity of different parts of *Tabebuia pallida* growing in Bangladesh. BMC Res Notes. 2015;8:621-630.

31. Gülçin İ. Antioxidant activity of food constituents: an overview. Arch Toxicol. 2012;86:345-391.

32. Faa G, Crisponi G. Iron chelating agents in clinical practice. Coord Chem Rev. 1999;184:291-310.

33. Aberoumand A, Deokule SS. Comparison of phenolic compounds of some edible plants of Iran and India. Pakistan J Nut. 2008;7:582-585.

34. Karimi E, Jaafar HZE, Ahmad S. Phenolics and flavonoids profiling and antioxidant activity of three varieties of Malaysian indigenous medicinal herb Labisia pumila Benth. J Med Plant Res. 2011;5:1200-1206.

35. Silva EM, Souza JNS, Rogez H, Rees JF, Larondella Y. Antioxidant activities and polyphenolic contents of fifteen selected plant species from the Amazonian region. Food Chem. 2006;101:1012-1018.

36. Essou JIL, Zanklan AS, Adomou AC, Assogba F. Studies on Phytochemistry and Antioxidant Potential of *Cleome Gynandra* L. (Capparidaceae) Collected from Contrasted Agro-Ecological Zones in Benin. Eur J Sci Res. 2017;147:251-274.

37. Ghimire BK, Seong ES, Kim EH, Ghimeray AK, Yu CY, Ghimire BK, Chung IM. A comparative evaluation of the antioxidant activity of some medicinal plants popularly used in Nepal. J Med Plants Res. 2011;5:1884-1891.

38. Yingming P, Ying L, Hengshan W, Min L. Antioxidant activities of several Chinese medicinal herbs. Food Chem. 2004;88:347-350.

39. Odabasoglu F, Aslan A, Cakir A, Suleyman H, Karagoz Y, Bayir Y, Halici M. Antioxidant activity, reducing power and total phenolic content of some lichen species. Fitoterapia. 2005;76:216-219.

40. Moghaddam PZ, Mohammadi A, Feyzi P, Alesheikh P. In vitro antioxidant and antibacterial activity of various extracts from exocarps and endocarps of walnut. Pak J Pharm Sci. 2017;30:1725-1731.

Turk J Pharm Sci 2021;18(1):17-20
DOI: 10.4274/tjps.galenos.2019.24993

ORIGINAL ARTICLE

Effect of *Panax ginseng* on Carbamazepine Pharmacokinetics in Rabbits

Panax ginseng'in Tavşanlarda Karbamazepin Farmakokinetiğine Etkisi

Issam Mohammed ABUSHAMMALA[1]*, Fatma Khaled EL-SHAIKH ALI[1], Kamal Fakher ABU SHAMMALEH[1], Mohammed Mahmoud TAHA[1], Mohammed Yousef MIQDAD[2]

[1]Al-Azhar University Faculty of Pharmacy, Department of Pharmaceutics and Industrial Pharmacy, Gaza Strip, Palestine
[2]Al-Azhar University-Gaza, College of Dentistry, Gaza Strip, Palestine

ABSTRACT

Objectives: Carbamazepine (CBZ) is a well-known drug prescribed to treat epilepsy and the preferred drug for trigeminal neuralgia. This study was conducted to investigate the effect of *Panax ginseng* extract (PGE) on the disposition of CBZ, a CYP3A4 substrate, in rabbits.

Materials and Methods: An *in vivo* randomized parallel design was used to examine herb-drug interactions in 12 male rabbits distributed into 2 groups. In the 1st group (control group), 6 rabbits (control group) were administered orally with CBZ suspension (30 mg/kg/day) as a single daily dose for 10 days. In the 2nd group (test group), 6 rabbits was treated concomitantly with CBZ and a dose of PGE (2.5 mg/kg/day) at the same time as in the 1st group. Blood samples were withdrawn from the marginal ear vein of the rabbits at intervals of 0.0, 0.5, 1.0, 1.5, 2.0, 2.5, 3.0, 4.0, 6.0, 12.0, and 24.0 h.

Results: CBZ had no significantly different pharmacokinetic (PK) parameters, namely, C_{max}, t_{max}, AUC_{0-24}, $AUC_{0-\infty}$, $t_{½}$, and K_e, when it was given alone or concurrently with PGE ($p \geq 0.05$).

Conclusion: PGE may unlikely interfere with the PK of CBZ when it is co-administered with CBZ. Therefore, PGE can be used safely without precautions or dose monitoring.

Key words: Carbamazepine, *Panax ginseng*, CYP3A4, drug interaction, pharmacokinetics

ÖZ

Amaç: Karbamazepin (CBZ), epilepsiyi tedavi etmek için reçete edilen, bilinen ve trigeminal nevraljide tercih edilen ilaçtır. Bu çalışma, *Panax ginseng* ekstresinin (PGE) tavşanlarda bir CYP3A4 substratı olan CBZ'nin dağılımı üzerindeki etkisini araştırmak için yapılmıştır.

Gereç ve Yöntemler: Bitki-ilaç etkileşimini incelemek için 12 erkek tavşan *in vivo* rastgele paralel bir tasarım kullanılarak 2 gruba ayrıldı. Birinci gruptaki 6 tavşana (kontrol grubu) 10 gün süreyle günde tek doz CBZ süspansiyonu (30 mg/kg/gün) oral yoldan uygulandı. İkinci gruptaki 6 tavşana (test grubu), 1. grupla eş zamanlı olarak CBZ ve bir doz PGE (2,5 mg/kg/gün) birlikte uygulandı. Uygulamayı takiben tavşanların kulak marjinal venlerinden 0,0, 0,5, 1,0, 1,5, 2,0, 2,5, 3,0, 4,0, 6,0, 12,0 ve 24,0. saatlerde kan örnekleri alındı.

Bulgular: Tek başına veya PGE ile birlikte verildiğinde CBZ'nin, C_{maks}, t_{maks}, AUC_{0-24}, $AUC_{0-\infty}$, $t_{½}$ ve K_e gibi farmakokinetik (PK) parametreleri arasında farklılık saptanmadı ($p \geq 0,05$).

Sonuç: PGE, CBZ ile birlikte uygulandığında, CBZ'nin PK parametreleri etkilenmeyecektir. Bu nedenle PGE, önleme gerek olmadan veya doz takibi yapılmadan güvenle kullanılabilir.

Anahtar kelimeler: Karbamazepin, *Panax ginseng*, CYP3A4, ilaç etkileşimi, farmakokinetik

***Correspondence:** issam.abushammala@uv.es, **Phone:** +00970599019757 **ORCID-ID:** orcid.org/0000-0002-3371-4718
Received: 29.06.2019, **Accepted:** 21.11.2019

INTRODUCTION

Carbamazepine (CBZ) is a well-known drug prescribed to treat epilepsy, trigeminal neuralgia, and bipolar depression.[1,2] The present study is performed to investigate the effect of *Panax ginseng* extract (PGE) on the disposition of CBZ, the substrate of CYP3A4, in rabbits.

CBZ has several properties involved in clinical interactions with co-administered drugs, herbs, and food.[3,4] It has a narrow therapeutic index.[5] It is a constructive inducing enzyme of several cytochrome P450 (CYP450) isoenzymes and subject to autoinduction.[3,6]

CBZ-10,11-epoxide (CBZ-E) is the active metabolite of CBZ whose concentration may be modified by concomitant drugs. It is mostly prescribed in codrug features because of its widespread and long-term use, thereby inducing drug interactions.[4]

Drug interactions are often classified as either pharmacokinetic (PK) or pharmacodynamic interactions.[7] The most tangible interactions that affect the PK of CBZ include those influencing its metabolic rate.[5] CBZ is mainly metabolized in the liver through oxidation catalyzed by the CYP450 3A4 enzyme, and less than 5% of CBZ becomes excreted and remains unchanged in urine.[4,8-10] CBZ-E is the major (up to 80%) active metabolite of CBZ, which is further metabolized before excretion through hydration to a trans-dihydrodiol (CBZ-diol).[4,11] CBZ is a substrate of CYP450 3A4 and inducer of its enzymatic activity.[8,11] It can induce its own metabolism[4,9] through autoinduction, which is a time- and dose-dependent process.[12] The inhibition or induction of CYP450 enzymes significantly influences drug interactions that can cause unpredictable adverse effects or even therapeutic failures.[13] Herb-drug interactions are expected, thereby eliciting various clinical effects. Moreover, the increased popularity of herbal medicines can explain the high incidence of herb-drug interactions.[14] These interactions can occur when the co-administered herbal preparations modulate drug metabolism either to be induced or inhibited by specific CYP enzymes.[15,16] CBZ-herb interactions are important and have been widely explored, especially when herbs affect the same enzymes involved in CBZ metabolism.[17]

PGE is one of the most popular and widely available herbal supplements.[18,19] It is mainly used as an adaptogenic, antineoplastic, immunomodulating, cardiovascular, CNS, endocrine, antiinflammatory, antioxidant, antineurological, and hypoglycemic agent.[20] Several studies have shown that PGE induces the activity of CYP3A4 in the liver and gastrointestinal tract.[21,22] Moreover, ginsenoside (an active compound in PGE) induces the CYP3A4 activity *in vitro* by interacting with CBZ, resulting in an increased CBZ metabolism.[14] The present *in vivo* research aims to determine the possible herb–drug interactions between PGE and CBZ disposition.

MATERIALS AND METHODS

Animals and study design

Twelve healthy male rabbits weighing 3200-3500 g were bought from Assdda Animal Center (Gaza, Palestine). Clinical tests and follow-up care were performed. The rabbits were subjected to fasting for 12 h and given free access to water before they were treated. The study was carried out at the AUG Faculty of Pharmacy, Gaza, Palestine.

An *in vivo* herb-drug interaction study between CBZ and PGE was conducted in healthy male rabbits. Experiments were carried out in 1 period, and 2 groups of male rabbits were used. The first group of 6 rabbits was given a single oral dose of CBZ (30 mg/kg/day) from an oral suspension of CBZ (Tegretol®), and the 2nd group of 6 rabbits was administered with the same volume of CBZ suspension combined with a single oral dose of PGE (2.5 mg/kg/day) prepared in laboratories via a special oral gavage for 10 days. CBZ oral suspension and PG capsules were purchased from private pharmacies. The dose was given to each rabbit via oral gavage by placing the drug in a corner of the rabbit's mouth, and the suspension was pushed down at a slow rate to prevent choking. Physical tests were subsequently carried out to assess clinical safety.

Blood sample collection

The hair on the rabbits' ear was removed as the marginal ear vein was located. Local anesthetic (4% lidocaine) was used to prevent the jerking of the rabbits. An IV cannula was installed in the marginal ear vein of each rabbit. Then, 1 mL of blood sample was collected in vacutainer tubes at the following time points: 0.0, 0.5, 1.0, 1.5, 2.0, 2.5, 3.0, 4.0, 6.0, 12.0, and 24.0 h after the last dose was received. Blood samples were centrifuged at 3,000 rpm for 5 min, and serum was separated, collected into clean tubes, and kept at 2°C-8°C for analysis within 24 h.

Analysis of CBZ serum samples

CBZ blood concentrations were assayed via a chemiluminescent immunoassay by using an ARCHITECT analyzer (1000 Abbott Laboratories, Abbott Park, IL, USA).

Pharmacokinetic analysis

The following PK parameters of both groups were determined: C_{max}, t_{max}, AUC_{0-t}, $AUC_{0-\infty}$, $t_{1/2}$, and K_e. C_{max} and t_{max} were directly identified from the plasma concentration versus time curves. AUC_{0-24} was calculated in accordance with the linear trapezoidal rule by using the following equation: $AUC_{0-\infty}=AUC_{0-24} + Ct/K_e$, where Ct is the last measured serum concentration at time t, and K_e is the elimination rate constant. K_e was determined via the least squares regression of plasma concentration-time data points in the terminal region by considering the semilogarithmic dependence that corresponds to first-order kinetics. $t_{1/2}$ was calculated as $0.693/K_e$. PK analysis was conducted via an independent model method (non-compartmental approach) in WinNonlin version 6.3 (Pharsight Corporation, Cary, NC) and GraphPad Prism version 4.00 (San Diego, CA, USA).

Statistical analysis

Statistical methods, including descriptive analysis and Mann-Whitney U test, were applied to compare the PK parameters of CBZ alone or with PGE. SPSS version 16.0 was applied to analyze data. Data were considered significantly different when $p \leq 0.05$.

RESULTS

The plasma concentration versus time profiles and PK parameters of CBZ (Figure 1) were compared after it was administered alone (control group) and combined with PGE (test group). The significant results of their comparison are given in Table 1.

DISCUSSION

CYP3A4 is one of the major CYP enzymes catalyzing 50% of drug metabolism[23,24] and participating in the metabolism of CBZ, so any drug affecting CYP3A4 has the potential to cause a drug interaction with CBZ.[4] Several popular herbs have been considered strong candidates for interactions with medicinal drugs. Therefore, herb-CYP interactions may have significant clinical and toxicological consequences.[15]

The plasma profiles of CBZ are illustrated in Figure 1. AUC_{0-24} and $AUC_{0-\infty}$ apparently decreased after the concomitant administration of CBZ with PGE, but this change was not statistically significant ($p \geq 0.05$). The other PK parameters of both groups were also not altered significantly after PGE administration. The mean C_{max} of the control group slightly decreased compared with that of the test group ($p=0.53$). Despite the decreased half-life ($t_{1/2}$) from 26.51±25.79 h to 16.99±8.58 h in the control and test groups, respectively, their differences were not statistically significant ($p=0.24$).

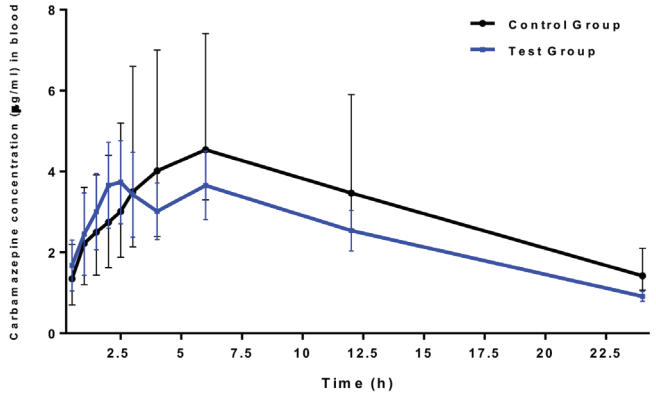

Figure 1. Plot of the mean serum concentration-time profile of CBZ alone (control group) and co-treatment with PGE (2.5 mg/kg/day; test group)
CBZ: Carbamazepine, PGE: *Panax ginseng* extract

PGE is an herbal medicine used worldwide for a variety of purposes.[25] With complicated PK and pharmacodynamics, PGE may pose a significant risk for patients once it is taken synchronously with other medications through PGE-drug interactions.[26]

Possible drug interactions have been reported between PGE and warfarin, phenelzine, and alcohol.[19,25] CBZ may reduce the blood concentrations of warfarin and induces mania if it is used synchronously with phenelzine.[27]

Similarly, Abushammala[17] found that valerian does not alter the PK parameters of CBZ in rabbits and concluded that CBZ can be used safely with valerian preparations. Moreover, clinical trials have shown that American ginseng does not significantly affect the PK of indinavir and zidovudine. No significant differences in the AUC of the plasma concentration versus time relationship are observed after the co-administration of American ginseng compared with that after either zidovudine or indinavir is administered alone.[28,29] Despite the stimulating effect of PGE on the CYP3A4 activity, the PK parameters of CBZ do not significantly affect healthy rabbits after the combined administration.

CONCLUSION

Under the experimental conditions, CBZ and PGE can be used safely without precautions or dose monitoring. However, more studies on humans should be designed to confirm our obtained results. Further research should also be performed by setting

Table 1. Pharmacokinetic parameters of CBZ alone and with PGE in healthy male rabbits (6 rabbits for each group)

PK parameter	Group	N	Mean ± SD	Median ± IQR	p value
C_{max}	CBZ alone	6	4.66±1.44	4.31±1.69	0.818
	CBZ + PGE	6	4.16±0.95	4.14±1.83	
t_{max}	CBZ alone	6	5.33±1.03	6.00±2.00	0.394
	CBZ + PGE	6	4.08±2.11	4.25±4.00	
$t_{1/2}$	CBZ alone	6	30.35±18.81	26.51±25.79	0.240
	CBZ + PGE	6	17.51±4.45	16.99±8.59	
K_e	CBZ alone	6	0.03±0.02	0.03±0.02	0.240
	CBZ + PGE	6	0.04±0.01	0.04±0.01	
AUC_{0-24}	CBZ alone	6	71.22±25.04	63.63±26.85	0.394
	CBZ + PGE	6	57.41±10.58	61.06±19.56	
$AUC_{0-\infty}$	CBZ alone	6	120.56±64.65	92.76±113.89	0.132
	CBZ + PGE	6	80.29±12.25	82.48±19.13	

CBZ: Carbamazepine, PGE: *Panax ginseng* extract, PK: Pharmacokinetic, SD: Standard deviation, IQR: Interquartile range

higher PGE doses, a longer treatment duration, and a larger sample size.

ACKNOWLEDGMENT

The authors would like to thank the staff of the Faculty of Pharmacy at AUG for providing support and help and Mr. Mohamed Abu Affash, the director of MRS-Gaza, for facilitating the analysis at the laboratory of their institution.

Conflicts of interest: No conflict of interest was declared by the authors. The authors alone are responsible for the content and writing of the paper.

REFERENCES

1. Bertilsson L, Tomson T. Clinical pharmacokinetics and pharmacological effects of carbamazepine and carbamazepine-10,11-epoxide. An update. Clin Pharmacokinet. 1986;11:177-198.
2. Whalen K, Finkel R, Panavelil TA. Lippincott illustrated reviews: pharmacology, 6th ed. Wolters Kluwer; 2015:158-163.
3. Patsalos PN, Fröscher W, Pisani F, van Rijn CM. The importance of drug interactions in epilepsy therapy. Epilepsia. 2002;43:365-385.
4. Spina E, Pisani F, Perucca E. Clinically significant pharmacokinetic drug interactions with carbamazepine. An update. Clin Pharmacokinet. 1996;31:198-214.
5. Pynnönen S, Mäntylä R, Iisalo E. Bioavailability of four different pharmaceutical preparations of carbamazepine. Acta Pharmacol Toxicol (Copenh). 1978;43:306-310.
6. Guengerich FP. Reactions and significance of cytochrome P-450 enzymes. J Biol Chem. 1991;266:10019-10022.
7. Bailie GR, Johnson CA, Mason NA, Peter W. Medfacts pocket guide of drug Interactions, 2nd ed. Verona, USA; Nephrology Pharmacy Associates Inc; 2004;3-7.
8. Ayano G. Bipolar disorders and carbamazepine: Pharmacokinetics, pharmacodynamics, therapeutic effects and indications of carbamazepine: review of articles. J Neuropsychopharmacol Ment Health. 2016;1:112.
9. Panday DR, Panday KR, Basnet M, Kafle S, Shah B, Rauniar GP. Therapeutic drug monitoring of carbamazepine. Int J Neurorehabil. 2017;4:245.
10. Tolou-Ghamari Z, Zara M, Habibabad JM, Najafi MR. A quick review of carbamazepine pharmacokinetics in epilepsy from 1953 to 2012. J Res Med Sci. 2013;18(Suppl 1):S81-85.
11. Larkin JG, McLellan A, Munday A, Sutherland M, Butler E, Brodie MJ. A double-blind comparison of conventional and controlled-release carbamazepine in healthy subjects. Br J Clin Pharmacol. 1989;27:313-322.
12. Rapeport WG. Factors influencing therelationship between carbamazepine plasma concentration and its clinical effects in pationts with epilepsy. Clin Neuropharmacol. 1985;8:141-149.
13. Lynch T, Price A. The effect of cytochrome P450 metabolism on drug response, interactions and adverse effects. Am Fam Physician. 2007;76:391-396.
14. Fong SYK, Gao Q, Zuo Z. Interaction of carbamazepine with herbs, dietary supplements, and food: A systematic review. Evid Based Complement Alternat Med. 2013;2013:898261.
15. Delgoda R, Westlake AC. Herbal interactions involving cytochrome P450 enzymes: a mini review. Toxicol Rev. 2004;23:239-249.
16. Hellum BH, Hu Z, Nilsen OG. The induction of CYP1A2, CYP2D6 and CYP3A4 by six trade herbal products in cultured primary human hepatocytes. Basic Clin Pharmacol Toxicol. 2007;100:23-30.
17. Abushammala I. The effect of valerian on the pharmacokinetics of carbamazepine in healthy rabbits. International Journal of Pharmaceutical Sciences and Research. 2014;9:3641-3645.
18. Seervi CH, Kirtawade R, Dhabale P, Salve P. Ginseng- multipurpose herb. J Biomed Sci Res. 2010;2:6-17.
19. Radad KH, Gille G, Rausch WD. Use of ginseng in medicine: Perspectives on CNS disorders. Iranian J Pharmacol Ther. 2004;3:30-40.
20. Kim J, Cho SY, Kim SH, Kim S, Park CW, Cho D, Seo DB, Shin SS. Ginseng berry and its biological effects as a natural phytochemical. Nat Prod Chem Res. 2016;4:209.
21. Hao M, Ba Q, Yin J, Li J, Zhang R, Wang H. Deglycosylated ginsenosides are more potent inducers of CYP1A1, CYP1A2 and CYP3A4 expression in HepG2 cells than glycosylated ginsenosides. Drug Metab Pharmacokinet. 2011;26:201-205.
22. Malati CY, Robertson SM, Hunt JD, Chairez C, Alfaro RM, Kovacs JA, Penzak SR. Influence of *Panax ginseng* on cytochrome P450 (CYP)3A and P-glycoprotein (P-gp) activity in healthy participants. J Clin Pharmacol. 2012;52:932-939.
23. Anzenbacher P, Anzenbacherova E. Cytochromes P450: Review on their basic principles. Proc Indian Natn Sci Acad. 2003;6:883-991.
24. Fasinu PS, Bouic PJ, Rosenkranz B. An Overview of the evidence and mechanisms of herb-drug interactions. Front Pharmacol. 2012;3:69.
25. Lakshmi T, Anitha R, Geetha RV. *Panax ginseng* a universal panacea in the herbal medicine with diverse pharmacological spectrum -a review. Asian Journal of Pharmaceutical and Clinical Research. 2011;4:14-18.
26. Qi LW, Wang CZ, Du GJ, Zhang ZY, Calway T, Yuan CS. Metabolism of ginseng and its interactions with drugs. Curr Drug Metab. 2011;12:818-822.
27. Izzo AA, Ernst E. Interactions between herbal medicines and prescribed drugs: a systematic review. Drugs. 2001;61:2163-2175.
28. Andrade AS, Hendrix C, Parsons TL, Caballero B, Yuan CS, Flexner CW, Dobs AS, Brown TT. Pharmacokinetic and metabolic effects of American ginseng (Panax quinquefolius) in healthy volunteers receiving the HIV protease inhibitor indinavir. BMC Complement Altern Med. 2008;8:50.
29. Lee LS, Wise SD, Chan C, Parsons TL, Flexner C, Lietman PS. Possible differential induction of phase 2 enzyme and antioxidant pathways by American ginseng, Panax uinquefolius. J Clin Pharmacol. 2008;48:599-609.

Turk J Pharm Sci 2021;18(1):21-27
DOI: 10.4274/tjps.galenos.2019.71300

ORIGINAL ARTICLE

A Synbiotic Mixture Ameliorates Depressive Behavior Induced by Dexamethasone or Water Avoidance Stress in a Mouse Model

Fare Modelinde Deksametazon ile İndüklenen Depresif Davranışı veya Sudan Kaçınma Stresini İyileştiren Sinbiyotik Bir Karışım

Azadeh MESRIPOUR*, Pooya RAKHSHANKHAH

Isfahan University of Medical Sciences, School of Pharmacy and Pharmaceutical Sciences, Department of Pharmacology and Toxicology, Isfahan, Iran

ABSTRACT

Objectives: Disruption of the hypothalamic-pituitary-adrenal axis by stress and glucocorticoid drugs is a major cause of depression. The benefits of probiotics may extend to systems beyond the gastrointestinal tract, i.e., the central nervous system. Therefore, the effect of a synbiotic (probiotic + prebiotic) mixture on dexamethasone (Dex) and stress-induced depression was investigated.

Materials and Methods: Male albino mice were used, the forced swimming test (FST) measured despair, and the sucrose preference test measured anhedonia. The synbiotic regimen ($12.5x10^6$ CFU) was supplemented in drinking water for 7 days. Dex was administered subcutaneously either in a single dose on the test day or for 7 days. Water avoidance stress (WAS) was induced for 1 hour each day for 4 days.

Results: Drinking the synbiotic reduced immobility time during the FST (54±7 sec vs. 111±6 sec in the control water group, $p<0.001$). Dex injection significantly increased the immobility time (single dose: 166±6 sec and 7 days: 174±9 sec) compared with the control groups, while adding the synbiotic to their drinking water reduced it (single dose: 81±6.6 sec, and 7 days: 84±14 sec), indicating that the synbiotic reversed Dex-induced depression. WAS increased the immobility time (148±11 sec vs. sham 99±6 sec, $p<0.001$) in the FST test. When the synbiotic treatment was added following WAS, the immobility time decreased (81±6.5 sec). The synbiotic groups also had a higher sucrose preference percentage.

Conclusion: The synbiotic mixture prevented the effects of WAS, acute or sub-acute Dex-induced depression in mice. Therefore, probiotics might be useful and safe supplements to prevent depression related to stress or glucocorticoid therapies, a phenomenon that deserves further evaluation.

Key words: Probiotics, depression, forced swimming test, glucocorticoid, stress

ÖZ

Amaç: Hipotalamik-hipofiz-adrenal eksenin stres ve glukokortikoid ilaçlarla bozulması, depresyonun başlıca nedenidir. Probiyotiklerin faydaları, gastrointestinal sistemin ötesindeki sistemlere, yani merkezi sinir sistemine kadar uzanabilir. Bu nedenle, bir sinbiyotik (probiyotik + prebiyotik) karışımın deksametazon (Dex) ve stres kaynaklı depresyon üzerindeki etkisi araştırıldı.

Gereç ve Yöntemler: Erkek albino fareler kullanıldı, zorlu yüzme testi (FST) umutsuzluğu, sükroz tercih testi ise anhedoniyi ölçmek için kullanıldı. Sinbiyotik rejim ($12,5x10^6$ CFU), içme suyunda 7 gün süreyle verildi. Dex, subkutan yollan test gününde tek doz olarak veya 7 gün süreyle uygulandı. Sudan kaçınma stresi (WAS) 4 gün boyunca her gün 1 saat süreyle indüklendi.

Bulgular: Sinbiyotik içilmesi FST'de hareketsizlik süresini azalttı (kontrol su grubunda 54±7 sn'ye karşılık 111±6 sn, $p<0,001$). Dex enjeksiyonu, kontrol gruplarına kıyasla hareketsizlik süresini (tek doz: 166±6 sn ve 7 gün: 174±9 sn) önemli ölçüde artırırken, sinbiyotiklerin içme suyuna eklenmesi ise hareketsizlik süresini azalttı (tek doz: 81±6,6 sn ve 7 gün: 84±14 sn). Bu, sinbiyotik uygulamasının Dex kaynaklı depresyonu tersine çevirdiğini gösterdi. WAS, FST testinde hareketsizlik süresini (148±11 sn karşı sham grubunda 99±6 sn, $p<0,001$) artırmıştır. WAS'nin ardından sinbiyotik tedavi eklendiğinde, hareketsizlik süresi azaldı (81±6,5 saniye). Sinbiyotik gruplar ayrıca daha yüksek bir sükroz tercih yüzdesine sahipti.

Sonuç: Sinbiyotik karışım, farelerde WAS'nin etkilerini, akut veya subakut Dex kaynaklı depresyonu önlemiştir. Bu nedenle probiyotikler, stres veya glukokortikoid tedavileriyle ilişkili depresyonu önlemek için yararlı ve güvenli takviyeler olarak daha fazla değerlendirmeyi hak etmektedirler.

Anahtar kelimeler: Probiyotikler, depresyon, zorlu yüzme testi, glukokortikoid, stres

***Correspondence:** a_mesripour@yahoo.com, **Phone:** +00983137927089 **ORCID-ID:** orcid.org/0000-0003-3150-5581

Received: 25.09.2019, **Accepted:** 28.11.2019

INTRODUCTION

Probiotics are defined as "living microorganisms, which when administered in adequate amounts induce beneficial effects on the host".[1] Gut bacterial microorganisms are present as 2 dominant phyla, *Bacteroidetes* and *Firmicutes*,[1] while *Bifidobacteria*, *Lactobacillus,* and *Bacteroides* types represent the most important beneficial probiotics.[2] Various lines of evidence suggest that probiotics have therapeutic importance in the treatment of several gastrointestinal (GI) disorders, such as inflammatory bowel disease, diarrhea, and irritable bowel syndrome.[3] More recently, it has been advocated that the effects of probiotic bacteria may extend to systems beyond the GI tract, i.e., central nervous system (CNS) disorders.[4,5] Animal studies have also suggested that probiotics could have a modulating role in neuroendocrine and neurochemical responses outside the gut.[6] In animal depression models, probiotic treatment has proved beneficial. Species of the genus *Lactobacillus* are especially considered to have an antidepressant effect.[7] *Bifidobacterium infantis* relieved depression in rat models of depression, probably via reduction of proinflammatory cytokines and regulation of tryptophan metabolism and CNS neurotransmitters.[6,8] Prebiotics, such as oligosaccharides, stimulate the proliferation of non-pathogenic intestinal microflora. It has been proven that prebiotics also have neurotropic effects by increasing brain-derived neurotropic factor expression in rats, probably via gut hormones.[9]

The microbiome-gut-brain axis refers to the connection that exists between the intestinal microbiota, the gut, and the CNS.[10,11] Additionally, research documents suggest that alteration of the gut microflora in mice affects the hypothalamic-pituitary-adrenal (HPA) axis reaction to stress[12,13] and anxiety behavior.[14] Probiotics (*L. rhamnosus* and *L. helveticus*) not only prevented the elevation of serum corticosterone and the increase in HPA axis activity following maternal separation in rats but also prevented depressive behavior. That is to say, probiotic organisms can adjust HPA axis dysregulation induced by early life stress.[15] The importance is that there is high comorbidity between GI functional illnesses and stress-related psychiatric illnesses, such as anxiety and depression.[16] On the other hand, pathogenic bacteria in rodents could cause anxiety-like behaviors, mediated through the vagal afferent nerves.[17]

Depression is often related to stress, possibly because a hypersensitive HPA axis results in chronically elevated cortisol levels as well as cortisol release in response to lower levels of stress.[18] Synthetic glucocorticoids (GC) are widely used to treat various allergic, inflammatory, and autoimmune disorders. These drugs may induce adverse psychiatric effects (also known as steroid-induced psychosis), including depressed mood.[19] Furthermore, administration of dexamethasone (Dex) and corticosterone have produced depression-like behaviors in animal models.[20,21] Previously, the antidepressant effects of a synbiotic [synonym (Syn); probiotic + prebiotic] mixture was proved in an animal model of depression.[22] The mixture was chosen on the basis that *Lactobacilli* and *Bifidobacteria* have antidepressant effects in animal studies; therefore, a manufactured, premixed product was chosen that comprised these genera and also a prebiotic, fructooligosaccharides.

GCs and stressful life events are risk factors for developing major depression, which is strongly linked to impairments in the HPA axis and serotonin (5-HT) neurotransmission; conversely, the beneficial effects of probiotics on the 5-HT system and HPA axis has been proven.[6,15] The primary aim of the following study was to induce depression in mice with a single dose or multiple doses of Dex and then to verify the effect of the Syn cocktail on depressive behavior. The secondary aim was to induce depression with stress in mice and ultimately verify the effect of the Syn cocktail on depressive behavior.

MATERIALS AND METHODS

Animals

Male albino mice weighing 25±2 g were housed at room temperature 23˚C±2˚C with free access to standard rodent chow and treated or untreated drinking water per the experiment, on a 12-12 h light-dark cycle (lights on at 6 am). Six animals were housed in each cage, and 24 h before the test they were placed in the experimental room for acclimatization. The total number of animals used, was 72, divided in 12 groups of animals each containing 6 animals. All the experiments were performed during 08:00-13:00 in daylight in the pharmacology laboratory. All animal procedures were performed in accordance with guidelines for the Care and Use of Laboratory Animals Issued by The National Ethical Committee (no: IR.MUI.RESEARCH.REC.1398.160). All efforts were made to reduce the number of animals used in each experiment and to minimize animal suffering. Animals were manipulated either by Dex administration or by stress induction.

Drug administration and the Syn cocktail

Dex (8 mg/2 mL ampule, Raha Industry, Iran) 250 mcg/kg was injected SC as single dose 3 hours prior the tests, or 15 mcg/kg was injected daily for 7 consecutive days and testing performed the following day, while control animals received normal saline.[6] Dex was freshly prepared in normal saline, and injections were adjusted to a volume of 10 mL/kg mouse body weight.

The Syn cocktail was prepared from a premixed product comprising 10^9 CFU probiotic strains and a prebiotic (*Lactobacillus casei, L. acidophilus, L. rhamnosus, L. bulgaricus, Bifidobacterium breve, B. infantis, Streptococcus thermophiles*, and *Fructooligosaccharides*; a product of Zisttakhmir Industry, Iran). Animals had free access to the Syn cocktail solution $12.5x10^6$ CFU;[22] in drinking water that was prepared fresh each day; control animals drank tap water ad libitum. The amount of the Syn cocktail solution or drinking water ingested by the animals was measured daily for 7 days, and the tests were performed on the next day.

Water avoidance stress (WAS)

WAS was performed in a Plexiglas tank comprising a block affixed in the middle of the floor. The tank was filled with room temperature shallow water (22˚C) within 1 cm of the top of the

block. The animals were placed on the block for a period of 1 h daily for 4 consecutive days.[23] The group of animals that had WAS and drank tap water throughout the experiment are referred to the WAS group. The animals administered synbiotic cocktail were subjected to WAS either during the first 4 days, referred to as WAS1, or during the last 4 days of ingesting the cocktail, referred to as WAS2.

The sham group consisted of animals that were placed similarly for 1 h daily for 4 days on the same platform in a waterless container.

Locomotor test

The first experiment was carried out in order to analyze the animal motor activity in an open arena (Borj Sanat, Iran) that was divided into 16 zones by red beams. Mice were allowed to explore the field for 3 min by passing through the beams. The zone entries were counted automatically, while rears on hind legs were recorded manually. The sum of zone entries (horizontal exploration) and rears (vertical exploration) were calculated as the total activity for each animal.

Forced swimming test (FST)

During the FST mice were forced to swim in 25°C water in a glass 2-liter beaker (diameter 12.5 cm, depth 12 cm) for 6 min. The immobility time was measured during the last 4 min of the 6 min trial after habituation was performed within the first 2 min. The immobility time is when no additional activity is observed other than that required to keep the animals' head above the water denoting a phenotype of depression. Swimming behavior, defined as horizontal movement around the beaker involving at least 2 limbs, and climbing behavior, defined as upward movement of the forepaws against the beaker wall, were also recorded.[24] The experiment was recorded by a camera and analyzed later. After the experiment, the animals were dried carefully to avoid hypothermia and returned to their home cages.

Sucrose preference test

This test measured another depression phenotype in rodents: Anhedonia. The test was conducted in 3 days: On the first day, two bottles of sucrose solution (5% w/v) were applied in the animals' home cage, and on the second day, one bottle of sucrose solution was replaced with water. After the habituation period, mice had access to 2 bottles containing 100 mL of sucrose solution and 100 mL of tap water that was finally measured after 24 h, and the percentage of sucrose preference was calculated according to the sucrose solution and water consumption. A decrease in sucrose preference measured to a level below 65% was taken as the criterion for anhedonia.[25]

Data processing and statistical analysis

Results are expressed as group means ± standard error of the mean (SEM). The results were analyzed by One-Way ANOVA, followed by Tukey's multiple comparison tests, and p values smaller than 0.05 were considered significant. The software programs used for data analysis and graph construction were Excel 2010 and GraphPad Prizm 6.

RESULTS

Daily food and drink intake and body weight change

As shown in Table 1, there was no significant difference in food consumption between groups. Drinking was significantly higher in Dex-treated animals that drank the Syn cocktail. The daily Syn consumption was then calculated according to the daily drink intake per body weight, which varied between 4.5 and $8.5x10^6$ CFU/g. There was a great rise in the percent body weight change in Dex-treated mice that drank Syn ($p<0.001$ vs. control and vs. Dex alone group) and in the WAS2 group that ingested Syn ($p< 0.001$ vs. control and $p<0.05$ vs. WAS group).

Effect of Dex and the synbiotic mixture on depressive behavior

As presented in Figure 1A, drinking the Syn cocktail reduced immobility time during the FST, which was significantly different from the control group that drank tap water (54±7 sec vs. 111±6 sec, $p<0.001$). Dex acute or sub-acute injection increased the immobility time (166±6 sec and 174±9 sec respectively, $p<0.001$ compared with their corresponding control groups), which clearly indicated animal depressive behavior. Adding the Syn cocktail to the animals' drinking water significantly reduced their immobility time, indicating that the Syn drink reversed Dex-induced depressant effects. As Figure 1B shows, the Syn mixture significantly increased the swimming time in normal animals (167±8 sec vs. water group 93±5 sec, $p<0.001$) or those

Table 1. Daily food intake, fluid intake, Syn ingestion, and percent body weight change

Groups	Daily food intake mg/g body weight	Daily fluid intake mL/g body weight	Daily synbiotic CFU/g body weight	Body weight increase (%)
Control	181.6±18	0.42±0.01	0	2.1±0.7
Syn	168.2±25	0.36±0.01	$4.5x10^6$	3.8±0.4
Dex	158±14	0.5±0.04	0	0.9±0.7
Dex + Syn	197±23	0.68±0.05*	$8.5x10^6$	$9.9±1^{***,ddd}$
WAS	132±5	0.54±0.03	0	2.9±0.7
WAS1 + Syn	178±22	0.58±0.03	$7.2x10^6$	4.5±0.7
WAS2 + Syn	173±24.4	0.56±0.1	$7x10^6$	$7.7±0.7^{***,s}$

Syn cocktail ($12.5x10^6$ CFU), Dex sub-acute (15 mcg/kg). Stress was imposed by WAS over 4 days, and daily measurements were performed during this period, while other groups were evaluated for 7 days. The animals administered synbiotic cocktail were subjected to WAS either during the first 4 days (WAS1) or during the last 4 days (WAS2) of ingesting the cocktail. ***: $p<0.001$ compared with the control group, ^{ddd}: $p<0.001$ compared with the Dex group, and ^{s}: $p<0.05$ compared with the WAS group, Syn: Synonym, Dex: Dexamethasone, WAS: Water avoidance stress

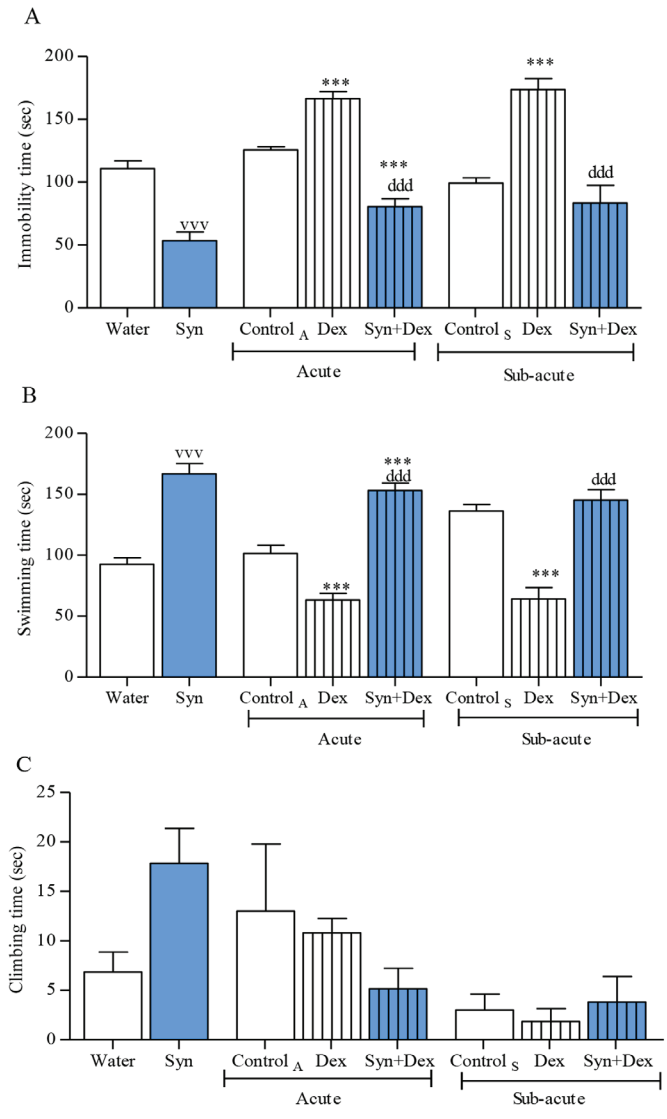

Figure 1. Effect of the synbiotic cocktail and dexamethasone on behavior during the forced swimming test. (A) Immobility time, (B) swimming time, and (C) climbing time. Synbiotic cocktail (Syn; 12.5x10^6 CFU) for 7 days, Dex acute (250 mcg/kg) single dose and control A normal saline, Dex sub-acute (15 mcg/kg) for 7 days and control S received normal saline. The number of animals in each group was 6. Results are expressed as group mean ± SEM and analyzed by ANOVA followed by Tukey's multiple comparison tests. ^{vvv}: p<0.001 compared with the water drinking group, ***: p<0.001 compared with control A or S groups, ^{ddd}: p<0.001 compared with Dex alone acute or sub-acute group, Syn: Synonym, Dex: Dexamethasone, SEM: Standard error of the mean

treated with Dex (acute 153±6 sec and subacute 145±8.5 sec, p<0.001 compared with their corresponding Dex alone groups). Climbing behavior was not significantly different among the various groups (Figure 1C). Table 2 shows the results of the sucrose preference test, which were in line with the FST results. By adding the Syn mixture to drinking water sucrose preference was increased to 82%, while Dex acute or sub-acute treatments reduced the preference for sucrose to levels under 60%, i.e., no preference of the sucrose solution over water, which indicates anhedonia in mice. Adding the Syn mixture to the drinking water clearly increased the sucrose preference in Dex acute and subacute groups. As shown in Table 3, the animals' locomotor activity in the open arena was not noticeably different between the groups.

Effect of WAS and the synbiotic mixture on depressive behavior

Figure 2A shows that exposing the animals to WAS increased immobility time during the FST (148±11 sec, vs. sham group 99±6 sec, p<0.001), which indicated animal despair behavior. Adding the Syn mixture to drinking water reduced immobility time in the WAS1 group (81±6.5 sec, p<0.001 compared with WAS alone), but the Syn cocktail was not effective in the WAS2 group (143±6 sec). This may indicate that the Syn mixture was not able to prevent the stress- induced rise in immobility during the FST. As shown in Figure 2B, C, in the WAS group, swimming time and climbing time were significantly lower than in the sham group. Adding the Syn cocktail to drinking water increased the swimming time significantly (Figure 2B) in the WAS1 group (142±18 sec, vs. the WAS alone group 68±10 sec, p<0.001), while climbing was lower than in the sham group (Figure 2C). The sucrose preference test results were parallel to the FST results (Table 2). As shown in the table, WAS reduced the sucrose preference to 59%, while in the sham group it was 84%. Meanwhile, adding the Syn mixture in the WAS1 group increased the sucrose preference to 90%, while it was 60% in the WAS2 group. Animals' locomotor activity in the open arena was not noticeably different between the various groups (Table 3).

DISCUSSION

Our results showed for the first time that a Syn mixture was able to remedy and prevent Dex-induced depression in mice during FST, which was confirmed by the sucrose preference test. We also observed that the Syn mixture treated depression induced by WAS1, but it was not useful to prevent depression induced by WAS2. The sucrose preference test also showed parallel results, as anhedonia was treated following ingestion of Syn after WAS1, but it did not prevent anhedonia induced by WAS2.

Changes in body weight showed that Dex reduced body weight, although the magnitude of the reduction did not reach a significant level. As in humans, GCs showed a powerful catabolic effect on experimental animals.[26] Body weight increased in animals that ingested the Syn mixture, but the increase was not statistically significant, and there was no noticeable rise in their food consumption. It has been proven that different *Lactobacillus* species could induce different effects on weight depending on the host.[27] In addition, certain *Lactobacillus* species, along with other bacterial species, have been associated with weight gain and obesity.[27] Therefore, the *Lactobacillus* present in the cocktail may have, at least in part, caused the weight gain. Wang and colleagues have demonstrated the opposite result, in their study *L. paracasei*, *L. rhamnosus*, and *B. animalis* were associated with weight reduction in high-fat-diet fed mice.[28] However, when the Syn cocktail was consumed following Dex treatment or WAS, it caused a significant body weight gain, and to some extent, greater food intake. Various mechanisms could

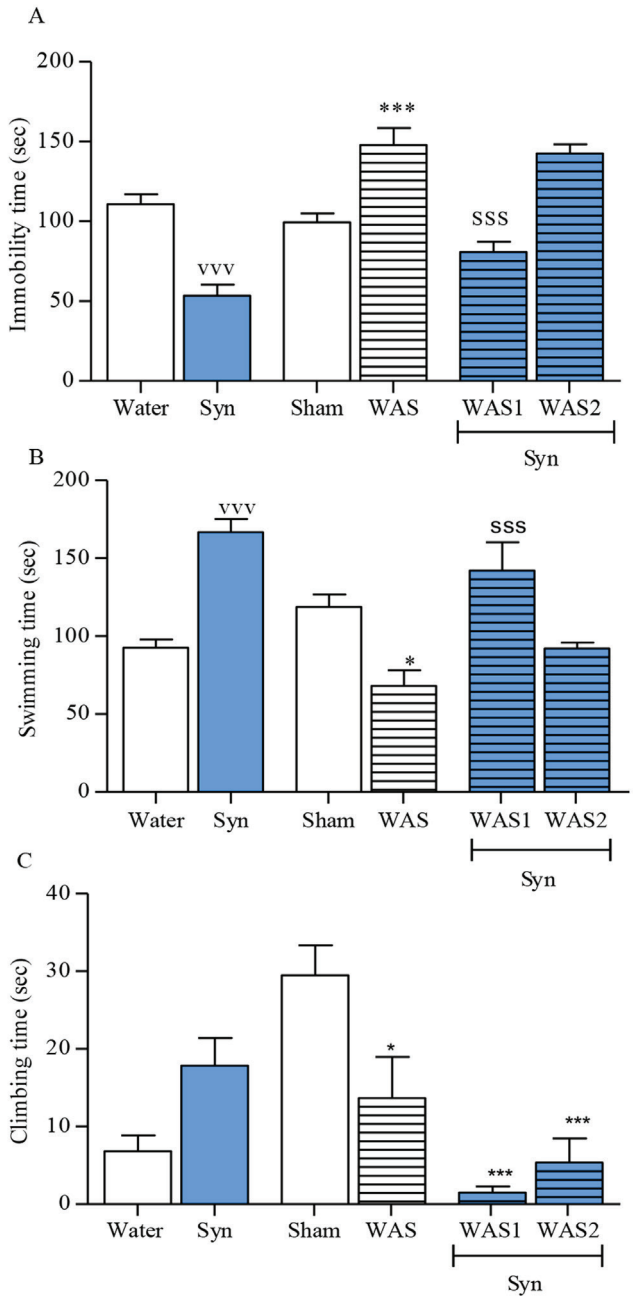

Figure 2. Effect of the synbiotic cocktail and stress on behavior during the forced swimming test. (A) The immobility time, (B) the swimming time, and (C) the climbing time. Syn cocktail ($12.5x10^6$ CFU) for 7 days. Stress was imposed by WAS during 4 days. The sham group animals were placed in a waterless container. The animals administered synbiotic cocktail were subjected to WAS either during the first 4 days (WAS1) or during the last 4 days (WAS2) of cocktail ingestion. The number of animals in each group was 6. Results are expressed as group mean ± SEM and analyzed by ANOVA followed by Tukey's multiple comparison tests. ^{vvv}: $p<0.001$ compared with the water drinking group, *: $p<0.05$, ***: $p<0.001$ compared with the sham group, ^{sss}: $p<0.001$ compared with WAS alone group. Syn: Synonym, Dex: Dexamethasone, WAS: Water avoidance stress, SEM: Standard error of the mean

have caused weight gain, apart from the cocktail, and increased food consumption could also have been responsible in these groups. Fructooligosaccharides are composed of fructose units

Table 2. Sucrose preference test results

Groups	Sucrose preference (%)	Groups	Sucrose preference (%)
Water	65	Sham	84
Syn	82	WAS	59
Control (acute)	65	WAS1 + Syn	90
Dex (acute)	53	WAS2 + Syn	60
Control (sub-acute)	75	Dex (acute) + Syn	95
Dex (sub-acute)	58	Dex (sub-acute) + Syn	72

Syn cocktail ($12.5x10^6$ CFU) for 7 days, Dex acute (250 mcg/kg) single dose and or sub-acute (15 mcg/kg) for 7 days and the control groups received normal saline. Stress was imposed by WAS over 4 days. The animals administered synbiotic cocktail were subject to WAS either during the first 4 days (WAS1) or during the last 4 days (WAS2) of ingesting the cocktail. The sham group animals were placed in a waterless container. The number of animals in each group was 6. Percentage of sucrose preference=(sucrose consumption/sucrose consumption + water consumption) x100. Syn: Synonym, Dex: Dexamethasone, WAS: Water avoidance stress

Table 3. Total activity during the locomotor test

Groups	Total activity (count)	Groups	Total activity (count)
Water	165±16	Sham	230±14
Syn	192±17	WAS	213±7
Control (acute)	173±12	WAS1 + Syn	179±16
Dex (acute)	155±6	WAS2 + Syn	171±20
Control (sub-acute)	170±13	Dex (acute) + Syn	199±14
Dex (sub-acute)	150±15	Dex (sub-acute) + Syn	188±13

Syn cocktail ($12.5x10^6$ CFU) for 7 days, Dex acute (250 mcg/kg) single dose and or sub-acute (15 mcg/kg) for 7 days, and the control groups received normal saline. Stress was imposed by WAS during 4 days. The animals administered synbiotic cocktail were subject to WAS either during the first 4 days (WAS1) or during the last 4 days (WAS2) of ingesting the cocktail. The sham group was placed in a waterless container. Total activity count during locomotor test=(horizontal + vertical) exploration. The number of animals in each group was 6. Results are expressed as group mean ± SEM and analyzed by ANOVA followed by Tukey's multiple comparison test. The differences between various groups did not reach statistical significance. Syn: Synonym, Dex: Dexamethasone, WAS: Water avoidance stress, SEM: Standard error of the mean

that occur naturally in plants, and they induce a low level of sweetness, although they are calorie free and non-cariogenic.[29] It seems unlikely that fructooligosaccharides were responsible for the observed weight gain.

During the FST, when the mouse is placed in the water, the animal gradually loses hope of escaping the stressful environment; thus, the immobility time reflects a measure of "behavioral despair". FST is not only a reliable tool in drug discovery in industrial settings where a high extent of screening of new compounds is essential but also in complementary depression medicine research.[30] In the same trend as previous results, the Syn cocktail presented antidepressant effects in mice by reducing immobility time.[22] Evidently the selective 5-HT reuptake inhibitor (SSRI) drug, fluoxetine decreases immobility time while increasing swimming behavior.[24] The 5-HT level was not measured in our experiment, but the changes during the FST with the Syn mixture were similar to

those induced by the SSRI drug, since the swimming time was augmented, which might be related to the serotonergic system. This statement is supported by a previous study that reported a decrease in the 5-hydroxyindoleacetic acid level in the frontal cortex following treatment of rats with *B. infantis*, indicating that 5-HT degradation was reduced, possibly due to decreased monoamine oxidase activity.[6]

Single dose and long-term Dex administration induced despair behavior during the FST, and anhedonia was deduced since the sucrose preference was reduced to levels under 60%. This was proven earlier, since it was shown that Dex dose-dependently increased the immobility time during the FST.[20] Addition of the Syn mixture reduced the immobility time in the FST not only when Dex was injected as single dose but also when it was administered for 7 days. This showed that the Syn mixture could have preventive effects on Dex-induced mental disorders. It has been shown previously that repeated corticosterone injections induce depressive behavioral and dysregulation of the HPA axis, since corticosterone could have blocked the HPA axis response that normally occurs after the animal is dropped in the water during FST testing.[31,32] GC receptor function may be impaired or it may become resistant to GCs in depression, thus causing HPA axis hyperactivity in depression, thereby causing high GC levels.[33] Evidently, the gut microbiota plays an imperative role in the regulation and development of the HPA axis.[7] Thus it could be deduced that consumption of the Syn mixture has a high likelihood of preventing HPA alterations induced by Dex and therefore preventing its depressive behavior in the FST. In order to further evaluate the possible effect of probiotics on HPA alteration-induced depression, a stress model was accomplished.

WAS is a well-recognized method that represents an effective psychological stressor with conspicuous boosts of adrenocorticotropic hormone and corticosterone within 30 min.[34] We observed that WAS induced despair behavior by increasing immobility time during the FST; meanwhile, anhedonia was assumed since there was no preference for sucrose over water consumption. During WAS1, when the Syn formulation was started with WAS and continued for 3 additional days, depressive symptoms went away in mice. However, during WAS2, which was imposed on the last 4 days of Syn formula ingestion, beneficial effects were not observed. On the other hand, Ait-belgnaoui and colleagues observed that a 2-week treatment with a probiotic formulation (consisting of *L. helveticus* R0052 and *B. longum* R0175) mitigated the HPA axis and autonomic nerve system response to WAS, as revealed by decreased levels of corticosterone and noradrenaline in stressed mouse plasma.[23] They administered the probiotic mixture orally at a concentration of 10^9 CFU/day to C57Bl6 mice and induced WAS at the end of this period. In our observational study, corticosterone plasma levels were not assessed; however, behavior studies showed interestingly that the Syn mixture could overcome depression induced by WAS but it could neither prevent it during FST nor during the sucrose preference test in mice. In addition, WAS caused a decrease in the swimming time, and Syn ingestion significantly increased it in the WAS1 experiment. It has been proven previously that swimming during the FST is related to the serotonergic pathway;[24] therefore, the Syn mixture may have overcome WAS-induced depression by altering the serotonergic system. This belief is supported by previous studies showing that chronic stress causes depression-related behavior through neurotransmitter changes in the CNS, suppression of hippocampal neurogenesis, and HPA axis dysfunction, which manipulates 5-HT activity and exacerbates the effects of stress.[35] Brain-gut communication is achieved by various interrelated systems, for example, through the hormones of the HPA axis, through neural pathways of the autonomic nervous system (which involves the vagus nerve and the adrenergic system), or through immune cytokines.[36]

It has been shown that various forms of stress change the composition of the intestinal microbiota in animals, for example, in one study, after a stressful experience the number of *Lactobacilli* and *Bifidobateria* in the gut were reduced.[37] Conversely, treatment with probiotic bacteria reduced the detrimental effects of stress.[8] Therefore, our results were in favor of previous reports of a high amount of comorbidity between CNS and GI disorders, where it has been reported that large number of those being treated for irritable bowel syndrome also suffer from psychiatric illness.[38]

CONCLUSION

This behavioral study clearly revealed that the Syn formulation can prevent depression induced by the GC drug Dex. In addition, it could remedy WAS-induced depression. Although extrapolating animal data to humans should be done judiciously, probiotics that could be easily inserted in the diet could be a useful alternative therapy in stress- or GC-related depression, while avoiding the harmful side effects of common antidepressants. The Syn effect on depressive behavior may be related to a number of aspects, including ameliorating GC- or stress-induced alterations in stress hormones, brain plasticity, and neurogenesis, which warrants further studies.

ACKNOWLEDGMENTS

This work was supported by the School of Pharmacy and Pharmaceutical Sciences Research Council (grant no: 398160; May 8, 2019), Isfahan University of Medical Sciences.

Conflicts of interest: No conflict of interest was declared by the authors. The authors alone are responsible for the content and writing of the paper.

REFERENCES

1. Hemarajata P, Versalovic J. Effects of probiotics on gut microbiota: mechanisms of intestinal immunomodulation and neuromodulation. Therap Adv Gastroenterol. 2013;6:39-51.
2. Round JL, Mazmanian SK. The gut microbiota shapes intestinal immune responses during health and disease. Nat Rev Immunol. 2009;9:313-323.
3. Floch MH, Walker WA, Guandalini S, Hibberd P, Gorbach S, Surawicz C, Sanders ME, Garcia-Tsao G, Quigley EM, Isolauri E, Fedorak RN, Dieleman LA. Recommendations for probiotic use--2008. J Clin Gastroenterol. 2008;42(Suppl 2):S104-108.

4. Dinan TG, Cryan JF. Melancholic microbes: a link between gut microbiota and depression? Neurogastroenterol Motil. 2013;25:713-719.
5. Cerdó T, Ruíz A, Suárez A, Campoy C. Probiotic, Prebiotic, and Brain Development. Nutrients. 2017;9:1247.
6. Desbonnet L, Garrett L, Clarke G, Bienenstock J, Dinan TG. The probiotic *Bifidobacteria infantis*: An assessment of potential antidepressant properties in the rat. J Psychiatr Res. 2008;43:164-174.
7. Wang Y, Kasper LH. The role of microbiome in central nervous system disorders. Brain Behav Immun. 2014;38:1-12.
8. Desbonnet L, Garrett L, Clarke G, Kiely B, Cryan JF, Dinan TG. Effects of the probiotic *Bifidobacterium infantis* in the maternal separation model of depression. Neuroscience 2010;170:1179-1188.
9. Savignac HM, Corona G, Mills H, Chen L, Spencer JP, Tzortzis G, Burnet PW. Prebiotic feeding elevates central brain derived neurotrophic factor, N-methyl-d-aspartate receptor subunits and d-serine. Neurochem Int. 2013;63:756-764.
10. Cryan JF, O'Mahony SM. The microbiome-gut-brain axis: from bowel to behavior. Neurogastroenterol Motil. 2011;23:187-192.
11. Forsythe P, Sudo N, Dinan T, Taylor VH, Bienenstock J. Mood and gut feelings. Brain Behav Immun. 2010;24:9-16.
12. Sudo N, Chida Y, Aiba Y, Sonoda J, Oyama N, Yu XN, Kubo C, Koga Y. Postnatal microbial colonization programs the hypothalamic-pituitary-adrenal system for stress response in mice. J Physiol. 2004;558(Pt 1):263-275.
13. Neufeld KM, Kang N, Bienenstock J, Foster JA. Reduced anxiety-like behavior and central neurochemical change in germ-free mice. Neurogastroenterol Motil. 2011;23:255-264, e119.
14. Diaz Heijtz R, Wang S, Anuar F, Qian Y, Björkholm B, Samuelsson A, Hibberd ML, Forssberg H, Pettersson S. Normal gut microbiota modulates brain development and behavior. Proc Natl Acad Sci U S A. 2011;108:3047-3052.
15. Gareau MG, Jury J, MacQueen G, Sherman PM, Perdue MH. Probiotic treatment of rat pups normalises corticosterone release and ameliorates colonic dysfunction induced by maternal separation. Gut. 2007;56:1522-1528.
16. Gros DF, Antony MM, McCabe RE, Swinson RP. Frequency and severity of the symptoms of irritable bowel syndrome across the anxiety disorders and depression. J Anxiety Disord. 2009;23:290-296.
17. Goehler LE, Gaykema RP, Opitz N, Reddaway R, Badr N, Lyte M. Activation in vagal afferents and central autonomic pathways: Early responses to intestinal infection with Campylobacter jejuni. Brain Behav Immun. 2005;19:334-344.
18. Dean J, Keshavan M. The neurobiology of depression: An integrated view. Asian J Psychiatr. 2017;27:101-111.
19. Brown ES, J Woolston D, Frol A, Bobadilla L, Khan DA, Hanczyc M, Rush AJ, Fleckenstein J, Babcock E, Cullum CM. Hippocampal volume, spectroscopy, cognition, and mood in patients receiving corticosteroid therapy. Biol Psychiatry. 2004;55:538-545.
20. Mesripour A, Alhimma F, Hajhashemi V. The effect of vitamin B6 on dexamethasone-induced depression in mice model of despair Nutr Neurosci. 2018;24:1-6.
21. Zhao Y, Ma R, Shen J, Su H, Xing D, Du L. A mouse model of depression induced by repeated corticosterone injections. Eur J Pharmacol. 2008;581:113-120.
22. Mesripour A, Meshkati A, Hajhashemi V. A synbiotic mixture augmented the efficacy of doxepin, venlafaxine, and fluvoxamine in mice model of depression. Turk J Pharm Sci. 2020;17:293-298.
23. Ait-belgnaoui A, Colom A, Braniste V, Ramalho L, Marrot A, Cartier C, Houdeau E, Theodorou V, Tompkins T. Probiotic gut effect prevents the chronic psychological stress-induced brain activity abnormality in mice. Neurogastroenterol Motil. 2014;26:510-520.
24. Cryan JF, Markou A, Lucki I. Assessing antidepressant activity in rodents: recent developments and future needs. Trends Pharmacol Sci. 2002;23:238-245.
25. Strekalova T, Spanagel R, Bartsch D, Henn FA, Gass P. Stress-induced anhedonia in mice is associated with deficits in forced swimming and exploration. Neuropsychopharmacology 2004;29:2007-2017.
26. Rooman R, Koster G, Bloemen R, Gresnigt R, van Buul-Offers SC. The effect of dexamethasone on body and organ growth of normal and IGF-II-transgenic mice. J Endocrinol. 1999;163:543-552.
27. Million M, Angelakis E, Paul M, Armougom F, Leibovici L, Raoult D. Comparative meta-analysis of the effect of *Lactobacillus* species on weight gain in humans and animals. Microb Pathog. 2012;53:100-108.
28. Wang J, Tang H, Zhang C, Zhao Y, Derrien M, Rocher E, van-Hylckama Vlieg JE, Strissel K, Zhao L, Obin M, Shen J. Modulation of gut microbiota during probiotic-mediated attenuation of metabolic syndrome in high fat diet-fed mice. ISME J. 2015;9:1-15.
29. Sabater-Molina M, Larqué E, Torrella F, Zamora S. Dietary fructooligosaccharides and potential benefits on health. J Physiol Biochem. 2009;65:315-328.
30. Yankelevitch-Yahav R, Franko M, Huly A, Doron R. The forced swim test as a model of depressive-like behavior. J Vis Exp. 2015;97:52587.
31. Marks W, Fournier NM, Kalynchuk LE. Repeated exposure to corticosterone increases depression-like behavior in two different versions of the forced swim test without altering nonspecific locomotor activity or muscle strength. Physiol Behav. 2009;98:67-72.
32. Johnson SA, Fournier NM, Kalynchuk LE. Effect of different doses of corticosterone on depression-like behavior and HPA axis responses to a novel stressor. Behav Brain Res. 2006;168:280-288.
33. Anacker C, Zunszain PA, Carvalho LA, Pariante CM. The glucocorticoid receptor: pivot of depression and of antidepressant treatment? Psychoneuroendocrinology. 2011;36:415-425.
34. Million M, Taché Y, Anton P. Susceptibility of Lewis and Fischer rats to stress-induced worsening of TNB-colitis: protective role of brain CRF. Am J Physiol. 1999;276:G1027-1036.
35. Mahar I, Bambico FR, Mechawar N, Nobrega JN. Stress, serotonin, and hippocampal neurogenesis in relation to depression and antidepressant effects. Neurosci Biobehav Rev. 2014;38:173-192.
36. Forsythe P, Sudo N, Dinan T, Taylor VH, Bienenstock J. Mood and gut feelings. Brain Behav Immun. 2010;24:9-16.
37. O'Mahony SM, Marchesi JR, Scully P, Codling C, Ceolho AM, Quigley EM, Cryan JF, Dinan TG. Early life stress alters behavior, immunity, and microbiota in rats: implications for irritable bowel syndrome and psychiatric illnesses. Biol Psychiatry. 2009;65:263-267.
38. Marks DM, Han C, Krulewicz S, Pae CU, Peindl K, Patkar AA, Masand PS. History of depressive and anxiety disorders and paroxetine response in patients with irritable bowel syndrome: post hoc analysis from a placebo-controlled study. Prim Care Companion J Clin Psychiatry. 2008;10:368-375.

Turk J Pharm Sci 2021;18(1):28-33
DOI: 10.4274/tjps.galenos.2019.53323

ORIGINAL ARTICLE

Masticatory Functional Load Increases the mRNA Expression Levels of ACTN2 and ACTN3 and the Protein Expression of α-Actinin-2 in Rat Masseter Muscle

Çiğneme Fonksiyonel Yükü Fare Masseter Kasında ACTN2 ve ACTN3'ün mRNA Ekspresyon Düzeylerini ve α-Aktin-2'nin Protein Ekspresyonunu Artırır

Nur MASITA SILVIANA[1]*, Sri ANDARINI[2], Diana LYRAWATI[3], Mohammad HIDAYAT[4]

[1]Universitas Brawijaya Faculty of Dentistry, Department of Orthodontics, Malang, Indonesia
[2]Universitas Brawijaya Faculty of Medicine, Department of Public Health, Malang, Indonesia
[3]Universitas Brawijaya Faculty of Medicine, Department of Pharmacy, Malang, Indonesia
[4]Syaiful Anwar General Hospital Faculty of Medicine, Universitas Brawijaya, Department of Orthopaedics, Malang, Indonesia

ABSTRACT

Objectives: α-actinins play structural and regulatory roles in cytoskeletal organization. They form a lattice structure that secures actin in thin filaments, which generate and transmit muscle contractile forces. The morphological and biochemical characteristics of rat masseter muscles are known to change reactions to masticatory functional loads, but their effect on α-actinins remains unknown. This study aimed to determine the response of α-actinins to masticatory functional loads.

Materials and Methods: Twenty-four male Wistar rats aged 3 weeks were divided randomly into 3 groups of liquid diet (LD), soft diet, and hard diet (HD). The rats were then sacrificed at the end of 8 weeks. The middle part of superficial masseter muscles was examined to investigate the masticatory effect of functional load on the mRNA expression levels of ACTN2 and ACTN3 and the protein expression levels of α-actinin-2 and α-actinin-3.

Results: The mRNA expression levels of ACTN2 and ACTN3 and the protein expression levels of α-actinin-2 of the HD group were significantly higher than those of the LD group, which served as the control group.

Conclusion: Masticatory functional load organizes the mRNA expression levels of ACTN2 and ACTN3 and the protein expression levels of α-actinin-2 in rat masseter muscles through stimuli during muscle physiological adaptation.

Key words: α-actinins, masseter muscles, masticatory function

ÖZ

Amaç: α-aktininler, hücre iskeleti organizasyonunda yapısal ve düzenleyici roller oynarlar. Aktin, kas kasılma kuvvetlerini üreten ve ileten ince filamentler halinde sabitleyen bir kafes yapısı oluştururlar. Sıçan masseter kaslarının morfolojik ve biyokimyasal özelliklerinin çiğneme fonksiyonel yüküne karşı verilen tepkiyi değiştirdiği bilinmektedir, ancak bunların α-aktininler üzerindeki etkisi bilinmemektedir. Bu çalışma, α-aktininlerin çiğneme fonksiyonel yüküne karşı verdiği tepkiyi belirlemeyi amaçlamıştır.

Gereç ve Yöntemler: Üç haftalık 24 erkek Wistar sıçan rastgele sıvı diyet (LD), yumuşak diyet ve sert diyet (HD) uygulanan gruplar olmak üzere 3'e ayrıldı. Sıçanlar daha sonra 8 haftanın sonunda sakrifiye edildi. Yüzeyel masseter kaslarının orta kısmı, fonksiyonel yükün ACTN2 ve ACTN3'ün mRNA ekspresyon seviyeleri ve α-aktin-2 ve α-aktin-3'ün protein ekspresyon seviyeleri üzerinde çiğnemenin etkisini araştırmak için incelendi.

*Correspondence: nurmasita.fk@ub.ac.id, Phone: +62341 576161 ORCID-ID: orcid.org/0000-0003-2981-1061
Received: 04.09.2019, Accepted: 05.12.2019

Bulgular: HD grubunun ACTN2 ve ACTN3'ün mRNA ekspresyon seviyeleri ve α-aktin-2'nin protein ekspresyon seviyeleri, kontrol grubu olan LD grubununkilerden anlamlı şekilde daha yüksekti.

Sonuç: Çiğneme fonksiyonel yükü, kas fizyolojik adaptasyonu sırasında uyarılar yoluyla, fare masseter kaslarında ACTN2 ve ACTN3'ün mRNA ekspresyon seviyelerini ve α-aktin-2'nin protein ekspresyon seviyelerini düzenler.

Anahtar kelimeler: α-aktininler, masseter kasları, çiğneme fonksiyonu

INTRODUCTION

Animal studies have revealed a straight causal relation between the transformation of masticatory muscle function induced by substituting diet consistency and muscular changes in a complete masticatory system. Kiliaridis and Shyu[1] reported that the strength of masticatory muscles after tetanic stimulation is lower with a soft diet (SD) food than with a hard diet (HD) food. The population of satellite cells in the masseter muscle with a reduced masticatory function is small.[2] A decrease in the physical consistency of diets can increase the fiber diameter, muscle mass, and cross-sectional area of type 2B fibers.[3-7] The masseter muscles of animals fed with SD have smaller proportion and cross-sectional area of fibers that co-expressing myosin heavy chain (MyHC)-I and MyHC-cardiac alpha than those in the control animals.[8]

α-actinins, which belong to the actinin-binding protein group, are classified into muscle and non-muscle isoforms. α-actinin-cross-linked actin filaments are located on the Z disk of sarcomeres to help stabilize and maintain the architecture of the contraction of skeletal muscles.[9] α-actinins participate in a wide range of signal transduction complexes by interacting with other proteins to accelerate physiological changes.[10] It is considered an important structural component associated with the contractile muscle of force generation and transmission as in the maintenance of regular myofibrillar arrays. α-actinins in the skeletal muscle have 2 isoforms, namely, α-actinin-2 and α-actinin-3.[11-13] α-actinin-2 is found in entire muscle fibers, including cardiac muscles and the brain, whereas α-actinin-3 is limited to most fast-contracting fibers, e.g., type 2. Both actinins initiate energy production of force-generating glycolytic at a high speed.

Through interactions with calcineurin signals, α-actinin-3, which is encoded by *ACTN3*, can contribute to muscle function to influence the proportion of fiber types during growth.[14] α-actinin-3 deficiency (XX) may influence the decrease in the performance of muscle strength, power, and endurance of elite athletes and general population.[15] Ogura et al.[16] claimed that the total protein level of α-actinin-2 increases in the plantaris and in the white and red gastrocnemius muscles, but no significant disparity is observed in the α-actinin-3 expression after an exercise training. Khaledi et al.[17] found that the mRNA and protein expression levels of actinins change in response to progressive resistance training. This finding shows that the mRNA expression levels of α-actinin-2 and α-actinin-3 are upregulated after 8 weeks of exercise in female Sprague-Dawley rats. The protein expression of α-actinin-2 significantly enhanced in the training group although no difference is detected in the protein expression of α-actinin-3.[17]

However, few studies have described the link of α-actinins to masseter muscle activities. Zebrick et al.[18] demonstrated the mRNA expression level of the masseter muscle differs from that in ACTN3 single nucleotide polymorphism genotypes. In the sagittal and vertical classifications of malocclusion, the frequency of ACTN3 genotypes significantly differs. In skeletal class 2 malocclusion, the clearest association is the enhancement of 577XX genotype. This genotype also produces fast type 2 fibers with small diameters within masseter muscles.[18] These results indicate that some aspects of muscle function may be affected by ACTN3 genotypes, such as α-actinin-3, to enhance the forceful and fast skeletal muscle contraction. The deficiency of α-actinin-3 implies the need of α-actinin-3 for rapid muscle contractions and optimal force.

However, the response of α-actinins to masticatory muscles is still unknown. The contraction velocity and maximum force generation of a closing jaw's muscle responsible for chewing are influenced by a decrease in the masticatory functional load during development. Our study aimed to examine the effect of masticatory functional load on the mRNA and protein expression levels of ACTN2 and ACTN3 in the masseter muscle of rats.

MATERIALS AND METHODS

Twenty-four 3-week-old male Wistar rats (body weight=approximately 60 g) were randomly classified into 3 groups, which contained eight rats in each group. In group 1 (control group), a liquid diet (LD) was given to the rats fed with a blended mixture of pellets and water with a ratio of 1:4. In group 2, a SD was prepared for the rats fed with a slurry mixture of pellets tempered in water with a 1:1 ratio. In group 3, the rats were fed with regular rat pellets set as a HD group. All the groups were fed ad libitum and given water. The rats were separately placed in suspended metal cages without other materials or objects that could be a masticatory stimulus. Every week, the body weight and physical condition were measured and recorded to monitor the rats' condition. After 8 weeks of examination, all the rats were anesthetized with pentobarbital sodium at a fetal overdose of 50 mg/kg and sacrificed through exsanguination. Then, the middle part of the rats' superficial masseter muscles was dissected, frozen in liquid nitrogen, and stored at -85°C. This experimental protocol was approved by the Ethics Committee for the Health Research of Universitas Brawijaya, Malang, Indonesia (269/EC/KEPK/07/2017).

Analysis of the mRNA expression levels of ACTN2 and ACTN3

RNA was isolated using a total RNA purification kit (Jena Bioscience, Jena, Thuringia, Germany). cDNA was synthesized with an iScript™ cDNA synthesis kit (Bio-Rad, Hercules, California, USA) under the following conditions:

priming at 25˚C for 5 min, reverse transcription at 46˚C for 20 min, and enzyme inactivation at 95˚C for 1 min. Quantitative real-time reverse transcription PCR (qRT-PCR) was conducted using SsoFast™ EvaGreen® Supermix (Bio-Rad, Hercules, California, USA) with the following primer sequences: ACTN2 F: 5'-CTATTGGGGCTGAAGAAATCGTC-3' and ACTN2 R: 5'-CTGAGATGTCCTGAATGGCG-3'. ACTN3 F: 5'-AGAAACAGCAGCGGAAAACC-3' and ACTN3 R: 5'-CAGGGCTTTGTTGACATTG-3'.[17] β-actin was chosen for quantitative data normalization, with the primers sequences as follow: β-actin F: 5'-ACCATGTACCCAGGCATTGC-3' and β-actin R: 5'-CACACAGAGTACTTGCGCTC-3'.[17] ACTN3 was amplified under the following conditions: enzyme activation at 95˚C for 3 min, denaturation at 95˚C for 5 sec, and annealing at 54.9˚C for 1 min (45 cycles). ACTN2 and β-actin were amplified under the following conditions: enzyme activation at 95˚C for 3 min, denaturation at 95˚C for 5 sec, annealing for 1 min at 57.3˚C (45 cycles). For all qPCR experiments comparative quantitation measured by a CFX96™ real-time PCR detection system (Bio-Rad, Hercules, California, USA).

Analysis of the protein expression levels of α-Actinin-2 and α-Actinin-3

Protein expression was analyzed via Western blot with α-actinin-2 (N1N3) and α-actinin-3 antibody (GeneTex, Irvine, California, USA). Protein bands in the gel were transferred to a PVDF membrane overnight and blocked with skim milk for 1 h. The membrane was incubated with 1:1000 anti-actinin antibody diluted in 1% PBS-skim milk overnight. Afterward, a secondary antibody was added, and BCIP/NBT was used as a substrate. Bands were analyzed using Quantity One (Bio-Rad, Hercules, California, USA).

Statistical analysis

Data were presented as mean ± standard error of the mean (SEM) and analyzed via One-Way ANOVA with Tukey's post hoc test. Differences were considered statically significant when $p<0.05$.

RESULTS

No significant differences were found in the rat body weight among the three experimental groups after 8 weeks (Table 1). The mean rat body weights in the LD, SD, and HD groups were 179.88±0.48, 179.30±0.75, and 179.64±0.72, respectively.

Table 1. Data are presented as mean body weight (grams) ± SD in liquid, soft, and hard diet groups for 8 weeks of the experiment (n=8 per group)

Week	2nd	4th	6th	8th
Diet	Mean ± SD	Mean ± SD	Mean ± SD	Mean ± SD
Liquid	79.06±0.26	136.91±0.18	158.31±0.49	179.88±0.48
Soft	78.64±0.47	136.5±0.46	157.89±0.45	179.30±0.75
Hard	78.96±0.19	136.95±0.21	158.51±0.52	179.64±0.72

SD: Standard deviation

mRNA expression of ACTN2 and ACTN3

The mRNA expression levels of ACTN2 and ACTN3 in the 3 experimental groups were assessed through qPCR. In the HD group, the mRNA expression levels of ACTN2 and ACTN3 from the masseter muscle significantly increased by mean factors of 2.29 (SEM: 0.41) and 2.19 (SEM: 0.2), respectively, in contrast to the LD group. In the SD group, the mRNA expression levels of ACTN2 and ACTN3 were upregulated, but they were not significantly different from that in the LD and HD groups ($p<0.005$) (Figure 1).

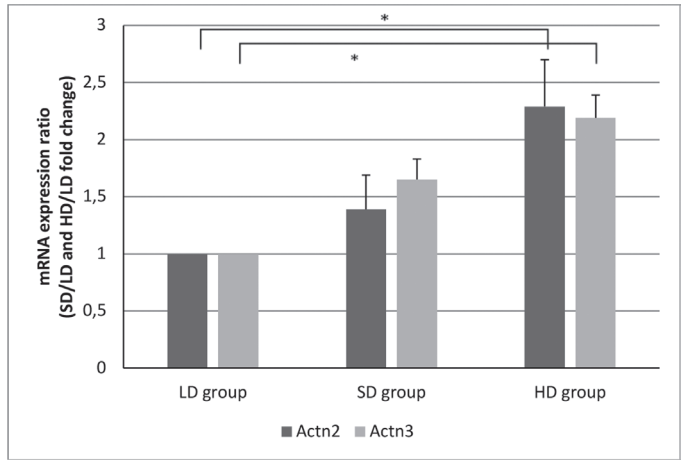

Figure 1. mRNA expression levels of ACTN2 and ACTN3 in masseter muscles shown as fold change compared with those in the liquid diet group as the control group. Statistical analysis was performed via One-Way ANOVA with Tukey's post-hoc test. *Significant with $p<0.05$. LD: Liquid diet SD: Soft diet HD: Hard diet

Protein expression of α-actinin-2 and α-actinin-3

The effects of masticatory muscle function on the protein expression levels of α-actinin-2 and α-actinin-3 in the 3 experimental groups were assessed through Western blot. The protein expression level of α-actinin-2 in the HD group (18.45, SEM: 0.78) was significantly higher than that in the LD group (14.40, SEM: 0.44; Figure 2A). The protein levels of α-actinin-3 in the HD group also increased compared with that in the SD and LD groups by mean factors of 16.75 (SEM: 0.72), 14.16 (SEM: 0.91) and 14.66 (SEM: 0.97), respectively. However, no significant difference in the protein expression levels of α-actinin-3 was observed in the 3 groups (Figure 2B).

DISCUSSION

This study investigated the functional influence of masticatory muscles on the mRNA expression levels of ACTN2 and ACTN3 and the protein expression levels of α-actinin-2 and α-actinin-3 with the consistency of diet variation. In the 3 experimental groups, no transformation was observed in the masticatory pattern in response to the consistency of diet variations. No significant body weight differences were observed in the LD, SD, and HD groups during the 8-week experiment. The mRNA expression levels of ACTN2 and ACTN3 were upregulated as the consistency of diet increased in the SD and HD groups compared with that in the LD group. The protein expression of α-actinin-2

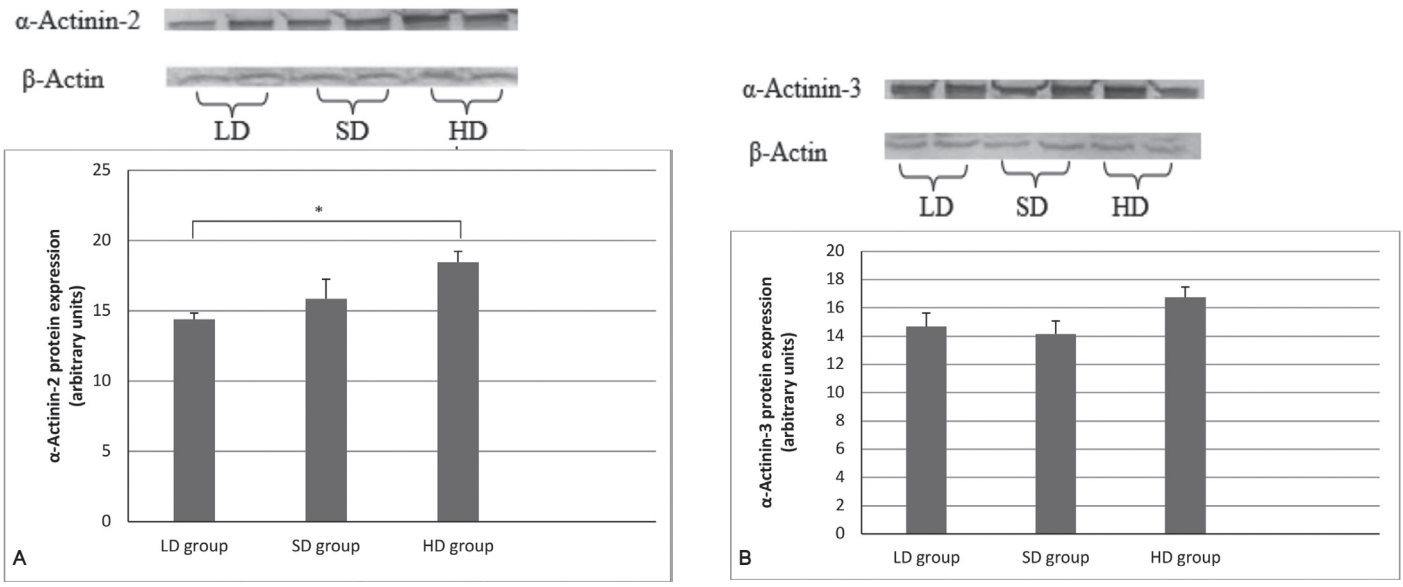

Figure 2. Western blot analysis. A) α-actinin-2 and B) α-actinin-3 protein expression in the LD, SD, and HD groups. β-actin was used as the sample loading control. The bar graphs on the right represent means ± SEM. *Significant with $p<0.05$. LD: Liquid diet SD: Soft diet HD: Hard diet, SEM: Standard error of the mean

increased as the consistency of diet increased. However, the expression levels of ACTN2, ACTN3, and α-actinin-2 in the LD group significantly differed from that in the HD group. However, the difference was not significant when the LD and HD groups were compared with the SD group. The expression levels of α-actinin-3 did not significantly differ among the three groups.

A previous study showed that about 16%-18% of the global population lacks α-actinin-3 possibly because of homozygosis for the common null of ACTN3 577X polymorphism.[19] This phenomenon is also associated with untrained adolescents, elite athletes, and young adults with low sprint performance, low muscle strength, and weak muscle power.[13] In the human skeletal muscle, the total protein level of α-actinins decreases after irregular exercise and recovers systematically in 7-8 days once exercise is complete.[20] This finding suggests that α-actinin-3 may be considered an important structural component to optimize forceful and rapid muscle contractions.[13]

The results of this study were similar to those of several animal studies on the effect of physiological stimuli on cellular α-actinins. Khaledi et al.[17] examined the effects of progressive resistance training on the gene and protein levels of ACTN3 and ACTN3. They found that the mRNA levels of ACTN2, ACTN3, and α-actinin-2 increase, but no transformation occurs in the protein expression of α-actinin-3. Ogura et al.[21] observed the effects of endurance exercise training on rats by using α-actinin-2 and α-actinin-3 levels. After exercise for 8 weeks on a treadmill, the α-actinin-2 expression in the plantaris muscles is slightly higher than the α-actinin-3 expression. They also demonstrated that α-actinin isoforms respond to other physiological stimuli. Therefore, the α-actinin-3 expression is slightly higher than the α-actinin-2 expression after hind limb unloading.[22]

Diet food consistency in laboratories changes the strength level of biting demands, masticatory activity, and behavior. It changes the composition and diameter of fiber types in animal masticatory muscles.[1,3-5] In the present study, physiological stimulation through masticatory functional load revealed that cellular α-actinins were involved in the masseter muscle. Zebrick et al.[18] used the masseter muscle obtained via orthognathic surgery to examine the expression and genetic variation in ACTN2 and ACTN3 and determined their associations with musculoskeletal malocclusion phenotypes. Masseter muscle samples from 60 subjects who underwent orthognathic surgery included the following vertical and sagittal classifications: class 2 and class 3 open bite, class 2 and class 3 deep bite, and class 2 and class 3 normal bite malocclusions. Their results demonstrated that the ACTN3 polymorphism R577X is related to class 2 and deep bite skeletal malocclusions. In masseter muscles, α-actinin-3 is lost with the small diameter of type 2 fiber. Real-time PCR demonstrated that the mRNA expression of ACTN3 is almost undetected with the 577XX genotype, and the expression level of ACTN2 remains unchanged. Therefore, ACTN2 may not compensate the loss of α-actinin-3 in masseter muscles.[18]

The adoption of consistency of diet variations is based on histological, morphological, and biochemical alterations in muscle fiber types. In the SD group, type 2A had a smaller percentage and type 2B had a larger percentage in the anterior deep masseter than those in the normal diet group.[1] Fundamentally, α-actinin-2 is found in the entire fibers of the skeletal muscle, whereas the α-actinin-3 expression is limited to type 2 fast-contracting skeletal muscle fibers.[11,13] Ogura et al.[22] indicated that the α-actinin-3 expression enhances in terms of the relative content of type 2 MyHC and fast myosin levels after hind limb unloading. Exercise training changes MyHC from 2B to 2A. Their study also suggested that changes in MyHC composition may affect the enhancement of the aerobic capacity of skeletal muscles after training.[22] The line

of fiber-type-specific gene expression-activated α-actinin-3 defines the type and size of fibers by binding to the calsarcin family of signaling proteins on the Z disk, which binds to the signaling protein calcineurin.[23,24]

This masticatory functional load showed that reactions were similar to those in skeletal muscle models. This finding indicated that the mRNA expression of ACTN2 and ACTN3 and the protein expression of α-actinin-2 were altered during masticatory muscle function. The mRNA expression of ACTN2 and ACTN3 and the protein expression of α-actinin-2 were significantly changed as the masticatory functional load increased between the HD and LD groups. Non-significant differences were shown in the SD group compared with the LD and HD groups. This difference likely indicated that the masticatory functional load in the SD group was insufficient to induce mRNA and protein expression. However, further investigation on the differences in the expression levels of ACTN2 and ACTN3 among LD, SD, and HD groups should be performed, which increased in time or remained stable is needed.

CONCLUSION

In summary, the mRNA expression levels of ACTN2 and ACTN3 and the protein expression level of α-actinin-2 are set in the rat masseter muscle as the masticatory functional load increases. Even though cellular α-actinins of the masseter muscle likely adapt to functional changes, the underlying mechanism should be further elaborated.

ACKNOWLEDGEMENTS

This study was financially supported by the Directorate General of Strengthening for Research and Development, the Ministry of Research, Technology, and Higher Education through a doctoral research grant (no: 338.178 / UN10.C10 / PN / 2018).

Conflicts of interest: No conflict of interest was declared by the authors. The authors alone are responsible for the content and writing of the paper.

REFERENCES

1. Kiliaridis S, Shyu BC. Isometric muscle tension generated by masseter stimulation after prolonged alteration of the consistency of the diet fed to growing rats. Arch Oral Biol. 1988;33:467-472.
2. Kuijpers MAR, Grefte S, Bronkhorst EM, Carels CEL, Kiliaridis S, Von den Hoff JW. Reduced masticatory function is related to lower satellite cell numbers in masseter muscle. Eur J Orthod. 2014;36:262-267.
3. Kiliaridis S, Engström C, Thilander B. Histochemical analysis of masticatory muscle in the growing rat after prolonged alteration in the consistency of the diet. Arch Oral Biol. 1988;33:187-193.
4. He T, Olsson S, Daugaard JR, Kiliaridis S. Functional influence of masticatory muscles on the fibre characteristics and capillary distribution in growing ferrets (Mustela putonusfuro) - A histochemical analysis. Arch Oral Biol. 2004;49:983-989.
5. Kitagawa Y, Mitera K, Ogasawara T, Nojyo Y, Miyauchi K, Sano K. Alterations in enzyme histochemical characteristics of the masseter muscle caused by long-term soft diet in growing rabbits. Oral Dis. 2004;10:271-276.
6. Saito T, Fukui K, Akutsu S, Nakagawa W, Ishibashi K, Nagata J, Shuler CF, Yamane A. Effects of diet consistency on the expression of insulin-like growth factors (IGFs), IGF receptors and IGF binding proteins during the development of rat masseter muscle soon after weaning. Arch Oral Biol. 2004;49:777-782.
7. Urushiyama T, Akutsu S, Miyazaki J-I, Fukui T, Diekwisch TGH, Yamane A. Change from a hard to soft diet alters the expression of insulin-like growth factors, their receptors, and binding proteins in association with atrophy in adult mouse masseter muscle. Cell Tissue Res. 2004;315:97-105.
8. Vreeke M, Langenbach GEJ, Korfage JAM, Zentner A, Grünheid T. The masticatory system under varying functional load. Part 1: Structural adaptation of rabbit jaw muscles to reduced masticatory load. Eur J Orthod. 2011;33:359-364.
9. Mills M, Yang N, Weinberger R, Vander Woude DL, Beggs AH, Easteal S, North K. Differential expression of the actin-binding proteins, alpha-actinin-2 and -3, in different species: implications for the evolution of functional redundancy. Hum Mol Genet. 2001;10:1335-1346.
10. Djinovic-Carugo K, Gautel M, Ylänne J, Young P. The spectrin repeat: a structural platform for cytoskeletal protein assemblies. FEBS Lett. 2002;513:119-123.
11. MacArthur DG, North KN. A gene for speed? The evolution and function of alpha-actinin-3. Bioessays. 2004;26:786-795.
12. MacArthur DG, North KN. ACTN3: A genetic influence on muscle function and athletic performance. Exerc Sport Sci Rev. 2007;35:30-34.
13. North KN, Beggs AH. Deficiency of a skeletal muscle isoform of alpha-actinin (alpha-actinin-3) in merosin-positive congenital muscular dystrophy. Neuromuscul Disord. 1996;6:229-235.
14. Vincent B, De Bock K, Ramaekers M, den Eede EV, Leemputte MV, Hespel P, Thomis MA . ACTN3 (R577X) genotype is associated with fiber type distribution. Physiol Genomics. 2007;32:58-63.
15. Yang N, Garton F, North K. alpha-actinin-3 and performance. Med Sport Sci. 2009;54:88-101.
16. Ogura Y, Naito H, Kakigi R, Akema T, Sugiura T, Katamoto S, Aoki J. Different adaptations of alpha-actinin isoforms to exercise training in rat skeletal muscles. Acta Physiol. 2009;196:341-349.
17. Khaledi N, Fayazmilani R, Gaeini AA, Javeri A. Progressive Resistance Training Modulates the Expression of *ACTN2* and *ACTN3* Genes and Proteins in the Skeletal Muscles. Am J Sport Sci Med. 2016;4:26-32.
18. Zebrick B, Teeramongkolgul T, Nicot R, Horton MJ, Raoul G, Ferri J, Vieira AR, Sciote JJ. ACTN3 R577X genotypes associate with Class II and deepbite malocclusions. Am J Orthod Dentofac Orthop. 2014;146:603-611.
19. North KN, Yang N, Wattanasirichaigoon D, Mills M, Easteal S, Beggs AH. A common nonsense mutation results in α-actinin-3 deficiency in the general population. Nat Genet. 1999;21:353-354.
20. Yu JG, Fürst DO, Thornell LE. The mode of myofibril remodelling in human skeletal muscle affected by DOMS induced by eccentric contractions. Histochem Cell Biol. 2003;119:383-393.
21. Ogura Y, Naito H, Kakigi R, Ichinoseki-Sekine N, Kurosaka M, Yoshihara T, Akema T. Effects of ageing and endurance exercise training on alpha-

actinin isoforms in rat plantaris muscle. Acta Physiol. 2011;202:683-690.

22. Ogura Y, Naito H, Kakigi R, Ichinoseki-Sekine N, Kurosaka M, Katamoto S. Alpha-actinin-3 levels increase concomitantly with fast fibers in rat soleus muscle. Biochem Biophys Res Commun. 2008;372:584-588.

23. Frey N, Olson EN. Calsarcin-3, a novel skeletal muscle-specific member of the calsarcin family, interacts with multiple Z-disc proteins. J Biol Chem. 2002;277:13998-14004.

24. Swoap SJ, Hunter RB, Stevenson EJ, Felton HM, Kansagra NV, Lang JM, Esser KA, Kandarian SC. The calcineurin-NFAT pathway and muscle fiber-type gene expression. Am J Physiol Cell Physiol. 2000;279:C915-924.

Turk J Pharm Sci 2021;18(1):34-43
DOI: 10.4274/tjps.galenos.2019.65624

ORIGINAL ARTICLE

Green Preparation of Citric Acid Crosslinked Starch for Improvement of Physicochemical Properties of *Cyperus* Starch

Cyperus Nişastasının Fizikokimyasal Özelliklerinin İyileştirilmesi için Sitrik Asit Çapraz Bağlanmış Nişastanın Yeşil Hazırlanması

Bunmi OLAYEMI[1]*, Christianah Yetunde ISIMI[1], Kokonne EKERE[1], Ajeh JOHNSON ISAAC[1], Judith Eloyi OKOH[1], Martins EMEJE[2]

[1]National Institute for Pharmaceutical Research and Development (NIPRD), Department of Pharmaceutical Technology and Raw Materials Development, Abuja, Nigeria
[2]National Institute for Pharmaceutical Research and Development (NIPRD), Centre for Nanomedicine and Biophysical Drug Delivery, Abuja, Nigeria

ABSTRACT

Objectives: This study was undertaken to assess the properties of *Cyperus esculentus* tuber starch crosslinked with citric acid from liquid substrates of orange peel derived via the natural solid-state fermentation process; a green approach.

Materials and Methods: The flow properties of the prepared starches were evaluated using standard methods. Water-holding capacity, swelling capacity, moisture sorption capacity, gelatinization temperature using differential scanning calorimetry, morphology, fourier infrared spectroscopy, and pH of the starches were evaluated.

Results: Results showed that the pH of the crosslinked starches were lower (3.39-4.07) than that of the native starch (5.25) and the flow profile was found to improve. The crosslinked starches' water-holding capacity (90.67%-96.69%) were higher, whereas its emulsion capacity (15.33) was similar to that of the native starch (15.33). No change was observed in the morphology of the crosslinked starches' granules. The infrared spectra of the native and crosslinked starches showed identical peaks; however, the enthalpy of gelatinization (ΔHgel) of the crosslinked products were found to differ from that of the native starch. Modified starches show propensity of being exploited as binding agents in food and pharmaceutical industries.

Conclusion: The green modification process proved to be a valuable addition to the available starch modification processes.

Key words: *Cyperus esculentus* tuber starch, crosslinking, citric acid, orange peel, crosslinked starch

ÖZ

Amaç: Bu çalışma yeşil bir yaklaşımla, doğal katı hal fermantasyon işlemi yoluyla portakal kabuğunun sıvı substratlarından elde edilen sitrik asit ile çapraz bağlanan *Cyperus esculentus* yumru nişastasının özelliklerini değerlendirmek için yapılmıştır.

Gereç ve Yöntemler: Hazırlanan nişastaların akış özellikleri standart yöntemler kullanılarak değerlendirildi. Nişastaların su tutma kapasitesi, şişme kapasitesi, nem tutma kapasitesi, jelatinleştirme sıcaklığı, diferansiyel tarama kalorimetresi kullanılarak morfolojisi, fourier kızılötesi spektroskopisi kullanılarak değerlendirildi ayrıca pH'leri belirlendi.

Bulgular: Bulgular, çapraz bağlı nişastaların pH'nin, doğal nişastanın (5,25) pH'sinden daha düşük olduğunu (3,39-4,07) ve akış profilinin iyileştiğini gösterdi. Çapraz bağlanmış nişastaların su tutma kapasitesi (%90,67-%96,69) daha yüksekti, oysa emülsiyon kapasitesi (15,33) doğal nişastanınkine (15,33) benziyordu. Çapraz bağlanmış nişasta granüllerinin morfolojisinde hiçbir değişiklik gözlenmedi. Doğal ve çapraz bağlı nişastaların kızılötesi spektrumları özdeş zirveler gösterdi; bununla birlikte çapraz bağlanmış ürünlerin jelatinleşme entalpisinin (ΔHgel) doğal nişastanınkinden farklı olduğu bulunmuştur. Değiştirilmiş nişastalar, gıda ve ilaç endüstrilerinde bağlayıcı maddeler olarak sömürülme eğilimi gösterir.

Sonuç: Yeşil modifikasyon prosesinin, mevcut nişasta modifikasyon proseslerine katkı sağlayacağı kanıtlandı.

Anahtar kelimeler: *Cyperus esculentus* yumru nişastası, çapraz bağlama, sitrik asit, portakal kabuğu, çapraz bağlı nişasta

***Correspondence:** olubunmibiala@yahoo.co.uk, **Phone:** +2348033532299 **ORCID-ID:** orcid.org/0000-0001-5759-7176

Received: 13.09.2019, **Accepted:** 05.12.2019

INTRODUCTION

Starch has been widely sourced from plant roots, seeds, leaves, and fruits in recent past, however, modern trends in technologies and processes have moved on to adopt other sources in obtaining starch. In the development of starch, non-conventional sources with wide applicability in pharmaceutical formulations as tablet binders and disintegrants, glidants, suspending, and emulsifying agents have been exploited.[1-6]

Although starch in its native form has many potentials, its poor flow properties, instability when exposed to high temperature and under high shear rate, variations in pH, high retrogradation, its limited solubility in common organic solvents, and freeze-thaw processes make them less desirable for industrial applications.[7-9] Therefore, to find means of overcoming these limitations while developing versatile starch-based excipients that have multifunctional applications is the goal of many formulation scientists. One solution to this demanding technological need is to modify native starch properties. This involves tweaking its physical and chemical characteristics to improve its functionality with useful structural attributes via physical, chemical, enzymatic, and genetic means.[10-13]

In the last century, the most prevalent means employed in modifying starch was chemical modification, and the developed products have found several applications in the food, textile, and pharmaceutical industries.[14] This type of adaptation involves the incorporation of functional groups through chemical reactions that can alter the starch molecule or substitute some functional groups. However, the modification outcome is influenced by factors like starch source, reactant type, reaction concentration and time, and the reacting medium's pH. Chemical modification through etherification, esterification, decomposition, grafting, and crosslinking techniques yields starch products.[12]

A covalent interconnection is introduced by crosslinking through hydrogen bonds in starch granules, which provides strong bonds between molecules and restrict polymer chain movement.[15,16] This decreases the rate of starch retrogradation, which consequently increases its gel rigidity and hardness, in addition to enhancing its solubility in organic solvents.[8,17]

In the crosslinking reaction, various reagents are used, which determines the property of the crosslinked product. Hirsch and Kokini[18] showed that the reaction of waxy maize starch with phosphorous oxychloride produced starch with high viscosity and minimum swelling. In Wattanachanta et al.[19] crosslinking sago starch with a mixture of sodium trimetaphosphate and sodium tripolyphosphate (STPP) produced starch with high resistance to acids, rigid gels, and high freeze-thaw stability. The reaction of chlorinated corn starch with formaldehyde was investigated in another study and it was observed that increasing the quantity of formaldehyde while reducing oxidation extent improved the reaction process' efficiency and the products.[20]

In a completely different study, Chowdary and Chaithanya[21] found that the product was insoluble in aqueous, alkaline, and acidic media, the process of crosslinking potato starch gelatinized with urea imparted better flow on the starch. However, prolonged drug release for up to 24 h was observed in the tablet formulations produced by the crosslinked starch; thus concluding that the product could be used in the preparation of extended-release tablet formulations.

The crosslinking effect of the *Icacina trichantha* tuber starch was investigated by Omojola et al.[7] and they observed that water absorption capacity in the modified starch was higher than in the native starch, with no gelatinization occurring upon heating. They proposed that the modified starch could be a more effective tablet disintegrant than the native *I. trichantha* tuber starch. In another study by Omojola et al.[22] the reaction of *Cola nitida* starch with acetic anhydride and STPP as explored, and results showed lower viscosity, solubility, and swelling in the obtained crosslinked starch than in the unreacted starch, and was thus suggested for use as a food thickener.

Isah et al.[9] reported that *Digitaria exilis* starch crosslinked with citric acid decreases the oil and water absorption capacities, foam capacity, and pH of the modified starch. By using scanning electron microscopy, they observed that the starch granule's shape and morphology were not altered by crosslinking; whereas the presence of an additional peak was shown using fourier transform infrared (FTIR). This suggested the use of the crosslinked *D. exilis* starch in the food and pharmaceutical industry.

In the crosslinking process, agents like citric acid have been commonly used. Citric acid is a very essential organic acid that is widely utilized in the food and pharmaceutical industries. It is an intermediate of the tricarboxylic acid cycle, and is found in a variety of acidic fruit juices, particularly the citrus family.[23]

Citrus fruits are readily available in most regions of the world. Annually, after the extraction of the citrus juice, processing industries generate tons of residues, including peels and segment membranes, for commercial purposes. However, these wastes are usually not put to use/reasonable use, thus creating environmental hazards. For example, the burden already present at landfills where solid wastes are deposited is increased; whereas liquid wastes disposed into the rivers could cause nutrient imbalance, loss of oxygen, and, consequently, death of the aquatic life. Failure to exploit these wastes' potential could also impact negatively on the economy. Citric acid, with an estimated annual production of about 10,000,000 tons, has one of the highest level of production worldwide among fermentation products.[24]

In recent years, various manufacturing processes and products with marginal likelihood of causing harm have been explored by researchers and scientists while also improving the sustainability of product development.[25,26] This can be achievable through the green approach system, which, in addition to reducing waste, entails manufacturing processes that create technologies that are safer for the environment and those working in those environment. Innovations through green synthesis has led to the development of diverse products for different applications, including the production of citric acid by fermentation of citrus byproducts using microorganisms.[27,28]

Submerged, surface, and solid-state are the different techniques employed in the production of citric acid through fermentation, with the latter being the simplest of all the techniques.[29,30]

To obtain citric acid from fruit wastes, we intend to use the green approach, which would serve as a precursor for the development of a pharmaceutical excipient. Therefore, this study aims to crosslink starch obtained from *Cyperus esculentus* seed using liquid substrates of orange peel derived by means of the natural solid-state fermentation process, and evaluate its physiochemical properties.

MATERIALS AND METHODS

Materials

Tigernut starch (TS) from *C. esculentus* tuber [extracted from the Department of Pharmaceutical Technology and Raw Material Development, National Institute for Pharmaceutical Research and Development (NIPRD), Abuja, Nigeria] and oranges (obtained from Karmo market, Abuja, Nigeria).

Orange peel substrate preparation

Fresh oranges were procured from the Karmo market in Abuja. They were washed with water, and the skin was separated from the fruit's pulpy segments. Orange peel of 900 g was soaked in 2.5 L of water, and the mixture's pH was recorded. The soaked peels' pH was subsequently recorded on days 1, 5, and 15.

Starch preparation

The method of Kunle et al.[31] was used to extract the TS.

Preparation of modified starch

The procedure described earlier[32] was adopted with some modifications. On day 5, the orange peel substrate's pH was determined, and 50 mL of the filtered substrate was poured in a beaker. Placed in another beaker was 50 g TS, where the filtered substrate was then added in aliquots and mixed until a smooth paste was obtained. The resulting paste was spread on a tray and left to dry at room temperature for about 18 h. The air-dried product was then oven-dried at 60°C for 1 h and 30 min. Using a mortar and pestle, the oven-dried product was size-reduced and after which it was further dried in the oven for 2 h at 130°C. The product (TS1) was then cooled, weighed, and then stored in the desiccator for further analysis.

Other products of the modified starch (TS2 and TS3) were prepared according to the procedure previously stated using orange peel substrate obtained on days 10 for TS2 and 15 for TS3.

Physicochemical properties evaluation of the modified starch

Morphology

Under a light microscope (Leica DM light microscope) at a magnification x400, a small quantity of TS was mounted on the microscope slide and was examined. The starch product's shape was extrapolated from the photomicrograph.

pH determination

The pH of a 10% w/v slurry of the starch product was determined at room temperature (28°C) using the pH meter. Triplicate determinations were made and the mean was computed.

Angle of repos

The funnel method was used; 20 g each of the dried products (TS0, TS1, TS2, and TS3) was allowed to flow through a funnel clamped at a fixed height from a flat surface. The powder heap's height (h) and radius (r) were measured, and the repose angle (A) was calculated as follows,

$A = \tan - 1\ {}^{h}/_{r}$.

Bulk and tapped densities

In a graduated cylinder, the volume occupied by the 20 g starch product was noted; and the bulk density (g/mL) was calculated as the ratio of the powder's weight to the volume occupied in the cylinder. Similarly, the tapped density (g/mL) was computed as the ratio of the powder's weight to the volume it occupied after tapping the cylinder 100 times.

Carr's compressibility index (CI) and Hausner ratio (HR)

Carr's CI, %) was calculated as follows:

$(\text{tapped density-bulk density}) / (\text{tapped density}) \times 100$.

HR was computed as the ratio between the tapped and bulk densities.

Swelling capacity

A slurry of the starch product (1% w/v) was made in distilled water. With intermittent stirring, the dispersion was heated on a water bath (Karl kolb, Dreiech West Germany) at 30°C for 30 min. This was then centrifuged at 1500 rpm for 30 min; the supernatant was discarded, the starch paste weight was determined, and the swelling capacity was calculated as follows:

$S\ (\%) = (\text{weight of wet starch}) / (\text{initial weight of dry starch}) \times 100$.

This procedure was carried out for each of the starch products (TS0, TS1, TS2, and TS3) at 30°C, 40°C, 50°C, 60°C, 70°C, 80°C, and 90°C.

Gelatinization temperature

Differential scanning calorimetry (DSC) was used to determine the gelatinization temperature. The starch samples (5 mg) were placed in an aluminum pan, and a drop of water was added. At a heating rate of 10°C under constant nitrogen flow, the samples were scanned between 60°C and 300°C.

Water-holding capacity

To obtain the water-holding capacity, the method of Kornblum and Stoopak[33] was adopted. The crosslinked starch dispersion (1% w/v) was placed in preweighed, stoppered centrifuge tube and shaken intermittently for 10 min and was left to stand for another 10 min. It was then centrifuged at 1,500 rpm for 5 min; the supernatant was discarded and the weight of the hydrated starch was determined. Hydration capacity was calculated using the equation below,

$H\ (\%) = (\text{weight of dry starch}) / (\text{weight of starch sediment} \times 100)$.

Foam capacity

For foam capacity, the method by Isah et al.[9] was adopted. The starch product's water dispersion of 2% w/v was homogenized for 5 min. It was poured into a measuring cylinder (50 mL), and the volume was recorded after 30 s. The percentage increase in volume expressed is the foam capacity.

Emulsion capacity

Emulsion capacity was also carried out based on the method of Isah et al.[9] The starch product was dispersed in water (2 % w/v) and homogenized for 2 min. After which, vegetable oil (2.5 mL) was gradually added to the mixture and stirred continuously for 30 sec. The suspension was centrifuged at 1,600 rpm for 5 min, and the volume of oil floating was determined. The computed quantity of oil emulsified per gram of the sample is the emulsion capacity.

Moisture content

The oven-dry method was used to determine moisture content. The starch product (0.5 g) was placed into a dry crucible (W_1) and was placed in an oven at for 10-12 h at 100-105°C until constant weight was obtained. The crucible was then allowed to cool in a desiccator for 30 min and was reweighed (W_2). Moisture content (%) was calculated as follows:

W_1-W_2 / W_1 x100.

Moisture sorption capacity

The starch product (1 g) was placed in a tarred porcelain dish and was weighed (W_1). The dish was then placed in a desiccator containing distilled water. The sample and dish were weighed daily (W_2) for 5 days, and the moisture sorption capacity was determined as follows,

W_1-W_2 / W_1 x 100.

FTIR spectral studies

Native TS and the crosslinked products (TS1, TS2, and TS3) were triturated with potassium bromide and were made into pellets (1 ton/cm^2). The Nicolet iS10, Thermo Scientific (USA), FTIR spectrometer was used to take the IR spectra between the scanning ranges of 4,000 and 400 cm^{-1}.

Statistical analysis

Results were obtained from at least three determination and were expressed as mean ± standard deviation.

RESULTS AND DISCUSSION

Organoleptic properties of TS and its crosslinked derivatives

Table 1 shows the organoleptic properties of TS and its crosslinked products. Native TS (TS0) was a white, tasteless, and odorless smooth powder, whereas the crosslinked productsthat had been reacted with orange peel substrates from days 5 (TS1), 10 (TS2), and 15 (TS3) were observed to be off-white in color, odorless with a characteristic taste, and is coarse to touch. The color change observed in the crosslinked products can be attributed to the color of the orange peel substrate used.

pH of orange peel substrate

Table 2 presents the pH of the orange peel substrate on days 0, 5, 10, and 15. Results show that during the study period, the substrate's pH was not consistent; the pH decreased to 2.00 by day 5 and increased to 2.79 by day 10 but decreased again to 2.30 by day 15. This could be a result of fermentation where microorganisms use carbohydrates from the substrate as a source of energy, thus influencing the substrate/medium's chemical environment. This process causes lactobacillus growth, which produce organic acids that lowers the medium's pH. The absence of a trend in the substrate's pH could be associated with the fact that microorganisms consumed the nutrients from the orange peels at the beginning fo the fermentation process and released organic acids into the medium, thus lowering the pH; however, shortage of these nutrients after a period of time could have resulted in the consumption of the organic acids, which led to an increase in the medium's pH. Because the initial decrease in pH is attributed to citric acid production, it implies that the crosslinking effect on starch products treated with substrate on day 5 (TS1) would be greater than that on day 10 (TS2) when the pH was observed to increase again. Factors that influence the medium's pH kinetics are the substrates' nature in the fermentation medium and the method by which the organic acids are produced.[34]

Flow properties of TS and its crosslinked derivatives

Flow properties results of TS products (TS0, TS1, TS2, and TS3) are shown in Table 3. A material's repose angle is a reflection of its flow ability; values less than 30° are an indication of excellent flow, whereas those between 31° and 35°, 36° and 40°, and those greater than 40° are indicative of good, fair, and poor flow, respectively.[35] Obtained values for TS0 (33.06°) and TS1 (34.66°) were observed to be similar, showing that they possess good flow; whereas TS2 (26.96°) and TS3 (30.39°) were lower, which reveal that they have good to excellent flow ability.

Table 2. pH of orange peel substrate

Day	pH
0	5.23±0.05
5	2.00±0.02
10	2.79±0.01
15	2.30±0.02

Number of determinations (n)=3, ± standard deviation

Table 1. Organoleptic properties of Tigernut starch products (TS0, TS1, TS2, and TS3)

Parameters	TS0	TS1	TS2	TS3
Color	White	Off-white	Off-white	Off-white
Odor	Odorless	Characteristic	Characteristic	Characteristic
Taste	Tasteless	Bland	Bland	Bland
Texture	Smooth	Coarse	Coarse	Coarse

Number of determinations (n)=6, TS: Tigernut starch

An increase in citric acid probably resulted in better modification as a substitution result of more OH groups on starch, leading to a less amorphous and better flowing product. Carr's CI is a parameter that assesses a material's ability to deform under pressure; whereas HR measures powdered material's cohesiveness by determining that material'sthe densification degree.[35] A material has excellent, moderate, or fair flow when CI ≤10%, CI: 16%-20%, or CI: 21%-25%, respectively. Consequently, the material is cohesive when HR ≤1.11, and become less cohesive when values are between 1.12 and 1.2.

The results presented in Table 3 show that increasing the fermentation period improved the flow of the crosslinked starch products (TS1, TS2, and TS3), with TS3 having lower CI (25.24%) and HR (1.34) than TS2 (CI, 29.24%; HR, 1.42) and TS1 (CI, 30.36%; HR, 1.45). Moreover, these values were also observed to be lower than those obtained for native starch (32.13% and 1.47), indicating that treating the starch with the orange peel substrate improved the flow of TS.

This indicates that when pressure is applied during tablet compression, the crosslinked starch (TS3) would produce good compacts. It also shows that there would be reproducible product manufacture and performance with consequent uniform drug distribution in the tablet batch.

Physicochemical properties of TS and its crosslinked derivatives

The pH of native TS (TS0, 5.25) was similar to that reported (5.60) by Kenneth et al.[36] in their characterization of TS. For the crosslinked products (TS1, TS2, and TS3), the values obtained were found to be lower (4.07, 3.39, and 3.87, respectively) and could be linked to the varying pH of orange peel substrate used. This may also be attributed to the presence of carboxylic acid on the starch molecule leading to increased acidity.

However, these values were within the range (3-9) specified for most starches used in pharmaceutical, cosmetics, and food industries.[37] This result is also similar to some earlier reports[7,34] where the pH of *I. trichantha* tuber starch and *Tacca involucrate* tuber starch crosslinked with citric were found to be 4.59 and 4.68, respectively. In addition, pastes from various modified starches have been documented to be acidic, therefore, the results of this study is consistent with earlier reports.[38-40]

Presented in Table 4 are the water-holding capacities of TS products. The crosslinked products' water-holding capacity (TS1, TS2, and TS3) were observed to increase with the orange peel substrate's length of stay. They were also found to be appreciable (91.37%, 90.37%, and 96.69%, respectively) compared with the native starch TS0 (85.55%). Water-holding capacity is a material's capacity to retain water when pressure is applied or when heated; it is also the measure of that material's hydration capacity.[41] The observed increase in water-holding capacity may be ascribed the carboxyl groups' attachment on the starch molecules, thus, improving its ability to imbibe water. Specifically in the application of starch products as disintegrants in solid dosage formulations or as drug carriers for controlled drug delivery systems, this phenomenon is desirable.[39] This result is in tandem with those of *Icacina* and *Tacca* starch citrate.[7,32] In Jyothi et al.,[42] cassava starch citrate was also reported to have higher water-holding ability than the native cassava starch.

Foam and emulsion capacities are vital functional properties that determine the behavior and applicability of these starches in processing, consumption, and storage. The crosslinked products' foam capacity were observed to be the same (3.33) but slightly higher than that of the native starch (3.07). On the other hand, their emulsion capacities were found to be the same (15.33%), indicating that their emulsifying property was not affected by starch modification. These results demonstrate the modified starches' ability (TS1, TS2, and TS3) to decrease

Table 3. Flow properties of Tigernut starch products (TS0, TS1, TS2, and TS3)

Parameters	TS0	TS1	TS2	TS3
Angle of repose (°)	33.06±1.79	34.66±1.05	30.39±1.01	26.96±1.02
Bulk density (g/mL)	0.46±0.01	0.49±0.01	0.48±0.01	0.50±0.01
Tapped density (g/mL)	0.68±0.01	0.71±0.02	0.68±0.01	0.67±0.01
Hausner ratio	1.47±0.02	1.45±0.01	1.42±0.04	1.34±0.03
Carr's index (%)	32.18±1.03	30.36±1.57	29.24±2.06	24.25±1.30

Number of determinations (n)=3, ± standard deviation, TS: Tigernut starch

Table 4. Physicochemical properties of Tigernut starch products (TS0, TS1, TS2, and TS3)

Parameters	TS0	TS1	TS2	TS3
pH	5.25±0.02	4.07±0.02	3.39±0.06	3.87±0.02
Water-holding capacity (%)	85.55±1.05	91.37±5.42	90.67±3.40	96.69±1.88
Foam capacity (%)	3.07±1.01	3.33±1.15	3.33±1.15	3.33±1.15
Emulsion capacity (%)	15.33±0.58	15.33±0.58	15.33±0.58	15.33±0.58
Moisture content (%)	8.00±0.30	7.80±0.10	8.10±0.10	9.20±1.00
Moisture sorption capacity (%)	5.87	5.42	5.84	5.54

Number of determinations (n)=3, ± standard deviation, TS: Tigernut starch

surface tension, and as such may be used as emulsifiers in food, cosmetic, and pharmaceutical products.

The crosslinked starches' moisture content increased with the increase of the crosslinking substrate's concentration (7.8%, 8.1%, and 9.2%, respectively) and were generally comparable with that of the native starch (8%). These values are within the limit specified for pharmaceutical starches[43] as presence of excessive moisture can impact negatively on the flow and mechanical properties of the material.[44] In addition, it can promote microorganism growth in the formulation during packaging and storage and decrease the formulation's stability and shelf-life.[45]

Moisture sorption capacity is a measure of moisture sensitivity and an indication of a material's physical stability under storage.[46] The crosslinked starches showed similar sorption capabilities (5.42%, 5.84%, and 5.54%, respectively) with the native starch (5.87%). Materials with low values less tendency to undergo hydrolytic degradation, thus, are beneficial in formulations containing moisture-sensitive drug components.

Table 5 shows the swelling capacity of TS0, TS1, TS2, and TS3 over a range of temperatures (30°C-90°C). Starch granules' ability to absorb water when exposed to heat is portrayed by its swelling characteristics. Swelling over different temperature ranges is important because it evaluates the starches' behavior under industrial conditions. Although swelling was found to be higher at higher temperatures (60°C-90°C) than at lower temperatures (30°C-50°C), the results show a general increase in starch volume as the exposure temperature increased for the native and crosslinked starches. This pattern is ascribed to intrinsic binding forces that tend to weaken at varying temperatures,[47] and as reported by Omojola et al.[48] However, an exception to this trend was observed with TS2, where swelling was observed to appreciably increase at 80°C but decreased at 90°C. TS1, TS2, and TS3 showed similar swelling patterns at 30°C, 40°C, 50°C, and 60°C. However, less swelling was observed in TS2 at 70°C than TS1 and TS3; at 90°C, no further swelling was observed in TS2 and TS3. Of all the starches, TS1's swelling profile was observed to be the most consistent (progressively increasing).

Table 5. Swelling power Tigernut starch products (TS0, TS1, TS2, and TS3)

Temperature (°C)	TS0	TS1	TS2	TS3
30	2.33±0.43	2.38±0.11	2.09±0.07	2.55±0.03
40	2.52±0.11	2.79±0.09	2.64±0.17	2.70±0.43
50	2.44±0.19	2.43±0.17	2.22±0.04	2.63±0.09
60	2.68±0.13	2.69±0.05	2.54±0.17	2.97±0.17
70	5.59±0.40	5.53±0.14	3.56±0.10	5.22±0.42
80	8.77±0.93	8.03±0.08	8.00±0.30	8.03±0.11
90	7.44±0.34	9.18±0.76	7.35±0.24	8.01±0.17

Number of determinations (n)=3, ± standard deviation, TS: Tigernut starch

Nonetheless, the swelling profile of the native and crosslinked starches were similar. This suggests that crosslinking did not have any effect on granule swelling and could be attributed to increased resistance to starch granule swelling because of higher bond strength conferred by crosslinking, which has also been reported by Xie and Liu.[49]

These starches may not be good disintegrant candidates for solid dosage formulations because of their limited water uptake into starch granules, which implies that structural granule break down will not take place. However, our result is different from those of Adebiyi et al.,[32] where *Tacca* starch citrate was observed to have higher swelling power than that of the native *Tacca* starch. This can be attributed to differences in the biological sources of starch materials and starch extraction methods employed.

Figure 1 illustrates the morphology of the native and crosslinked starches. The native starch (TS0) have small and large-sized, oval-shaped, smooth granules occurring mostly in single un-aggregated forms. The crosslinked starches (TS1, TS2, and TS3) are more uniform in size, oval-shaped, and occur in aggregates that are observed to increase with the time of crosslinking (TS1 > TS2 > TS3). Here, application of the orange peel substrate to modify TS did not rupture or change the granule morphology, which shows that under applied pressure resulting in higher bond strength, modified starch would pack more closely and consolidate better than the native starch. Starch granules with small and uniform sizes are widely used in pharmaceutical and food industries,[50] as such, this cheap substrate crosslinked starches could find application in these industries.

FTIR of TS and its crosslinked derivatives

Figure 2 presents the FTIR spectra of the starch products. The native starch shows significant peaks at 3240 cm^{-1}, whereas those of TS1, TS2, and TS3 are 3257.7, 3235.3, and 3250.2 cm^{1}, respectively, all indicating OH stretching. The band 2929.7 cm^{-1} of the native starch is characteristic of C-H stretches associated with ring hydrogen atoms and was observed to slightly decrease to 2926 cm^{-1} in all the crosslinked products. The change in

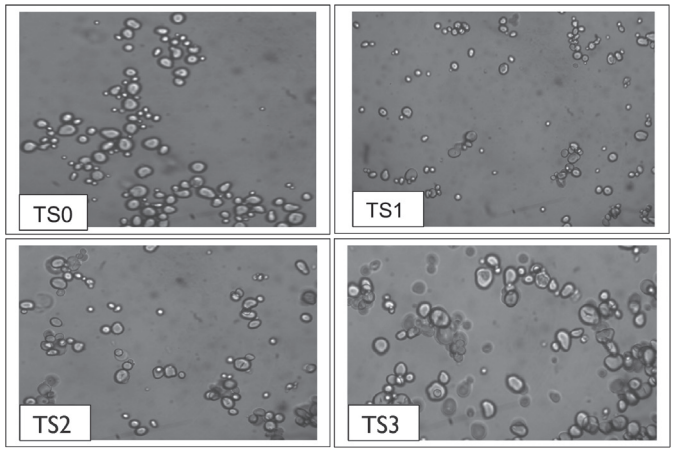

Figure 1. Photomicrograph of native Tigernut starch (TS0), crosslinked starches from day 5 (TS1), day 10 (TS2), and day 15 substrate (TS3)
TS: Tigernut starch

intensity in the C-H stretch could be because of the possible change in starch's amylose and amylopectin content, which is known to be responsible for variation in the physicochemical properties of starch. All the starches showed peaks at about 1640, 1338, and 1140 cm^{-1}, indicating the presence of intra-molecular hydrogen bonds, C-H bending, and C-O stretching. Bands at 708-928 cm^{-1} portray the characteristic identity of the starch.[50]

DSC of TS and its crosslinked derivatives

Presented in Figure 3A-C are DSC thermograms of the behavior of the starch granules of all the samples (TS0, TS1, TS2, and TS3) when subjected to heat. A series of processes that occur when starch is heated and converted to paste is referred to as starch gelatinization; and the temperature at which gelatinization occurs is dependent on the starch molecules' crystalline nature. This transitional phase of starch granules is an important characteristic that makes them applicable in industrial processes.

Thermal properties of the native and modified starches are presented in Table 6. The onset temperature of gelatinization (T_o) of TS0 is observed to be lower (60.35°C) than those of TS2 and TS3 (104.16°C and 113.18°C, respectively). This is attributable to increased granule strength conferred as a result of crosslinking, thus higher temperature is required to initiate starch gelatinization. Increase in gelatinization temperature also indicates better binding ability of the starch, which shows that crosslinked starches possess better binding capability than native starch. Some studies have also reported an increase in gelatinization temperature with other crosslinked starches, relating to decreased mobility of amorphous chains in the starch granule.[16,38] Similarly, peak (T_p) temperature and conclusion temperature (T_c) of the modified starches were observed to be generally higher than those of TS0 (125.59°C and 134.44°C, respectively). This suggests that modified starches acquire more crystalline forms than the native starch; this is in tandem with literature where positive correlation between onset and peak temperature of gelatinization and the materials' amorphous/crystalline nature have been reported.[50,51]

The enthalpy of gelatinization (ΔH) is directly related to the starch granules' crystalline nature (amylopectin), and demonstrates the extent to which the bond order within the

Table 6. Differential scanning calorimetry (DSC) parameters of the native and modified starches

Parameter	TS0	TS1	TS2	TS3
Onset temperature (°C)	60.35	59.84	104.16	113.18
Peak temperature (°C)	125.59	141.60	124.47	132.88
Conclusion temperature (°C)	134.44	293.41	129.52	132.92
Enthalpy of gelatinization [J/(g*K)]	1926.95	2120.73	488.44	1096.20
ΔT (°C)	74.09	233.57	25.36	25.74
Peak height index (PHI)	26.01	9.07	19.26	42.59

TS: Tigernut starch, ΔT: Gelatinization temperature range

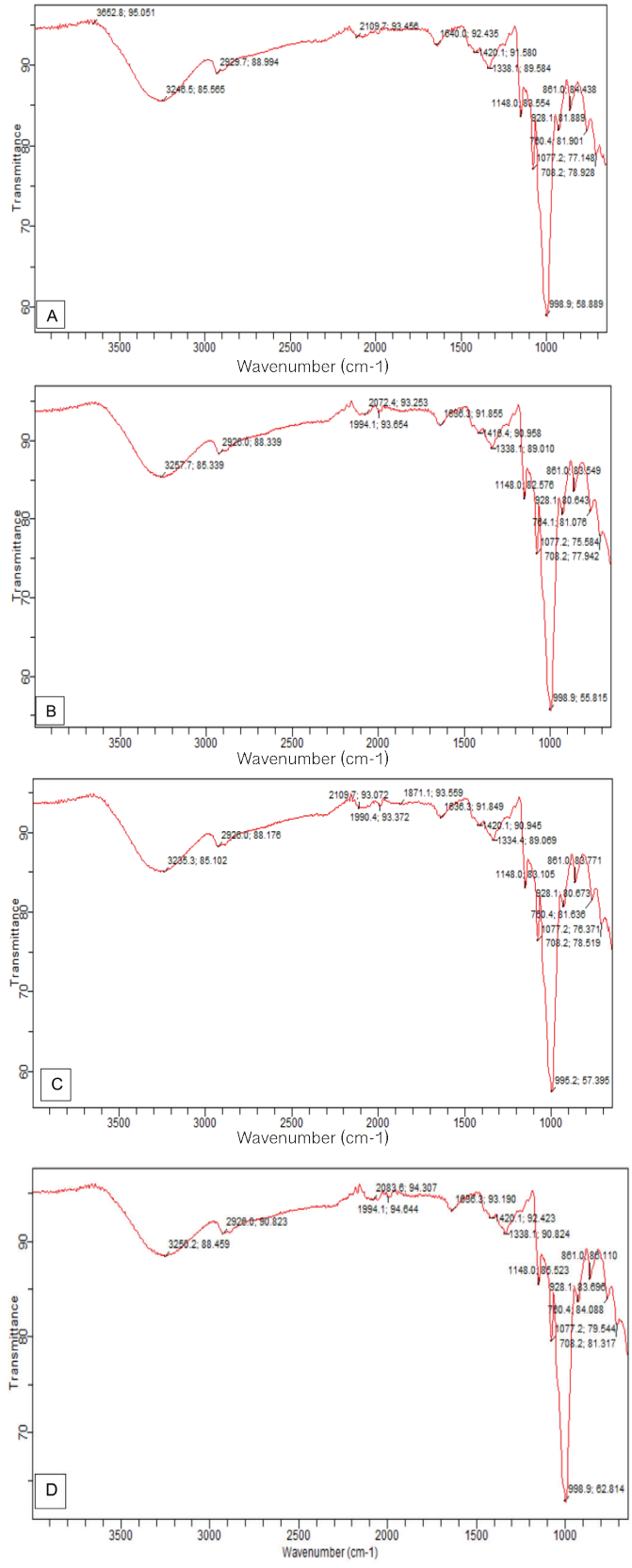

Figure 2. Fourier transform infrared (FTIR) spectra of (A) native Tigernut starch, (B) crosslinked starch from day 5 substrate, (C) crosslinked starch from day 10 substrate, (D) crosslinked starch from day 15 substrate

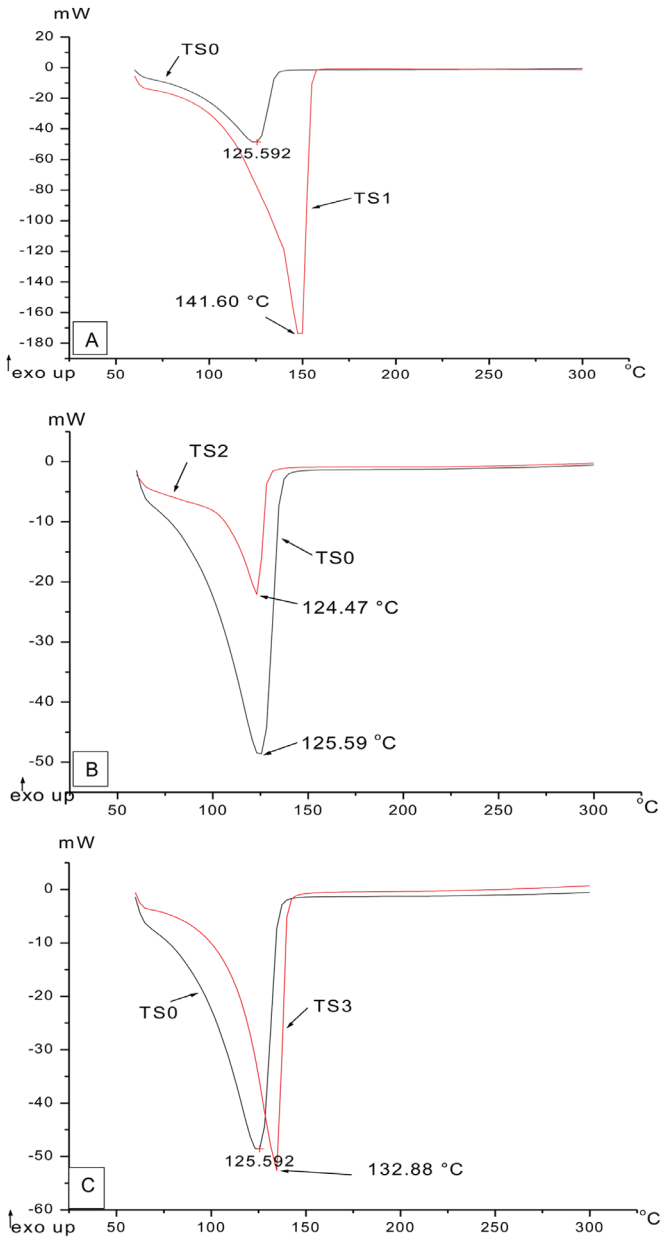

Figure 3. (A) Native Tigernut starch (TS0) and crosslinked starch from day 5 substrate (TS1); (B) TS0 and crosslinked starch from day 10 substrate (TS2); (C) TS0 and crosslinked starch from day 15 substrate (TS3)

starch molecule is broken and melted during the heating process. Considered to be the result of dissimilar bond forces within the starch granules are the differences in ΔH.[52] Higher gelatinization enthalpies as observed with TS0 and TS1, 1926.95 and 2120.73 J/(g*K), respectively, shows that higher energy is required to disentangle these bonds compared with those of TS2 and TS3; thus, showing the crosslinking effect on bond rearrangement within the starch granules. Therefore, TS1 would function as a better binder than TS2 and TS3.

Generally, higher T_o, T_p, and T_c of the modified starches suggest high degree of crystalline association within those granules than in TS0; these resulted in higher structural stability and resistance to gelatinization as previously reported.[53] Low temperatures observed in TS0 could be an indication of low stability of starch molecules because of weak molecular arrangement, which corroborates with the theory that native starches are generally unable to withstand industrial temperatures.

Peak height index (PHI) is an indication of starch granules distribution and its uniformity during gelatinization. Table 6 shows a reduction in the peak height of TS1 and TS2 in relation to TS0, which could be attributed to the effect of increasing the concentration of the crosslinking substrate. PHI and ΔT are observed to be negatively related; the wider the temperature range as a result of higher gelatinization temperature, the smaller the PHI as observed with TS1. This suggests that the modified starches could be effective as a binding agent in solid dosage formulations.

CONCLUSION

We proved in this study that agricultural waste constituting environmental nuisance, such as orange peels, could be employed as raw material for the green synthesis of starch obtained from *C. esculentus* tubers. Results obtained shows that modified TS had better water-holding capacity and thermal stability while retaining its microstructural properties, which suggests that it may perform well as binding agents in food and pharmaceutical industries.

ACKNOWLEDGMENTS

The authors are grateful to the technical staff of the Department of Pharmaceutical Technology and Raw Materials Development, NIPRD for their support during the course of this study.

Conflicts of interest: No conflict of interest was declared by the authors. The authors alone are responsible for the content and writing of the paper.

REFERENCES

1. Adebayo AS, Itiola OA. Effects of breadfruit and cocoyam starch mucilage binders on disintegration and dissolution behaviors of paracetamol tablet formulations. J Pharm Tech. 2003;80:78-90.
2. Manek RV, Builders PF, Kolling WM, Emeje M, Kunle OO. Physicochemical and binder properties of starch obtained from *Cyperus esculentus*. AAPS PharmSciTech. 2012;13:379-388.
3. Esezobo S, Ambujam V. An evaluation of starch obtained from plantain *Musa paradisiaca* as a binder and disintegrant for compressed tablets. J Pharm Pharmacol. 1982;34:761-765.
4. Muazu J, Musa H, Bhatia PG. Evaluation of the glidant property of Fonio starch. Res J App Sci Eng Tech. 2010;2:149-152.
5. Khunkitti W, Aromdee C, Vorarat S, Chitropas P. The potential of jackfruit starch for use as suspending agent and emulsifying agent. Songklanakarin J Sci Technol. 2006;8:145-155.
6. Onyishi IV, Chime SA, Kanu I. Application of *Ipomea batatas* starch as suspending agent in Acetaminophen suspension. Afr J Pharm Pharmacol. 2014;8:24-30.

7. Omojola M, Orishadipe AT, Afolayan M, Adebiyi AB. Preparation and physicochemical characterization of *icacina* starch citrate - a potential pharmaceutical/industrial starch. Agric Biol J N Am. 2012;3:11-16.
8. Alcázar-Alay CS, Meireles MAA. Physicochemical properties, modifications and applications of starches from different botanical sources. Food Sci Tech (Campinas). 2015;35:215-236.
9. Isah S, Oshodi AA, Atasie VN. Physicochemical properties of cross linked acha (*Digitaria exilis*) starch with citric acid. Chem Int. 2017;3:150-157.
10. Tomasik P, Zaranyika MF. Nonconventional methods of modification of starch. Adv Carbohd Chem Biochem. 1995;51:243-318.
11. Rusli D, Azronnizan Q, Maaruf AG, Nik IND, Bohari MI. Hydroxypropylation and acetylation of sago starch. Malay J Chem. 2004;6:48-52.
12. Neelam K, Vijay S, Lalit S. Various techniques for the modification of starch and the applications of its derivatives. Int Res J Pharm. 2012;3:25-31.
13. Yadav BS, Guleria P, Yadav RB. Hydrothermal modification of Indian water chestnut starch: Influence of heat-moisture treatment and annealing on the physicochemical, gelatinization and pasting characteristics. LWT - Food Sci Tech (Campinas). 2013;53:211-217.
14. Abbas KA, Khalil SK, Hussin ASM. Modified starches and their usages in selected food products: A Review Study. J Agric Sci. 2010;2:90-100.
15. Maitra J, Shukla VK. Cross-linking in Hydrogels - A Review. Amer J Pol Sci. 2014;4:25-31.
16. Shah N, Mewada RK, Mehta T. Crosslinking of starch and its effect on viscosity behavior. Rev Chem Eng. 2016;32:265-270.
17. Singh J, Kaur L, McCarthy OJ. Factors influencing the physicochemical, morphological, thermal and rheological properties of some chemically modified starches for food applications: A Review. Food Hydrocoll. 2007;21:1-22.
18. Hirsch JB, Kokini JK. Understanding the mechanism of cross-linking agents (POCL3, STMP, and EPI) through swelling behavior and pasting properties of cross-linked waxy maize starches. Cereal Chem. 2002;79:102-107.
19. Wattanachanta S, Muhammad K, Hashimb DM, Rahmanb RA. Effect of crosslinking reagents and hydroxypropylation levels on dual-modified sago starch properties. Food Chem. 2003;80:463-471.
20. Yin L, Zhu Z. Research on the preparation of crosslinked starch chlorinated with sodium hypochlorite. Wuhan University J Nat Sci. 2003;8:861-865.
21. Chowdary KPR, Chaithanya KK. Preparation and evaluation of cross linked starch urea. A new polymer for controlled release of Aceclofenac. Asian J Chem. 2010;22:4265-4270.
22. Omojola MO, Manu N, Thomas SA. Effect of cross linking on the physicochemical properties of *cola* starch. Afr J Food Sci. 2012;6:91-95.
23. Torrado AM, Cortés S, Manuel Salgado J, Max B, Rodríguez N, Bibbins BP, Converti A, Manuel Domínguez J. Citric acid production from orange peel wastes by solid-state fermentation. Braz J Microbiol. 2011;42:394-409.
24. Soccol CR, Vandenberghe LPS. Overview of applied solid state fermentation in Brazil. Biochem Eng J. 2013;13:205-218.
25. Balasundram N, Sundram K, Samman S. Phenolic compounds in plants and agri-industrial by-products: Antioxidant activity, occurrence, and potential uses. Food Chem. 2006;99:191-203.
26. Rabetafika HN, Bchir B, Blecker C, Richel A. Fractionation of apple by-products as source of new ingredients: Current situation and perspectives. Trends Food Sci Technol. 2014;40:99-114.
27. Dhandayuthapani K, Thiyageswaran G, Kumar R. Production of citric acid from banana waste by *Aspergillus niger*. Int J App Bioeng. 2008;2:1-3.
28. Vafina A, Proskurina V, Vorobiev V, Evtugin VG, Egkova G, Nikitina E. Physicochemical and morphological characterization of potato starch modified by bacterial amylases for food industry applications. J Chem. 2018;8:1-9.
29. Rohr M, Kubicek CP, Kominek J. Citric acid. In- Biotechnology, Reed, G. and Rehm, HJ. (Eds.), Verlag-Chemie, Weinheim; 1983:419-454.
30. Pandey A, Soccol CR. Bioconversion of biomass: A case study of lignocellulosics bioconversions in solid state fermentation. Brazilian Arch Biol Technol. 1998;41:379-390.
31. Kunle OO, Ibrahim YE, Emeje MO, Shada S, Kunle Y. Extraction and physicochemical compaction properties of *Tacca* starch- a Potential Pharmaceutical excipient. Starch/Stärke. 2003;55:319-325.
32. Adebiyi AB, Omojola MO, Orishadipe AT, Afolayan MO, Olalekan D. *Tacca* starch citrate - A potential pharmaceutical excipient. Arch. Appl. Sci. Res. 2011;3:114-121.
33. Kornblum SS, Stoopak SB. A new tablet disintegrating agent: Cross-linked polyvinylpyrrolidone. J Pharm Sci. 1973;62:43-49.
34. Yokoya F. Citric Acid Production. In: Industrial Fermentation Series, Campinas, SP, Brazil; 1992:1-82.
35. Mohammadi MS, Harnby N. Bulk density modelling as a means of typifying the microstructure and flow characteristics of cohesive powders. Powder Technol. 1997;92:1-8.
36. Kenneth A, Afolayan MO, Oberafo AA, Thomas S. Isolation and physicochemical characterization of Tigernut (*Cyperus esculentus*) starch as a potential industrial biomaterial. Int J Mat Sci App. 2014;3:37-41.
37. Coursey DG, Rasper V. Properties of starches of some West African yams. J Sci Food Agric. 1967;18:240-248.
38. Akpa JG, Dagde KK. Modification of cassava starch for industrial uses. Int J Eng Tech. 2012;2:913-919.
39. Emeje M, Kaita R, Isimi C, Buragohain A, Kunle O, Ofoefule S. Synthesis, physicochemical characterization and functional properties of an esterified starch. Afr J Food Agric Nutr Dev. 2012;65:369-374.
40. Isah S. Chemical modification of grains starch for improved functionality. Int J Chem Mat Sci. 2018;1:6-16.
41. Mariod AA. Gum arabic: structure, properties, application and economics, London, United Kingdom: Elsevier Ltd. Academic Press; 2018.
42. Jyothi AN, Moorthy SN, Sreekumar JN, Rajasekharan KN. Studies on the properties of citrate derivatives of cassava (*Manihot esculenta Crantz*) starch synthesized by microwave technique. J Sci Food Agric. 2007;87:871-879.
43. British Pharmacopoeia (BP).Vol. I and II: Her Majesty's stationary office, university, press, Cambridge, London; 2002.
44. Adane M, Endale A, Bultosa G, Abdel-Mohsen MG, Gebre-Mariam T. Isolation and physicochemical characterization of Godare (*Colocasia esculenta*) starch from Ethiopia. Ethiop Pharm J. 2006;24:13-22.

45. Emeje M, Isimi C, Kunle O. Effect of Grewia gum on the mechanical properties of paracetamol tablet formulations. Afr J Pharm Pharmacol. 2008;2:1-6.

46. Ohwoavworhua FO, Adelakun TA. Some physical characteristics of microcrystalline cellulose obtained from raw cotton of *Cochlospermum planchonii*. Trop J Pharm Res. 2005;4:501-507.

47. Loss PJ, Hood LF, Graham HD. Isolation and characterization of starch from Breadfruit. Cereal Chem. 1981;58:282-286.

48. Omojola MO, Akinkunmi YO, Olufunsho KO, Egharevba HO, Martins EO. Isolation and physicochemical characterization of *Cola* starch. Afr J *Food* Agric Nutr Dev. 2010;10:2884-2900.

49. Xie X, Liu Q. Development and physicochemical characterization of new resistant citrate starch from different corn starches. Starch/Stärke. 2004;56:364-370.

50. Babu AS, Parimalavalli R, Jagannadham K, Rao JS. Chemical and structural properties of sweet potato starch treated with organic and inorganic acid. J Food Sci Technol. 2015;52:5745-5753.

51. Park IM, Ibanez AM, Zhong F, Shoemaker CF. Gelatinization and Pasting Properties of Waxy and Non-waxy Rice Starches. Starch/Stärke. 2007;59:388-396.

52. McPherson AE, Jane J. Comparison of waxy potato with other root and tuber starches. Carbohyd Polym. 1999;40:57-70.

53. Bhupender SK, Rajneesh B, Baljeet SY. Physicochemical, functional, thermal and pasting properties of starches isolated from pearl millet cultivars. Int Food Res J. 2013;20:1555-1561.

Turk J Pharm Sci 2021;18(1):44-55
DOI: 10.4274/tjps.galenos.2019.98624

ORIGINAL ARTICLE

Development of a Novel Freeze-dried Mulberry Leaf Extract-based Transfersome Gel

Dondurularak Kurutulmuş Dut Yaprağı Ekstresi Bazlı Yeni Bir Transferzom Jelinin Geliştirilmesi

Sopan NANGARE[1]*, Dhananjay BHATANE[2], Rushikesh MALI[2], Mayuri SHITOLE[3]

[1]H.R. Patel Institute of Pharmaceutical Education and Research, Department of Pharmaceutical Chemistry, Dhule, India
[2]Bharati Vidyapeeth College of Pharmacy, Department of Pharmaceutics, Maharashtra, India
[3]Murli Krishna Pharma Pvt. Ltd., Department of Process Development Lab, Maharashtra, India

ABSTRACT

Objectives: Nowadays, antioxidants are important for health-related concerns related to acne vulgaris. Acne vulgaris is interrelated with the development of free radicals that interact with cells. Mulberry leaves contain phenolic compounds, including antioxidants such as quercetin. An antioxidant is a scavenger of free radicals. The current study addresses the development of a mulberry leaf extract-based transfersome gel containing quercetin by a thin-layer hydration method for topical antioxidant delivery. The process was optimized by encapsulating the drug in a variety of transfersome formulations.

Materials and Methods: Batch optimization was carried out by particle size and zeta analysis, entrapment efficiency (%), polydispersity index, *in vitro* drug release, and drug content analysis.

Results: The optimized batch MF5 provided 86.23% entrapment efficiency of quercetin in the vesicles and 95.79% drug release. It furnished a spherical shaped vesicle with an average diameter of 118.7 nm and zeta potential of -45.11 mV. The MG1 formulation provided superior antioxidant activity, drug content, and entrapment efficiency, *ex vivo* drug release, spreadability, homogeneity, and stability to MG2. The presence of quercetin in the extract and gel formulation was confirmed by using high performance thin layer chromatography.

Conclusion: It is evident from this study that a mulberry leaf extract-based transfersome gel is a promising prolonged delivery system for quercetin and has reasonably good stability characteristics. This research recommends that mulberry leaf extract-based transfersome gel can potentially be used in the treatment of acne vulgaris through a transdermal drug delivery system.

Key words: Transfersomes, mulberry leaves, quercetin, antioxidant activity, transfersome gel

ÖZ

Amaç: Günümüzde antioksidanlar, akne vulgaris bağlantılı sağlık sorunları için önemlidir. Akne vulgaris, hücrelerle etkileşime giren serbest radikallerin gelişimi ile ilişkilidir. Dut yaprakları, kuersetin gibi antioksidanlar da dahil olmak üzere fenolik bileşikler içerir. Bir antioksidan, serbest radikal temizleyicisidir. Bu çalışma, topikal antioksidan taşınımı için ince tabaka hidrasyon yöntemi ile kuersetin içeren dut yaprağı ekstresi bazlı transferzom jeli geliştirilmesini ele almaktadır. İşlem, ilacı çeşitli transferzom formülasyonları ile enkapsüle ederek optimize edildi.

Gereç ve Yöntemler: Seri optimizasyonu için partikül boyutu, zeta analizi, yükleme etkinliği (%), polidispersite indeksi, *in vitro* ilaç salımı ve ilaç içeriği analizleri gerçekleştirildi.

Bulgular: Optimize edilmiş MF5 serisinin, enkapsülasyon etkinliği %86,23 ve kersetin salımı %95,79 olarak bulundu. Ortalama çapı 118,7 nm ve zeta potansiyeli -45,11 mV olan küresel şekilli morfolojiye sahip oldukları tespit edildi. MG2 formülasyonuna göre MG1 formülasyonu üstün antioksidan aktivite, ilaç içeriği, enkapsülasyon etkinliği, *ex vivo* ilaç salımı, dağılabilirlik, homojenlik ve stabilite sağladı. Ekstre ve jel formülasyonunda kersetin varlığı, yüksek performanslı ince tabaka kromatografisi kullanılarak doğrulandı.

Sonuç: Bu çalışmada, dut yaprağı ekstresi bazlı transferzom jelin, kuersetin için ümit verici uzun süreli ilaç salım sistemi olduğu ve oldukça iyi stabilite özelliklerine sahip olduğu belirlendi. Bu araştırma, dut yaprağı ekstresi bazlı transferzom jelin potansiyel olarak bir transdermal ilaç taşıyıcı sistem aracılığıyla akne vulgaris tedavisinde kullanılabileceğini önermektedir.

Anahtar kelimeler: Transferzomlar, dut yaprakları, kuersetin, antioksidan aktivite, transferzom jel

***Correspondence:** snangareopan@gmail.com, **Phone:** +919561141110 **ORCID-ID:** orcid.org/0000-0002-6513-3336
Received: 06.08.2019, **Accepted:** 05.12.2019

INTRODUCTION

In the modern era, acne is the most common skin disease worldwide.[1] The research scenario indicates that approximately 85% of the world's population between 11 and 30 years is affected at some point in their lifetime. Approximately 4.8 million peoples per year are affected by acne.[2,3] Principally, it is a multifactorial disease of the pilosebaceous unit, which manifests as comedones or severe inflammatory lesions[4,5] in the skin, mainly on the face. This is related to the elevated rate of sebum excretion, abnormal proliferation of keratinocytes, overload production of male hormone androgens, oil-producing glands on the face, and inflammatory response initiated by bacterial antigens and cytokines.[6] In addition, oxidative stress is a major factor responsible for skin diseases such as acne. Principally, oxidative stress is initiated by free radicals/reactive oxygen species (ROS).[7,8] In acne vulgaris, the sebum contains hydroxyl radicals, nitrous oxide, and ROSs such as superoxide, which creates irritation during acne, inflammation, etc. Interestingly, active ingredients in plants contain exceptional antioxidant capacity, and scientific reports have revealed that herbal formulations showed the ability to repair damage caused by ROS. Additionally, various scientific reports have revealed that natural antioxidants show fewer adverse effects than synthetic antioxidant compounds.[8] The encapsulation of antiacne drugs in vesicular and particulate delivery systems is in the pioneering stage, and the substitution approach is being taken to minimize their side effects while preserving their efficacy. Presently, the development of a novel drug delivery system has the goal of high therapeutic activity along with patient compliance while conquering the penetration difficulties associated with transdermal drug delivery systems.[9] Traditionally, Morus alba L. (mulberry), generally known as a medicinal plant, has been used. The main content of mulberry leaf extract, which is normally referred to as phenolics such as quercetin [quercetin 3-(6-malonylglucoside)], isoquercetin, rutin, and some other flavonoids, has been identified in mulberry leaves.[10] It has been used to treat inflammation, cough, hypertension, cancer, and fever due to its medicinal value. The polyphenolic compounds in mulberry leaves provide its antioxidant properties by scavenging free radicals and guard many organs against oxidative stress.[11] The utilization of mulberry leaves in formulation development can offer several advantages such as easy availability, low cost, non-toxic formulation, and enhancement of sericulture farming. Plenty of literature has revealed that quercetin reduces the production of interleukin-6 and the expression of metalloproteinase-1 and, consequently, reduces inflammation and fibroblast proliferation.[12] Also, as an antioxidant, quercetin scavenges ROS and ultimately repairs damaged cells. Over the past few decades, sustained and efficient drug delivery systems have gained the noteworthy attention of researchers; transdermal drug delivery is one such system that offers productive significance and advantages.[13] The novel era of drug delivery introduced the use of transfersomes, developed by Gregor Cevc in the year 1991. Transferomes consist of a hydrated core surrounded by an ultra-deformable lipid layer complex.[14] Generally, transfersomes are made by intercellular sealing of lipids, which increases their flexibility, reduces the risk of absolute vesicle rupture in the skin, and permits transfersomes to penetrate the natural water gradient across the epidermis following application to the skin. Transferomes can thus be utilized for the delivery of synthetic and herbal drugs.[15,16] Recently, considerable attention has been focused on developing a new lipidic nanovesicle-based transdermal drug delivery system. Transfersomes are deformable and flexible and have a high affinity for penetration through the skin to the systemic circulation. Transdermal administration of transfersome vesicles offers a great advantage over other vesicles; therefore, we attempted to develop a transfersomal gel formulation of mulberry leaf extract. Subsequently, prepared transfersome gels were evaluated for entrapment efficiency, particle morphology, particle size, zeta potential, polydispersity index (PDI), swelling index, viscosity and pH behavior, fourier transform infrared spectroscopy (FTIR), antioxidant activity, deformability index, and penetration using Franz diffusion cells. High performance thin layer chromatography (HPTLC) was used to analyze the level of active substances contained in the extract. In conclusion, novel transfersomal prepared gel could be used to explore the application of natural mulberry leaf extract containing an antioxidant (quercetin) for the treatment of acne-like skin diseases. Also, it could overcome the drug resistivity and adverse effects of currently challenging acne therapy.

MATERIALS AND METHODS

Material

Mulberry leaves were procured from a local market in Indapur, Maharastra. Ethanol AR (70%) and TWEEN80 were from Loba Chemie (Pvt. Mumbai). PHOSPHOLIPON 90G, Carbapol 940, PROPYLENE GLYCOL, and Formic acid were from Merk Life Sciences. Diethyl ether, Ethyl acetate, Toulene, Petroleum ether, 2,2-diphenyl-1-picrylhydrazyl (DPPH), ascorbic acid, and quercetin were from Yucca Enterprises (Mumbai).

Processing and extraction of mulberry leaves

Mulberry leaves were collected from the local market in Indapur, (MS) India, in July. Briefly, the collected leaves were washed systematically under running water to remove soil and other debris adhered to them. Clean leaves were dried, ground, and passed through a sieve ASTM #30. Mulberry leaf powder (50 g) was subjected to Soxhlet extraction using 70% Ethanol AR as the solvent.[17] Finally, the extract was subjected to physical and phytochemical characterization.

Freeze drying (FD)

The mulberry leaf extract solution was frozen at -20°C for 24 h and then dried using a lyophilizer (Labconco, United Kingdom) at 0.013 mbar pressure and -49°C. The obtained extract powder was milled by mortar and pestle to achieve a fine powder.

Isolation of phytoconstituents

FD extract (3 g) was successively extracted with 50 mL of petroleum ether (fraction 1), 50 mL of diethyl ether (fraction 2), and 50 mL of ethyl acetate (fraction 3), with the assistance of a separatory funnel. Complete extraction was ensured by repeating the extraction 3 times for every batch. Owing to the presence of fatty acids and free flavonoids, respectively, fractions 1 and 2 were rejected. As fraction 3 contained quercetin, it was further processed by concentration and hydrolyzed using 7% sulfuric acid (10 mL/g extract) for up to 5 h. The hydrolyzed fraction was filtered and extracted with ethyl acetate (1:1/ thrice) via a separatory funnel.[18]

Thin-layer chromatography

The isolated portion was chromatographed in comparison with quercetin as a reference standard (std.) along with Silica gel G TLC plates (Indian Herbal Pharmacopeia, 2002) by using toluene:ethyl acetate:formic acid (5:4:0.2) as the mobile phase.[19]

Ultraviolet (UV)-spectrometric analysis

The UV spectra of the isolated quercetin from mulberry leaves, std. quercetin, and the extract were recorded using a UV-visible (Vis) spectrophotometer (Jasco V-630).[20]

Calibration curve

Calibration curve of std. and isolated quercetin

Five working solutions of quercetin with concentrations of 10, 20, 30, 40 and 50 µg/mL in methanol were prepared, and the absorbance was recorded at 246 nm λmax for each sample.

FTIR spectroscopy

The FTIR absorption spectrum of FD mulberry leaf extract was determined by ATR-FTIR (Jasco V-530 model) using the KBr dispersion method.

Antioxidant assay

In vitro antioxidant activity by the DPPH method

DPPH is a rapid and sensitive method to estimate the antioxidant capacity of different plant extracts. Also, the visual observation of antioxidant activity is possible. In brief, antioxidants react with DPPH, which is a steady free radical, and the DPPH is reduced to DPPH-H. Reduction in the absorbance of the solution was measured using a UV-Vis spectrophotometer at 517 nm.[8,21] The potential to scavenge the DPPH radical was measured by the following formula (1).

$$\text{DPPH scavenged (\%)} = \frac{\text{Absorbance of control-absorbance of test}}{\text{Absorbance of control}} \quad \text{.....(1)}$$

Optimization of transfersomes of FD mulberry leaf extract

Preparation of transfersomes

Transfersomes of FD mulberry leaf extract were formulated by the thin-layer hydration method.[22] The composition of transfersomes for batches MF1, MF2, MF2, MF3, MF4, MF5, and MF6 is reported in Table 1. In these techniques, phopholipon 90G (phospholipids), tween 80 (age activator), and mulberry leaf extract were added to a round bottom flask and dissolved in dichloromethane (solvent). Then, the organic solvent was evaporated by using a rotary evaporator above the lipid transition temperature at 50˚C, under reduced pressure at a velocity of 60 rpm. After complete evaporation of the solvent, a thin layer on the inner wall of the flask was observed. Then, the deposited lipid film was rehydrated using phosphate buffer (pH 7.4) until the entire thin layer peeled off. The rehydration process was carried out at a temperature of 37±2˚C, with rotation at 100 rpm for 30 min in the absence of a vacuum. Finally, fully hydrated transfersome suspensions were collected in a vial, then the particle size of the vesicle was reduced by ultrasonication for 5 min with an amplitude of 25.

Morphological characterization

Prepared transfersomes was subjected to morphology evaluation. Herein, the vesicular morphology of transfersomes was observed by Motic microscope.

Percentage entrapment efficiency (%EE)

The %EE test was performed by using an ultracentrifugation method (indirect method) at 10,000 rpm for 10 min at 4˚C, which produces a supernatant as a released drug. Measurement of the total concentration of active compound was performed by dissolving a 1 mL suspension of transfersomes with poly (butylene succinate) pH 6.8 in a 10 mL flask. The concentration measurement was performed by using UV-Vis spectroscopy at 254 nm.[23] The %EE was calculated by using equation (2).

$$\%EE = \frac{\text{C total-C released}}{\text{C total}} \times 100 \quad \text{.....(2)}$$

Where,

C_{total}: Total concentration of quercetin (µg/mL) in transfersomes.

$C_{released}$: Untrapped concentration of active substances (µg/mL) in transfersomes.

Optimization of transfersomes

The number of process variables accounts for the characterization and optimization of the transfersome formulation. Herein, the batch optimization was carried out by particle size analysis, zeta potential, PDI, and %EE.[24]

Table 1. Preparation of Mulberry leaf extract transfersomes

Material name	Concentration (% w/w)					
	MF1	MF2	MF3	MF4	MF5	MF6
Mulberry leaf extract	10	10	10	10	10	10
Tween 80	0.3	0.3	0.3	0.4	0.4	0.4
Phopholipon 90G	2	2.5	3	2	2.5	3
Phosphate buffer (saline pH 7.4)	Add 100	Add 100	Add 100	Add 100	Add 100	Add 100

In vitro drug release of transfersomes

An *in vitro* drug release study was performed by using modified Franz diffusion cells. A dialysis membrane (Hi-Media, Molecular weight 5.000D) was arranged between the receptor and donor compartments. Subsequently, the transfersomes of mulberry leaf extract were kept in the donor compartment, and the receptor compartment was filled sufficiently with phosphate buffer, pH 7.4 (25 mL). The diffusion cells were maintained at 37±0.5˚C with constant stirring at 40 rpm throughout the experiment. At 30, 60, 90, 120, 150, 180, 210, 240, 270, 300, and 360 min intervals, 5 mL aliquots were withdrawn from the receiver compartment through the side tube and again filled with 5 mL and analyzed for drug content by UV-Vis spectroscopy.[25]

Preparation of transfersome gel

Herein, we used the optimized batch of transfersomes (MF5) for preparation of the gel. A 10% (w/v) transfersome suspension was weighed for gel formation. Carbapol 940 was added to purified water with stirring and allowed to hydrate for 24 h. The transfersome suspension was dispersed in the hydrated carbapol 940 slurry and stirred continuously for 30 min. Then, propylene glycol was added slowly to the slurry. The pH of the formulation was adjusted with triethanolamine, and the same procedure was carried out for the control extract-based gel (MG2) (Table 2).[26]

Evaluation of MG and MG2 gel formulation

MG1 and MG2 gel formulations were subjected to organoleptic evaluation, FTIR, homogeneity rate, pH and viscosity measurements, flow property measurements, drug content analysis,[27] and %EE.[28]

Homogeneity rate

The homogeneity of the formulated gel was determined by pressing a small amount of both gels (MG1 and MG2) between the thumb and the index finger. The uniformity was a resolute as a harmonized or not.[29]

Spreadability

A spreadability test of MG1 and MG2 gels was carried out by pressing 0.5 g of the final formulation. Briefly, a sample of the gel from each batch was pressed between 2 translucent spherical glass slides, and the highest degree of spreading was permitted by leaving them for 5 min. The diameter of the formed circle was calculated to articulate the spreadability of the formulated gel.[30]

HPTLC analysis

HPTLC analysis was performed by application of the std. and isolated quercetin, and MG1 formulation. The samples were prepared by using methanol. Subsequently, the analysis of quercetin was performed on the HPTLC plate of silica gel 60F254 (5 cm x10 cm) using a mixture of toluene:ethyl acetate:formic acid as the mobile phase in proportions of 5:4:0.2. Finally, the quercetin dark brown colored bands were identified and confirmed via R_f.[31]

Limit of detection (LOD) and limit of quantification (LOQ)

LOD and LOQ are 2 important terms used to describe the smallest concentration of an analyte that can be reliably measured by an analytical procedure. The LOD and LOQ of compounds were determined based on R_f values as well as UV/Vis spectral overlaying of respective standard compounds. The LOD was determined based on the lowest concentration detected by the instrument from each of 2 standards, while the LOQ was determined based on the lowest concentration quantified in the samples.

The determination of LOD and LOQ was calculated using the formula,

LOD = ¼ 3.3(SD/S).....(3)

LOQ = ¼ 10(SD/S).....(4)

Where,

SD: Standard deviation of the response

S: Slope

Drug content (%)

Accurate quantities of MG1 and MG2 gel were measured into in separate beakers, lysed with 50 mL methanol for 15 min using ultrasonication, and centrifuged at 10,000 rpm for 30 min (25˚C). The clear supernatant was collected, added to 10 mL methanol, and diluted with pH 7.4. The quercetin content was calculated from the absorbance determined using a UV spectrophotometer at 246 nm.

Ex vivo release studies

Fresh hairless abdominal goat skin was collected from a slaughterhouse and used for release studies after peeling the skin from the underlying cartilage placed inside the receptor compartment.[32,33] In brief, using a Franz diffusion cell apparatus, the drug release studies were performed. Goat skin was placed between the donor and receptor compartments. The receptor compartment was filled with the phosphate buffer and ethanol mixture in a ratio of 8:2 (15 mL) at 37±0.5˚C, and gel samples were exposed to the donor compartment. Receptor compartment containing dissolution media was continuouslystirred using magnetc stirrer at 25 rpm, which help to avoid the saturation of dissolution media during the penetration of the active content.[34] For the calculation of percent *ex vivo* drug release, sampling was performed at different time intervals.

Statistical analysis

All outcomes in this work are expressed as a mean ± SD. A paired Student's t-test was used for the comparison of percent

Table 2. Transfersome gel of mulberry leaf extract (MG1) and control extract gel (MG2)

Composition / Concentration (% w/w)	Transfersomes	Extract	Carbapol 940	Triethanolamine	Propylene glycol	Water
MG1	Equal to 10% extract	-	1	0.1	12.5	Add 100
MG2	-	10	1	0.1	12.5	Add 100

ex vivo drug release of 2 related gel samples (MG1 and MG2). Differences at $p<0.05$ was considered significant.

Ex vivo penetration test

An *ex vivo* penetration test of the transfersome gel was carried out on fresh hairless abdominal goat skin through a Franz diffusion cell apparatus assembly. The goat skin was assembled between the donor and receptor compartment with an effective diffusion area of 2.26 cm^2 and a cell volume of 25 mL. Briefly, the receptor compartment contained phosphate buffer and ethanol (8:2) media (15 mL) at body temperature 37±0.5°C and the media in the receptor compartment was stirred. The gel was placed in the donor compartment, and samplings were carried out periodically for 24 h from the receptor compartment. Simultaneously, the sink condition was maintained, and the collected samples were subjected to UV spectrophotometry analysis. Based on the experimental findings, the permeation coefficient was calculated by using the cumulative amounts of drug permeated per unit area (μg/cm^2) vs time graph. The transdermal flux was calculated from the slope of the linear portion of the graph.

Stability study

MG1 and MG2 formulations were stability tested for 3 months at 4°C±2°C and 40°C±2°C 75%±5% RH stations for determination of the physical and chemical stability of the formulations (as per International Council for Harmonisation guidelines).

RESULTS

Characterization of mulberry leaf extract

The extraction was performed by the successive hot continuous Soxhlet extraction method. The ethanolic extract of mulberry leaves was greenish in color. The phytoconstituent analysis revealed the presence of sterols, tannins, phenols, and alkaloids. The pH of the extract was 6.5.

TLC analysis

TLC fingerprinting of mulberry leaf extracts was performed along with std. quercetin under UV 254. It showed that spots representing std. quercetin and isolated quercetin had R_f values of 0.38 and 0.31, respectively (Figure 1). In conclusion, quercetin analysis using TLC confirmed the presence of quercetin in the extract.

Subsequently, the UV spectra of std. quercetin was observed at 254 nm, which confirmed the purity and presence of quercetin in the prepared sample (Figure 2a). Also, the UV spectra of isolated quercetin from mulberry leaf extract were obtained at 246 nm and confirmed the existence of quercetin in the extract (Figure 2b).

Calibration curve of standard quercetin and isolated quercetin

The calibration curve of the std. (Figure 3a) and isolated quercetin (Figure 3b) showed linearity along with 0.999 and 0.996 R^2, respectively, providing confirmation of the purity of quercetin.

FTIR spectra of std and quercetin isolated from mulberry extract

FTIR investigations revealed the presence of quercetin. In brief, std. quercetin showed the peak of O-H stretching vibration at 3387.47 cm^{-1}, whereas O-H bending of phenol function was detectable at 1316 cm^{-1}. The C=C aromatic ring stretch band was at 1605.47 cm^{-1}. The in-plane bending band of in aromatic hydrocarbon was detectable C-H at 1446.70 cm^{-1}. The C=O aryl ketonic stretch absorption was evident at 1659.83 cm^{-1}. Bands at 1165.63 cm^{-1} was attributable to the C-O stretching in the aryl ether ring (Figure 4a). The observed frequencies for isolated quercetin from the extract of mulberry leaves are shown in Figure 4b. It showed the O-H (strong) stretching vibration at 3288.26 cm^{-1}, and C-H stretching vibration at 2916.94 cm^{-1}. The C=O aryl ketonic stretch absorption was evident at 1731.51cm^{-1}.The in plane bending band of in aromatic hydrocarbon was detectable C-H bending at 1415.10 cm^{-1}. Bands at 1026.95 cm^{-1} was attributable to the C-O stretching in the aryl ether ring at 1026.95 cm^{-1}. Overall, it provides confirmation of quercetin present in the extract (Figure 4b). These pragmatic frequencies confirmed that the isolated fraction was quercetin in reference to std. quercetin.

Antioxidant activity

The antioxidant activity of the FD extract showed an excellent result in contrast to standard ascorbic acid. Quercetin isolated from mulberry leaves, ascorbic acid (std.), and std. quercetin furnished antioxidant activity of 67.2%, 83.20%, and 69.54%

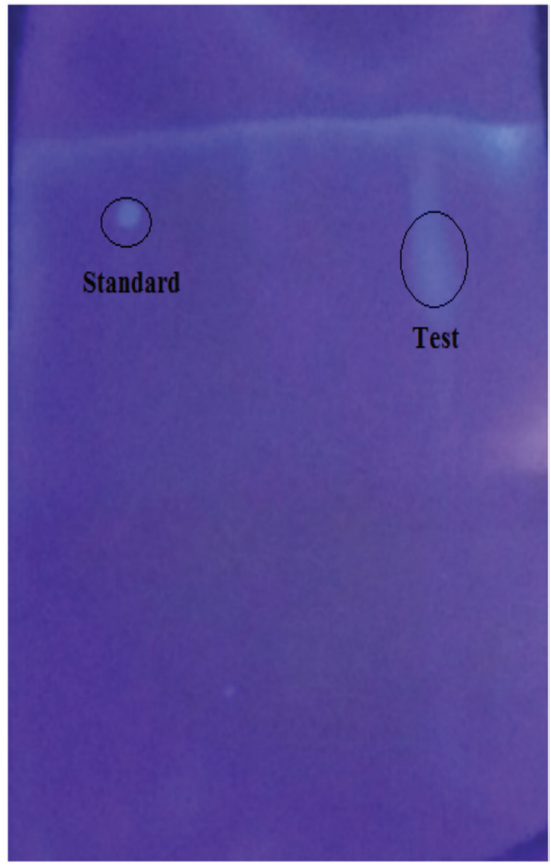

Figure 1. TLC plate developed under UV light at 254 nm
TLC: Thin layer chromatography, UV: Ultraviolet

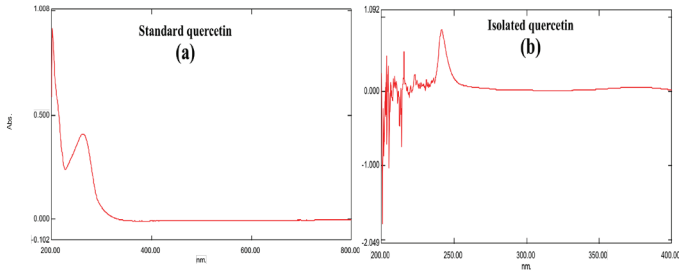

Figure 2. UV spectra of standard quercetin (a) isolated quercetin (b)
UV: Ultraviolet

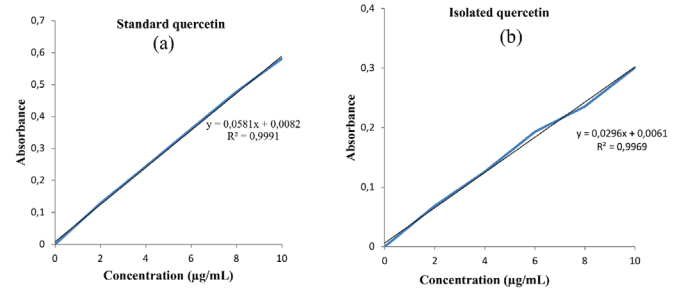

Figure 3. Calibration curve of standard quercetin (a) and isolated quercetin (b)

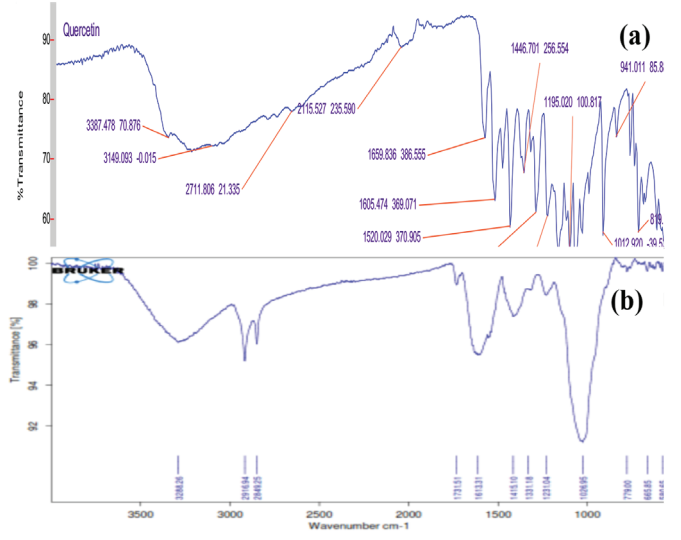

Figure 4. FTIR spectra of standard quercetin (a) and isolated quercetin (b)
FTIR: Fourier transform infrared spectroscopy

consistently. In conclusion, free- radical scavenging capacity of isolated quercetin and standard quercetin was found similar.

Characterization and optimization of transfersomes

Shape of the vesicle

The shape of the vesicle by Motic microscopy revealed no aggregation or irregularities in transfersomes, and the spherical structures of vesicles were observed in the range of 110 to 460 nm in diameter. Hence, the successful construction of transfersome vesicles was confirmed (Figure 5).

Optimization of transfersomes

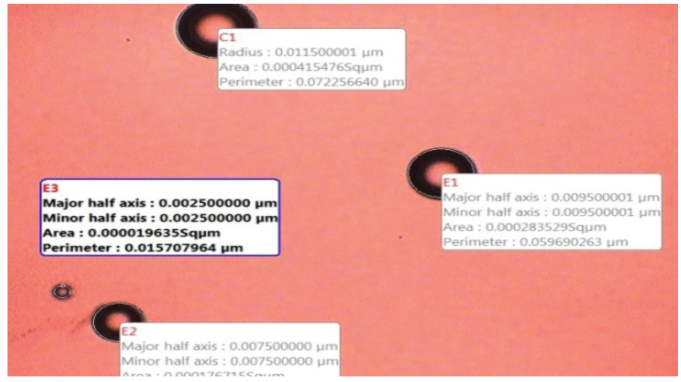

Figure 5. Unsonicated transfersomes vesicles by Motic microscopy

Particles size analysis and PDI

The size distribution of the transfersome suspension was determined by a particle size analyzer (nanoplus) which works by photon correlation spectroscopy (Table 3). Owing to the surfactant, the vesicle size observed was within the range of 114.5 to 416.6 mm. The PDI values of the formulation were observed in the range of 0.270 to 0.628. Based on the particle size and PDI value, it was concluded that the particle size distribution was consistent within the formulation.

Zeta potential

The Zeta potential provides knowledge of particle aggregation or flocculation in suspension. Herein, the transfersome batch (MF1 to MF6) showed a zeta potential in the range of -21.19 to -45.11 mV. These results specify the stability of the transfersomes in a suspension.

Percent entrapment efficiency

Table 3. Characterization and optimization of prepared transfersomes

Batch no	Particle size	Zeta potential	PDI	%EE	Deformability index
MF1	381.9 nm	21.19 mV	0.511	68.23±1.2	3.52±0.9
MF2	214.5 nm	-44.56 mV	0.421	65.23±1.1	3.63±0.5
MF3	268.3 nm	-21.91 mV	0.448	76.23±0.9	2.25±1.3
MF4	401.9 nm	-22.39 mV	0.270	77.65±1.6	3.5±2.1
MF5	**118.7** nm	**-45.11** mV	**0.389**	**86.23±2.1**	**1.03±0.8**
MF6	416.6 nm	-27.73 mV	0.628	80.23±1.8	2.05±1.5

n=3, ± standard deviation, PDI: Poly dispersity index, EE: Entropment afficiency

%EE was calculated by using the ultracentrifugation method. In brief, the un-entrapped drug was separated and the amount of it calculated. Subsequently, the EE was calculated for transfersomes. From the estimation of the %EE, the MF1 to MF6 showed 57.65 to 86.23 %EE.

In vitro release of transfersomes

The determination of percent drug release in phosphate (pH 7.4) was carried out by using the slope of quercetin in phosphate buffer (pH 7.4) calibration curve (Figure 6). The comparison *in vitro* cumulative release from batches MF1 to MF6 in the diffusion study is shown in Figure 7; it was 90.34%, 92.07%, 91.69%, 92.03%, 95.79%, and 91.42%, respectively. Among all the batches, MF5 showed the highest extended-release of 95.79% after 6 h (Figure 7). Herein, based on the %EE, particle size analysis, zeta potential, and PDI, we selected the MF5 batch as the optimized batch and used it for further processes of gel formulation.

FTIR spectra of transfersomes

The FTIR spectra of transfersome gels showed peaks for O-H stretching, C-H stretching, C-O stretching, C=O stretching, C-H bending, and C-O starching around 3334 cm^{-1}, 2923 cm^{-1}, 2853 cm^{-1}, 1620 cm^{-1}, 1453 cm^{-1}, and 1035 cm^{-1}, respectively, which is about same as for std. quercetin FTIR. The appearance of the above peaks in Figure 8 confirmed the presence of quercetin and other compounds. No interaction was found between quercetin and the excipients used in formulation development.

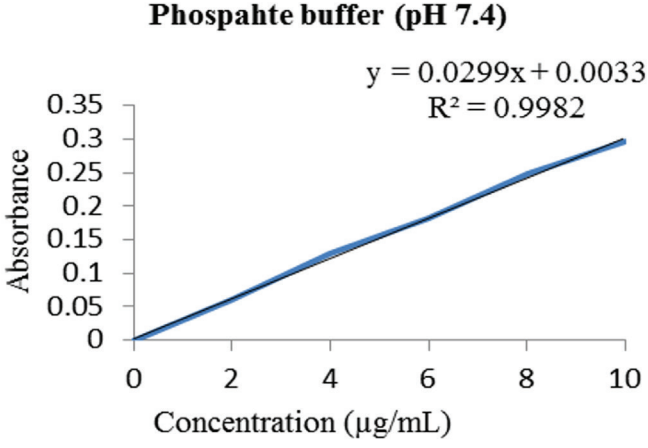

Figure 6. Calibration curve of extract (pH 7.4)

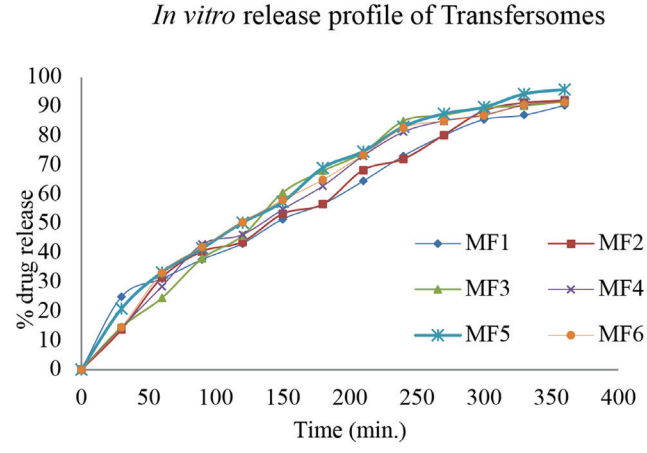

Figure 7. *In vitro* release profile of transfersomes

Evaluation of MG1 and MG2

The MG2 gel showed a greenish color and a glossy appearance due to direct contact between the extract and the gel-forming agent. The MG1 gel furnished a slightly greenish color and a transparent as well as glossy appearance, because the extract was entrapped in the lipid vesicles. Both gels gave off a somewhat sweet odor and demonstrated exceptional homogeneity.

Measurement of the viscosity of MG1 and MG2

The viscosity of MG1 and MG2 gel formulations were determined by using a Brookfield Viscometer at different time intervals (Figure 9). MG1 and MG2 showed a remarkable result for viscosity. This was is because of carbopol, and it could be advantageous to resist drug leakage. Concurrently, the pH of the gel was determined with a digital pH meter (Figure 10), and it showed that MF1 gave a constant pH after 6 h and in the case of MF2, variation in the pH was observed.

Swelling index

The MG1 gel showed good water-holding capacity. Herein, hydrogen bonding facilitates the formation of a structure that

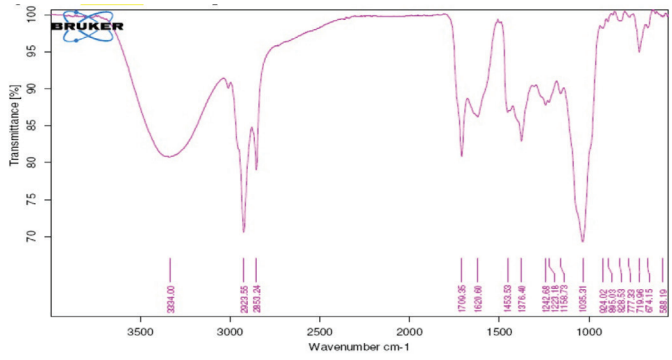

Figure 8. FTIR spectra of transfersomes
FTIR: Fourier transform infrared spectroscopy

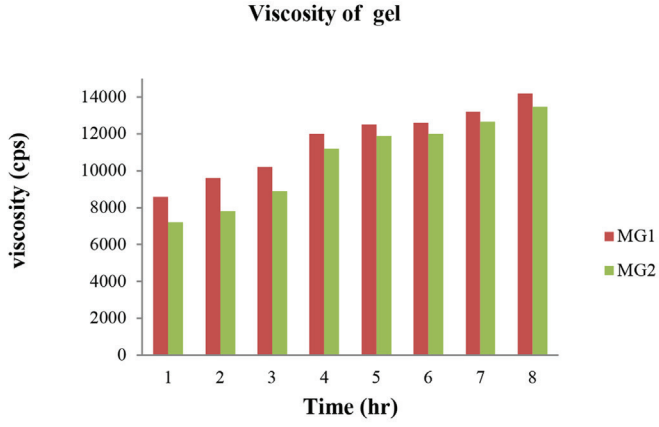

Figure 9. Viscosity of MG1 and MG2 gel

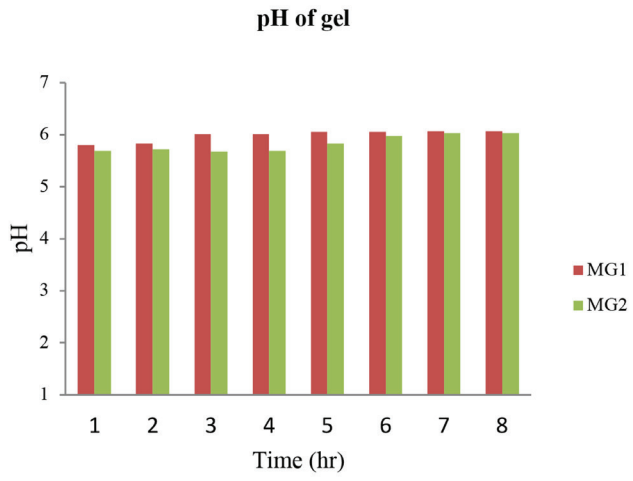

Figure 10. pH of MG1 and MG2 gel

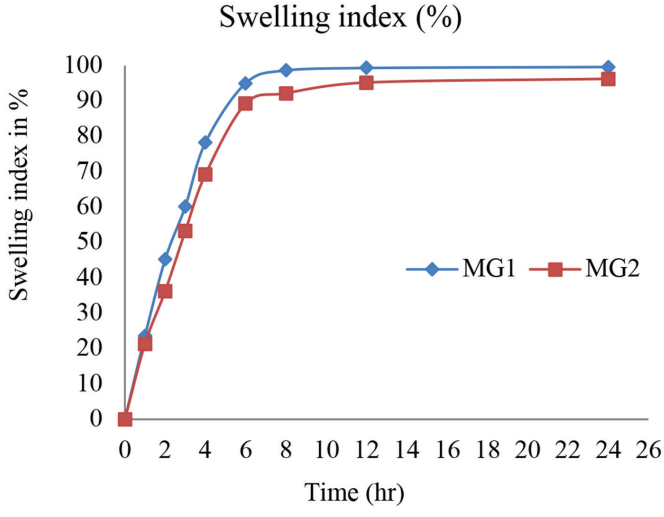

Figure 11. Swelling index of transferosomal gel

allows swelling of the excipients. A comparison of MG1 and MG2 showed a swelling index of up to 99.61% and 96.27 %, respectively (n=3, Figure 11).

Flow properties

The flow properties of MG1 and MG2 gels were computed at different day intervals. It was observed that the MG1 gel showed better flow properties than the MG2 as shown in Table 4. Outcomes of the flow properties concluded that the MG1 provides exceptional tensile strength, elongation rate, and spreadability. MG1 also exhibited a good homogeneity rate as compared with the MG2 batch.

Entrapment efficiency, drug content, and antioxidant activity

The % drug content of the MG1 and MG2 formulations was found to be 98.23% and 89.52%, respectively (Figure 12a). Moreover, the MG1 gel formulation showed superior antioxidant activity (66.72%) as compared with the MG2 gel formulation (59.23%) as shown in Figure 12a. The MG2 gel antioxidant activity and drug content were found to be quite a bit less; this may have been because of the extract becoming degraded during the manufacturing process of the gel. The MG1 and MG2 gel formulation showed 85.6% and 81.20% EE. The formation of multi-laminar vesicle complexes in transfersomes enhances the %EE (Figure 12b).

HPTLC analysis

Optimized parameters for std quercetin, isolated quercetin, and the gel formulation (MG1) containing quercetin by HPTLC at 246 nm are reported in Table 5. The spectrum scan of std. quercetin is comparable with that of an isolated compound and the formulation containing quercetin (Figure 13). For the extract, the retention time was found to be 8.4 min, which coincided with standard quercetin. The results of tests carried on standard and isolated Quercetin and the formulation are summarized in Figure 14. It confirmed the presence of quercetin in the gel formulation, along with the absence of an interaction between excipients and quercetin.

LOD and LOQ

The LOD were determined to be 0.25 and 0.23 ng/spot, and the LOQ was found to be 0.6 and 0.5 ng/spot for std quercetin and isolated quercetin, respectively. The values remained quite similar for both compounds, which revealed the sensitivity of the method.

Ex vivo percent drug release

The *ex vivo* percent drug release of MG1 and MG2 was carried out in phosphate buffer pH 7.4 through goat skin using Franz diffusion cells (Figure 15). The dissolution profile of MG1 (96.86%) showed an excellent drug release as compared with the MG2 (88.23%) up to 24 h. A statistically significant test for comparison of *the ex vivo release* of MG1 and MG2 was performed by a paired t-test. By conventional criteria, the considered difference between MG 1 (transferosome gel) and MG 2 (control gel) was statistically significant at the level of $p<0.05$.

Table 4. Flow properties of MG1 and MG2

Properties	MG1		MG2	
	0 days	10 days	0 days	10 days
Homogeneity rate (1/10 mm)	60.54±1.6	99.58±2.9	59.23±1.2	99.03±3.6
Tensile strength (kg/cm)	30.25±0.9	35.62±1.7	30.01±1.9	33.87±2.8
Elongation rate (%)	200.21±1.4	282.3±2.5	199.56±1.6	276.2±3.1
Spreadability (cm)	9.80±0.9	9.98±0.9	8.01±0.9	8.26±0.9

n=3, ± standard deviation

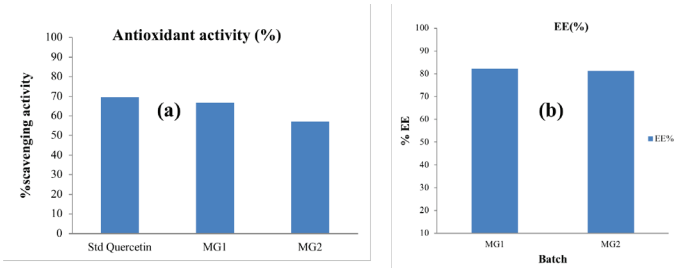

Figure 12. (a, b) Antioxidant properties and %EE of MG1 and MG2 gel

EE: Entropment efficiency

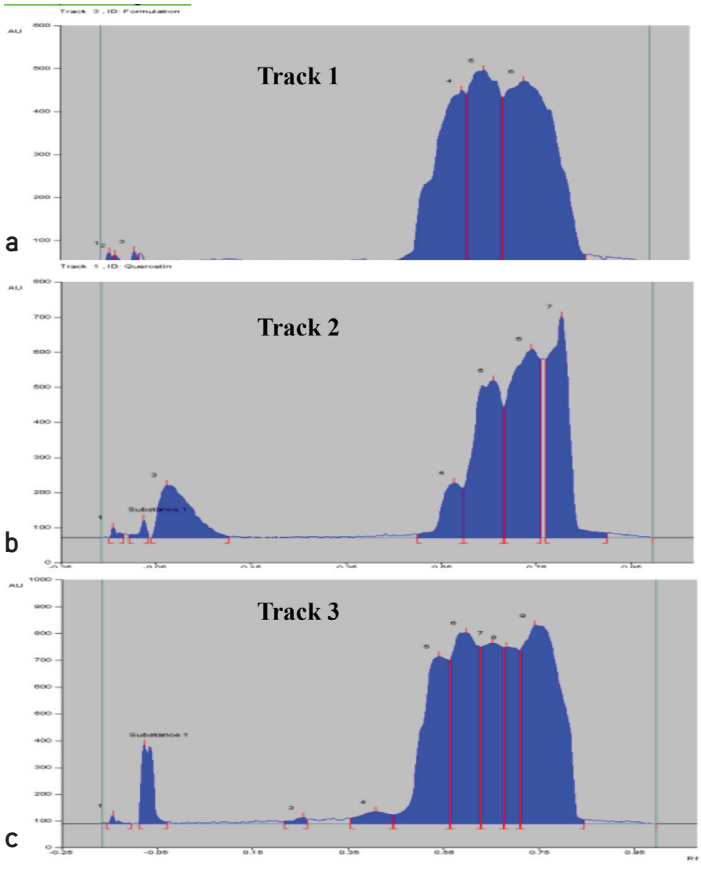

Figure 13. a) standard quercetin (track 1), b) isolated quercetin (track 2) and c) gel formulation (track 3)

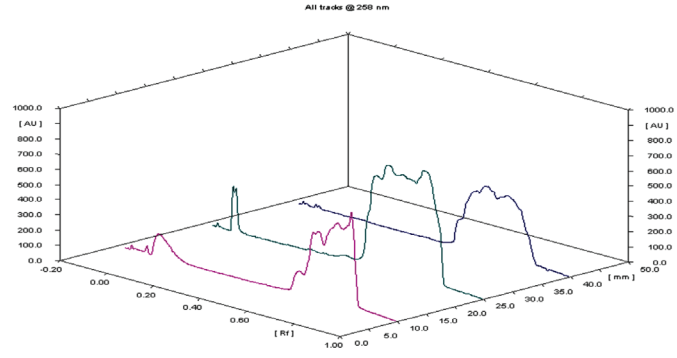

Figure 14. Overlay at 246 nm of standard quercetin, isolated quercetin, and formulation (MG1) in HPTLC

HPTLC: High performance thin layer chromatography

Ex vivo permeation test

The MG1 gel showed better transdermal flux as compared with the MG2 (35.52±3.02 and 26.01±2.02, respectively). Moreover, a superior permeation coefficient was shown for the MG1 (0.016±0.0009) than the MG2 (0.012±0.0003) gel formulation.

Stability studies

After 3 months of stability testing at 4±2˚C and 40±2˚C in sealed glass ampules, negligible drug leakage was confirmed. Based on observation, it was concluded that the MG1 gel formulation was more stable at 4±2˚C as compared with the 40±2˚C. Furthermore, leakage of the drug from the MG1

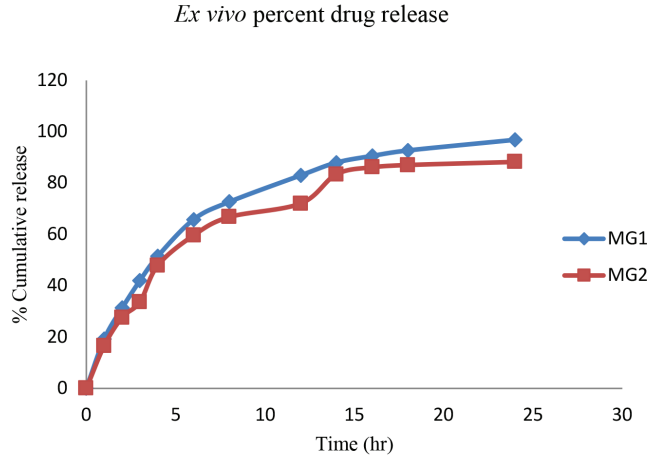

Figure 15. Dissolution profile of MG2 and MG2 gel

Table 5. Optimized Parameters of HPTLC for quercetin isolation

Parameters	Description	Parameters	Description
Stationary phase	Merck Silica gel 60 F254 HPTLC pre-coated plates	Plate size	4.0 cm x10.0 cm
Mode of separation	Normal phase	Development chamber	Camag twin trough chamber
Mobile phase	Ethyl acetate: toluene: formic acid (4:3.5:0.5v/v/v)	Bandwidth	7.0 mm
Chamber saturation	30 min	Space between the bands	7.0 mm
Sample applicator	Camag linomat V	Syringe	Hamilton, 100.0 µL
Distance from the edges of the plat	13.0 mm	Rate of a sample application	150 nL/sec
Lamp and wavelength	Deuterium, 246 nm	Development distance	85.0 mm
Densitometric scanner	Camag scanner IV equipped with win-CATS planar chromatography manager software version 1.4.7		

HPTLC: High performance thin layer chromatography

batch was found to be minimum as compared with the MG2 gel formulation at both stability stations. The viscosity of the carbopol-containing gel prevented the movement and fusion of transfersomes, which resulted in the low drug leakage in gel formulation (MG1). As compared with the drug release of the MG1 gel formulation at zero days after stability, it demonstrated excellent product stability. As a result, there is no major variation seen in MG1, before and after stability (Table 6). Hence, the MG1 transfersome-based gel formulation is more stable without causing any incompatibility, and it shows promising potential for topical application.

Table 6. Stability evaluation of transferosomal gel after 3 months

Properties MG1		Gel formulation MG2	
(4˚C±2˚C)	a- Color	Slightly yellowish	Greenish
	b- pH	5.62±0.23	5.89±0.95
	c- Viscosity (CPS)	14005±230	13202±456
	d- EE (%)	84.96±2.35	78.35±3.69
	e- Drug content (%)	98.01±2.61	89.40±3.10
(40˚C±2˚C)	a- Color	Slightly yellowish	Greenish
	b- pH	5.95±1.02	6.23±1.63
	c- Viscosity (CPS)	13750±412	12889±362
	d- EE (%)	83.69±4.02	73.23±5.06
	e- Drug content (%)	97.96±00.97	84.25±2.96

n=3, ± standard deviation, EE: Entrapment efficiency

DISCUSSION

Gels are a semi-solid dosage form system of drug delivery and constitute a method of good repute among novel pharmaceutical dosage forms. Nowadays, herbal nano lipid vesicle-based gel formulations are gaining attention due to their safe and effective use. In this study, the transfersomes of mulberry leaf extract were prepared by a thin-layer hydration method. Numerous investigations have revealed that quercetin has exceptional antioxidant potential and decreases the production rate of interleukin-6 and the expression of metalloproteinase-1. Consequently, it reduces inflammation and fibroblast proliferation during the healing process. Moreover, plenty of literature claims that ROS is a major factor in skin diseases (example; acne vulgaris), and antioxidant have scavenging potential against ROS. Synthetic antioxidant agents have some adverse/side effects. Thus, the nontoxic nature of herbal antioxidants such as quercetin can be effective in the treatment of acne vulgaris[12]. Herein, the mulberry leaves containing the active antioxidant quercetin were isolated by using TLC and HPTLC, confirmed by using UV spectroscopy and FTIR, and compared by using std quercetin. The fruitful outcomes of TLC and UV spectroscopy provide evidence of successful isolation and confirmation of the purity of quercetin. The FTIR spectra of std. quercetin, isolated quercetin, and the gel formulation (MG1) showed the confirmation of quercetin content and excipient compatibility. In the development of a transfersome formulation, various factors are important. The sizes and shape of the vesicle mainly depend on the concentration of phopholipon 90G and the concentration of surfactants. An increase in the concentration of surfactant increases the EE of vesicles and ultimately prevents drug leakage.[35,36] Outcomes of the experiment are tabulated in Table 3, which reveals that the transfersomes prepared by using a specific concentration of tween 80 and phospholipid showed a superior result as compared with other formulations. Also, the proper proportion of excipients in batch MF5 showed the highest value of %EE (86%). Principally, the particle size of vesicles is an important parameter in the formulation of transfersomes. Generally, particle size distribution is based on volume. Moreover, the dynamic light scattering DLS technique determines the PDI value, which generally ranges from 0 to 0.6. If the value of PDI >0.6, it indicates that the sample has a very broad size distribution. The results showed that the PDI value of each batch changed with particle size (Table 3). The highest PDI value of MF6 was caused by the large particles, which were prone to aggregation.[26,37,38] Zeta potential is an important parameter to describe the stability of the dispersion system. It is used to measure the magnitude of the electrostatic potential or repulsive force among the same electrical charge of particles in suspension. Also, it gives an idea that particles in suspension undergo aggregation or flocculation. Various scientific reports revealed that the zeta potential is stable when more positive than of +30 mV or more negative than -30 mV.[24,26,39] Herein, the results revealed that the MF5 transfersomes were more stable than other formulations because their zeta potential was comparatively high. A negative value of zeta potential might be derived from the lipid composition in the formula. Phosphatidylcholine is a zwitterionic compound with an isoelectric point of 6-7. Also, phosphate buffered saline at pH 7.4 was used as the hydrating medium in the process of vesicle formulation. In that, the pH was slightly higher than the isoelectric point of phosphatidylcholine and due to this, the phosphatidylcholine carried a negative charge.[24] The deformability index is an important parameter in transfersome preparation and generally is used to examine the flexibility of transfersomes. The deformability index value is influenced by the concentrations of phospholipid and surfactant used. The use of excessive surfactant can lower the deformability index value as it can lead to the formation of micelles. At a larger index value of deformability, the transfersomes will be more flexible, which will allow them to penetrate through skin pores smaller than themselves.[40] The results show that MF5 transfersomes had the lowest deformability index. Based on the transfersome characterization results, batch optimization was carried out and the optimal batch further formulated into a gel. The formula selected was a batch with the highest percentage of drug entrapped, an uniform nano-size distribution, a value of the PDI more than ±0.30, and a value of zeta potential more negative than -30 mV. Based on the summary results, MF5 transfersomes was chosen because they had a spherical shape, the highest

percentage of drug entrapped (86.23±2.1%), a PDI of 0.389, a zeta potential value of -45, a Dv90 particle size of 118.7 nm, and a deformability index of 1.03±0.8. Simultaneously, mulberry leaf extract-based gel (MG2) was prepared for evaluation and comparison with MG1. FTIR of the MG1 gel confirmed that there was no interaction between quercetin and excipients. Besides, the MG1 gel formulation showed satisfactory flow properties, viscosity, and stable pH. Also, MG1 gel showed a superior swelling index and the homogeneity rate. The antioxidant assay of MG1 gel showed that the good antioxidant activity as compared with the MG2. In the MG2 formulation, there may be a chance of degradation or interaction between quercetin and excipients and, due to that, the antioxidant activity is slightly diminished. HPTLC analysis was used for further phytochemical and pharmacological investigation of the gel formulation. In the present study, the phytochemical constituent (quercetin) was identified and confirmed based on the color zone obtained during the HPTLC analysis. The color of the zone with isolated quercetin and transferosomes gel formulation the color of the reference compound (std. quercetin) under daylight and UV light after derivatization in the chromatogram confirmed the presence of stable and pure quercetin. This detailed chemical profile may be useful in the identification and quality evaluation of drugs concerning plants. *Ex vivo* percent drug release results conducted on transfersome and control gels showed a significant difference ($p<0.05$). Furthermore, the penetration rate of MG1 was higher vs MG2. These fruitful findings could be related to the negative charge of transfersomes.[41] These negative charges generated the weak electrostatic repulsion between transfersomes and intercellular components of the skin. Subsequently, this repulsion accelerates the penetration of negatively charged transfersomes through follicles of different skin layers. Additionally, the rapid penetration of transfersomes into the intact part of the basal area of follicles occurred.[42] Herein, the hydration and rehydration temperature, as well as rpm used for the development of transfersomes are key parameters in the penetration mechanism of transfersomes. Also, the phase transition temperature of the surfactant, hydrophile-lipophile balance value of the surfactant, saturation, and unsaturation of alkyl chain length play major roles in the penetration mechanism. The prepared M1 gel showed less drug release as compared with the control formulation. A possible reason involved less leakage from vesicles of transfersomes and greater hydration temperature than the gel to liquid phase transition temperature, and along with that, it provides a superior %EE.[43,44] The stability study revealed that the MG1 gel formulation had admirable stability at 4˚C±2˚C and 40˚C±2˚C. The outcomes of the present investigation confirmed that transfersomes of mulberry leaf extract in a gel system offer a new substitute for transdermal drug delivery. Thus, based on the prolific findings, the MG1 gel formulation could be utilized in the treatment of acne.

CONCLUSION

The present study revealed the development of a novel transferosome gel of mulberry leaf extract, with enhanced antioxidant activity as compared with MG2 gel. The optimized batch of transfersomes confirms the excellent zeta potential, particle size, EE (%), PI, deformability index, and *in vitro* percent drug release. Moreover, the MG1 gel *ex vivo* drug release and penetration studies indicated that the developed transfersome gel formulation may serve as a promising carrier for better penetration through the skin as compared with the MG2. Although MG1 gel demonstrated good homogeneity, spreadability, excipient compatibility, and drug content as compared with the MG2, the percent EE and antioxidant properties of MG1 were admirable. Consequently, MG1 batch transfersome gel of mulberry leaf extract offers tremendous antioxidant potential, which creates new opportunities for the topical application for the treatment of acne vulgaris.

ACKNOWLEDGMENTS

The authors wish to thank Ms. Neha Desai, Assistant Professor (Ashokrao Mane College of Pharmacy, Peth-Vadgaon) for her technical support.

Conflicts of interest: No conflict of interest was declared by the authors. The authors alone are responsible for the content and writing of the paper.

REFERENCES

1. Prabu SL, Umamaheswari A, Rajakumar S, Bhuvaneswari P, Muthupetchi S. Development and Evaluation of Gel Incorporated with Synthesized Silver Nanoparticle from Ocimum gratissimum for the Treatment of Acne Vulgaris. American Journal of Advanced Drug Delivery. 2017;5:107-117.
2. Vats A, Sharma P. Formulation and evaluation of topical anti acne formulation of coriander oil. International Journal of Pharmacy and Pharmaceutical Science Research. 2012;2:61-66.
3. Baghel S, Gidwani B, Gupta A. Novel drug delivery systems of herbal constituents used in acne. International Journal of Contemporary Research and Review. 2017;7:57-67.
4. Latter G, Grice JE, Mohammed Y, Roberts MS, Benson HAE. Targeted Topical Delivery of Retinoids in the Management of Acne Vulgaris: Current Formulations and Novel Delivery Systems. Pharmaceutics. 2019;11:490.
5. Ghovvati M, Afshari GK, Nasrollahi SA, Firooz A, Samadi A, Karimi M, Talebi Z, Kolahdooz S, Vazirian M. Efficacy of topical cinnamon gel for the treatment of facial acne vulgaris: A preliminary study. Biomedical Research and Therapy. 2019;6:2958-2965.
6. Tahir CM. Pathogenesis of acne vulgaris: simplified. Journal of Pakistan Association of Dermatology. 2016;20:93-97.
7. Baek J, Lee MG. Oxidative stress and antioxidant strategies in dermatology. Redox Rep. 2016;21:164-169.
8. Vora J, Srivastava A, Modi H. Antibacterial and antioxidant strategies for acne treatment through plant extracts. Informatics in Medicine Unlocked. 2018;13:128-132.
9. Thakur N, Jain P, Jain V. Formulation development and evaluation of transferosomal gel. Journal of Drug Delivery Therapeutics. 2018;8:168-177.

10. Bown D. The Royal Horticultural Society encyclopedia of herbs & their uses: Dorling Kindersley Limited; 1995.
11. Pujari A, Jadhav N. Design and development of anti-diabetic tablet formulation containing spray dried extract of mulberry leaves. Int J Pharm Sci Res. 2019;10:1501-1509.
12. Lubtikulthum P, Kamanamool N, Udompataikul M. A comparative study on the effectiveness of herbal extracts vs 2.5% benzoyl peroxide in the treatment of mild to moderate acne vulgaris. J Cosmet Dermatol. 2019;18:1767-1775.
13. Bhasin B, Londhe VY. An overview of transfersomal drug delivery. International Journal of Pharmaceutical Sciences and Research. 2018;9:2175-2184.
14. Vinod KR, Kumar MS, Anbazhagan S, Sandhya S, Saikumar P, Rohit RT, Banji D. Critical issues related to transfersomes - novel vesicular system. Acta Sci Pol Technol Aliment. 2012;11:67-82.
15. Rajan R, Jose S, Mukund VP, Vasudevan DT. Transferosomes - A vesicular transdermal delivery system for enhanced drug permeation. J Adv Pharm Technol Res. 2011;2:138-143.
16. Malakar J, Sen SO, Nayak AK, Sen KK. Formulation, optimization and evaluation of transferosomal gel for transdermal insulin delivery. Saudi Pharm J. 2012;20:355-363.
17. Zou Y, Liao S, Shen W, Liu F, Tang C, Chen CY, Sun Y. Phenolics and antioxidant activity of mulberry leaves depend on cultivar and harvest month in Southern China. Int J Mol Sci. 2012;13:16544-16553.
18. Sanghavi N, Srivastava R, Malode Y. Isolation and identification of the flavonoid "quercetin" from tridax procumbens linn. International Journal of Pharmaceutical Sciences and Research. 2014;5:1454-1459.
19. Sajeeth C. Quantitative estimation of gallic acid, rutin and quercetin in certain herbal plants by HPTLC method. Der Chemica Sinica. 2010;1:80-85.
20. Patil V, Angadi S, Devdhe S. Determination of quercetin by uv spectroscopy as quality control parameter in herbal plant: Cocculus hirsutus. J Chem Pharm Res. 2015;7:99-104.
21. Iqbal S, Younas U, Sirajuddin, Chan KW, Sarfraz RA, Uddin K. Proximate composition and antioxidant potential of leaves from three varieties of Mulberry (Morus sp.): a comparative study. Int J Mol Sci. 2012;13:6651-6664.
22. Chauhan P, Tyagi BK. Herbal novel drug delivery systems and transfersomes. Journal of Drug Delivery and Therapeutics. 2018;8:162-168.
23. Rahmi AD, Pangesti DM. Comparison of the Characteristics of Transfersomes and Protransfersomes Containing Azelaic Acid. J Young Pharm. 2018;10:S11-15.
24. Duangjit S, Opanasopit P, Rojanarata T, Ngawhirunpat T. Characterization and *In Vitro* Skin Permeation of Meloxicam-Loaded Liposomes versus Transfersomes. J Drug Deliv. 2011;2011:418316.
25. Laxmi M, Zafaruddin M. Design and characterization of transferosomal gel of repaglinide. Int Res J Pharm. 2015;6:37-41.
26. Surini S, Djajadisastra J. Formulation and *in vitro* Penetration Study of Transfersomes Gel Containing Gotu Kola Leaves Extract (Centella asiatica L. Urban). J Young Pharm. 2018;10:27-31.
27. Ali MFM, Salem HF, Abdelmohsen HF, Attia SK. Preparation and clinical evaluation of nano-transferosomes for treatment of erectile dysfunction. Drug Des Devel Ther. 2015;9:2431-2447.
28. Laxmi M, Zafaruddin M, Kuchana V. Design and characterization of transferosomal gel of repaglinide. Int Res J Pharm. 2015;6:37-41.
29. Preeti MSK. Development of celecoxib transfersomal gel for the treatment of rheumatoid arthritis. Indian J Pharm Biol Res. 2014;2:7-13.
30. Mulani H, Bhise K. QbD Approach in the formulation and evaluation of Miconazole Nitrate loaded ethosomal cream-o-gel. Int Res J Pharm Sci. 2017;8:1-37.
31. Movaliya V, Zaveri M. HPTLC method development and estimation of quercetin in the alcoholic extract of Aerva javanica root. Advance Research in Pharmaceuticals and Biologicals. 2012;2:222-228.
32. Patel R, Singh S, Singh S, Sheth N, Gendle R. Development and characterization of curcumin loaded transfersome for transdermal delivery. J Pharm Sci Res. 2009;1:71-80.
33. Kaza R, Pitchaimani R. Formulation of transdermal drug delivery system: matrix type, and selection of polymer-their evaluation. Kaza R, Pitchaimani R. Formulation of transdermal drug delivery system: matrix type, and selection of polymer- their evaluation. Curr Drug Discov Technol. 2006;3:279-285.
34. Marwah H, Garg T, Rath G, Goyal AK. Development of transferosomal gel for trans-dermal delivery of insulin using iodine complex. Drug Deliv. 2016;23:1636-1644.
35. Jain S, Jain P, Umamaheshwari R, Jain N. Transfersomes-a novel vesicular carrier for enhanced transdermal delivery: development, characterization, and performance evaluation. Drug Dev Ind Pharm. 2003;29:1013-1026.
36. Lichtenberg D, Robson RJ, Dennis EA. Solubilization of phospholipids by detergents. Structural and kinetic aspects. Biochim Biophys Acta. 1983;737:285-304.
37. Ascenso A, Raposo S, Batista C, Cardoso P, Mendes T, Praça FG, Bentley MV, Simões S. Development, characterization, and skin delivery studies of related ultradeformable vesicles: transfersomes, ethosomes, and transethosomes. Int J Nanomedicine. 2015;10:5837-5851.
38. Malvern A. Basic Guide to Particle Characterisation. Malvern Instruments, Ltd.: Malvern, UK; 2012.
39. Liu J, Hu G. Advances in studies of phospholipids as carriers in skin topical application. Journal of Nanjing Medical University. 2007;21:349-353.
40. Chaudhary H, Kohli K, Kumar V. Nano-transfersomes as a novel carrier for transdermal delivery. Int J Pharm. 2013;454:367-380.
41. Mitkari B, Korde S, Mahadik K, Kokare C. Formulation and evaluation of topical liposomal gel for fluconazole. Indian J Pharm Educ Res. 2010;44:324-333.
42. Shaji J, Lal M. Novel double loaded transferosomes: evidence of superior anti-inflammatory efficacy-a comparative study. Int J Curr Pharm Res. 2014;6:16-25.
43. Sultana SS, Krishna Sailaja A. Formulation and evaluation of diclofenac sodium transferosomes using different surfactants by thin film hydration method. Der Pharmacia Lettre. 2015;7:43-53.
44. Gupta A, Aggarwal G, Singla S, Arora R. Transfersomes: a novel vesicular carrier for enhanced transdermal delivery of sertraline: development, characterization, and performance evaluation. Sci Pharm. 2012;80:1061-1080.

Turk J Pharm Sci 2021;18(1):56-60
DOI: 10.4274/tjps.galenos.2019.47108

ORIGINAL ARTICLE

Evaluation of Antiinflammatory Activity of Ethanol Extract of *Nelumbo nucifera* Fruit

Nelumbo nucifera Meyvesinin Etanol Ekstresinin Antiinflamatuvar Aktivitesinin Değerlendirilmesi

Muhammad Ali RAJPUT[1]*, Tabassum ZEHRA[2], Fizzah ALI[2], Gunesh KUMAR[3]

[1]Multan Medical and Dental College, Department of Pharmacology, Multan, Pakistan
[2]Liaquat National Medical College, Department of Pharmacology , Karachi, Pakistan
[3]Liaquat University of Medical and Health Sciences, Department of Pharmacology, Sindh, Pakistan

ABSTRACT

Objectives: In recent times, the use of natural remedies, which are rich in varieties of vitamins and flavonoids, for treatment of inflammation has increased substantially. These natural remedies are expected to be safe and economical when compared with other conventional allopathic drugs. Thus, existing research investigated the anti-inflammatory effect of *Nelumbo nucifera* fruit (NNF), in view of estimating its traditional and pharmacologic use against disorders associated with pain and inflammation.

Materials and Methods: To estimate the antiinflammatory effect of NNF, carrageenan-induced paw edema method was employed with equally distributed (n=7) Wistar male rats (N=35). The paw edema was measured by volume displacement method with plethysmometer.

Results: The NNF extract significantly reduced the inflammation of the paw and decreased the edema volume in rats administered carrageenan at all doses from the 3rd to 5th hour when compared to control, whose maximum percent reduction of edema was estimated as 100 mg/kg dose (that is, 73.92% at the 5th hour after administration of carrageenan).

Conclusion: NNF exhibited a strong antiinflammatory effect, due to its phytochemical constituents, including flavonoids, saponins, and tannins, all of which synergistically exert inhibitory effects on arachidonic acid metabolism, neutrophil degranulation, and enzyme systems that promote cell proliferation and regulation of complement system. However, more preclinical and clinical evaluations are mandatory to validate these findings.

Key words: *Nelumbo nucifera*, flavonoids, carrageenan, arachidonic acid

ÖZ

Amaç: Son zamanlarda enflamasyon tedavisinde vitaminler ve flavonoidler açısından zengin çeşitli doğal ilaçların kullanımı önemli oranda artmıştır. Bu doğal ilaçların diğer geleneksel allopatik ilaçlarla karşılaştırıldığında güvenli ve ekonomik olması beklenmektedir. Bu nedenle, bu çalışmada, geleneksel ve farmakolojik olarak ağrı ve enflamasyon ile ilişkili bozukluklara karşı kullanılan *Nelumbo nucifera* meyvesinin (NNF) antiinflamatuvar etkisi araştırıldı.

Gereç ve Yöntemler: NNF'nin antiinflamatuvar etkisini belirlemek için, carrageenan kaynaklı pençe ödemi yöntemi, eşit olarak dağıtılmış (n=7) Wistar erkek sıçanlarda (N=35) kullanıldı. Pençe ödemi, pletismometre ile hacim değiştirme yöntemi ile ölçüldü.

Bulgular: NNF ekstresi, ödemdeki maksimum azalma yüzdesi 100 mg/kg doz olarak tahmin edilen kontrole kıyasla 3. ile 5. saatte tüm dozlarda carrageenan uygulanan sıçanlarda pençenin enflamasyonunu önemli ölçüde azalttı ve ödem hacmini azalttı (carrageenan uygulamasından sonraki 5. saatte %73,92).

Sonuç: NNF, flavonoidler, saponinler ve taninler de dahil olmak üzere fitokimyasal bileşenleri nedeniyle güçlü antiinflamatuvar etki gösterdi; bunların tümü, hücre proliferasyonunu ve kompleman sistem regülasyonunu tetikleyen araşidonik asit metabolizması, nötrofil degranülasyonu ve enzim sistemleri üzerinde sinerjistik inhibitor etki gösterdi. Bununla birlikte, bu bulguların pre klinik ve klinik deneyler ile doğrulanması gerekmektedir.

Anahtar kelimeler: *Nelumbo nucifera*, flavonoidler, carrageenan, araşidonik asit

***Correspondence:** drmuhammadali2016@gmail.com, **Phone:** +0923463881721 **ORCID-ID:** orcid.org/0000-0003-3688-8518
Received: 10.10.2019, **Accepted:** 12.12.2019

INTRODUCTION

A lot of individuals who experience severe, inexorable, and excruciating pain resulting from any deleterious painful condition, such as myocardial infarction or injury secondary to accidents, rely primarily on opioids, in spite of their established adverse effects. Similarly, unceasing anti-nflammatory conditions, such as rheumatoid arthritis and osteoarthritis, are generally cured with non-steroidal antiinflammatory drugs (NSAIDs). Although NSAIDs are dominating in the market, the toxicity associated with their prolonged use cannot be overlooked. The most frequent toxicity associated with NSAIDs includes gastro-intestinal tract bleeding and ulcers.[1,2] Therefore, this instigates the need to develop new, safe, effective, economical, and innocuous analgesics.[3]

The use of herbal drugs is progressively becoming more popular, since they are natural and have no adverse effects.[4] Basically, plant-derived drugs are taken randomly with no adequate knowledge of their local application for the treatment of various diseases. It is therefore important to appropriately guide the general population on the use of natural products. In addition, it is necessary to scientifically prove the effectiveness of these medicinal plants.[5]

Nelumbo nucifera (NNF) (Lotus), a member of the *Nymphaeaceae* family of plants, is commonly cultivated in hot and humid climate zones of Thailand, Pakistan, India, and China.[6] Its fruit contains seeds and pods. The green colored pods offer add-on to the seeds, which are usually black in color, tough, and roundish in shape (diameter: 1.5x1.0 cm). They are organized in whorls.[7] The seeds are the edible part of the fruit, which have to be skinned separately before consumption.[8]

The seeds of NNF are good sources of protein, fat, asparagines, unsaturated fatty acids, and starch. The key active components in the seeds are flavonoids, alkaloids, carbohydrates, gallic acid, and ample amount of various minerals, in addition to zinc, iron, potassium, sodium, and calcium.[9,10]

A recently conducted study on NNF pods revealed the existence of numerous active bioactive principles, such as flavonoids, alkaloids, saponins, terpenoids, and tannins.[11] Procyanidin (flavonoid) was also extracted from NNF pods.[6]

Customarily, the fruits are used as a healthy component of Asian cuisine. They are also used as a traditional cure for various ailments, such as hypertension, palpitation, arrhythmia, fever, pain, inflammation, sleep disorders, chronic diarrhea, spermatorrhea, leucorrhoea, bad breath, leprosy, and menorrhagia.[12,13] Recent research revealed that the LD_{50} value of NNF was higher than 5g/kg, whereas its neuropharmacological role was also established to be anxiolytic, antidepressant, and antiepileptic.[11,14] However, there insufficient information in literature regarding its ameliorative effect on inflammation. In this regard, this study aimed to evaluate the antiinflammatory activity of NNF, in view of justifying its traditional and pharmacologic use against disorders associated with pain and inflammation.

MATERIALS AND METHODS

Study design and methodology

This study was performed with the assistance of the laboratory services of the Department of Pharmacology, UoK, following approval from the Board of Advance Studies and Research, UoK.

Animals care

The research board, which comprise members of Faculty of Pharmacy, permitted the use of animals for the experiments in accordance with the protocols described by NIH and NACLAR.[15,16]

Animals were kept in plastic cages and maintained at a temperature near 25°C and humidity of 50% to 60% in an interchanging twelve hour cycle. Each mouse was given free access to normal diet and water. Rats were carried to the workroom about an hour prior to the trials initiation. Prior to administration of the dose, complete health of the rats was assessed based on the absence of movements, edema, diarrhea, and ulceration during the acclimatization process using the laboratory settings for 7 days.

Preparation of extract

After obtaining fruits from the domestic fruit bazaar of Hyderabad, Pakistan in July 2015, they were initially presented to Pharmacognosy Department, UoK for identification and authentication and, afterward, the receipt no NNF-03 was assigned and deposited in the same department.

Crude extract was prepared through cold extraction procedure.[17,18] In brief, fruits (6 kg) were initially rinsed with clean water and seeds were manually separated from the fruit. Since the seeds have high contents of water, they need to be chopped first and left for 6 days to dry out in shade. The dried material obtained was thick and, as a result, the seeds need to be ground into fine powder. In contrast, pods were chopped once and allowed to dry in shade for 3 days. The dried pod material was in a coarse powder form. For better separation and collection of NNF constituents (secondary metabolites), they need to be chopped and dried separately before soaking them in ethanol (98%) for 30 days with occasional shaking.

Afterward, it was filtered with whatman no. 1 filter paper. Then, it was evaporated with a rotary evaporator under condensed pressure at a temperature of 40°C-45°C. The condensed material was freeze-dried with a freeze dryer (-30°C) and stored in a refrigerator. The final yield of the extract was 0.4 kg (dry weight).

Grounding of drugs

Carrageenan and gum tragacanth were obtained from Merck. Aspirin was purchased from a well-known pharmacy in Karachi.

2% tragacanth gum (powder form) was procured from Merck, which was used to prepare suspensions of 3 different dosages for the test group (NNF 50, 100, and 200 mg/kg). Control group was given tragacanth gum (10 mL/kg PO) as placebo. On each occasion, new suspensions were prepared for the dosage.[19,20]

Carrageenan suspension (0.1 mL of 1% w/v) was prepared in normal saline and inoculated via the planter aponeurosis of right hind paw to induce hind paw edema in the experimental rats.[21]

Aspirin (300 mg tablet) was crushed and suspended in tragacanth gum (2%), which was then administered to the rats at the dosage of 150 mg/kg PO (as reference agent) using an orogastric tube.[22]

Hind paw edema method

Hind paw edema method is an established technique for assessing the antiinflammatory effect of NNF extract, following the induction of edema in the hind paw of rat by carrageenan. Generally, carrageenan is used as a phlogistic agent, a substance that induces inflammation or edema.[23]

The test was performed on 35 Wistar rats that were equally distributed into 5 groups (n=7). The control group was administered 2% tragacanth gum; the reference group was administered 150 mg/kg aspirin; and the 3 test groups were administered 50, 100, and 200 mg/kg NNF. All drugs were administered orally (PO) at an hour prior to the delivery of carrageenan injection. Carrageenan suspension (0.1 mL of 1% w/v) prepared in normal saline was introduced under the planter aponeurosis of right hind paw of rats to induce hind paw edema in the experimental rats.[21]

The paw edema was estimated by volume displacement technique using a plethysmometer (UGO Basile 7140, Italy), which, perhaps, is the most efficient method for estimating the antiinflammatory effect of a drug. Plethysmometer is a volume meter that is composed of water-filled Perspex cell, in which the hind paw of rat was submerged with the transducer, which records small changes in water level caused by volume displacement, as well as with a digital meter, which displays the exact volume of water being displaced by the edema in the hind paw of rats. The swelling was estimated as mL of edema at different time interval, that is, the paw volume before carrageenan administration (time=0 baseline) and paw volume after carrageenan administration from the 1st to 5th hour was noted. Changes in the paw volume estimated earlier, as well as the succeeding administration of phlogistic agent points toward the significance of edema. Lastly, percent reduction of paw swelling was estimated in terms of % inhibition as follows:[24]

% inhibition: A-B/A x100

Where;

A: The average paw volume for test groups

B: The average paw volume for control group

Statistical analysis

The statistical analysis was done by applying Student's independent samples t-test to the mean and standard error of mean. P values less than 0.05 were considered significant and p values less than 0.005 were considered highly significant. Analysis of data was performed by using IBM SPSS Statistics for Windows, Version 20.0 (IBM Corp., Armonk, N.Y., USA).

RESULTS

Hind paw edema method

Table 1 and 2 showed that the carrageenan injection produced a localized edema at the right hind paw of rats, which attained its peak at the 3rd hour after the carrageenan administration, but gradually reduced after this period. Administration of 50, 100, and 200 mg/kg NNF significantly reduced the paw edema volume from the 3rd to 5th hour when compared to control, whose maximum percent reduction of edema was estimated as 100 mg/kg (that is, 73.92% at the 5th hour after administration of carrageenan). The initial phase of the edema (1st and 2nd hour) was not affected by the fruit extract. On the other hand, 150 mg/kg aspirin substantially decreased paw edema volume from the 1st to 5th hour when compared to control. Maximum percent inhibition of edema (88.17%) was estimated at the 5th hour after the carrageenan administration.

DISCUSSION

Several individuals who experience severe, inexorable, and excruciating pain resulting from cancer, injury, or from various autoimmune disorders and other degenerative diseases rely on opioids, such as morphine, in spite of their established adverse effects. Although NSAIDs are dominating in the market, toxicity associated with their prolonged use cannot be overlooked.[1,2] This instigates the need to develop novel, safe, and effective substances for ameliorating the effect of inflammation.

Acute inflammation induced by carrageenan is the most appropriate technique for screening antiinflammatory agents.

Table 1. Antiinflammatory activity of NNF and aspirin estimated by hind paw edema method in rats

Groups	Average paw size (mL) ± SEM						Average rise in paw volume (mL) ± SEM				
	Pre drug	1 h	2 h	3 h	4 h	5 h	1 h	2 h	3 h	4 h	5 h
Control	2.0±0.02	2.8±0.10	3.5±0.17	4.3±0.18	4.2±0.16	3.8±0.16	0.8±0.07	1.5±0.14	2.3±0.15	2.1±0.13	1.8±0.13
NNF 50 mg/kg	2.1±0.03	3.3±0.21	3.9±0.18	3.2±0.18**	2.8±0.20**	2.9±0.21**	1.2±0.18	1.8±0.15	1.1±0.15**	0.8±0.16**	0.8±0.18**
NNF 100 mg/kg	2.0±0.01	2.8±0.10	3.1±0.11	3.0±0.18**	2.6±0.07**	2.5±0.18**	0.7±0.08	1.1±0.09	1.0±0.16**	0.65±0.05**	0.48±0.16**
NNF 200 mg/kg	1.9±0.02	2.8±0.18	3.4±0.14	3.0±0.11**	2.8±0.14**	2.6±0.16**	0.84±0.15	1.43±0.11	1.11±0.08**	0.9±0.11**	0.66±0.13**
Aspirin 150 mg/kg	1.8±0.04	1.9±0.05**	2.1±0.18**	2.3±0.06**	2.1±0.06**	2.0±0.05**	0.19±0.02	0.35±0.14	0.5±0.03**	0.34±0.02**	0.22±0.01**

n=7, data are expressed as mean ± SEM, **: P value less than 0.005 was considered highly significant. SEM: Standard error of mean, NNF: *Nelumbo nucifera* fruit

Table 2. Percent inhibition of edema in rats treated with NNF and aspirin

Groups	% inhibition of edema		
	3 h	4 h	5 h
Control	-	-	-
NNF 50 mg/kg	51.29	63.30	55.91
NNF 100 mg/kg	55.12	70.18	73.92
NNF 200 mg/kg	52.15	58.71	64.51
Aspirin 150 mg/kg	78.44	84.40	88.17

n=7, NNF: *Nelumbo nucifera* fruit

The time required for edema to appear in carrageenan-induced hind paw edema model in rats is often estimated by a biphasic curve. The initial phase of inflammation arises within an hour of carrageenan administration, due to trauma at the injection site, serotonin, and histamine element.[25] The 2nd phase of edema starts from the 3rd hour and is sensitive to cyclooxygenase (COX) inhibitors, such as NSAIDs.[3]

This study revealed the antiinflammatory effect of NNF, which incredibly decreased the paw edema volume at all doses from the 3rd to 5th hour as compared to control, with maximum percent reduction of edema estimated at 100 mg/kg (that is, 73.92% at the 5th hour after administration of carrageenan). The first phase of the edema (that is, 1st and 2nd hour) was not affected by the fruit extract. Hence, in the present study, there was no inhibition of histamine and serotonin at the first phase of the test; however, COX pathway was effectively inhibited at the second phase of the test.

Flavonoids, which are also one of the significant constituents of NNF, exert its antiinflammatory effects via several mechanisms. One of these mechanisms pertains to their proposed capability of diminishing neutrophil degranulation. This represents the shortest possible approach to inhibit the liberation of arachidonic acid by neutrophils and other immune cells. Neutrophils carrying lipoxygenase produce chemotactic factors from arachidonic acid, which also stimulate the release of cytokines.[26,27]

Certain flavonoids are capable of reducing complement system activation, thus diminishing the attachment of inflammatory cells to the endothelium, thus reducing the inflammatory response.[28]

Saponins and tannins, which are also present in NNF, have also been reported to show inhibitory effects on arachidonic acid breakdown.[29] A recently conducted study has revealed the analgesic activity of NNF in various animal models, postulating that it may be connected with the synergistic actions of flavonoids, saponins, and tannins on arachidonic acid inhibition.[30] Therefore, it can be stated that the antiinflammatory effects of NNF are largely due to their flavonoids, saponins, and tannins content, which is believed to synergistically exert inhibitory effects on arachidonic acid metabolism, neutrophil degranulation, and enzyme systems that promote cell growth and regulates complement system.

CONCLUSION

The antiinflammatory activity of NNF demonstrated in this study was due to the existence of phytochemical constituents, which make it a useful agent for the treatment of patients with chronic inflammatory disorders. However, further preclinical and clinical evaluation is required to validate these findings.

ACKNOWLEDGEMENTS

The authors are thankful to the Chairman of Pharmacognosy Department, UoK for identifying and authenticating the NNF. We also appreciate the support of the Director, International Center for Chemical and Biological Sciences, for permitting us to use their facilities to complete this piece of work.

Conflicts of interest: No conflict of interest was declared by the authors. The authors alone are responsible for the content and writing of the paper.

REFERENCES

1. Yesilada E, Ustun O, Sezik E, Takaishi Y, Ono Y, Honda G. Inhibitory effect of Turkish folk remedies on inflammatory cytokines: Interleukins-1-alpha, interleukins-1-beta and tumor necrosis factor-alpha. J Ethnopharmacol. 1997;58:59-73.
2. Corley DA, Kerlikowske K, Verma R, Buffler P. Protective association of aspirin/NSAIDS and esophageal cancer: A systemic review and meta-analysis. Gastroenterology. 2003;124:47-56.
3. Singh M, Kumar V, Singh I, Gauttam V, Kalia AN. Anti-inflammatory activity of aqueous extract of *Mirabilis jalapa* Linn. leaves. Pharmacognosy Res. 2010;2:364-367.
4. da Costa Lopes L, Albano F, Augusto Travassos Laranja G, Marques Alves L, Fernando Martins e Silva L, Poubel de Souza G, de Magalhães Araujo I, Firmino Nogueira-Neto J, Felzenszwalb I, Kovary K. Toxicological evaluation by *in vitro* and *in vivo* assays of an aqueous extract prepared from Echinodorus macrophyllus leaves. Toxicol Lett. 2000;116:189-198.
5. Agbaje EO, Adeneye AA, Daramola AO. Biochemical and toxicological studies of aqueous extract of Syzigium aromaticum (L.) Merr. & Perry (Myrtaceae) in rodents. Afr J Tradit Complement Altern Med. 2009;6:241-254.
6. Mukherjee PK, Mukherjee D, Maji AK, Rai S, Heinrich M. The sacred lotus (*Nelumbo nucifera*) - phytochemical and therapeutic profile. J Pharm Pharmacol. 2009;61:407-422.
7. Sridhar KR, Bhat R. Lotus: a potential nutraceutical source. J Agri Technol. 2007;3:143-155.
8. Carlo FM, Masami Y, Yoshiaki K, Ganesh KA, Randeep Rakwal. Lotus - A Source of Food and Medicine: Current Status and Future Perspectives in Context of the Seed Proteomics. IJLS 2013;7:1-5.
9. Indrayan AK, Sharma S, Durgapal D, Kumar N, Kumar M. Determination of nutritive value and analysis of mineral elements for some medicinally valued plants from Uttaranchal. Curr Sci. 2005;89:1252-1255.
10. Pal I, Dey P. A review on lotus (*Nelumbo nucifera*) seed. IJSR. 2015;4:1659-1666.
11. Rajput MA, Khan RA. Phytochemical screening, acute toxicity, anxiolytic and antidepressant activities of Nelumbo nucifera fruit. Metab Brain Dis. 2017;32:743-749.

12. Chopra RN, Nayar SL, Chopra IC, Asolkar LV, Kakkar KK, Chakre OJ, Varma BS. Glossary of Indian Medicinal Plants. New Delhi: Council of Scientific and Industrial Research, 1996;3:174.

13. Varshney CK, Rzoska J. Aquatic weeds in South East Asia. 1st ed. New Delhi: Springer; 1976; p. 39.

14. Rajput MA, Khan RA, Assad T. Anti-epileptic activity of *Nelumbo nucifera* fruit. Metab Brain Dis. 2017;32:1883-1887.

15. National Advisory Committee for Laboratory Animal Research. Guidelines on the care and use of animals for scientific purposes. 2004; p. 24.

16. National Institute of Health Guidelines for Care and Use of Laboratory Animals in Biomedical Research. Guide for the care and use of laboratory animals. Prepublication draft. 8thed. The National Academies Press Washington DC 2010; 6, 47.

17. Hossain MS, Ahmed M, Islam A. Hypolipidemic and hepatoprotective effects of different fractions of ethanolic extract of immature leaves of *Mangifera indica* Linn in alloxan induced diabetic rats. IJPSR. 2010;1:132-138.

18. Assad T, Khan RA, Rajput MA. Effect of *Trigonella foenum-graecum* Linn seeds methanol extract on learning and memory. Metab Brain Dis. 2018;33:1275-1280.

19. Madhu A, Keerthi PHV, Singh J, Shivalinge GKP. To evaluate the anti-epileptic activity of aqueous root extract of *Hemidesmus indicus* in rats. Arch Pharm Sci Res. 2009;1:43-47.

20. Khan RA, Rajput MA, Assad T. Effect of Nelumbo nucifera fruit on scopolamine induced memory deficits and on motor coordination. Metab Brain Dis. 2018;34:87-92.

21. Ocete MA, Risco S, Zarzuelo A, Jimenez J. Pharmacological activity of the essential oil of Bupleurum gibraltaricum: anti-inflammatory activity and effects on isolated rat uteri. J Ethnopharmacol. 1989;25:305-313.

22. Ahmed S, Naved A, Khan RA, Siddiqui S. Analgesic Activities of Methanol Extract of *Terminalia chebula* Fruit. Pharmacology Pharmacy 2015;6:547-553.

23. Winter CA, Risely EA, Nuss GW. Carrageenan induced edema in hind paw of the rat as an assay for antiinflammatory drugs. Proc Soc Exp Biol Med. 1962;111:544-547.

24. Palanichamy S, Nagarajan S. Anti-inflammatory activity of Cassia alata leaf extract and kaempferol 3-O-sophoroside. Fitoterapia. 1990;61:44-47.

25. Crunkhorn P, Meacock SC. Mediators of the inflammation induced in the rat paw by Carrageenan. Br J Pharmacol. 1971;42:392-402.

26. Hoult JR, Moroney MA, Paya M. Actions of flavonoids and coumarins on lipoxygenase and cyclooxygenase. Methods Enzymol. 1994;234:443-454.

27. Tordera M, Ferrandiz ML, Alcaraz MJ. Influence of anti-inflammatory flavonoids on degranulation and arachidonic acid release in rat neutrophils. Z Naturforsch C J Biosci. 1994;49:235-240.

28. Friesenecker B, Tsai AG, Intaglietta M. Cellular basis of inflammation, edema and the activity of Daflon 500 mg. Int J Microcirc Clin Exp. 1995;15(Suppl):17-21.

29. Ahmadiani A, Hosseiny J, Semnanian S, Javan M, Saeedi F, Kamalinejad M, Saremi S. Anti-nociceptive and anti-inflammatory effects of *Eleagnusangusti folia* Fruit Extract. J Ethnopharmacol. 2000;72:287-292.

30. Rajput MA, Tabassum, Z, Fizzah A, Gunesh K. Assessment of analgesic activity of *Nelumbo nucifera* fruit ethanol extract. Int J Pharm Sci. 2019;11:1-5.

Turk J Pharm Sci 2021;18(1):61-67
DOI: 10.4274/tjps.galenos.2019.32656

ORIGINAL ARTICLE

Design and Optimization of Febuxostat-loaded Nano Lipid Carriers Using Full Factorial Design

Febukostat Yüklü Nano Lipit Taşıyıcıların Tam Faktör Tasarımı Kullanılarak Tasarımı ve Optimizasyonu

Shailendra BHATT[1]*, Jai Bharti SHARMA[1], Ruchi KAMBOJ[1], Manish KUMAR[1], Vipin SAINI[2], Shailendra MANDGE[3]

[1]Maharishi Markandeshwar College of Pharmacy, Department of Pharmaceutics, Haryana, India
[2]Maharishi Markandeshwar University, Department of Pharmaceutics, Solan, India
[3]Pacific University, Department of Pharmaceutics, Rajasthan, India

ABSTRACT

Objectives: This work aims to develop nanostructured lipid carriers (NLCs) to improve the oral bioavailability of febuxostat (FEB).

Materials and Methods: High shear homogenization, a well-known technique, followed by bath sonication with slight modifications was used to prepare FEB-loaded NLCs using oleic acid as liquid lipid and stearic acid as solid lipid. A total of 3^2 full factorial design was utilized to examine the effect of 2 independent variables, namely, X1 (liquid to solid lipid ratio) and X2 (surfactant concentration) on the Y1 (particle size) and Y2 (% entrapment efficiency) of the drug. The prepared NLCs were evaluated for particle size, polydispersity index, zeta potential, and (%) entrapment efficiency.

Results: The drug's highest solubility was found in the stearic (solid lipid) and oleic acid (liquid lipid), which were further chosen for NLC preparation. Result of the present study showed an increase in entrapment efficiency and a decrease in particle size with the increase in liquid lipid to solid lipid ratio. With increased surfactant concentration, a small particle size is observed. The optimized formulation's particle size and (%) entrapment efficiency was found to be 99 nm and 80%, respectively. The formulations' zeta potential and polydispersity index were found within the range. Compared to plain drug suspension, the optimized formulation showed higher drug release, which may be due to the presence of the higher amount of liquid lipid. The particles shown in the transmission electron microscopy were round in shape and have smooth surface. Stability studies showed that the NLC formulation can be stored for a longer time period under room condition.

Conclusion: FEB-loaded NLC were successfully prepared using full 3^2 factorial design, and can be further used for oral delivery of FEB for gout treatment.

Key words: Febuxostat, nanostructured lipid carriers, oral drug delivery, oleic acid

ÖZ

Amaç: Bu çalışmada, febukostatın (FEB) oral biyoyararlanımını iyileştirmek için nano yapılı lipit taşıyıcıların (NLC) geliştirilmesi amaçlanmıştır.

Gereç ve Yöntemler: Sıvı lipit olarak oleik asit ve katı lipit olarak stearik asit kullanarak FEB yüklü NLC'leri hazırlamak amacıyla iyi bilinen bir teknik olan yüksek hızlı homojenizasyon ve ardından, modifiye edilmiş su banyosu sonikasyonu kullanıldı. X1 (sıvı/katı lipit oranı) ve X2 (yüzey aktif madde konsantrasyonu) olmak üzere iki bağımsız değişkenin Y1 (partikül boyutu) ve Y2 (% ilaç yükleme etkinliği) üzerindeki etkisini belirlemek için 3^2 faktöryel tasarım kullanılmıştır. Hazırlanan NLC'ler, partikül boyutu, polidispersite indeksi, zeta potansiyeli ve (%) ilaç yükleme etkinliği açısından değerlendirildi.

Bulgular: İlacın çözünürlüğü, stearik (katı lipit) ve oleik asitte (sıvı lipit) kombinasyonunda en yüksek bulunduğu için NLC hazırlanmasında bunlar kullanıldı. Bu çalışma ile, sıvı lipit/katı lipit oranının artmasıyla ilaç yükleme etkinliğinin arttığı, partikül boyutunun ise azaldığı gösterilmiştir. Artan yüzey aktif madde konsantrasyonu ile de partikül boyutunun azaldığı gözlemlendi. Optimize edilmiş formülasyonun partikül boyutu ve (%) ilaç yükleme etkinliği sırasıyla 99 nm ve %80 olarak bulundu. Formülasyonların zeta potansiyeli ve polidispersite indeksi, aralık içinde bulundu. İlaç süspansiyonu ile karşılaştırıldığında, optimize edilmiş formülasyonunun daha yüksek ilaç salımı gösterdiği, bunun da daha yüksek miktarda sıvı lipitin varlığından kaynaklanıyor olabileceği sonucuna varıldı. Transmisyon elektron mikroskobunda parçacıkların sferik şekilde ve pürüzsüz bir yüzeye sahip oldukları tespit edildi. Stabilite çalışmaları, NLC formülasyonunun oda koşullarında daha uzun süre saklanabileceğini göstermiştir.

Sonuç: FEB yüklü NLC, 3^2 faktöryel tasarım kullanılarak başarıyla hazırlanmıştır. Gut tedavisi için FEB'nin oral yolla verilmesi için FBE yüklü NLC'ler kullanılabilir.

Anahtar kelimeler: Febuksostat, nanoyapılı lipit taşıyıcılar, oral ilaç uygulama, oleik asit

***Correspondence:** shailu.bhatt@gmail.com, **Phone:** +8107663903 **ORCID-ID:** orcid.org/0000-0001-9405-3311

Received: 16.07.2019, **Accepted:** 12.12.2019

INTRODUCTION

The most convenient route for drug administration is the oral route because it offers multiple dosage forms selectivity and high patient compliance.[1] Not just the drug's solubility but also its other inherent characteristics, like physiological milieu in the gastrointestinal tract including pH value and bile salts, slows down the drug's absolute absorption.[2,3]

In mid-90's, Professor R. H. Müller (Germany) and Professor M. Gasco (Italy) started to research on the capability of lipid-based drug delivery system, that is, solid lipid nanoparticles.[4] However, drug loading is a significant disadvantage of such dosage form. The incorporation of a liquid lipid in the nanoparticle preparation helps incorporate more drugs in the nanoparticle and enhance the nanocarrier's physical stability. This liquid lipid-containing nanoparticles were further named nanostructured lipid carriers (NLCs).[5,6] These are made up of biocompatible solid and liquid lipids.[7] NLCs are better than other colloidal carriers because of their drug loading capacity; and thus, have been investigated to more extent in pharmaceutical modernization.[8] NLCs are also helpful in other administration routes of administration, such as dermal, oral, ocular, and pulmonary. In topical transporter, NLC also shows high drug release, drug targeting, and proper lipophilic and hydrophilic drug molecules absorption.[9,10]

One of the most common crystal-induced arthropathies is gout, which is caused by arthritis inflammation. Other gout problems that may arise are metabolic syndrome, renal disease, and cardiovascular disease.[11] Hyperuricemia is an abnormality that is mostly found in children and adolescents. Because of its low concentration in the serum, even pediatricians cannot measure children's uric acid level. According to a recent study, hyperuricemia occurs because of obesity and non-communicable diseases like cardiovascular disorders. More attention has been given to it in children and adolescents.[12,13]

Another powerful, non-purine particular xanthine oxidase inhibitor is febuxostat (FEB). It is used to treat hyperuricemia in grown-ups with gout.[14] FEB is a biopharmaceutics classification system class 2 drug and is acidic in nature (pKa~3.08).[15] According to the Food and Drug Administration, FEB tablets show low oral bioavailability of 49.9% because of its low water solubility and low enzymatic degradation.[16] This research aims to develop the FEB-loaded NLC formulation using high shear homogenization technique followed by bath sonication method.

MATERIALS AND METHODS

FEB was received as a gift sample from Arbindo pharmaceuticals in Dehradun, India. Oleic acid, methanol AR, and sodium hydroxide pellets were purchased from Qualikems fine chemicals in Mumbai, India. Disodium hydrogen phosphate and potassium dihydrogen phosphate were purchased from S. D. Fine Chemicals, Ltd in Mumbai, India. Stearic acid and Tween 80 were purchased from Central Drug House Ltd. Vardaan House Daryaganj in New Delhi, India. All ingredients were of analytical grade.

Methods

Selection of lipids

Solid and liquid lipid was selected based on the drug's extreme solubility in various lipids.[17] The solid lipid was selected based on the solubility studies of the drug in stearic acid, glyceryl monostearate, cetyl alcohol, palmitic acid, whereas liquid lipid was examined in castor oil, isopropyl myristate, and oleic acid. In glass vials, the solid lipid was accurately weighed and heated to 70°C. FEB of 10 mg was added to these vials with continuous stirring. It was cooled to room temperature and was microscopically examined for precipitation. Solid lipids that did not show any precipitation were selected for further studies.[18]

Formulation of FEB-loaded NLC

Design of the experiment

To study the effect of 2 independent variables X_1 (liquid to solid lipid concentration) and X_2 (surfactant concentration) on the drug's particle size (Y_1) and entrapment efficiency [(EE); Y_2), a full 3^2 factorial design was used. Table 1 represents the 3^2 factorial design along with factors and levels.

Statistical analysis

DESIGN-EXPERT® version 13.0 was used to perform the statistical analysis.

Preparation of FEB-loaded NLC

The NLC was prepared by high shear homogenization followed by bath sonication with slight modifications.[8] The lipid phase was melted in a water bath at 85°C, and then the drug was added. The lipid and aqueous phases were prepared separately. The surfactant solution or aqueous phase was prepared by adding Tween 80 in water. To form a suspension, a preheated surfactant solution was added to the melted lipid. It was further homogenized for 15 min at 12,000 rpm by the high shear homogenizer (Remi Motors Ltd, Mumbai, India). All the formulations were subjected to a 5-min bath sonication (Hwashin Technology, Seoul, Korea) for uniform size distribution.[19] In a cooling centrifuge, the dispersion was centrifuged at 10,000 rpm for 60 min at 10°C, thereafter. To get the desired particle size, the sedimented soft pellet was separated from supernatant and resuspended in 20 mL of distilled water, which contained 2%-3% Tween 80 as stabilizer, with stirring for 10 minutes and again subjected to ultrasonication for 1 min.

Evaluation of FEB-loaded NLC

Particle size

After proper dilution with distilled water, the particle size and zeta potential were measured. The scattering angle was fixed at 173°C, and the temperature was maintained at 25°C.

Entrapment efficiency

The formulation was centrifuged at 10,000 rpm, and the supernatant was collected and was used to calculate the EE. Then, dilution was made up to 10 mL with phosphate-buffered saline pH 7.4, and FEB content was determined using an ultraviolet spectrophotometer at 315 nm.

Table 1. Experimental design for Febuxostat-loaded nanostructured lipid carriers

Formulation code	X_1	X_2	Zeta potential	Polydispersity index	Particle size	Entrapment efficiency
F_1	0	1	-15.1	0.144	145	76.8±2.13
F_2	-1	1	-18.7	0.152	198	70.3±2.42
F_3	0	-1	-25.9	0.412	189	72.9±2.76
F_4	0	0	-12.3	0.136	182	74.2±1.89
F_5	1	0	-14.8	0.131	109	79.5±2.57
F_6	-1	0	-20.7	0.346	215	67.8±1.77
F_7	0	0	-21.2	0.128	182	74±1.94
F_8	1	1	-17.9	0.187	99	80±1.58
F_9	0	0	-27.3	0.254	182	73.9±2.63
F_{10}	1	-1	-12.9	0.437	115	78±2.54
F_{11}	0	0	-25.5	0.135	181	74.1±1.87
F_{12}	-1	-1	-28.3	0.452	229	65.2±2.11

X_1: Liquid lipid to solid lipid ratio (-1=1:9, 0=5:5, +1=9:1), X_2: Concentration of surfactant (-1=3%, 0=4%, +1=5%)

The drug's EE was calculated as follows:[8]

$$(\%)\ EE: \frac{\text{Total amount of drug - drug in supernatant}}{\text{Total amount of drug}} \times 100$$

Optimization of formulation

The design master was used for optimization. Highest (%) EE and minimum particle size was the basis in selecting the optimized formulation.

Interaction between the factors

To statistically evaluate all the results, One-Way analysis of variance was used. P value gives the different independent variables' impact on dependent responses such as EE and particle size. Further, the reduced model was generated by omitting non-significant terms ($p>0.05$) from the full polynomial model. The reduced polynomial model was used to evaluate the effect of independent variables on the responses.

In vitro drug release studies

The plain drug suspension and prepared NLC's *in vitro* drug release study was carried out using the dialysis sac method, based on a previously published method with slight modifications.[19] An accurately measured amount of plain drug solution and prepared NLC equivalent to 5 mg of FEB were introduced into the sac; and the sac was properly tied with a thread at both ends. The sac was then hanged in 200 mL of phosphate buffer pH 7.4, with 1% polysorbate 80 and kept on a magnetic stirrer. The receptor compartment temperature was maintained at 37°C±1°C at a predetermined time, and, with the help of a pipette, aliquots of 5 mL were withdrawn and replaced with fresh buffer at each time. The sample was filtered using a membrane filter (0.45 µm) and was analyzed spectrophotometrically at 315 nm. For blank solutions, the same procedure was repeated.

Characterization of optimized FEB-loaded NLC

Surface morphology study

To study the surface morphology of optimized formulations, transmission electron microscopy [(TEM); Philips Tecnai-20, USA] with an accelerating voltage of 120.0 kv was used. The NLC dispersion was prepared in distilled water, and a drop of dispersion was placed on the carbon-coated copper grid followed by drying.

Stability study

Freeze-dried optimized formulation was used to carry out stability studies, according the International Conference on Harmonisation regulations. The samples were stored in vials for 3 mo and kept at atmospheric conditions of 25±2°C/60±5% relative humidity (RH) and 40±2°C/75±5% RH in a stability chamber (Macro Scientific Work Pvt Ltd., New Delhi, India) in order to check their stability. Also, at specified intervals, such as 0, 15, 30, 60, and 90 d, these samples' physical appearance and EE were determined.

RESULTS AND DISCUSSION

Solid and liquid lipid selection

Compared with other lipids, the solid and liquid lipid drug solubility was found highest in stearic and oleic acid, respectively. The were selected for NLC preparation as they did not show precipitation in the solubility studies of FEB.

Evaluation of optimized NLC

Zeta potential and polydispersity index

Colloidal dispersion stability is evaluated by zeta potential. It measures the repulsion degree between similarly charged particles to prevent the particle aggregation. Polydispersity ranges from 0 to 1, and its index is the width measurement of the particle size distribution. An index near 0 has narrow-size distribution. As shown in Table 1, the mean polydispersity index

value and zeta potential of drug-loaded NLC formulations F_1 to F_{12} varied in the range of 0.135 to 0.452 and -12.3 to -28.3 mv, respectively. In Figure 1, the optimized formulation F_8 showed zeta potential of -17.9 mv. It was found in previous studies that only the electrostatic repulsion is not responsible for the stability of nanoparticles but to formulate stable nanoparticles, steric stabilizer also has a significant effect. The surfactant's high concentration compensates missing electrostatic repulsion and stabilizes the dispersion for a long duration.[20] The steric stability fto NLC is provided by Tween 80's high concentration.

Optimization of formulation

Entrapment efficiency

As shown in Table 1, all the NLC formulations' EE was remarkably increased from 65.2±1.25 to 80±2.27%. EE was found to be 80% for optimized formulation. Results on the incorporation of liquid to solid lipids shows that more drug is entrapped in the NLC.[21] regression analysis was used to obtain the polynomial equation of the full model for EE. The full model is as follows:

Y_1: 74.23+5.70X_1+1.83X_2-0.9375X_1^2+0.2625X_2^2-0.7750X_1X_2

The non-significant terms from the full model were removed (p>0.05) to obtain a reduced model as follows:

Y_2: 74.23+5.70X_1+1.83X_2-0.9375X_1^2+0.2625X_2^2

The higher positive coefficient in the equation indicates the raising variable increasing the response and effect of factor on the response. X_1, X_2, X_1X_2, and X_1^2 factors were found to be significant based on their p values. The calculated f value for the given model was found very low compared with the tabular f value (α: 0.05, 2, respectively), which clearly demonstrates that the omitted terms does not significantly affect the prediction of EE. It was found in this study that EE increases significantly by increasing the surfactant concentration and liquid to solid lipid ratio. The high drug solubility in the melted lipids and more space provided for drug accommodation resulted in high EE.

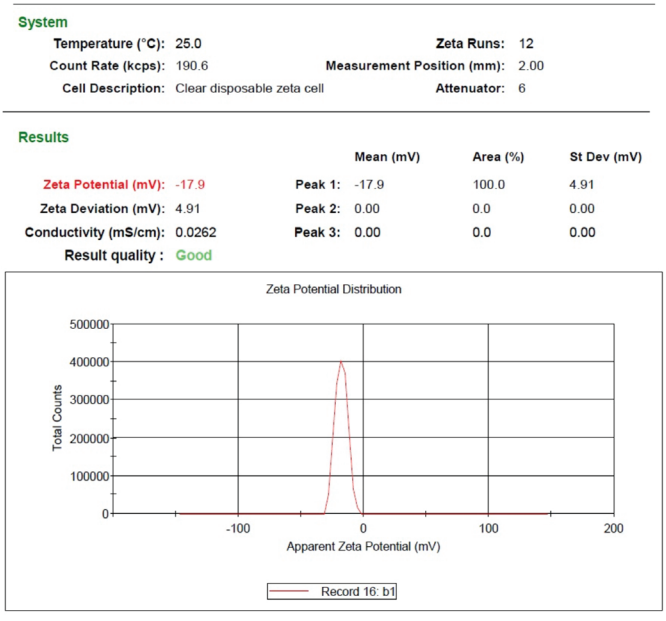

Figure 1. Zeta potential of optimized formulation

High liquid lipid proportion helps increase drug solubility in the lipid matrix, hence, high % EE was observed. The 3D surface response plot for % EE is shown in Figure 2.

Particle size

To confirm the produced particles' nano-range, particle size measurement was required and are presented as z-average diameter. All the formulations' particle size ranges from 99-229 nm, as shown in Table 1. Formulation F_8 showed considerably smaller mean particle size of 99 nm. It was confirmed from the data obtained from the experimental design that the model is significant. The polynomial equation of the full model for the particle size was obtained by regression analysis. The full model is as follows:

Y_2: 179.58-53.17X_1-15.17X_2-13.25X_1^2-8.25X_2^2+3.75X_1X_2

Non-significant terms from the full model were removed (p>0.05) to obtain a reduced model as follows:

Y_2: 179.58-53.17X_1-15.17X_2-13.25X_1^2-8.25X_2^2

Based on the p value, X_1, X_2, X_1^2 and X_2^2 factors were found to be significant. The calculated f value for the given model was found very low compared with the tabular f value (α: 0.05, 2, respectively), which clearly demonstrates that the omitted terms does not significantly affect particle size prediction. From the above study, it was found that particle size decreases when the liquid to solid lipid ratio increases.[22,23] The surfactant concentration (X_2) is also a critical factor that significantly affects the particle size. An increase in NLC formulation's surfactant concentration reduces the interfacial tension between the lipid and dispersion; thus, NLC with smaller particle size are formed. The optimized formulation's particle size was found to be 99 nm. Figure 3 shows the 3D surface response plot for particle size.

Characterization of optimized FEB-loaded NLC

Surface morphology study

From TEM study, it was found that NLC particles are spherical in shape and have a smooth surface, which is illustarated in Figure 4. The NLC's shape is in correlation with the previous findings. TEM study also proved that the NLC's particle size is

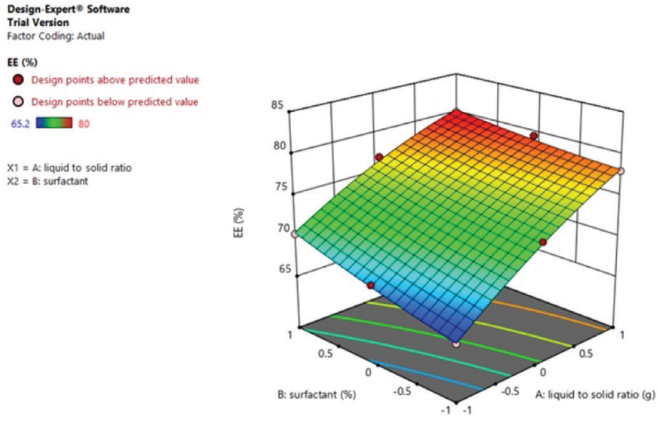

Figure 2. 3D surface response plot for entrapment efficiency

EE: Entrapment efficiency

less than 100 nm, which is reliably equal to the particle sizes calculated by zetasizer.

In vitro drug release

Figure 5 shows the percent cumulative drug release that was studied over a period of 12 h. In the second hour, NLC demonstrated a high burst release. Optimized formulation (F_8) showed enhancement in drug release compared to a plain drug suspension, and this is because of the presence of a higher liquid lipid amount. More liquid lipid stays at the outer shell of nanoparticles and shown essentially greater solubility for hydrophobic drugs which gives burst release in drug profile. As shown in Figure 6, the drug release was then fitted into the zero order, first order, and Higuchi kinetic model. NLC's drug release characteristics were best fitted to the Higuchi model. The correlation was determined for kinetics models. As shown in Table 2, the value of R^2 indicates that the drug release characteristics were best fitted to Higuchi kinetic model.

Stability study

This table provides data for the optimized formulation stability of (F_8). At the given stability conditions, no change in physical appearance was observed. It was also observed in accelerated conditions that there is a slight decrease in EE. The results show that storage of lipid-based formulation is not suitable under the accelerated temperature because the drug starts degrading under this condition or temperature. Table 3 shows the data for the stability study. Thus, with the help of this table, it can be concluded that the formulated NLC can be stored for longer period of time under room condition rather than in the accelerated condition.

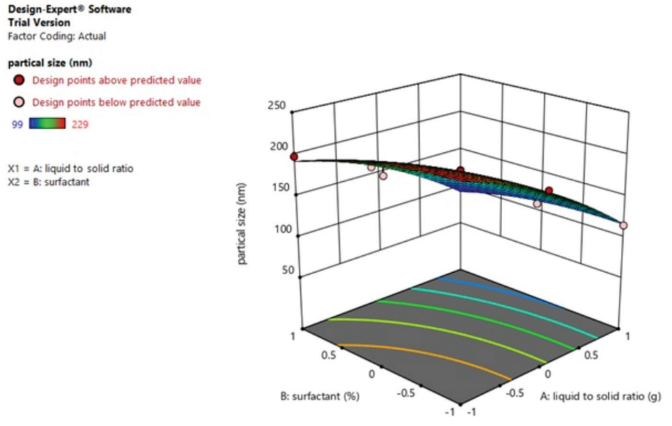

Figure 3. 3D surface response plot for particle size

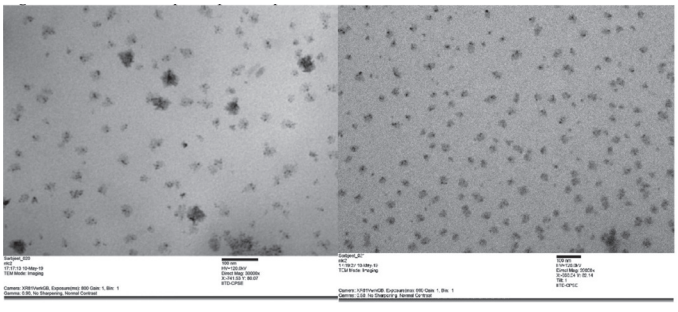

Figure 4. Transmission electron microscopy (TEM) image of optimized formulation

CONCLUSION

With the use of high shear homogenization followed by bath sonication technique, NLC was successfully prepared and optimized. To study the effect of liquid to solid lipid ratio and surfactant concentration on the drug's particle size and EE, a full 3^2 factorial design was utilized. Based on the solubility studies, stearic and oleic acid were selected as the solid and liquid lipid, respectively, and tween 80 was used as the surfactant. From the above study, it was found that particle size and (%) EE are significantly affected by both liquid to solid lipid

Table 2. Slope and R^2 values of drug release kinetics by various models

Slope no.	Model	Slope	R^2
1	Zero order	6.570	0.973
2	First order	-0.069	0.95
3	Higuchi equation	0.038	0.978
4	Korsemeyer Peppas equation	1.089	0.638

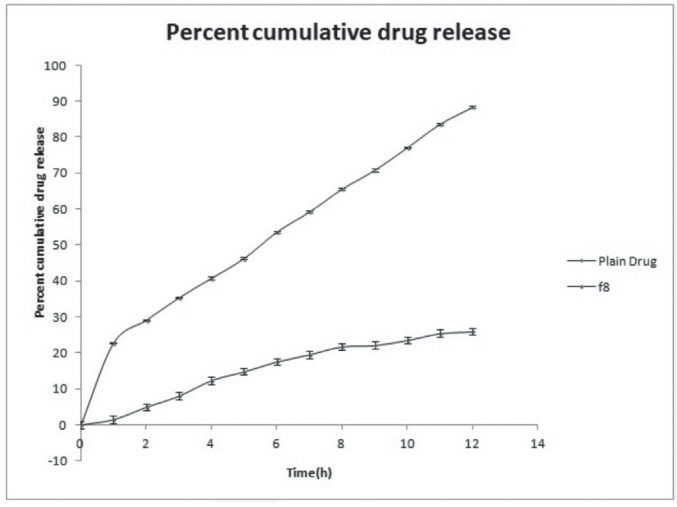

Figure 5. Comparison of *in vitro* release profile of optimized formulation and plain drug suspension

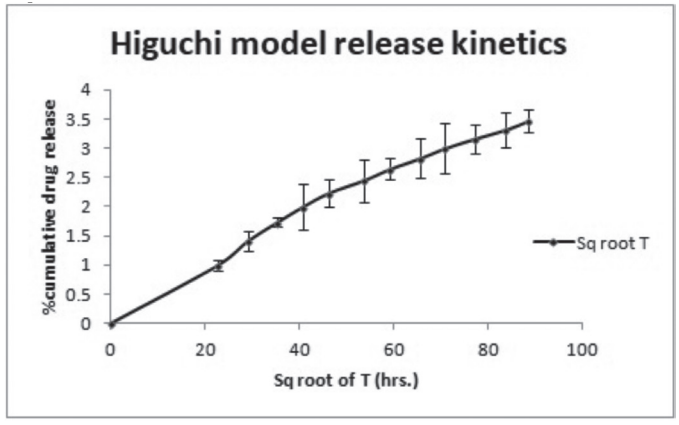

Figure 6. Drug release kinetics by Higuchi model

Table 3. Stability study data for optimized formulation (F_8)

		25˚C±2˚C/60%±5% RH		40˚C±2˚C/75%±5% RH	
Slope no.	Time (days)	Physical appearance	Entrapment efficiency ± SD (%)	Physical appearance	Entrapment efficiency ± SD (%)
1	0	White colored suspension throughout the study	80±2.79	White suspension throughout the study	80±2.79
2	15		79.87±2.68		79.97±2.63
3	30		79.80±2.57		78.52±2.52
4	60		79.74±3.52		77.44±1.15
5	90		78.85±2.32		75.93±2.12

RH: Relative humidity, SD: Standard deviation

ratio and surfactant concentration significantly. By increasing the surfactant concentration and liquid to solid lipid ratio, EE was found to be increased. High % EE resulted from high liquid lipid proportion, which helps increase drug solubility in the lipid matrix. The interfacial tension between the lipids are reduced with the increase in surfactant; and a decrease in particle size is resulted from dispersion. All formulations' zeta potential and polydispersity index were within range. The high concentration of tween 80 compensates missing electrostatic repulsion and provides steric stability to NLC. TEM images show the spherical globules nanosized particles with a smooth surface area; and NLC's particle size is obtained less than 100 nm, which is in good agreement with the zetasizer results. *In vitro* drug release study showed the sustained release of drug up to 12 h. Stability study showed that the formulation possesses good stability at room temperature, whereas the accelerated temperature is not an appropriate storage condition for lipid-based formulation. FEB-loaded NLCs were successfully prepared and can be used for oral delivery of FEB in gout treatment.

Conflicts of interest: No conflict of interest was declared by the authors. The authors alone are responsible for the content and writing of the paper.

REFERENCES

1. Soni K, Rizwanullah M, Kohli K. Development and optimization of sulforaphane-loaded nanostructured lipid carriers by the Box Behnken design for improved oral effcacy against cancer: *in vitro*, *ex vivo* and *in vivo* assessments. Artif Cells Nanomed Biotechnol. 2018;46(Sup1):15-31.
2. Porter CJ, Trevaskis NL, Charman WN. Lipids and lipid-based formulations: optimizing the oral delivery of lipophilic drugs. Nat Rev Drug Discov. 2007;6:231-248.
3. Liu C, Kou Y, Z Xin Z, Cheng H, Chen X, Mao S. Strategies and Industrial Perspectives to Improve Oral Absorption of Biological Macromolecules. Expert Opin Drug Deliv. 2018;15:223-233.
4. Müller RH, Mäde K, Gohla S. Solid lipid nanoparticles (SLN) for controlled drug delivery - a review of the state of the art. Eur J Pharm Biopharm. 2000;50:161-177.
5. Müller RH, Shegokar R, Keck CM. 20 years of lipid nanoparticles (SLN and NLC): present state of development and industrial applications. Curr Drug Discov Technol. 2011;8:207-227.
6. Müller RH, Radtke M, Wissing SA. Nanostructured lipid matrices for improved microencapsulation of drugs. Int J Pharm. 2002;242:121-128.
7. Muchow M, Maincent P, Muller RH. Lipid nanoparticles with a solid matrix (SLN, NLC, LDC) for oral drug delivery. Drug Dev Ind Pharm. 2008;34:1394-1405.
8. Gadad AP, Tigadi SG, Dandagi PM, Mastiholimath SV, Bolmal BU. Rosuvastatin Loaded Nanostructured Lipid Carrier: For Enhancement of Oral Bioavailability. Indian J Pharm Edu Res. 2016;50:605-611.
9. Luan J, Zheng F, Yang X, Yu A, Zhai G. Nanostructured Lipid carriers for Oral delivery Of baicalin: *In Vitro* and *in Vivo* evaluation. Colloids Surf A Physicochem Eng Asp. 2015;466:154-159.
10. Motawea A, Gawad AE, Borg T, Motawea M, Tarshoby M. The Impact of Topical Phenytoin Loaded Nanostructured Lipid Carriers in Diabetic Foot Ulceration. Foot (Edinb). 2019;40:14-21.
11. Kuo CF, Grainge MJ, Zhang W, Doherty M. Global epidemiology of gout: prevalence, incidence and risk factors. Nat Rev Rheumatol. 2015;11:649-662.
12. Wilcox WD. Abnormal serum uric acid levels in children. J Pediatr. 1996;128:731-741.
13. Yamanaka H. Gout and hyperuricemia in young people. Curr Opin Rheumatol. 2011;23:156-160.
14. Maddileti D, Jayabun SK, Nangia A. Soluble Cocrystals of the Xanthine Oxidase Inhibitor Febuxostat. Cryst Growth Des. 2013;13:3188-3196.
15. Ernst ME, Fravel MA. Febuxostat: a selective xanthine-oxidase/xanthine-dehydrogenase inhibitor for the management of hyperuricemia in adults with gout. Clin Ther. 2009;31:2503-2518.
16. Khosravan R, Grabowski B, Wu JT, Joseph-Ridge N, Vernillet L. Effect of food or antacid on pharmacokinetics and pharmacodynamics of febuxostat in healthy subjects. Br J Clin Pharmacol. 2008;65:355-363.
17. Shete H, Patravale V. Long chain lipid based tamoxifen NLC. Part I: Preformulation studies, formulation development and physicochemical characterization. Int J Pharm 2013;454:573-583.
18. Lakhani P, Patil A, Taskar P, Ashour E, Majumdar S. Curcumin-loaded Nanostructured Lipid Carriers for ocular drug delivery: Design optimization and characterization. J Drug Deliv Sci Technol. 2018;18:30184-30189.
19. Shah NV, Seth AK, Balaraman R, Aundhia CJ, Maheshwari RA, Parmar GR. Nanostructured lipid carriers for oral bioavailability enhancement of raloxifene: Design and *in vivo* study. J Adv Res. 2016;7:423-434.
20. Thatipamula R, Palem C, Gannu R, Mudragada S, Yamsani M. Formulation and *in vitro* characterization of domperidone loaded solid

lipid nanoparticles and nanostructured lipid carriers. Daru. 2011;19:23-32.

21. Abbas H, Refai H, Sayed NE. Superparamagnetic iron oxide-loaded lipid nanocarriers incorporated in thermosensitive *in situ* gel for magnetic brain targeting of clonazepam. J Pharm Sci. 2018;107:2119-2127.

22. Fathi HA, Allam A, Elsabahy M, Fetih G, El-Badry M. Nanostructured lipid carriers for improved oral delivery and prolonged antihyperlipidemic effect of simvastatin. Colloids Surf B Biointerfaces. 2018;162:236-245.

23. Khan AA, Mudassir J, Akhtar S, Murugaiyah V, Darwis Y. Freeze-Dried Lopinavir-Loaded Nanostructured Lipid Carriers for Enhanced Cellular Uptake and Bioavailability: Statistical Optimization, *in Vitro* and *in Vivo* Evaluations. Pharmaceutics. 2019;11:97.

Turk J Pharm Sci 2021;18(1):68-74
DOI: 10.4274/tjps.galenos.2019.23500

ORIGINAL ARTICLE

Repurposing of Tamoxifen Against the Oral Bacteria

Tamoksifenin Oral Bakterilere Karşı Yeniden Konumlandırılması

Ali Abdul Hussein S. AL-Janabi

Karbala University College of Medicine, Department of Microbiology, Karbala, Iraq

ABSTRACT

Objectives: Tamoxifen (TAM), which is used for treating breast cancer, has exhibited another important function as an antimicrobial agent. The objective of this study is to investigate the antibacterial action of TAM against the bacteria present in the human oral cavity.

Materials and Methods: The bacteria present in the human oral cavity were isolated from healthy individuals. Different concentrations of TAM were tested against the isolated bacteria. Additionally, bactericidal and bacteriostatic effects of TAM were also determined.

Results: Out of 23 isolated bacteria, a greater number of Gram-positive bacteria were highly susceptible to the low concentrations of TAM than Gram-negative bacteria. *Kytococcus sedentarius*, which is Gram-positive bacterium, and *Pseudomonas stutzeri*, which is Gram-negative bacterium, needed a high minimum inhibitory concentration value of TAM (2.5 mg/mL) to be inhibited by TAM's bacteriostatic action. Resistance to TAM was also observed in three strains of Gram-positive and four strains of Gram-negative bacteria.

Conclusion: TAM has shown a potential antibacterial effect against the bacteria present in the oral cavity, especially against Gram-positive bacteria. This effect is mostly bacteriostatic. This study also found bacterial resistance toward TAM.

Key words: Bacteria, oral cavity, tamoxifen, Gram-positive, Gram-negative

ÖZ

Amaç: Meme kanserinin tedavisinde kullanılan tamoksifenin (TAM), antimikrobiyal ajan olarak önemli bir etkisi daha vardır. Bu çalışmanın amacı, TAM'nin insan ağız boşluğunda bulunan bakterilere karşı antibakteriyel etkinliğini araştırmaktır.

Gereç ve Yöntemler: İnsan ağız boşluğunda bulunan bakteriler sağlıklı bireylerden izole edildi. İzole edilen bakterilere karşı farklı TAM konsantrasyonları test edildi. Ek olarak, TAM'nin bakterisidal ve bakteriyostatik etkileri de belirlendi.

Bulgular: İzole edilen 23 bakteriden Gram-negatif bakterilere kıyasla daha fazla sayıda Gram-pozitif bakterinin, düşük TAM konsantrasyonlarına yüksek oranda duyarlı olduğu saptandı. Gram-pozitif bakteri olan *Kytococcus sedentarius* ve Gram-negatif bakteri olan *Pseudomonas stutzeri*, TAM'nin bakteriyostatik etkisiyle inhibe edilebilmeleri için yüksek bir minimum inhibitör konsantrasyon değerine (2,5 mg/mL) ihtiyaç duydukları saptandı. TAM'ye direnç, üç Gram-pozitif ve dört Gram-negatif bakteri suşunda da gözlenmiştir.

Sonuç: TAM, özellikle Gram-pozitif bakteriler olmak üzere ağız boşluğunda bulunan bakterilere karşı potansiyel antibakteriyel etki göstermiştir. Bu etki çoğunlukla bakteriyostatiktir. Bu çalışmada aynı zamanda TAM'ye karşı bakteriyel dirençte gösterilmiştir.

Anahtar kelimeler: Bakteri, ağız boşluğu, tamoksifen, Gram-pozitif, Gram-negatif

***Correspondence:** aljanabi_bio@yahoo.com, **Phone:** +07811411260 **ORCID-ID:** orcid.org/0000-0002-2479-3282

Received: 01.10.2019, **Accepted:** 12.12.2019

INTRODUCTION

As a member of selective estrogen receptor modulators, tamoxifen (TAM) is mainly used in the treatment and prevention of estrogen-positive breast cancer.[1,2] It was first introduced by AstraZeneca, UK as a more effective therapy for estrogen-positive breast cancer in women of Pakistan and Australia.[3] After more than four decades, TAM is considered as a golden drug for the treatment of breast cancer and extending the lives of approximately 500,000 women every year worldwide.[3-5] The chemopreventive usage of TAM is another approach approved by the US Food and Drug Administration to protect women from breast cancer for at least five years.[4,6] After two years of postoperative application, a study also found that TAM had the ability to reduce mortality resulting from coronary heart disease.[7]

The potential antimicrobial activities of TAM against various pathogenic organisms have prompted researchers to conductdrug repurposing.[8] Various studies have confirmed the direct and indirect antibacterial activities of TAM against different types of bacteria. TAM has shown a direct inhibitory action on the growth of *Staphylococcus aureus* and methicillin-resistant *S. aureus* (MRSA) strains,[9] and also against *Mycobacterium tuberculosis*.[10,11] The growth of *Enterococcus faecium* and its pathogenesis was found to be reduced by TAM after its administration in a *Galleria mellonella* infection model.[12] Meanwhile, the indirect antibacterial action of TAM was observed when it enhanced the activity of immune cells represented by neutrophils against various pathogenic bacteria such as MRSA, *Pseudomonas aeruginosa*, and *Escherichia coli* through the agonist activity of the G protein-coupled estrogen receptor.[13] Moreover, the antibacterial action of standard antibiotics such as polymyxin Bis also increased against various bacteria after combination with TAM.[14]

The treatment of breast cancer by TAM usually takes a longer period that could extend up to five years;[3] therefore, the normal bacterial flora of the human body, such as in the oral cavity, could be affected by the potential antibacterial activity of TAM. Hence, the objective of this study is to investigate the *in vitro* antibacterial activity of TAM against the oral flora of the human body.

MATERIALS AND METHODS

Chemicals

TAM citrate was purchased from Ebewe Pharma, Austria. Müller Mueller-Hinton agar (MHA) and Müller Mueller-Hinton broth (MHB) were purchased from HiMedia, India.

Isolation of bacteria

The swab samples were collected from the oral cavity of the healthy volunteers by sterilized cotton swabs. Then, the collected samples were cultured on blood agar and MacConkey agar (HiMedia, India). Inoculated media were incubated at 37°C for 24 hours for growing suspected bacteria. Diagnosis of the isolated bacteria was performed by the Vitek® 2 system using Vitek® 2 YST ID diagnostic cards for Gram-positive and Gram-negative bacteria (BioMérieux, France).

Determination of minimum inhibitory concentration (MIC) of TAM

The MIC of TAM was determined by the methods of dilution antimicrobial susceptibility tests for bacteria that grow aerobically as mentioned by CLSI-M07-A10 (2015).[15] A broth culture of isolated bacteria was prepared by the selected inoculum bacteria in MHB and was incubated at 37°C for 24 hours. The turbidity of growing bacterial cells was adjusted with 0.5 McFarland standard to contain approximately $1x10^8$ CFU/mL. Serial concentrations of TAM (5, 2.5, 1.25, and 0.625 mg/mL) were prepared from a stock solution (10 mg/mL). Plastic microdilution plates (96-well plates) were used to determine the MIC values of TAM. Each well of the plate received 50 µL from the standard count of each bacterial suspension and 100 µL from MHB, followed by adding 50 µL of specific concentration of TAM. Several controls were used within a microdilution plate, including MHB with only bacteria, MHB without bacteria, and MHB with only TAM. The inoculated plate was incubated at 37°C for 24 hours. The results were visually read observed as the presence or absence of bacteria growth.

Bactericides and the bacteriostatic effect of TAM were determined by re-culturing the growth-inhibited bacteria from the microdilution plate on MHA and then incubating the same at 37°C for 24 hours. The growth of inhibited bacteria indicated bacteriostatic action, whereas the absence of growth showed bactericidal effects.

Ethical approval

The study was ethically approved by the local Ethics Committee of the College of Medicine of the University of Karbala in July 20, 2019.

Statistical analysis

Data of all the tests were expressed as mean ± standard deviation. The values were statistically analyzed with One-Way ANOVA using Microsoft Excel for Windows version 10. The minimum level of p value >0.05 was considered as statistically significant.

RESULTS

In total, 23 isolated strains of bacteria were diagnosed after culturing the swab samples from the oral cavity. There were 13 strains of Gram-positive and 10 strains of Gram-negative bacteria. Most of the Gram-positive bacteria were highly susceptible to the low concentration of TAM as compared to the Gram-negative bacteria. *Kytococcus sedentarius* as one Gram-positive and *Pseudomonas stutzeri* as one Gram-negative bacterium needed higher concentrations of TAM (MIC: 2.5 mg/mL) to be inhibited by the same. Additionally, the effect of TAM on these two types of bacteria was determined as bacteriostatic action (Table 1 and 2).

The effective low concentrations of TAM on susceptible bacteria, which showed MIC at 0.625 mg/mL, were mostly determined as bacteriostatic action. This bacteriostatic action was clearly shown in the five isolated strains of Gram-positive and in the two strains of Gram-negative bacteria, whereas TAM

demonstrated bactericidal action against three strains of Gram-positive and one strain of Gram-negative bacteria at the same concentration (Table 1 and 2).

The resistance to TAM was observed in three strains of Gram-positive bacteria, namely *Granulicatella elegans*, *Kocuria kristinae*, and *K. varians*, and in four strains of Gram-negative bacteria, namely *Acinetobacter haemolyticus, E. coli*, *Enterobacter cloacae*, and *Klebsiella pneumonia* (Table 1 and 2).

DISCUSSION

TAM is an effective drug for the treatment of breast cancer in both women and men.[3,4] A clinical trial study conducted worldwide demonstrated that TAM can reduce the incidence of breast cancer by 50% in high-risk pre- and post-menopausal women.[6] It has also been used as an adjuvant therapy with an efficacy of more than five years for treating postmenopausal, node-positive, and estrogen or progesterone receptor-positive women since the mid-1980s.[3,6] Hence, TAM is commonly used by more than 7 million patients in a year and had saved the lives of approximately 500,000 women.[3,4,6] In addition to the antagonist binding property of TAM with estrogen receptor to prevent the development of breast cancer.[4,6] It also has another mechanism to prevent this type of cancer via the stimulated production of transforming growth factor (TGF)-calmodulin and protein kinase C, and also by blocking the angiogenesis process by lowering the production of IGF-1 and TGF.[16]

Table 1. The minimum inhibitory concentration of TAM in Gram-positive bacteria

No	Bacteria	MIC value (mg/mL)	MBC
1	*Dermacoccus nishinomiyaensis*	0.625	-
2	*Gemella sanguinis*	0.625	+
3	*Granulicatella adiacens*	0.625	-
4	*Granulicatella elegans*	R	+
5	*Helcococcus kunzii*	0.625	+
6	*Kocuria kristinae*	R	+
7	*Kocuria rosea*	1.25	+
8	*Kocuria varians*	R	+
9	*Kytococcus sedentarius*	2.5*	-
10	*Leuconostoc mesenteroides* ssp. *cremoris*	0.625	-
11	*Staphylococcus aureus*	0.625	+
12	*Staphylococcus pseudintermedius*	0.625	+
13	*Staphylococcus warneri*	0.625	+

*Significant difference between bacterial species at p<0.05, MIC: The minimum inhibitory concentration, TAM: Tamoxifen, MBC: Minimum bactericidal concentration

Table 2. The minimum inhibitory concentration of TAM in Gram-negative bacteria

No	Bacteria	MIC value (mg/mL)	MBC
1	*Acinetobacter haemolyticus*	R	+
2	*Aeromonas salmonicida*	1.25	+
3	*Burkholderia cepacia*	0.625	-
4	*Escherichia coli*	R	+
5	*Enterobacter cloacae* complex	R	+
6	*Klebsiella pneumoniae* ssp. *pneumoniae*	R	+
7	*Pseudomonas fluorescens*	1.25	-
8	*Pseudomonas stutzeri*	2.5*	-
9	*Ralstonia insidiosa*	0.625	+
10	*Sphingomonas paucimobilis*	0.625	+

*Significant difference between bacterial species at p<0.05, MIC: The minimum inhibitory concentration, TAM: Tamoxifen

In recent times, the resistance of bacteria to the most common antibacterial agents has increased progressively because of the massive overuse of these types of agents.[17] The misuse and overprescription of antibacterial agents is considered as the most important factor that has contributed to the rise of resistant bacterial strains for such type of agents.[18] The bacteria present in the oral cavity have also developed drug resistance toward many common types of antibiotics because of the genetic changes in their genomic structure.[19] The resistance of the oral bacteria to erythromycin due to the activity of *mef* and *erm* (B) genes is one example of such antibiotic resistance.[20] However, the list of antibiotics has hardly changed in four decades, and most of the pharmaceutical companies have left the antibiotic field due to the absence of a new class of antibacterial agents.[17] Hence, antibiotic resistance is emerging as one of the modern crises, and now is the right time for a global commitment to develop new antibacterial drugs.[17,21] The repurposing of existing drugs can be introduced as a solution to resolve the limited number of antimicrobial agents and for the enhancement of the treatment of most severe bacterial and fungal infections.[22] The repurposing process is usually employed to discover a new therapeutic action of a specific drug to add to its previously known usage.[8] TAM is one of those drugs, whose potential antimicrobial effect has been determined by many studies. These studies have presented promising data to repurpose the use of TAM from an anticancer drug into an antimicrobial agent.[9-12,23] Low side-effect profile and cheaper price are other important characteristics that could encourage the continued usage of TAM for the treatment of cancer and microbial infections.[6]

Out of 23 strains of the oral bacteria isolated in this study, 19 of them revealed susceptibility to TAM with variable MIC values. Alow concentration of TAM (7.1 µg/mL) exhibited moderate antibacterial effect against *M. tuberculosis*,[23] whereas a high concentration of TAM (MIC_{50}: 5-10 mg/mL) is required to suppress its growth.[12] However, drug-sensitive strains of *M. tuberculosis* could be inhibited by low concentrations of TAM (3.125-6.25 µg/mL) as compared with drug-resistant strains (6.25-12.5 µg/mL).[10] Antibacterial effects of TAM were also recorded against various other types of bacteria such as *E. faecium* and *S. aureus*[9,11] and also against more drug-resistant bacterial strains such as MRSA and *M. tuberculosis*.[9,10] The chemical derivatives of TAM have also shown potent antibacterial action. 4-hydroxytamoxifen,

ametabolic derivative of TAM, exerted an inhibitory action against *M. tuberculosis* with an MIC_{50} value of 5-10 mg/mL.[12] The newly synthesized triaryl butane, which is an analog of TAM, exhibited antibacterial activity against Gram-positive and Gram-negative food-borne pathogens, such as *Listeria monocytogenes*, *Listeria ivanovii*, *Enterococcus faecalis*, *S. aureus,* and *E. coli*.[24] Triphenylethylene, which is considered as a backbone of TAM, has also shown antibacterial activity against various types of pathogens including bacteria.[8] Otherwise, TAM had shown synergistic action with many known antibiotics to make them more effective against pathogenic bacteria as with polymyxin B against the polymyxin-resistant *P. aeruginosa*, *K. pneumoniae*, and *Acinetobacter baumannii*[14,25] and the three first-line antibiotics (rifampin, isoniazid, and ethambutol) against *M. tuberculosis*.[12] The activity of chitosan against *E. coli* and *Staphylococcus* spp. was increased in the presence of TAM when they were prepared in the nano-fiber polycaprolactone structure.[26] Moreover, TAM can increase the defensive ability of the immune cells. This process is well proven when the bactericidal activity of neutrophils is increased by TAM against various bacteria such as MRSA, *P. aeruginosa*, and *E. coli*. TAM can also enhance the bacterial clearance by this immune cell with 2.4-4.2 log reductions in bacterial counts in several types of tissue samples.[13] Intracellular tuberculosis in macrophages was also decreased after its treatment with TAM in a dose-dependent manner.[10]

The results of this study have shown that Gram-positive bacteria are more susceptible to TAM than Gram-negative bacteria. The resistance rate in Gram-negative bacteria was also found to be higher (36-73%) toward many antibiotics as compared to that in Gram-positive bacteria.[27] Generally, the resistance of Gram-negative bacteria is clearly identified toward various types of antibiotics because of its cell wall components, which make them a formidable barrier against any dangerous materials.[28] The inhibition of function of the bacterial cell membrane is the proposed mechanism of TAM action against bacteria.[23,24,29] This type of antibacterial action is mostly related to the hydrophobicity of TAM because of the presence of alkyl groups that are attached to the amino group in its structure.[9] Ultrastructural alterations in the components of the cell membrane of *Bacillus stearothermophilus,* which cause bacterial cell killing after treatment with TAM shows evidence that TAM is a membrane-active drug.[29] This type of alteration, which leads to high K^+ and Na^+ efflux from bacterial cells and causes severe damage in the inner and outer membranes, is also recognized after the treatment of *E. coli* and *L. ivanovii* with an analog of TAM (triaryl butane).[24] The mitochondrial membrane of *M. tuberculosis* was also observed to be collapsing by the ionic protonophore uncouplers of TAM and its lipophilic nature.[23]

Seven of the isolated bacteria, including three types of Gram-positive and four types of Gram-negative bacteria, in this study showed resistance to TAM. This resistance may related to the modification of the lipid or protein composition of the outer membrane of bacterial cells as observed in most of the antibiotic-resistant bacteria.[28] Other membrane modifications may include changes in the action of efflux pumps, the expression of various drug-deactivating agents, and proteolytic degradation.[30]

As one of four members of Gram-negative bacteria that was resistant to TAM, *A. haemolyticus* also showed resistance against other antibiotics. This bacterium, which usually causes nosocomial infections and is frequently isolated from the intensive care unit (ICU) of the hospitals, is emerging to be one of the bacteria that are to most of antimicrobial agents.[31] Isolates of *A. haemolyticus* from patients with immunocompromised status revealed a high level of resistance toward a wide range of antibiotics, including ampicillin-sulbactam, ampicillin, aztreonam, cefuroxime, and ceftazidime.[32] This resistance was also observed among isolated strains from patients receiving treatment at ICU against ciprofloxacin, cefepime, ceftazidime, piperacillin, and amikacin.[31,33] Like clinical isolates, *A. haemolyticus* isolated from the natural environment also showed resistance toward antibiotics such as cefotaxime and ceftazidime.[34] However, the resistance of *A. haemolyticus* mainly depends on its acquisition of beta-lactamase and cephalosporinase enzymes, whereas resistance to quinolone is related to the mutations in *gyrA* and/or *parC* genes.[35]

E. coli was a second Gram-negative bacterium that was resistant to TAM. This type of bacterium is usually sensitive to almost all the relevant antibiotics, but it also has the ability to acquire resistance genes from other species of bacteria via horizontal gene transfer.[36] Another source of multiple antibiotic resistance may result from the change in amino acids of *mar* locus regulator or mutation in the operator-promoter region *marO* of the bacterium.[37] In total, 137 *E. coli* isolates extracted from the cases of urinary tract infection (UTI) exhibited a high resistance (51.1-94.3%) toward ten types of antibiotics,[38] whereas 17 non-pathogenic *E. coli* strains extracted from different sources revealed multiple antibiotic resistance because of the genes carried by class 1 and class 2 integrons.[37] However, the transfer of resistance genes acquired by *E. coli* could result from plasmids and from other mobile genetic elements, such as transposons and gene cassettes in class 1 and class 2 integrons.[36]

Our study results showed that *Enterobacter cloacae* complex (ECC), which contains common nosocomial bacteria that can cause various types of infection,[39] exhibited resistance to TAM. The greatest antibiotic resistance by *E. cloacae* was against penicillin, cephalosporins (cefotaxime, ceftazidime, ceftriaxone), aminoglycosides, colistin, and fluoroquinolones.[40,41] Moreover, a study recorded an emerging resistance of ECC to a new generation of carbapenems.[39] The pathogenic strains of *E. cloacae* that caused bacteremia were found to be resistant against cephalothin and ampicillin and a smaller number to these strains against aminoglycosides.[42] However, this bacterium becomes resistant by acquiring resistance genes just like the other members of Gram-negative bacteria.[39]

K. pneumoniae, which causes various nosocomial infections, sepsis in neonates and bacteremia,[43,44] is another bacterium of the Gram-negative group that showed resistance against

TAM. A study conducted from 1998 to 2010 in the USA also showed such resistance of *K. pneumoniae* against a wide range of antibiotics.[45] The emergence of such types of multidrug-resistant bacteria have been increasing nowadays because of their production of extended-spectrum beta-lactamases[43] and a mutation in the *mgrB* regulatory gene that lead to resistance against colistin.[46]

Our results also exhibited resistance of three isolates of Gram-positive bacteria, namely *Granulicatella elegans, K. kristinae* and *K. varians*, and *G. elegans*, to TAM. These bacteria are related to the nutritionally variant *streptococci* that is usually found as one of the oral flora with an ability to cause infections and endocarditis under some conditions.[47,48] It is considered as the most sensitive species to most antibiotics than other species of its genus, especially *G. adiacens*.[49,50] The resistance of *G. elegans* to macrolide and beta-lactam antibiotics was recently noticed because of the presence of *erm* and *mef* genes.[47,49,51] This resistance could be increased in the case of biofilm formation by this bacterium.[52]

Our results also showed that the two isolates of *Kocuria* spp., namely *K. kristinae* and *K. varians*, were resistant to TAM. This Gram-positive *cocci* bacterium is mostly non-pathogenic, and it mostly causes infection in the patients with immunocompromised status such as those with cancer diseases.[53,54] Antibiotic resistance had been hardly recognized in this bacterium because of very limited available data.[53] Thus, the absence of useful guidelines for determining the antibiotic resistance of *Kocuria* spp. makes the susceptibility test necessary according to the *Staphylococcus* guidelines.[54] However, *K. kristinae* was found to be more resistant to antibiotics than *K. varians*. All the isolates of *K. varians* extracted from patients with endophthalmitis were found to be sensitive to all the tested antibiotics, whereas *K. kristinae* showed resistance against amikacin and cefazolin.[55] Other isolates of *K. kristinae* from patients with UTI, immunosuppressive conditions, and cancer diseases also exhibited resistance against a wide range of antibiotics.[56,57] Meanwhile, all the isolates of *K. varians* from periodontitis and brain abscess exhibited sensitivity to all the tested antibiotics.[58,59]

CONCLUSION

The antibacterial action of TAM was clearly observed against oral bacteria, especially Gram-positive bacteria. The action was mostly determined as a bacteriostatic effect. The repurposing of TAM from cancer therapy to antimicrobial treatment could be encouraged by many factors; for example, TAM is a cheap drug with a few adverse effects. Although some bacteria show resistance, most of the known virulent species of isolated bacteria were found to be sensitive to TAM. This result will provide a promising view to use TAM in the treatment of infections caused by such types of bacteria.

REFERENCES

1. Osborne CK. Tamoxifen in the treatment of breast cancer. N Engl J Med. 1998;339:1609-1618.
2. Bekele RT, Venkatraman G, Liu R, Tang X, Benesch MG, Mackey JR, Godbout R, Curtis JM, McMullen TP, Brindley DN. Oxidative stress contributes to the tamoxifen-induced killing of breast cancer cells: implications for tamoxifen therapy and resistance. Sci Rep. 2016;6:21164.
3. Shahbaz K. Tamoxifen: Pharmacokinetics and pharacodynamics. J Pharm Res. 2017;1:1-8.
4. Jordan VC. Tamoxifen: a most unlikely pioneering medicine. Nat Rev Drug Discov. 2003;2:205-213.
5. Bogush TA, Polezhaev BB, Mamuchey IA, Bogush EA, Polotsky BE, Tjulandin SA, Ryabov AB. Tamoxifen never ceases to amaze: New findings on non-estrogen receptor molecular targets and mediated effects. Cancer Invest. 2018;36:211-220.
6. Jordan VC. Tamoxifen. In: Schwab M, ed. Encyclopedia of Cancer. Philadelphia; Springer; 2017.
7. Rosell J. Long-term effects of adjuvant tamoxifen treatment on cardiovascular disease and cancer. Linköping University Medical Dissertations No. 1430. Linköping University, Faculty of Health Sciences, Department of Clinical and Experimental Medicine, Sweden; Division of Clinical Sciences, Oncology; 2014.
8. Montoya MC, Krysan DJ. Repurposing estrogen receptor antagonists for the treatment of infectious disease. mBio. 2018;9:1-10.
9. Levinson NS. Towards the elucidation of the mechanism of the antibiotic activity of tamoxifen. MS dissertation in Chemistry, College of Science. Georgia Institute of Technology; 2017. https://smartech.gatech.edu/bitstream/handle/1853/58251/LEVINSON-THESIS-2017.pdf
10. Jang WS, Kim S, Podder B, Jyoti MA, Nam KW, Lee BE, Song HY. Anti-Mycobacterial Activity of Tamoxifen Against Drug-Resistant and Intra-Macrophage Mycobacterium tuberculosis. J Microbiol Biotechnol. 2015;25:946-950.
11. Chen FC, Liao YC, Huang JM, Lin CH, Chen YY, Dou HY, Hsiung CA. Pros and cons of the tuberculosis drugome approach--an empirical analysis. PLoS One. 2014;9:e100829.
12. Jacobs AC, Didone L, Jobson J, Sofia MK, Krysan D, Dunman PM. Adenylate kinase release as a high-throughput-screening-compatible reporter of bacterial lysis for identification of antibacterial agents. Antimicrob Agents Chemother. 2013;57:26-36.
13. Flores R, Insel PA, Nizet V, Corriden R. Enhancement of neutrophil antimicrobial activity by the breast cancer drug tamoxifen. FASEB Journal. 2016;30:969.
14. Hussein M, Han M, Zhu Y, Schneider-Futschik EK, Hu X, Zhou QT, Lin Y, Anderson D, Creek DJ, Hoyer D, Li J, Velkov T. Mechanistic insights from global metabolomics studies into synergistic bactericidal effect of a polymyxin B combination with tamoxifen against cystic fibrosis MDR Pseudomonas aeruginosa. Comput Struct Biotechnol J. 2018;16:587-599.
15. Clinical and Laboratory Standards Institute (CLSI). Methods for dilution antimicrobial susceptibility tests for bacteria that grow aerobically; Approved standard 10th ed. Document M07-A10. Wayne. Pennsylvania; 2015:29.
16. Karn A, Jha AK, Shrestha S, Acharya B, Poudel S, Bhandari RB. Tamoxifen for breast cancer. JNMA J Nepal Med Assoc. 2010;49:62-67.
17. Bartlett JG, Gilbert DN, Spellbergs B. Seven ways to preserve the miracle of antibiotics. Clin Infect Dis. 2013;56:1445-1450.
18. Nature Editorial. The antibiotic alarm. Nature. 2013;495:141.
19. Roberts MC. Antibiotic resistance in oral/respiratory bacteria. Crit Rev Oral Biol Med. 1998;9:522-540.

20. Villedieu A, Diaz-Torres ML, Roberts AP, Hunt N, McNab R, Spratt DA, Wilson M, Mullany P. Genetic basis of erythromycin resistance in oral bacteria. Antimicrob Agents Chemother. 2004;48:2298-2301.
21. Infectious Diseases Society of America. The 10 x '20 Initiative: pursuing a global commitment to develop 10 new antibacterial drugs by 2020. Clin Infect Dis. 2010;50:1081-1083.
22. Miró-Canturri A, Ayerbe-Algaba R, Smani Y. Drug repurposing for the treatment of bacterial and fungal infections. Front Microbiol. 2019;10:41.
23. Feng X, Zhu W, Schurig-Briccio LA, Lindert S, Shoen C, Hitchings R, Li J, Wang Y, Baig N, Zhou T, Kim BK, Crick DC, Cynamon M, McCammon JA, Gennis RB, Oldfield E. Antiinfectives targeting enzymes and the proton motive force. Proc Natl Acad Sci U S A. 2015;112:E7073-7082.
24. El Arbi M, Théolier J, Pigeon P, Jellali K, Trigui F, Top S, Aifa S, Fliss I, Jaouen G, Hammami R. Antibacterial properties and mode of action of new triaryl butane citrate compounds. Eur J Med Chem. 2014;76:408-413.
25. Hussein MH, Schneider EK, Elliott AG, Han M, Reyes-Ortega F, Morris F, Blastovich MAT, Jasim R, Currie B, Mayo M, Baker M, Cooper MA, Li J, Velkov T. From breast cancer to antimicrobial: Combating extremely resistant Gram-negative "superbugs" using novel combinations of polymyxin B with selective estrogen receptor modulators. Microb Drug Resist. 2017;23:640-650.
26. Saeidi Z, Ashjaran A, Dabirsiyaghi SAR. Study of anti-cancer drug release (tamoxifen) of the nanofibers made of poly-caprolactone-chitosan. International J Advanced Biotechnology and Research. 2016;7:897-906. https://bipublication.com/files/ijabr20167304Morteza.pdf
27. Zorgani AA, Belgasim Z, Ziglam H, Ghenghesh KS. Antimicrobial susceptibility profiles of Gram-negative Bacilli and Gram-positive cocci isolated from cancer patients in Libya. Archives of Clinical Microbiology. 2012;3:1-8.
28. Delcour AH. Outer membrane permeability and antibiotic resistance. Biochim Biophys Acta. 2009;1794:808-816.
29. Luxo C, Jurado AS, Madeira VM, Silva MT. Tamoxifen induces ultrastructural alterations in membranes of *Bacillus stearothermophilus*. Toxicol In Vitro. 2003;17:623-628.
30. Steinbuch KB, Fridman M. Mechanisms of resistance to membrane-disrupting antibiotics in Gram-positive and Gram-negative bacteria. Med Chem Comm. 2016;7:86-102.
31. Tripathi PC, Gajbhiye SR, Agrawal GN. Clinical and antimicrobial profile of *Acinetobacter* spp.: An emerging nosocomial superbug. Adv Biomed Res. 2014;3:13.
32. Dimple R, Nupur S, Mahawal BS, Ankit K, Ajay P. Speciation and antibiotic resistance pattern of *Acinetobacter* species in a tertiary care hospital in Uttarakhand. Int J Med Res Health Sci. 2016;5:89-96.
33. Kumari M, Batra P, Malhotra R, Mathur P. A 5-year surveillance on antimicrobial resistance of *Acinetobacter* isolates at a level-1 trauma center of India. J Lab Physicians. 2019;11:34-38.
34. Kittinger C, Kirschner A, Lipp M, Baumert R, Mascher F, Farnleitner AH, Zarfel GE. Antibiotic resistance of *Acinetobacter* spp. isolates from the river Danube: Susceptibility stays high. Int J Environ Res Public Health. 2017;15:52.
35. Espinal P, Roca I, Vila J. Clinical impact and molecular basis of antimicrobial resistance in non-*baumannii Acinetobacter*. Future Microbiol. 2011;6:495-511.
36. Poirel L, Madec JY, Lupo A, Schink AK, Kieffer N, Nordmann P, Schwarz S. Antimicrobial resistance in *Escherichia coli*. Microbiol Spectr. 2018;6.
37. Sáenz Y, Briñas L, Domínguez E, Ruiz J, Zarazaga M, Vila J, Torres C. Mechanisms of resistance in multiple-antibiotic-resistant *Escherichia coli* strains of human, animal, and food origin. Antimicrob Agents Chemother. 2004;48:3996-4001.
38. Olorunmola FO, Kolawole DO, Lamikanra A. Antibiotic resistance and virulence properties in *Escherichia coli* strains from cases of urinary tract infections. Afr J Infect Dis. 2013;7:1-7.
39. Annavajhala MK, Gomez-Simmonds A, Uhlemann A. Multidrug-resistant *Enterobacter cloacae* complex emerging as a global, diversifying threat. Frontiers in Microbiology. 2019;10:1-8.
40. Uzunović S, Ibrahimagić A, Bedenić B. Antibiotic resistance in *Enterobacter cloacae* strains with derepressed/partly derepressed/inducible AmpC and extended-spectrum beta-lactamases in Zenica-Doboj Canton, Bosnia and Herzegovina. Med Glas (Zenica). 2018;15:37-45.
41. Lima TB, Silva ON, de Almeida KC, Ribeiro SM, Motta D, Maria-Neto S, Lara MB, Filho CR, Ombredane AS, de Faria Junior C, Parachin NS, Magalhães BS, Franco OL. Antibiotic combinations for controlling colistin-resistant *Enterobacter cloacae*. J Antibiot (Tokyo). 2017;70:122-129.
42. John JF, Jr Sharbaugh RJ, Bannister ER. *Enterobacter cloacae*: Bacteremia, epidemiology, and antibiotic resistance. Rev Infect Dis. 1982;4:13-28.
43. Khaertynov KS, Anokhin VA, Rizvanov AA, Davidyuk YD, Semyenova DR, Lubin SA, Skvortsova NN. Virulence factors and antibiotic resistance of *Klebsiella pneumoniae* strains isolated from neonates with sepsis. Front Med (Lausanne). 2018;5:225.
44. Garbati MA, Godhair AI. The growth resistance of *Klebsiella pneumoniae*: the need to expand our antibiogram: Case report and review of the literature. Afr J Infect Dis. 2013;7:8-10.
45. Sanchez GV, Master RN, Clark RB, Fyyaz M, Duvvuri P, Ekta G, Bordon J. *Klebsiella pneumoniae* antimicrobial drug resistance, United States, 1998-2010. Emerg Infect Dis. 2013;19:133-136.
46. Kidd TJ, Mills G, Sá-Pessoa J, Dumigan A, Frank CG, Insua JL, Ingram R, Hobley L, Bengoechea JA. A *Klebsiella pneumoniae* antibiotic resistance mechanism that subdues host defenses and promotes virulence. EMBO Mol Med. 2017;9:430-447.
47. Madison G, Golamari R, Bhattacharya P. Endocarditis caused by Abiotrophia and Granulicatella species. In: Michael S, ed. Advanced Concepts in Endocarditis. United Kingdom; IntechOpen; 2018:41-58.
48. Cargill JS, Scott KS, Gascoyne-Binzi D, Sandoe JA. Granulicatella infection: diagnosis and management. J Med Microbiol. 2012;61:755-761.
49. Alberti MO, Hindler JA, Humphries RM. Antimicrobial susceptibility of *Abiotrophia defectiva, Granulicatella adiacens*, and *Granulicatella elegans*. Antimicrob Agents Chemother. 2015;60:1411-1420.
50. Kanamoto T, Terakubo S, Nakashima H. Antimicrobial susceptibility of oral isolates of *Abiotrophia* and *Granulicatella* according to the consensus guidelines for fastidious bacteria. Medicines (Basel). 2018;5:129.
51. Zheng X, Freeman AF, Villafranca J, Shotridge D, Beyer J, Kabat W, Dembkowski K, Shulman ST. Antimicrobial susceptibility of invasive pediatric *Abiotrophia* and *Granulicatella* isolates. J Clin Microbiol. 2004;42:4323-4326.

52. Moreno MG, Wang L, De Masi M, Winkler T, Trampuz A, Di Luca M. *In vitro* antimicrobial activity against *Abiotrophia defectiv*a and *Granulicatella elegans* biofilms. J Antimicrob Chemother. 2019;74:2261-2268.

53. Savini V, Catavitello C, Masciarelli G, Astolfi D, Balbinot A, Bianco A, Febbo F, D-Amario C, D-Antonio D. Drug sensitivity and clinical impact of members of the genus *Kocuria*. J Med Microbiol. 2010;59:1395-1402.

54. Purty S, Saranathan R, Prashanth K, Narayanan K, Asir J, Sheela Devi C, Kumar Amarnath S. The expanding spectrum of human infections caused by *Kocuria* species: a case report and literature review. Emerg Microbes Infect. 2013;2:71.

55. Dave VP, Joseph J, Pathengay A, Pappuru R. Clinical presentations, management outcomes, and diagnostic dilemma in *Kocuria* endophthalmitis. J Ophthalmic Inflamm Infect. 2018;8:21.

56. Lakshmikantha M, Devki V, Yogesh C. Is *Kocuria kristinae* an upcoming pathogen?. Int J Curr Microbiol App Sci. 2015;4:885-889.

57. Tewar R, Dudeja M, Das AK, Nandy S. *Kocuria kristinae* in catheter associated urinary tract infection: A case report. J Clin Diagn Res. 2013;7:1692-1693.

58. Tsai CY, Su SH, Cheng YH, Chou YL, Tsai TH, Lieu AS. Kocuria varians infection associated with brain abscess: a case report. BMC Infect Dis. 2010;10:102.

59. Meletis G, Gogou V, Palamouti M, Spiropoulos P, Xanthopoulou K, Tantou P, Rizou A, Thomoglou V. Catheter-related relapsing peritonitis due to *Kocuria varians* in a patient undergoing continous ambulatory peritoneal dialysis. Nefrologia. 2012;32:541-542.

Turk J Pharm Sci 2021;18(1):75-79
DOI: 10.4274/tjps.galenos.2019.04657

ORIGINAL ARTICLE

Effect of Probucol on Proliferation of Leukemia, Multiple Myeloma, Lymphoma, and Fibroblast Cells

Probukolün Lösemi, Multipl Miyeloma, Lenfoma ve Fibroblast Hücre Hatlarının Proliferasyonu Üzerindeki Etkileri

Aslı KOÇ*, Arzu Zeynep KARABAY, Ali YAPRAK, Zeliha BÜYÜKBİNGÖL, Fügen AKTAN

Ankara Universtiy Faculty of Pharmacy, Department of Biochemistry, Ankara, Turkey

ABSTRACT

Objectives: Probucol is a bisphenol antioxidant with antiinflammatory, antilipidemic and antidiabetic effect. Development and progression of cancer is closely related to chronic inflammation and oxidative stress. Agents that target these processes have been shown to modulate cancer cell proliferation. In this regard, the effect of probucol on proliferation of different cancer cell lines was investigated.

Materials and Methods: Different concentrations of probucol solutions were prepared and applied to the following cancer cell lines: K562S (imatinib sensitive) and K562R (imatinib resistant) chronic myeloid leukemia (CML) cells; U937 histiocytic lymphoma cells; HL60 acute myeloid leukemia cells; U266, H929, and RPMI8226 multiple myeloma cells; and L929 fibroblast cells. Cell viability was conducted by 3-(4,5-dimethylthiazol-2-yl)-2,5-diphenyltetrazolium bromide assay.

Results: Significant toxicity was not exhibited due to probucol treatment (0.1-10 μM) in K562S and K562R CML cells, U937 histiocytic lymphoma cells, HL60 acute myeloid leukemia cells, U266 multiple myeloma cells, and L929 fibroblast cells. However, probucol treatment significantly inhibited the viability of H929 and RPMI8226 multiple myeloma cells at the concentration of 0.5-10 μM and 5-10 μM, respectively.

Conclusion: Probucol treatment slightly inhibited the viability of other cancer cell lines, but significantly inhibited the viability of H929 and RPMI8226 multiple myeloma cells. However, its effect was not potent, since a 50% reduction in cell viability could not be achieved at the concentrations of probucol treatment administered.

Key words: Probucol, chronic myeloid leukemia, multiple myeloma, histiocytic lymphoma, acute myeloid leukemia

ÖZ

Amaç: Probukol, antiinflamatuvar, antilipidemik ve antidiyabetik aktivitelere sahip bisfenol bir antioksidandır. Kanser gelişimi ve ilerlemesi kronik inflamasyon ve oksidatif stres ile yakından ilişkilidir ve bu süreçleri hedefleyen ajanların kanser hücre proliferasyonunu modüle ettikleri gösterilmiştir. Bu bağlamda, bu çalışmada, probukolün farklı kanser hücre hatlarının proliferasyonu üzerindeki etkileri araştırılmıştır.

Gereç ve Yöntemler: Probukolün farklı konsantrasyonlarda hazırlanan çözeltileri kullanılarak K562S (imatinib duyarılı), K562R (imatinib dirençli) kronik miyeloid lösemi (KML), U937 histiositik lenfoma, HL60 akut miyeloid lösemi, U266 multipl miyeloma ve L929 fibroblast hücre hatlarında hücre canlılığı 3-(4,5-dimethylthiazol-2-yl)-2,5-diphenyltetrazolium testi ile belirlenmiştir.

Bulgular: Probukol uygulaması (0,1 μM-10 μM), K562S, K562R KML, U937 histositik lenfoma, HL60 akut miyeloid lösemi, U266, H929, RPMI8226 multipl miyelom ve L929 fibroblast hücre hatlarında anlamlı bir etki göstermemiştir. Diğer taraftan, probukol uygulaması, H929 ve RPMI8226 hücre serilerinin canlılığını sırasıyla 0,5-10 μM and 5-10 μM konsantrasyon aralığında anlamlı olarak azaltmıştır ($p<0,05$).

Sonuç: Probukol uygulaması H929 ve RPMI8226 multipl miyelom hücre hatlarının canlılığını anlamlı olarak inhibe etmiştir. Fakat, probukolün bu etkisi potent bulunmamıştır ve uygulanan konsantrasyon aralığında, hücre canlılığında %50 ve üzerinde azalma sergilemediği belirlenmiştir.

Anahtar kelimeler: Probukol, kronik miyeloid lösemi, multipl miyelom, histositik lenfoma, akut miyeloid lösemi

***Correspondence:** aslikoc79@gmail.com, **Phone:** +90 505 403 20 96**ORCID-ID:** orcid.org/0000-0002-4679-9079

Received: 25.10.2019, **Accepted:** 16.12.2019

INTRODUCTION

Probucol is a bisphenol, which was originally synthesised as an antioxidant compound with antilipidemic effect.[1,2] Probucol has been shown to inhibit the oxidation of low density lipoprotein (LDL) and lower the level of cholesterol in the bloodstream by increasing the rate of catabolism of LDL.[3] Although probucol has been used extensively as a lipid-lowering drug in Japan, its reducing effect on serum high density lipoprotein cholesterol has posed a major setback, thus limiting its use in western countries.[4] Nevertheless, the effect of probucol is currently being reexamined, as various studies aim to elucidate its pleiotropic functions and effects. According to these studies, probucol has been shown to inhibit neurovascular inflammation as a single agent,[5] inhibit atherosclerosis when combined with atorvastatin,[6] exert beneficial effects on cognitive functions[7] and exhibit neuroprotective effect in animal models of Parkinson's[8] and Huntington's disease.[9] In addition, probucol has been demonstrated to inhibit inflammation due to its antiinflammatory effect in beta cells,[10] as well as its inhibitory activity on nuclear Factor kappa B (NF-κB) in spinal cord inflammation.[11]

Oxidative stress and chronic inflammation are among the characteristic features of neoplastic diseases. Overproduction of reactive oxygen species within the cell plays a major role in signaling pathways, leading to the initiation and progression of cancer and possible drug resistance.[12] In contrast, some studies showed that increasing oxidative stress may aid the elimination of cancer.[13] Type, stage, oxygen dependence, metastasis, and angiogenesis status under hypoxia are among the determinants of the modulation of cancer cell viability by oxidative stress.[14] Therefore, targeting oxidative stress has a great potential in cancer therapy. Treatment of cancer cells with antioxidants or oxidative stress inducing agents have been widely examined in different studies. In literature, a wide range of antioxidant compounds, such as N-acetyl cysteine,[15] vitamin E,[16] epigallocatechin gallate,[17] vitamin C,[18] and curcumin[19] have been examined for their potential effects in cancer prevention. Antioxidants, including ascorbic acid, naringenin, and curcumin, have been examined to induce apoptosis in K562 chronic myeloid leukemia (CML) and HL60 acute myeloid leukemia cells.[20-22] In addition to the aboved mentioned antioxidant compounds, resveratrol has been shown to inhibit proliferation, migration, and invasion of U266 multiple myeloma cells;[23] however, quercetin (an antioxidant and antiinflammatory compound) was found to inhibit RPMI8226 multiple myeloma cell proliferation by inducing cell cycle arrest and apoptosis.[24]

Based on these findings, we aimed to analyze the effects of a known antioxidant and antiinflammatory agent (probucol) on viability of K562S and K562R CML cells, U937 histiocytic lymphoma cells, HL60 acute myeloid leukemia cells, U266 multiple myeloma cells, and L929 fibroblast cells.

MATERIALS AND METHODS

Cell culture

Human multiple myeloma cell lines [H929, U266, and RPMI8226 multiple myeloma; human CML (K562), human histiocytic lymphoma (U937), human acute myeloid leukemia (HL60), and mouse fibroblast (L929)] were cultured in RPMI-1640 (Sigma) cell culture medium including: 10% heat inactivated fetal bovine serum, L-glutamine (2 mmol/L), 100 µ/mL penicillin, and 100 µg/mL streptomycin. Cells were incubated at 37˚C, 5% CO_2, and 95% humidity. At 80% confluence, adherent L929 cells were passaged with trypsinization.

Imatinib resistant K562 cell line

K562R cells, which are resistant to 5 µM imatinib, were used in our experiments. 0.6 µM imatinib resistant cells were kindly provided by Prof. Carlo Gambacorti-Passerini from University of Milano-Bicocca, Monza, Italy. The Imatinib resistant cells were increased to 5 µM by incubating the cells with increasing concentration of imatinib at time intervals.[25]

Cell viability

3-(4,5-dimethylthiazol-2-yl)-2,5-diphenyltetrazolium bromide (MTT) assay was conducted to test the effect of probucol on the various human cancer cell lines and mouse fibroblast cells. For this purpose, cells (20,000 cells/well) were seeded onto 96-well plates. 20 mM stock solution of probucol was pepared by dissolving probucol in dimethyl sulfoxide (DMSO) and further dilutions were prepared with culture medium. Maximum concentration of probucol applied to cells was 10 µM, due to low solubility of the compound at higher concentrations. H929, U266, RPMI8226, U937, and HL60 cells were treated with 0.1-10 µM probucol for 72 h at 37˚C. Control cells were incubated with the same concentration of DMSO as the probucol-treated cells and the DMSO concentration never exceeded 0.5%. For each cell line, the same protocol was followed. K562S (imatinib sensitive) and K562 R (imatinib resistant) cells were treated with probucol 0.1-10 µM), imatinib, and imatinib/probucol combination for 72 h. Imatinib concentrations used for K562S and K562R cells were 0.5 µM and 20 µM, respectively. Since imatinib is a first line therapeutic option for CML, we determined its single effect or combination effect with probucol. The effect of probucol was also detemined in non-cancerous L929 fibroblast cell line. After proper incubation, MTT solution (5 mg/mL) was prepared with phosphate buffer saline and cells were incubated with MTT solution for a period of four hours. Insoluble formazan crystals were dissolved by SDS-HCl solution. Absorbance was measured at 550 nm using a microplate reader (Molecular Devices-Spectra Max spectrophotometer, Sunnyvale, CA, USA).

Statistical anaylsis

One-way analysis of variance with Tukey post hoc test was performed with StatistiXL Software (Nedlands, Western Australia, 6009). Data were presented as mean ± standard deviation. P values less than 0.05 was considered statistically significant.

RESULTS

According to our experiments, probucol significantly decreased the viability of H929 and RPMI8226 cells at the concentrations of 0.5-10 µM and 5-10 µM, respectively. However, we did not

observe any antiproliferative effect on the other cell lines (Figure 1).

In our previous study, we administered 0.5 μM and 20 μM imatinib to K562S and K562 R cells, respectively, which are the known cytotoxic concentrations of imatinib in these cells. Treatment with imatinib alone significantly decreased the viability of K562S and K562R cells to 36.92±3.44% and 48.02±1.55%, respectively ($p<0.001$). On the other hand, probucol did not exhibit any antiproliferative effect on both cell lines either as a single agent or in combination with imatinib (Figure 2 and 3).

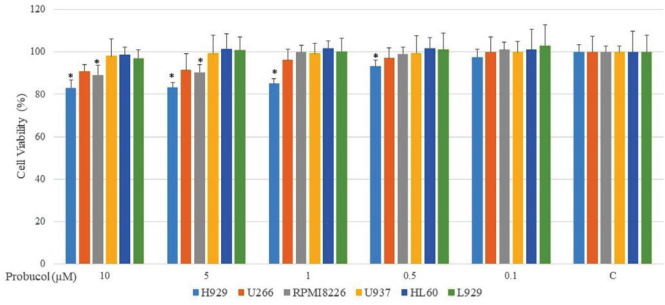

Figure 1. Human multiple myeloma (H929, U266, and RPMI8226), human histiocytic lymphoma (U937), human acute myeloid leukemia (HL60), and mouse fibroblast cell lines (L929) were treated with 0.1-10 μM probucol and cell viability was determined by MTT assay. *: $p<0.05$ indicates significant differences between control and probucol-treated groups. Probucol significantly decreased the cell viability of H929 and RPMI8226 at the concentrations of 0.5-10 μM and 5-10 μM, respectively, MTT: 3-(4,5-dimethylthiazol-2-yl)-2,5-diphenyltetrazolium bromide

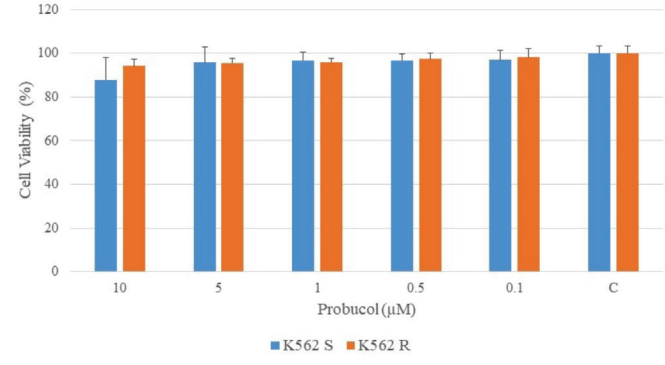

Figure 2. Imatinib-sensitive and -resistant human chronic myeloid leukemia cell lines (K562S and K562R) were treated with probucol (0.1-10 μM). Cell viability was tested by MTT assay. Probucol had no significant effect on the cell viability. MTT: 3-(4,5-dimethylthiazol-2-yl)-2,5-diphenyltetrazolium bromide

DISCUSSION

In literature, various studies have investigated the efficacy of probucol treatment in cancer. In one of these studies, directed nanoassembly formulation of probucol was shown to suppress lung metastasis of breast cancer[26] and, in another study, it inhibited benzopyrene-induced lung tumorigenesis.[27] In

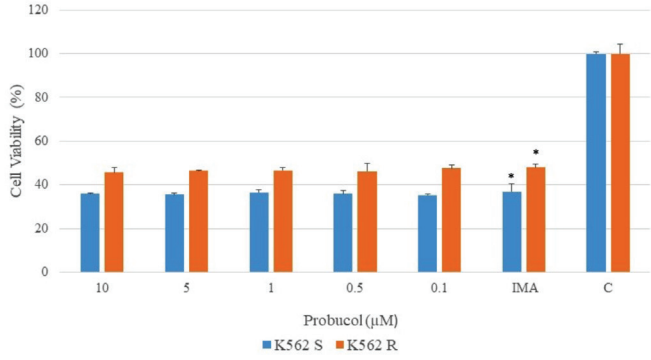

Figure 3. Imatinib-sensitive and -resistant human chronic myeloid leukemia cell lines (K562S and K562R) were treated with probucol (0.1-10 μM), imatinib (0.5 μM for K562S cells, 20 μM for K562R cells), or probucol/imatinib combination. Imatinib treatment significantly decreased the viability of both K562S and K562R cells. *$p<0.05$ indicates significant differences between control and imatinib-treated group. Viability of cells treated with imatinib and probucol also reduced when compared to the control cells. No significant difference was found between imatinib and imatinib/probucol combination treatment in both K562S and K562R cells. IMA: Imatinib

addition, probucol was reported to exhibit its antiproliferative effects via inhibition of cell cycle progression and inactivation of NF-κB and mitogen-activated protein kinase pathways in human ovarian cancer cells.[28] Probucol was also reported to exert chemopreventive effect in kidney cancer[29] and probucol treatment of κB cell xenografts in mice showed a significant anticancer effect via antiangiogenic- and apoptosis-inducing mechanisms.[30] To the best of our knowledge, this is the first study investigating the effects of probucol on K562S and K562R CML cells; U266, H929, and RPMI8226 multiple myeloma cells, and L929 fibroblast cells. In contrast to studies that reported a reduction of cancer cell proliferation by probucol treatment, we did not observe any potent inhibition of cell viability at 0.1-10 μM probucol treatment for all the cell lines investigated. Probucol treatment significantly inhibited the viability of H929 and RPMI8226 multiple myeloma cell lines at the concentrations of 0.5-10 μM and 5-10 μM, respectively. However, the percentage viability in these cell lines was higher than 80% following probucol treatment, since 50% higher viability inhibition could not be achieved at the applied concentrations of probucol. According to our results, probucol had no significant effect on viability of U937 cells. In literature, probucol has been tested on U937 cells. However, most studies aimed to reveal its effects on atherosclerosis.[31] In parallel to our study, one of these studies reported that the viability of U937 cells was greater than 90% followng incubation with 5 μM probucol.[32]

CONCLUSION

Our results collectively showed that probucol was not effective in inducing cell death as a single agent in U937 histiocytic lymphoma cells, HL60 acute myeloid leukemia cells, and U266 multiple myeloma cells. Although probucol significantly inhibited H929 and RPMI8226 cell proliferation at particular doses, its effects were not potent. Probucol combined with imatinib did not alter the viability of K562S and K562R cells,

thus showing its ineffectiveness as a combinatorial therapeutic agent in CML.

ACKNOWLEDGEMENTS

This study was supported by Scientific Research Projects (BAP) of Ankara University (16L0237007).

Conflicts of interest: No conflict of interest was declared by the authors. The authors alone are responsible for the content and writing of the paper.

REFERENCES

1. Heel RC, RN Brogden, TM Speight, GS Avery. Probucol: A review of its pharmacological properties and therapeutic use in patients with hypercholesterolaemia. Drugs. 1978;15:409-428.
2. Buckley MM, KL Goa, AH Price, RN Brogden. Probucol. A reappraisal of its pharmacological properties and therapeutic use in hypercholesterolaemia. Drugs. 1989;37:761-800.
3. Parthasarathy S, SG Young, JL Witztum, RC Pittman, D Steinberg. Probucol inhibits oxidative modification of low density lipoprotein. The Journal of clinical investigation. 1986;77:641-644.
4. Yamashita S, D Masuda, Y Matsuzawa. Did we abandon probucol too soon? Current opinion in lipidology.2015;26:304-316.
5. Takechi R, MM Pallebage-Gamarallage, V Lam, C Giles, JC Mamo. Long-term probucol therapy continues to suppress markers of neurovascular inflammation in a dietary induced model of cerebral capillary dysfunction. Lipids in health and disease. 2014;13:91.
6. Keyamura Y, C Nagano, M Kohashi, M Niimi, M Nozako, T Koyama, R Yasufuku, A Imaizumi, H Itabe, T Yoshikawa. Add-on effect of probucol in atherosclerotic, cholesterol-fed rabbits treated with atorvastatin. PloS one. 2014;9:e96929.
7. Mamo JC, V Lam, E Brook, A Mooranian, H Al-Salami, N Fimognari, M Nesbit, R Takechi. Probucol prevents blood-brain barrier dysfunction and cognitive decline in mice maintained on pro-diabetic diet. Diabetes & vascular disease research. 2019;16:87-97.
8. Ribeiro RP, EL Moreira, DB Santos, D Colle, AA Dos Santos, KC Peres, CP Figueiredo, M Farina. Probucol affords neuroprotection in a 6-OHDA mouse model of Parkinson's disease. Neurochemical Research. 2013;38:660-668.
9. Colle D, Santos DB, Moreira EL, Hartwig JM, dos Santos AA, Zimmermann LT, Hort MA, Farina M. Probucol increases striatal glutathione peroxidase activity and protects against 3-nitropropionic acid-induced pro-oxidative damage in rats. PLoS One. 2013;14;8:e67658.
10. Mooranian A, Zamani N, Luna G, Al-Sallami H, Mikov M, Goločorbin-Kon S, Stojanovic G, Arfuso F, Kovacevic B, Al-Salami H. Bile acid-polymer-probucol microparticles: protective effect on pancreatic β-cells and decrease in type 1 diabetes development in a murine model. Pharm Dev Technol. 2019;24:1272-1277.
11. Zucoloto AZ, Manchope MF, Borghi SM, Dos Santos TS, Fattori V, Badaro-Garcia S, Camilios-Neto D, Casagrande R, Verri WA Jr. Probucol Ameliorates Complete Freund's Adjuvant-Induced Hyperalgesia by Targeting Peripheral and Spinal Cord Inflammation. Inflammation. 2019;42:1474-1490.
12. Snezhkina AV, Kudryavtseva AV, Kardymon OL, Savvateeva MV, Melnikova NV, Krasnov GS, Dmitriev AA. ROS Generation and Antioxidant Defense Systems in Normal and Malignant Cells. Oxid Med Cell Longev. 2019;2019:6175804.
13. Hanikoglu A, Ozben H, Hanikoglu F, Ozben T. Hybrid Compounds & Oxidative Stress Induced Apoptosis in Cancer Therapy. Curr Med Chem. 2020;27:2118-2132.
14. Udensi UK, Tchounwou PB. Dual effect of oxidative stress on leukemia cancer induction and treatment. J Exp Clin Cancer Res. 2014;33:106.
15. Agarwal A, Muñoz-Nájar U, Klueh U, Shih SC, Claffey KP. N-acetyl-cysteine promotes angiostatin production and vascular collapse in an orthotopic model of breast cancer. Am J Pathol. 2004;164:1683-1696.
16. Fontana F, Moretti RM, Raimondi M, Marzagalli M, Beretta G, Procacci P, Sartori P, Montagnani Marelli M, Limonta P. δ-Tocotrienol induces apoptosis, involving endoplasmic reticulum stress and autophagy, and paraptosis in prostate cancer cells. Cell Prolif. 2019;52:e12576.
17. Zan L, Chen Q, Zhang L, Li X. Epigallocatechin gallate (EGCG) suppresses growth and tumorigenicity in breast cancer cells by downregulation of miR-25. Bioengineered. 2019;10:374-382.
18. Zeng LH, Wang QM, Feng LY, Ke YD, Xu QZ, Wei AY, Zhang C, Ying RB. High-dose vitamin C suppresses the invasion and metastasis of breast cancer cells via inhibiting epithelial-mesenchymal transition. Onco Targets Ther. 2019;12:7405-7413.
19. Sun C, Zhang S, Liu C, Liu X. Curcumin Promoted miR-34a Expression and Suppressed Proliferation of Gastric Cancer Cells. Cancer Biother Radiopharm. 2019;34:634-641.
20. Sarkar R, Mukherjee A, Mukherjee S, Biswas R, Biswas J, Roy M. Curcumin augments the efficacy of antitumor drugs used in leukemia by modulation of heat shock proteins via HDAC6. J Environ Pathol Toxicol Oncol. 2014;33:247-263.
21. Mastrangelo D, Massai L, Lo Coco F, Noguera NI, Borgia L, Fioritoni G, Berardi A, Iacone A, Muscettola M, Pelosi E, Castelli G, Testa U, Di Pisa F, Grasso G. Cytotoxic effects of high concentrations of sodium ascorbate on human myeloid cell lines. Ann Hematol. 2015;9:1807-1816.
22. Li RF, Feng YQ, Chen JH, Ge LT, Xiao SY, Zuo XL. Naringenin suppresses K562 human leukemia cell proliferation and ameliorates Adriamycin-induced oxidative damage in polymorphonuclear leukocytes. Exp Ther Med. 2015;9:697-706.
23. Geng W, Guo X, Zhang L, Ma Y, Wang L, Liu Z, Ji H, Xiong Y. Resveratrol inhibits proliferation, migration and invasion of multiple myeloma cells via NEAT1-mediated Wnt/beta-catenin signaling pathway. Biomed Pharmacother. 2018;107:484-494.
24. Najibi A, Heidari R, Zarifi J, Jamshidzadeh A, Firoozabadi N, Niknahad H. Evaluating the Role of Drug Metabolism and Reactive Intermediates in Trazodone-Induced Cytotoxicity toward Freshly-Isolated Rat Hepatocytes. Drug Res (Stuttg). 2016;66:592-596.
25. Hekmatshoar Y, Ozkan T, Altinok Gunes B, Bozkurt S, Karadag A, Karabay AZ, Sunguroglu A. Characterization of imatinib-resistant K562 cell line displaying resistance mechanisms. Cell Mol Biol (Noisy-le-Grand). 2018;64:23-30.
26. Zhang Z, H Cao, S Jiang, Z Liu, X He, H Yu, Y Li. Nanoassembly of probucol enables novel therapeutic efficacy in the suppression of lung metastasis of breast cancer. Small (Weinheim an der Bergstrasse, Germany). 2014;10:4735-4745.
27. Zarkovic M, Qin X, Nakatsuru Y, Zhang S, Yamazaki Y, Oda H, Ishikawa T, Ishikawa T. Inhibitory effect of probucol on benzo[a]pyrene induced lung tumorigenesis. Carcinogenesis. 1995;16:2599-2601.

28. Chuang LY, Guh JY, Ye YL, Lee YH, Huang JS. Effects of probucol on cell proliferation in human ovarian cancer cells. Toxicol Res (Camb). 2016;5:331-339.

29. Iqbal M, Okazaki Y, Okada S. Probucol modulates iron nitrilotriacetate (Fe-NTA)-dependent renal carcinogenesis and hyperproliferative response: diminution of oxidative stress. Mol Cell Biochem. 2007;304:61-69.

30. Nishimura G, Yanoma Y, Mizuno H, Kawakami, Tsukuda M. An antioxidant, probucol, induces anti-angiogenesis and apoptosis in athymic nude mouse xenografted human head and neck squamous carcinoma cells. Jpn J Cancer Res. 1999;90:1224-1230.

31. Kaneko M, Hayashi J, Saito I, Miyasaka N. Probucol downregulates E-selectin expression on cultured human vascular endothelial cells. Arterioscler Thromb Vasc Biol. 1996;16:1047-1051.

32. Chen JW, Chen YH, Lin FY, Chen YL, Lin SJ. Ginkgo biloba extract inhibits tumor necrosis factor-α–induced reactive oxygen species generation, transcription factor activation, and cell adhesion molecule expression in human aortic endothelial cells. Arterioscler Thromb Vasc Biol. 2003;23:1559-1566.

Turk J Pharm Sci 2021;18(1):80-90
DOI: 10.4274/tjps.galenos.2019.29000

ORIGINAL ARTICLE

Antiplasmodial Activity and Phytochemical Constituents of Selected Antimalarial Plants Used by Native People in West Timor Indonesia

Batı Timor Endonezya Yerel Halkının Kullandığı Bazı Antimalaryal Bitkilerin Antiplazmodiyal Aktiviteleri ve Fitokimyasal Bileşenleri

Maximus M. TAEK[1]*, Gerardus D. TUKAN[1], Bambang E.W. PRAJOGO[2], Mangestuti AGIL[2]

[1]Widya Mandira Catholic University Faculty of Mathematics and Natural Sciences, Department of Chemistry, Kupang, Indonesia
[2]Airlangga University Faculty of Pharmacy, Department of Pharmacognosy and Phytochemistry, Surabaya, Indonesia

ABSTRACT

Objectives: To document traditional antimalarial plants used by Tetun ethnic people in West Timor Indonesia and evaluate the antiplasmodial activity and phytochemicals of several plants that are widely used as oral medicine.

Materials and Methods: A field study to document antimalarial plants followed by laboratory works to test antiplasmodial activity and identify the phytochemical constituents of some selected plants extract were applied. The inhibitory potency of ethanolic extracts of *Strychnos ligustrina* wood, roots of *Calotropis gigantea, Fatuoa pilosa,* and *Neoalsomitra podagrica*, whole plant of *Cleome rutidosperma* and *Physalis angulata*, stem barks of *Alstonia spectabilis, Alstonia scholaris, Jatropha curcas* and *Plumeria alba*, and leaves of *Melia azedarac*h on the *Plasmodium falciparum* 3D7 strain *in vitro* were tested. Gas chromatography-mass spectrometry instrument was used to analyze the phytochemicals of the extracts.

Results: The Tetun ethnic people use 50 plant species as antimalarials. *P. angulata, J. curcas*, and *A. spectabilis* extracts show strong antiplasmodial activity with IC_{50} values of 0.22, 0.22, and 1.23 µg/mL, respectively; *N. podagrica, A. scholaris, F. pilosa,* and *P. alba* were moderate antiplasmodials with IC_{50} values of 11.60, 15.46, 24.92, and 36.39 µg/mL, respectively; and *C. rutidosperma, M. azedarach, S. ligustrina, and C. gigantea* were weak antiplasmodials with IC_{50} values of 54.25, 63.52, 63.91, and 66.49 µg/mL, respectively. The phytochemicals identification data indicate that these 11 plants contain alkaloids, terpenoids, steroids, coumarins, alcohols, thiols, phenolics, aldehydes, fatty acids, esters, and so forth.

Conclusion: Plants widely used as antimalarials by the Tetun ethnic people is proven to have antiplasmodial activity.

Key words: Ethnomedicine, medicinal plant, malaria, antiplasmodial activity

ÖZ

Amaç: Endonezya Batı Timor'unda Tetun etnik halkı tarafından kullanılan geleneksel antimalaryal bitkileri, yaygın oral ilaçlar olarak kullanılan bazı bitkilerin antiplazmodial aktivitelerini ve fitokimyasallarını belirlemek.

Gereç ve Yöntemler: Antimalaryal bitkileri belirleyen alan çalışmasını takiben, antiplazmodiyal aktiviteyi test etmek ve seçilen bitki ekstraktlarından fitokimyasal bileşenleri belirlemek için laboratuvar çalışması yapılmıştır. *Strychnos ligustrina* bitkisinin odunsu kısımları, *Calotropis gigantea, Fatuoa pilosa* ve *Neoalsomitra podagrica* bitkilerinin kökleri, *Cleome rutidosperma* ve *Physalis angulata* bitkilerinin tamamı, *Alstonia spectabilis, Alstonia scholaris, Jatropha curcas* ve *Plumeria alba* bitkilerinin gövde kabukları ile Melia azedarach yaprakları etanol ekstrelerinin inhibitör potansiyelleri *Plasmodium falciparum* 3D7 suşunda *in vitro* koşullarda belirlendi. Ekstrelerin fitokimyasal içerikleri gaz kromatografisi-kütle spektrometresi ile analiz edildi.

Bulgular: Tetun etnik halkının antimalaryal olarak kullandığı 50 bitki türü olduğu belirlendi. *P. angulata, J. curcas* ve *A. spectabilis* ekstreleri, sırasıyla 0,22, 0,22 ve 1,23 µg/mL IC_{50} değerleriyle güçlü antiplazmodiyal aktivite gösterirken, *N. podagrica, A. scholaris, F. pilosa* ve *P. alba*, sırasıyla 1,60, 15,46, 24,92 ve 36,39 µg/mL IC_{50} değerleriyle, ve *C. rutidosperma, M. azedarach, S. ligustrina* ve *C. gigantea*, sırasıyla 54,25, 63,52, 6391 ve 66,49 µg/mL IC_{50} değerleriyle zayıf antiplazmodiyal aktivite gösterdi. Fitokimyasal tanımlamanın verileri, bu 11 bitkinin alkaloitler, terpenoidler, steroidler, kumarinler, alkoller, tiyoller, fenolikler, aldehitler, yağ asitleri, esterler ve diğer bileşikleri içerdiğini gösterdi.

Sonuç: Tetun etnik halkı tarafından yaygın olarak antimalaryal olarak kullanılan bitkilerin antiplazmodiyal aktivite gösterdiği kanıtlanmıştır.

Anahtar kelimeler: Etnotıp, şifalı bitki, sıtma, antiplazmodiyal aktivite

***Correspondence:** maximusmt2012@gmail.com, **Phone:** +6282245811193 **ORCID-ID:** orcid.org/0000-0002-4597-2167
Received: 22.10.2019 **Accepted:** 26.12.2019

INTRODUCTION

Plants are very valuable source in obtaining various pharmacological active substances to deal with various human health problems.[1] It has been the basis and an important part of various traditional medical systems for thousands of years. It is estimated that around 25% or 40,000-70,000 of the total number of plant species known today are used as medicinal plants in various places all over the world.[2,3]

More recently, natural product chemicals isolated from plants have been a good source of lead compounds used to treat various infectious diseases, including malaria. Two examples of phenomenal lead compounds that have greatly contributed in reducing malaria deaths worldwide are quinine isolated from *Cinchona* sp. stem bark and artemisinin from Chinese medicinal plants *Artemisia annua*.[4] Derivatives such as chloroquine, amodiaquine, primaquine, and mefloquine have been synthesized from quinine; and compounds such as artemether, arteether, and sodium artesunate have been produced from artemisinin. However, *Plasmodium* has shown in the last few decades increasing resistance to antimalarial quinine derivatives, especially chloroquine, which made them no longer effective. *Plasmodium falciparum* has also showed an increase in resistance to artemisinin-based antimalarials as reported in several recent publications.[5]

Plasmodium's increasing resistance to currently used antimalarial drugs encouraged researchers to continue searching for new and more effective antimalarials.[6] Plants have become one of the most important sources in searching new potential antimalarials in traditional medicine of various ethnics worldwide.[7] A promising and better approach in finding new antimalarial(s) is selecting plants that have been traditionally used in treating malaria. With this, resources such as high investment and skills are saved, and the time of plant selection and testing of its antimalarial activity is shown to be accelerated compared with the random selection approach. For the development of important active antimalarials, research on medicinal plants of various traditional medicine systems could provide useful leads.[8]

The experience of the Tetun people, a native ethnic in West Timor, in interacting with malaria for a long time led to them to develop their own methods of treatment. They identified malaria as sick of hot body or fever. A variety of medicinal plant formula called ai tahan or kwa were carried out by the Tetun community as a traditional treatment for malaria, which is applied by drinking, bathing, massage, inhaling, and cataplasm.[9] In-depth exploration of the antimalarial plants used in the community's traditional medicine might provide a valuable contribution in discovering new sources of antimalarial substances.

This research is an ethnomedicine study that was first conducted in the Tetun community. In our study, two research steps were performed. For the first step, a field research was conducted to document various species of medicinal plants and formula of traditional medicines for oral treatment of malaria used by the Tetun people. In the second step, some of the high-frequency mentioned plants were selected to test their antiplasmodial activity. *In vitro* antiplasmodial activity testing was carried out against the chloroquine-sensitive *P. falciparum* 3D7 strain.

MATERIALS AND METHODS

Field study

The field research was carried out in several subdistricts of Belu (9˚15,0 S, 124˚40 E) and Malaka Districts (9˚34 S, 124˚54 E). These two districts are located along the borderline of East Nusa Tenggara Province (Indonesia) and the Republic Democratic de Timor Leste. In this field study, information was collected through interviews and discussions. This study consists of 94 informants, 42 males and 52 females, who were traditional healers, former malaria patients that have undergone traditional medicine, and others who have knowledge and experience in the traditional treatment of malaria. These informants were between the ages of 40 and 90 years old, and almost all of them have settled in their area since they were born.

Data collected on traditional medicinal plants used for malaria treatment include: the plant's local name, place where the plant was obtained, part of the plant used as a medicine, methods of processing and usage, dosage and duration of use, and the medication's claimed effect. To prepare an herbarium, the plants mentioned by the informants were then collected in parts. First, all plants were identified by matching their local name with the scientific names of the species listed in the Timorese local plants book.[10] Second, experts from the Lembaga Ilmu Pengetahuan Indonesia-Bogor Botanic Garden identified the plants again. Part(s) of some plants mentioned by the informants with high frequency were collected in greater quantities for laboratory evaluation of their antimalarial activity and phytochemicals identification. Those plant part samples were collected from the area where the plant was mentioned.

Preparation of the plant extract

The attached dirt on the plant part samples, that is the whole plant, stem bark, wood, roots, and leaves, were cleaned using tap water. They were then air-dried at room temperature until they were completely dry and then grounded into powder. The extracts were prepared by maceration. Plant powder of 20 g each was macerated with 95% ethanol for 24 h at room temperature and then filtered. Maceration was repeated three times, and the filtrates were collected and then evaporated to dry using a vacuum rotary evaporator at 40˚C. The dried extracts were stored in a closed container, and were then used for antiplasmodial activity test against *P. falciparum* and phytochemical analysis.

In vitro antiplasmodial activity test

In vitro antimalarial activity testing was carried out on the chloroquine-sensitive 3D7 strain of *P. falciparum* obtained from the Institute of Tropical Diseases Airlangga University, Surabaya Indonesia. In 96 microwells plate, *Plasmodium* was cultivated according to a method developed by Trager and Jenssen.[11] It was carried out using O type human red blood cells (RBC) with 5% hematocrit suspended in RPMI 1640 medium.

In a CO_2 incubator, the culture was incubated at 37°C, and the medium was replaced every day until parasitemia reaches 1%-2%. Dried plant extracts were dissolved in dimethylsulphoxide and filtered through a 0.22 µm membrane filter. The solution of each extract was then placed in microwells containing *Plasmodium* suspension with 1% parasitemia. To obtain the final concentrations of 100, 10, 1.0, 0.1, and 0.01 µg/mL, the solutions were diluted in a series of tenfold dilution with the RPMI 1640 medium. Two series of controls were set up: as a positive control, in which parasitized blood cells without the addition of plant extract; and as a positive control where parasitized blood cells were added with chloroquine diphosphates. To make final concentrations of 100, 10, 1.0, 0.1, and 0.01 µg/mL, preparation for chloroquine diphosphates were similar to plant extracts. The culture was then incubated at 37°C in a CO_2 incubator for 48 h. Duplicate tests were performed. RBC culture was harvested after 48 h of incubation. On a glass object, a thin blood was smeared, dried and fixed with methanol, and stained with Giemsa. A light microscope with 1000x magnification was then used to count the number of parasitized RBC.

Statistical analysis

A total of 1000s RBC was counted by observing blood smear slides under a microscope, and the number of infected RBC (iRBC) was obtained from the antiplasmodial activity test. The amount of iRBC to the total RBC was expressed as percentage of parasitemia, which was calculated using the numerical formula as follows:

Percentage of parasitemia, p=[(ΣiRBC/ΣRBC) x100%].

From the percentage of parasitemia data in treated groups and negative control, *Plasmodium*'s growth and inhibition percentages were calculated as follows:

Percentage of growth: (Pt/Pnc) x100%,

Percentage of inhibition: 100% - percentage of growth,

where *Pt* is the percentage of parasitemia in treated groups and *Pnc* is the percentage of parasitemia in the negative control group. *Pt* and *Pnc* were calculated at the beginning of test (0 h, P_0) and when the culture was harvested (48 h, P_{48}). The parasitemia's actual percentage value was P_{48} - P_0. The inhibition percentage range is 0%, which means no inhibition, to 100%, which is complete inhibition.

Probit analysis was used to statistically calculate the 50% inhibitory concentration (IC_{50}) by plotting the data on inhibition percentage versus concentration of each extract. To classify the antimalarial potency of each extract, the IC_{50} value was compared with the value given by the literature.

Identification of phytochemicals in extracts

Gas chromatography-mass spectrometry (GC-MS) was used to analyze the phytochemicals contained in each extract. An Agilent 6980N Network GC system with autosampler was linked to a detector of Agilent 5973 inert MSD. A column of J and W Scientific HP-5MS 30 m × 0.25 mm × 0.25 µm was used. To interpret the compounds, the GC-MS instrument used a Wiley version 7.0 database. The GC-MS operational conditions were set up as follows: Inlet temperature of 250°C; and oven temperature programmed at 50°C for 5 min and increased to 10°C/min up to 280°C, maintained constant for 15 min. Temperatures of Aux, MS Quad, and MS Source were 250°C, 150°C, and 230°C, respectively. Used as sample carrier was helium gas with 99.999% purity. Gas flow in the column was set constant at 1.0 mL/min for 50 min running time. Scan mode ranged from 20 amu to 600 amu.

Each extract was first dissolved in 5 mL ethanol, sonicated for 15 min, and filtered through a 0.45-µm nylon membrane filter before running the analysis of the chemical content. The filtrate of 0.2 µL was then injected into the GC-MS system. The results were printed out after the analysis process in the instrument was finished.

Ethics committee approval statement

All field research designs have been approved by the Government of East Nusa Tenggara Province (no: 070/535/DPM-PTSP/2017 and no: 070/535/DPM-PTSP/2017, dated February 28, 2017), the Government of Malaka District (no: 070/150/IV/2017, dated March 3, 2017), and the Government of Belu District (no: BKBP-070/75/III/2017, dated March 29, 2017) to guarantee the ethics and legality of human involvement in this study.

RESULTS AND DISCUSSION

Plants used for malaria treatment

Documented in this study are 50 plant species belonging to 27 families that used by the Tetun ethnic group for malaria treatment in the Malaka and Belu Districts (Table 1). These plants were used as single formula or combination of plants in various recipes for oral application. Some of the plants that are most frequently mentioned by the informants are *Strychnos ligustrina* Blume, *Calotropis gigantea* (L.) R. Br., *Cleome rutidosperma* DC., *Physalis angulata* L., *Carica papaya* L., *Alstonia spectabilis* R.Br., *Alstonia scholaris* (L.) R. Br., *Melia azedarach* L., *Plumeria alba* L., *Swietenia macrophylla* King, and *Momordica balsamina* L.

The highest number of plant species belong to seven families: Apocynaceae and Fabaceae (five species each), Cucurbitaceae (four species), and Meliaceae, Moraceae, Euphorbiaceae, and Rubiaceae (three species each). The most widely used plant parts in its utilization as medicinal materials are the stem bark (21 species), leaves (19 species), and root (11 species). Some plants are used more than one part at a time. Decoction and infusion are the common preparation modes of various formula for oral use of these plants.

Plant selection for antiplasmodial activity test

For antiplasmodial activity testing, 11 plants species with high citation frequency were selected. These are *S. ligustrina* Blume (34.04%), *C. gigantea* (L.) R. Br. (24.47%), *C. rutidosperma* DC. (18.09%), *P. angulata* L. (18.09%), *A. spectabilis* R. Br. (17.02%), *A. scholaris* (L.) R. Br. (13.83%), *M. azedarach* L. (13.83%), *Fatoua pilosa* Gaudich. (7.45%), *Jatropha curcas* (6.38%), *P. alba* L. (6.38%), and *Neoalsomitra podagrica* Steenis (4.26%).

Table 1. Plants used by the Tetun ethnic people for malaria treatment

Botanic name	Family	Local name	Plants' part used	Frequency of citation n (%)*
Strychnos ligustrina Blume	Loganiaceae	Bakumoru	Wood, stem bark	32 (34.04)
Calotropis gigantea (L.) R. Br.	Asclepediaceae	Fuka	Root	23 (24.47)
Cleome rutidosperma DC.	Capparaceae	Lakaur	Whole plant	17 (18.09)
Physalis angulata L.	Solanaceae	Babotore	Whole plant	17 (18.09)
Carica papaya L.	Caricaceae	Dila	Leaves	16 (17.02)
Alstonia spectabilis R.Br.	Apocynaceae	Kroti metan	Stem bark	16 (17.02)
Alstonia scholaris (L.) R.Br.	Apocynaceae	Kroti mutin	Stem bark	13 (13.83)
Melia azedarach L.	Meliaceae	Samer	Leaves, stem bark	13 (13.83)
Fatoua pilosa Gaudich	Moraceae	Lorowen	Root	7 (7.45)
Jatropha curcas L.	Euphorbiaceae	Badut malaka mutin	Stem bark	6 (6.38)
Swietenia macrophylla King	Meliaceae	Mahoni	Seed	6 (6.38)
Plumeria alba L.	Apocynaceae	Mukrin	Stem bark	6 (6.38)
Momordica balsamina L.	Cucurbitaceae	Bria fuik	Leaves, fruit	5 (5.32)
Neoalsomitra podagrica Steenis	Cucurbitaceae	Masin borat	Root	4 (4.26)
Wrightia pubescens R. Br.	Apocynaceae	Lalitin feto	Leaves, root, stem bark	3 (3.19)
Tabernaemontana pandacaqui Lam.	Apocynaceae	Lalitin mane	Stem bark	3 (3.19)
Aegle marmelos (L.) Correa	Rutaceae	Dilabutak	Stem bark, root, leaves	3 (3.19)
Andrographis paniculata (Burm.f.) Nees.	Acanthaceae	Karlulu	Whole plant	2 (2.13)
Cassia fistula L.	Fabaceae	Liman tohar	Stem bark	2 (2.13)
Cassia siamea Lam.	Fabaceae	Krui	Leaves, stem bark	2 (2.13)
Coccinia grandis (L.) Voigt	Cucurbitaceae	Kabasa	Leaves	2 (2.13)
Ficus callosa Willd.	Moraceae	Salur	Stem bark	2 (2.13)
Ficus hispida L.f.	Moraceae	Baulenuk	Leaves	2 (2.13)
Phyllanthus niruri L.	Phyllanthaceae	Renes	Whole plant	2 (2.13)
Acacia leucophloea (Roxb.) Willd.	Fabaceae	Besak	Stem bark	1 (1.06)
Blumea balsamifera (L.) DC.	Compositae	Fafok	Stem bark	1 (1.06)
Bridelia ovata Decne.	Euphorbiaceae	Knabu	Leaves	1 (1.06)
Brucea javanica (L.) Merr.	Simaroubaceae	Ai lakar	Leaves, stem bark, root	1 (1.06)
Capsicum frutescens L.	Solanaceae	Masimanas	Fruit	1 (1.06)
Ceiba pentandra (L.) Gaertn.	Malvaceae	Kabidawa	Leaves	1 (1.06)
Curcuma domestica Val.	Zingiberaceae	Kinur	Rhizome	1 (1.06)
Dendropthoe pentandra (L) Miq.	Loranthaceae	Tau tiu ten	Leaves	1 (1.06)
Dysoxylum gaudichaudianum (A. Juss.) Miq.	Meliaceae	Meda lasan	Leaves	1 (1.06)
Garuga floribunda Decne.	Burseraceae	Feu	Stem bark	1 (1.06)
Gossypium herbaceum L.	Malvaceae	Kabas fuan mean	Root	1 (1.06)
Grewia koodersiana Burrett	Tilliaceae	Lenok	Root	1 (1.06)
Gymnopetalum chinense (Lour.) Merr.	Cucurbitaceae	Kolokoen	Root	1 (1.06)
Imperata cylindrica (L.) P. Beauv.	Poaceae	Hae manlain	Root	1 (1.06)
Indigofera suffruticosa Mill.	Fabaceae	Taun	Leaves	1 (1.06)
Jatropha gossypifolia L.	Euphorbiaceae	Badut malaka mean	Stem bark	1 (1.06)
Morinda citrifolia L.	Rubiaceae	Nenuk	Leaves, fruit, stem bark	1 (1.06)

Table 1 continue

Nauclea orientalis (L.) L.	Rubiaceae	Kafiru	Stem bark	1 (1.06)
Piper cubeba L.f.	Piperaceae	Kunus aleten	Leaves	1 (1.06)
Sterculia foetida L.	Sterculiaceae	Abano	Stem bark	1 (1.06)
Tamarindus indica L.	Fabaceae	Sukaer	Leaves	1 (1.06)
Uvaria rufa Blume	Annonaceae	Koke	Root	1 (1.06)
Wendlandia burkillii Cowan	Rubiaceae	Katimun	Stem bark	1 (1.06)
Ziziphus timoriensis DC.	Rhamnaceae	Ai sisi	Leaves	1 (1.06)
Not identified	Not identified	Moat tiris	Leaves	1 (1.06)
Not identified	Not identified	Uas laomea	Tuber	1 (1.06)

*: The total percentage is greater than 100% because each informant (N=94) mentioned more than one plant

C. papaya L. (17.02%), *S. macrophylla* King (6.38%), and *M. balsamina* L. (5.32%) were three other plants with high citation frequency but were not included antiplasmodial activity testing because of several reasons. The *C. papaya* was not selected testing for the reason that it is a food plant that is consumed every day as a vegetable. The wild bitter melon *M. balsamina* was also not included because it was difficult to obtain, very rarely cultivated, usually only grow wild, and is seasonal. The *S. macrophylla* was excluded because according to the informants, the use of its seeds as an antimalarial medicine was not sourced from traditional practice of the Tetun people's ancestors.

Antiplasmodial activity

A graphical comparison of the extracts' ability to inhibit *Plasmodium* growth is shown in Figure 1. It can be seen from this graph that with an increase in concentration, three extracts, *P. angulata* L., *J. curcas* L., and *A. spectabilis* R. Br. show a more significant increase in their inhibitory activity compared with the other extracts. The graph presents that on average, a tenfold increase in the concentration of these three extracts increases their antiplasmodial activity twice.

Table 2 lists the antiplasmodial activity of each extract in the form of percentage of inhibition at each concentration level and their IC_{50} values. The concentration that causes 50% reduction in *Plasmodium* growth is represented by IC_{50}. A smaller IC_{50} value indicates the better the extract's antiplasmodial activity; and vice versa, greater IC_{50} indicates low inhibitory activity. In the positive control, with the same experimental condition, chloroquine diphosphate has an IC_{50} value of 0.005 µg/mL.

Ouattara et al.[12] categorized an extract as very active or strong antiplasmodial if IC_{50} <5 µg/mL, active or moderate antiplasmodial if IC_{50}: 5-50 µg/mL, less active or weak antiplasmodial if IC_{50}: 50-100 µg/mL, and inactive if IC_{50} >100 µg/mL. Based on these categories, ethanolic extracts of *P. angulata* L. (IC_{50} 0.22 µg/mL), *J. curcas* L. (IC_{50} 0.22 µg/mL), and *A. spectabilis* R. Br. (IC_{50} 1.23 µg/mL) are strong antiplasmodials; whereas *N. podagrica* Steenis (IC_{50} 11.60 µg/mL), *A. scholaris* (L.) R. Br. (IC_{50} 15.46 µg/mL), *F. pilosa* Gaudich. (IC_{50} 24.92 µg/mL), and *P. alba* L. (IC_{50} 36.39 µg/mL) are moderates. The extracts of *C. rutidosperma* DC. (IC_{50} 54.25 µg/mL), *M. azedarach* L. (IC_{50} 63.52 µg/mL),

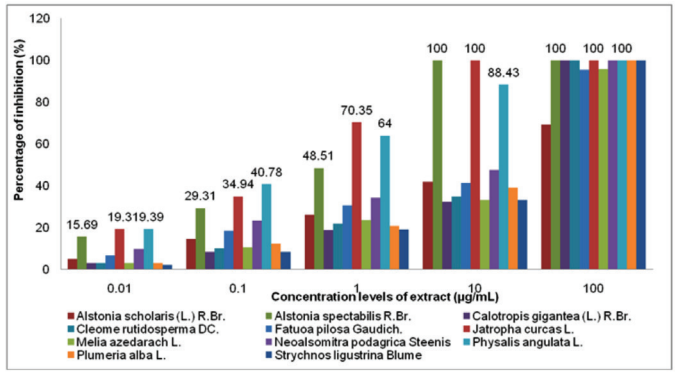

Figure 1. Graphical comparison of the plant extract's inhibitory ability on *Pasmodium falciparum* 3D7 strain *in vitro*

S. ligustrina Blume (IC_{50} 63.91 µg/mL), and *C. gigantea* (L.) R. Br. (IC_{50} 66.49 µg/mL) are weak antiplasmodial. In general, although they are relatively weaker than chloroquine diphosphates, *P. angulata* L., *J. curcas* L., and *A. spectabilis* R. Br. ethanolic extracts showed good antiplasmodial effects on *P. falciparum* 3D7 strain.

Among the 11 plant extracts, *P. angulata* L. showed the strongest antiplasmodial activity. This result is in line with the findings of previous studies using methanol and dichloromethane extracts of *P. angulata* L. leaves, where these extracts presented very high activity with IC_{50} <3 µg/mL against the chloroquine-sensitive 3D7 and chloroquine-resistant W2 strains of *P. falciparum in vitro*. *P. angulata* extracts also showed good *in vivo* parasitemia inhibition on mice infected by *Plasmodium berghei*.[13]

In this study, the ethanolic extract of *J. curcas* L. stem bark showed strong antiplasmodial activity, equivalent to *P. angulata* L. In another study, it was found that mice infected by *P. berghei* treated with 250, 500, and 750 mg/kg body weight doses of aqueous extract of *J. curcas* L. stem bark decreases parasitemia percentage from 9.25% to 7.80%, suggesting that the plant extract possesses antiplasmodial properties.[14]

Results in this study showed that ethanolic extract of *P. alba* L. stem bark is a moderate antiplasmodial. Another study showed that water extract (300 mg/kg body weight) and dichloromethane-methanol extract (300 mg/kg body weight) of this plant's stem bark reduces parasitemia level of mice

Table 2. Antiplasmodial activity of plant extracts

Plant extract	Inhibition percentage of extract on *Plasmodium* (%) at each level of concentration (µg/mL)					IC_{50} (µg/mL)
	0.01	0.1	1.0	10	100	
Alstonia scholaris (L.) R. Br.	5.06	14.52	26.20	41.89	69.26	15.46
Alstonia spectabilis R. Br.	15.69	29.31	48.51	100.00	100.00	1.23
Calotropis gigantea (L.) R. Br.	2.96	8.43	18.96	32.44	100.00	66.49
Cleome rutidosperma DC.	3.04	10.25	22.09	34.96	100.00	54.25
Fatuoa pilosa Gaudich	6.70	18.69	30.78	41.39	95.56	24.92
Jatropha curcas L.	19.30	34.94	70.35	100.00	100.00	0.22
Melia azedarach L.	2.96	10.78	23.74	33.22	95.91	63.52
Neoalsomitra podagrica Steenis	9.74	23.39	34.26	47.74	100.00	11.60
Physalis angulata L.	19.39	40.78	64.00	88.43	100.00	0.22
Plumeria alba L.	2.98	12.45	20.88	39.04	100.00	36.39
Strychnos ligustrina Blume	2.20	8.56	19.19	33.33	100.00	63.91

infected by *P. berghei* to 16.4% and 20.0%, respectively, in eight days of evaluation.[15]

Although the ethanolic extract of *A. scholaris* (L.) R. Br. stem bark in this study showed a moderate activity, the results in another study showed that methanolic extract of its stem bark showed excellent antiplasmodial activity against *P. falciparum* 3D7 strain, with a mean IC_{50} of 0.1650±0.1100 µg/mL.[16] The stem bark of *A. scholaris* (L.) R. Br. contains villalstonine and macrocarpamine alkaloids, which are antimalarial active, with the IC_{50} values of 0.27 and 0.36 µM, respectively, against chloroquine-resistant *P. falciparum* K1 strain.[17]

Ethanolic extracts of *S. ligustrina* Blume, *C. gigantea* (L.) R. Br., *C. rutidosperma* DC., and *M. azedarach* L. in this study showed weak activity against *P. falciparum* 3D7 strain, with IC_{50} >50 µg/mL. However, it was found in several other studies that these plants showed a good antiplasmodial activity when different solvents were used for extraction. Water extract of *S. ligustrina* Blume wood was classified as a strong antiplasmodial as it inhibited *P. falciparum* growth *in vitro* by 98.1% at a concentration of 1.0 mg/mL.[18] Methanolic extract of *C. gigantea* (L.) R. Br. leaves showed moderate antimalarial activity against *P. falciparum in vitro* with an IC_{50} value of 12.17 µg/mL, and very good activity against *P. berghei in vivo*.[19] Ethanolic extract of *C. rutidosperma* DC. whole plant showed moderate antimalarial activity with IC_{50} of 34.4 µg/mL; however, its water extract was less active with IC_{50} >100 µg/mL against chloroquine-sensitive *P. falciparum* D10 strain *in vitro*.[20]

The results of this antimalarial activity evaluation did not linear to rank of the plants based on their percentage of citation listed in Table 1. In laboratory testing, the informants' most frequently mentioned plants, which are the *S. ligustrina* Blume, *C. gigantea* (L.) R. Br., and *C. rutidosperma* DC., turned out to show weak antiplasmodial activity. However, it does not mean that these plants' effectiveness claims as antimalarials are incorrect. Possible causes of non-synchronous data between frequency of citation of the informants and the laboratory antiplasmodial evaluation of these plants can be explained as follows. Firstly, the use of ethanol as an extraction solvent can cause differences in type and amount of antiplasmodial active compounds extracted into it, which causes differences in the antiplasmodial activity shown by each plant extract. Secondly, the *in vitro* system is very different from the biochemical system in the human body, therefore, *in vitro* antimalarial activity results cannot directly describe the actual events in human body. Therefore, it is possible for an antimalarial plant to be active in human and be inactive in an *in vitro* testing, and vice versa. Thirdly, certain plants may not be true antimalarial (antiplasmodial) that works to kill or inhibit *Plasmodium* growth. It may more likely be an indirect antimalarial (antipyretic, analgesic or antiinflammatory) that works to heal malaria-related symptoms, and therefore, the test showed no significant activity as antiplasmodial. As is known, traditional treatment of malaria is a symptomatic healing, which mainly aims to reduce heat or fever; therefore, it is possible that a plant used in this treatment is more likely antipyretic than antiplasmodial.[21,22] Plants having antimalarial properties can show a direct effect on *Plasmodium* by inhibiting growth or killing it; or indirect effects on the relationship between parasites and the human body. A plant that inhibits or kills *Plasmodium* is called antiplasmodial or true antimalarial. Other plants may serve as indirect antimalarial, which affects the relationship between the human body as a host and *Plasmodium*, for example as immunostimulant or antipyretic, or causing hemolysis and membrane structure changes, which inhibits *Plasmodium* growth.[23]

This report of antiplasmodial activity of *N. podagrica* Steenis and *F. pilosa* Gaudich. against *P. falciparum* 3D7 strain is the first based on our search of previous studies in any publications. A study on the antimalarial activity of these two plants was not carried out by other researchers before. The *F. pilosa* Gaudich. was only reported to have pharmacological activity as an antimycobacterial,[24] whereas *N. podagrica* Steenis had no known pharmacological activities. Therefore, it is an open

chance to make further evaluation on the antimalarial activity of these two plants, and to identify their antimalarial active compound(s).

Phytochemicals content of the extracts

Table 3 shows the phytochemical analysis results using GC-MS. It can be seen in this table that, overall, these 11 extracts contain various types of natural products, such as alkaloids, terpenoids, steroids, coumarins, alcohols, thiols, phenolics, aldehydes, fatty acids, esters, and so forth. Several studies showed that many secondary plant metabolites, such as alkaloid, flavonoid, xantone, quassinoid, triterpene, and sesquiterpene, have antiplasmodial activity; thus, having the potential to be developed as antimalarial.[4,17]

Although identifying the types and amounts of compounds by GC-MS is limited to volatile compounds, results showed each of the extracts contained quite a number of previously unknown compounds; for example, the alkaloid brucine in *M. azedarach* L leaves. Some of the compounds identified from the 11 plant extracts, such as alstonine, alstomacroline, pleiocarpamine, lupeol, amyrin, and brucine, are known to have antiplasmodial activity.[13,15,17,25-27]

CONCLUSION

The Tetun ethnic people use at least 50 plant species as oral antimalarial medicine. The *A. scholaris* (L.) R. Br., *A. spectabilis* R. Br., *C. gigantea* (L.) R. Br., *C. rutidosperma* DC., *F. pilosa* Gaudich., *J. curcas* L., *M. azedarach* L., *N. podagrica* Steenis, *P. angulata* L., *P. alba* L., and *S. ligustrina* Blume are some of the frequently cited plants. These 11 plants have proven to have antiplasmodial activity, ranged from strong to weak antiplasmodial. The *P. angulata* L., *J. curcas* L., *A. spectabilis* R. Br., *N. podagrica* Steenis, and *F. pilosa* Gaudich. May have a potential to be developed as new sources of antimalarials.

The novelty of this study is the fact that *N. podagrica* Steenis have never been reported used as antimalarial in other traditional medicine systems elsewhere, and this is the first publication of *N. podagrica* Steenis and *F. pilosa* Gaudich.'s antiplasmodial activity against the *P. falciparum* 3D7 strain.

ACKNOWLEDGEMENTS

This study was supported by The Directorate of Research and Community Service, Ministry of Research, Technology and Higher Education, Republic of Indonesia (Research Contract no: 0668/K8/KM/2018), Father Rector of Widya Mandira Catholic University, and Head of Yayasan Pendidikan Katolik Arnoldus Kupang. Thanks to all the informants for their participation in our field study in Belu and Malaka Districts, and to the analyst of Malaria Laboratory, Institute of Tropical Diseases, Airlangga University, for her assistance in the examination of antiplasmodial activity.

Conflicts of interest: No conflict of interest was declared by the authors. The authors alone are responsible for the content and writing of the paper.

Table 3. Phytochemical contents of the plants'extracts identified using gas chromatography-mass spectrometry

Plant's extract	Ret-time (min)	Compound	Area (%)
Alstonia scholaris (L.) R. Br.	20.63	*n*-hexadecanoic acid	0.15
	22.25	*Z*-9-oxtadecenoic acid	0.20
	22.41	Linoleic acid ethyl ester	0.08
	26.93	4, 11-dimethoxy-1H-cyclopent[b]anthracene-2,5,10(3H)-trione	0.14
	27.86	2,2-dimethyl-6,11-dioxo-2,3,6,11-tetrahydro anthra[1,2-b]furan-4-carbaldehyde	0.13
	27.94	Pleiocarpamine	0.11
	28.50	*E*-3,3'-bis-ethylmercapto-1,1'-biisoindolylidene	0.18
	29.22	Dihydroxycrinane	0.22
	30.91	Campesterol	0.66
	31.33	2,2-dimethyl-cholest-4-en-3-one	0.83
	32.24	(23*S*)-ethylcholest-5-en-3β-ol	0.97
	32.69	β-amyrin	27.61
	33.17	Aristolone	5.12
	33.77	Isomultiflorenyl acetate	0.54
	34.25	Maragenin I acetate	18.94
	35.17	Lupenyl acetate	32.03
	35.32	Dihydroagnosterol acetate	0.11
	35.85	Friedoursan-3-one	0.11
Alstonia spectabilis R. Br.	18.33	Coniferol	0.71
	20.67	*n*-hexadecanoic acid	0.53
	22.26	*E*-9-octadecanoic acid	0.46
	25.85	Strictamine	0.44
	26.30	Eupomatenoid-17	0.32
	26.43	Pleiocarpamine	1.70
	26.50	10-aza-8-oxyprotoberberine	2.54
	27.07	2,5-bis(3,5-dimethyl-4-methoxyphenyl)-thiophene	0.26
	27.14	Fluorocarpamine	0.43
	28.18	Vincamajine	2.09
	28.70	Alstomacroline	10.27
	30.36	Homoegonol	0.39
	30.91	*E*-5,10-secocholest-1 (10)-en-3,5-dione	0.89
	31.29	2,2-dimethylcoles-4-en-3-one	1.59
	31.99	(23*S*)-ethylcolest-5-en-3β-ol	1.15
	32.56	β-amyrene	0.27
	32.95	α-amyrin	1.26
	33.05	1-amino-8-methyl-3,6-diazahomodamantan-9-ol	0.51
	33.82	Norolean-12-ene	0.71
	34.54	Aristolone	0.40

Table 3 continue

Calotropis gigantea (L.) R. Br.	1.99	1,1-diethoxy-ethane	0.19
	20.56	Ethyl hexadecanoate	0.10
	22.07	Ethyl linoleate	0.30
	32.91	Urs-12-en-24-oic acid, 3-oxo-, methyl ester	0.54
	33.53	α-amyrin acetate	0.98
	35.12	Dammaradienyl acetate	0.49
	38.17	β-amyrene	0.26
Cleome rutidosperma DC.	2.10	1,1-diethoxy-ethane	0.20
Fatuoa pilosa Gaudich	19.40	Angelicin	6.57
	20.67	*n*-hexadecanoic acid	0.18
	21.48	Heraclin	0.48
	21.61	Seselin	0.55
	22.47	Ethyl oleate	0.13
	22.97	Brayelin	0.12
	25.69	Vincanine	1.79
	26.66	Strictamine	0.19
	30.76	Cycloartenol	0.33
	31.75	Friedelin	0.48
	32.08	Aristolone	3.49
	32.46	β-amyrin	2.55
	32.83	Lupene-3-one	14.04
	33.27	Lupeol	15.40
	34.11	Urs-12-en24-oic acid, 3-oxo-, methyl ester	7.76
	34.28	Fern-7-en-3β-ol	1.75
	34.47	Moretenol	0.67
	34.88	α-amyrin acetate	12.38
	35.38	9,19-cyclolanost-7-en-3-ol	1.15
	36.30	3β-Lup-20(29)-en-3-ol acetate	1.15
Jatropha curcas L.	21.71	2,4-bis(1-phenylethyl)phenol	0.47
	24.76	Isocryptotanshinon	1.08
	31.04	5-methoxy-6-[1-(4-ethoxyphenyl)ethyl]-1,3-benzodioxol	1.02
	31.27	7-bromo-cycloisolongifolene	1.07
	31.65	Ferruginol methyl ether	1.95
	31.88	13, 27-cycloursane	2.85
	32.93	4, 14-dimethyl-9, 9-cyclocholestan-3-one	0.55

Table 3 continue

Melia azedarach L.	2.10	2-allyl-1,3-dioxolan	0.19
	19.05	Ethylpentylacetylene	0.14
	20.51	*n*-hexadecanoic acid	0.81
	22.10	Methyl hexadeca-7,10,13-trienoate	0.56
	22.15	(9*Z*,12*Z*,15*Z*)-octadecatrien-1-ol	0.21
	32.11	(22*E*,24*S*)-stigmasta-4,22-dien-6-one	0.10
	32.92	2,2-dimethylcholest-4-en-3-one	0.35
	35.09	Dibenz[a,h]anthracene	0.23
	36.29	Brucine	0.96
	39.54	4,6-di-m-tolyl-1H-[1,3,5]triazin-2-one	0.28
Neoalsomitra podagrica Steenis	20.63	*n*-Hexadecanoic acid	0.61
	22.26	9, 12, 15-octadecatrien-1-ol	0.99
	22.48	*n*-octadecanoic acid	0.58
	27.62	2, 5, 8-trimethyl-1-naphtol	0.27
	28.25	Plectrinon A	0.43
	29.21	β-tocopherol	0.35
	31.17	3-phenoxyphenol	0.56
	31.96	3β, 5α-stigmasta-7, 25-dien-3-ol	7.94
	32.46	3β, 5α-stigmasta-7, 16-dien-3-ol	2.43
	33.53	Trans, cis-1,2,4-trimethylcyclohexane	1.72
	33.82	Norolean-12-ene	0.77
	34.27	3-methoxy-N-(4-chlorophenyl)sulfonyl benzenecarboximidamide	1.22
	34.51	1-chloro-4-(methylsulfonyl)-benzene	3.91
	34.80	1-(2-thienyl)-1-butanone	2.06
Physalis angulata L.	2.09	1, 1-diethoxy-ethane	0.19
	31.72	Medroxyprogesterone acetate	0.27
	31.88	3β-lupa-1, 20 (29)-dien-3-ol	0.14
	32.40	Ergosta-4, 24 (28)-dien-3-one	0.16
Plumeria alba L.	2.10	1, 1-diethoxy-ethane	0.16
	31.25	3-keto-urs-12-ene	0.37
	31.82	Friedooleanan-3-one	1.07
	32.99	β-amyrin acetate	1.03
	33.86	3β-lup-20 (29)-en-3-ol acetate	9.22
	34.98	Olean-18-en-28-oic acid, 3-oxo-, methyl ester	0.10
Strychnos ligustrina Blume	2.05	1,1-diethoxy-ethane	0.24
	36.10	Brucine	0.73

REFERENCES

1. Verpoorte R. Medicinal plants: A renewable resource for novel leads and drugs. In: Ramawat KG, ed. Herbal drugs: Ethnomedicine to modern medicine. Berlin Heidelberg: Springer-Verlag, 2009.
2. Schippmann U, Leaman DJ, Cunningham AB. Plants as source of medicines: New perspectives. In: Bogers RJ, Craker LE, Lange D, eds. Medicinal and aromatic plants - Agricultural, commercial, ecological, legal, pharmacological and social aspects. Dordrecht: Springer, 2006.
3. Ramawat KG, Goyal S. The Indian herbal drugs scenario in global perspectives. In: Ramawat KG, Merillon JM, eds. Bioactive molecules and medicinal plants. Berlin: Springer, 2008.
4. Schwikkard S, van Heerden F. Antimalarial activity of plant metabolites. Nat Prod Rep. 2002;19:675-692.
5. Htut ZW. Artemisinin resistance in *Plasmodium falciparum* malaria. N Engl J Med. 2009;361:1807-1808.
6. Akuodor GC, Ajoku GA, Ezeunala MN, Chilaka KC, Asika EC. Antimalarial potential of the ethanolic leaf extract of *Pseudocedrala kotschyi*. J Acute Dis. 2015;14:23-27.
7. Willcox ML, Bodeker G. Traditional herbal medicines for malaria. Br Med J. 2004;329:1156-1159.
8. Lemma MT, Ahmed AM, Elhady MT, Ngo HT, Vu TL, Sang TK, Campos-Alberto E, Sayed A, Mizukami S, Na-Bangchang K, Huy NT, Hirayama K, Karbwang J. Parasitol Int. 2017;66:713-720.
9. Taek MM, Prajogo BEW, Agil M. Plants used in traditional medicine for treatment of malaria by Tetun ethnic people in West Timor Indonesia. Asian Pac J Trop Med. 2018;11:630-637.
10. Drees EM. List of Tree and Shrub Names from Timor. Bogor: Balai Penyelidikan Kehutanan, 1950.
11. Trager W, Jenssen JB. Human malaria parasites in continuous culture. Science. 1976;193:673-675.
12. Ouattara Y, Sanon S, TraorÃ Y, Mahiou V, Azas N, Sawadogo L. Antimalarial activity of *Swartzia madagascariensis* Desv. (Leguminosae), *Combretum glutinosum* Guill. & Perr. (Combretaceae) and *Tinospora bakis* Miers. (Menispermaceae), Burkina Faso medicinal plants. Afr Trad CAM. 2006;3:75-81.
13. Lusakibanza M, Mesia G, Tona G, Karemere S, Lukuka A, Tits M, Angenot L, Frédérich M. *In vitro* and *in vivo* antimalarial and cytotoxic activity of five plants used in Congolese traditional medicine. J Ethnopharmacol. 2010;129:398-402.
14. Sarkiyayi S, Zailani HA, Simon JG. Effects of aqueous stem bark extract of *Jatropha curcas* on some biochemical indices of mice infected with *Plasmodium berghei*. Am J Biochem. 2016;6:130-135.
15. Johnson NB, Ameyaw EO, Kyei S, Aboagye B, Asare K, Afoakwah R, Boye A, Donfack JH. *In vivo* antimalarial activity of stem bark extracts of *Plumeria alba* against *Plasmodium berghei* in imprinting control region mice. Rep Parasitol. 2013;3:19-25.
16. Abdillah S, Tambunan RM, Farida Y, Sandhiutami NMD, Dewi RM. Phytochemical screening and antimalarial activity of some plants traditionally used in Indonesia. Asian Pac J Trop Dis. 2015;5:454-457.
17. Saxena S, Pant N, Jain DC, Bhakuni RS. Antimalarial agents from plant sources. Curr Sci. 2003;85:1314-1326.
18. Murnigsih T, Subeki, Matsuura H, Takahashi K, Yamasaki M, Yamato O, Maede Y, Katakura K, Suzuki M, Kobayashi S, Chairul, Yoshihara T. Evaluation of the inhibitory activities of the extracts of Indonesian traditional medicinal plants against *Plasmodium falciparum* and *Babesia gibsoni*. J Vet Med Sci. 2005;67:829-831.
19. Chan EW, Wong SK, Chan HT. Apocynaceae species with antiproliferative and/or antiplasmodial properties: A review of ten genera. J Integr Med. 2016;14:269-284.
20. Bose A, Smith PJ, Lategan CA, Gupta JK, Si S. Studies on *in vitro* antiplasmodial activity of Cleome rutidosperma. Acta Pol Pharm. 2010;67:315-318.
21. Taek MM, Prajogo BEW, Agil M. Ethnomedicinal plants used for the treatment of malaria in Malaka, West Timor. J Young Pharm. 2018;10:187-192.
22. Taek MM, Prajogo BEW, Agil M. Ethnomedicine of Tetun ethnic people in West Timor Indonesia: Philosophy and practice in the treatment of malaria. Integr Med Res. 2019;8:139-144.
23. Mambu L, Grellier P. Antimalarial compounds from traditionally used medicinal plants. In: Colegate SM, Molyneux RJ, eds. Bioactive natural products: Detection, isolation and structural determination 2nd edition. New York: CRC Press; 2007.
24. Chiang CC, Cheng MJ, Peng CF, Huang HY, Chen IS. A novel dimeric coumarin analog and antimycobacterial constituents from *Fatoua pilosa*. Chem Biodivers. 2010;7:1728-1736.
25. Widyastuti Y, Adi MBS, Widodo H, Widayat T, Subositi D, Supriyati N, Haryanti S, Damayanti A, Hidayat T. 100 top tanaman obat Indonesia. Cakarta; Kemenkes RI; 2011.
26. Abiodun O, Gbotosho G, Ajaiyeoba E, Happi T, Falade M, Wittlin S, Sowunmi A, Brun R, Oduola A. *In vitro* antiplasmodial activity and toxicity assessment of some plants from Nigerian ethnomedicine. Pharm Biol. 2011;49:9-14.
27. Sura J, Sumeet D, Raghvendra D. Pharmacological, phytochemical, and traditional uses of *Plumeria alba* L. an Indian medicinal plant. SPER J Anal & Drug Reg. 2016:14-17.

Turk J Pharm Sci 2021;18(1):91-95
DOI: 10.4274/tjps.galenos.2019.94914

ORIGINAL ARTICLE

Polymorphisms of Estrogen Receptor-α and Estrogen Receptor-β Genes and its Expression in Endometriosis

Östrojen Reseptör-α ve Östrojen Reseptör-β Genlerinin Polimorfizmi ve Endometriozisde İfadelenmeleri

Eldafira ELDAFIRA[1,2*], Vivitri Dewi PRASASTY[3], Abinawanto ABINAWANTO[2], Luthfiralda SYAHFIRDI[2], Dwi Ari PUJIANTO[1]

[1]Universitas Indonesia, Faculty of Medicine, Department of Medical Biology, Depok, Indonesia
[2]Universitas Indonesia, Faculty of Mathematics and Natural Sciences, Department of Biology, Jakarta, Indonesia
[3]Atma Jaya Catholic University of Indonesia, Faculty of Biotechnology, Jakarta, Indonesia

ABSTRACT

Objectives: Endometriosis is a common gynecological disorder, characterized by the presence of endometrial-like tissue in the extrauterine location. The increasing estradiol concentration can influence endometriosis risk and estrogen receptor (ER) activity. Polymorphism in ER causes gene expression alteration and influences hormone-receptor interaction. This research aims to determine ER genetic polymorphisms in endometriosis pathogenesis.

Materials and Methods: This study was performed on case-control polymorphisms, which compared 83 women with endometriosis and 76 women without endometriosis. However, the samples used for *ER* gene expression analysis and estrogen level measurement were obtained from 18 women with endometriosis and 18 women without endometriosis. Polymerase chain reaction-restriction fragment length polymorphism was used to determine ER genetic polymorphisms. Chi-square, Mann-Whitney test, Spearman's correlation (p), t-independent, and two-tailed tests were used to analyze the data.

Results: Association between the allele ERα rs9340799 A/G and endometriosis was significantly different (p=0.012), whereas rs2234693 T/C polymorphism showed no association with endometriosis. The correlation between the genotype frequencies of allele ERβ rs4986938 G/A and endometriosis was found significantly different (p=0.015; p=0.034).

Conclusion: Estradiol level and ERβ expression increases, polymorphism genotypes and alleles of *ERβ rs4986938 G/A* gene and allele frequency of *ERα rs9340799 A/G* gene have roles in endometriosis.

Key words: Estradiol (E2), estrogen receptor (ERα and ERβ), endometriosis

ÖZ

Amaç: Endometriozis, ekstrauterin lokasyonda endometrial benzeri dokunun varlığı ile karakterize yaygın bir jinekolojik hastalıktır. Östradiol konsantrasyonunun artması, endometriozis riskini ve östrojen reseptörlerinin (ER) aktivitesini etkileyebilir. ER'deki polimorfizm, gen ekspresyonunda değişikliğe neden olur ve hormon-reseptör etkileşimini etkiler. Bu araştırma, endometriozis patogenezinde ER'nin genetik polimorfizmini belirlemeyi amaçlamaktadır.

Gereç ve Yöntemler: Bu olgu-kontrol çalışması, endometriozisi olan 83 kadın ile endometriozisi olmayan 76 kadını karşılaştıran bir polimorfizm çalışmasıdır. Ancak *ER* gen ekspresyon analizi ve östrojen düzeyi ölçümü için kullanılan örnekler 18 endometriozisi olan ve 18 endometriozisi olmayan kadından elde edildi. ER genetik polimorfizmlerini belirlemek için polimeraz zincir reaksiyonu restriksiyon parça uzunluğu polimorfizmi kullanıldı. Veriler ki-kare, Mann-Whitney test, Spearman rho, t-bağımsız ve iki-kuyruklu testleri kullanılarak analiz edildi.

Bulgular: Allel ERα rs9340799 A/G ile endometriozis arasındaki ilişki anlamlıydı (p=0,012). Aksine, rs2234693 T/C polimorfizmi ile endometriozis arasında bir ilişki bulunamadı. Genotip ve allel Erβ rs4986938 G/A frekanslari ile endometriozis arasındaki ilişki anlamlı bulundu (p=0,015; p=0,034).

Sonuç: Östradiol düzeyi ve ERβ ekspresyonu, polimorfizm genotipleri ve *Erβ 4986938 G/A* geninin alelleri ve *ERα rs9340799 A/G* geninin allel sıklığı endometriozisde rol oynamaktadır.

Anahtar kelimeler: Estradiol (E2), östrojen reseptörü (ERα, ve ERβ), endometriozis

***Correspondence:** eldafira96@yahoo.com, **Phone:** +062217867222**ORCID-ID:** orcid.org/0000-0003-0592-8978
Received: 23.09.2019, **Accepted:** 26.12.2019

INTRODUCTION

Chronic gynecological disorder manifested by the presence of endometrium-like tissue that grows outside the uterine cavity is called endometriosis.[1,2] Endometriosis incidence is estimated at 10%-15%, and reached 13.6%-69.5% of the infertile group based on clinical data from various hospitals in Indonesia.[2-4] Endometriosis etiology and pathophysiology is not fully understood yet. The interaction of various factors, such as the environment, immunology, and genetics, causes a multifactorial disease called endometriosis.[5,6]

It is closely related to estrogen levels. Generally, patients with endometriosis have higher estrogen levels than normal women, which can stimulate endometrial tissue and stromal cell growth outside the uterine cavity, causing pain and inflammation. Estrogen levels in the serum are twice the highest peak of the proliferative phase (before ovulation) and the luteal phase based on the women menstrual cycle. Although high estradiol concentrations in the endometriosis tissues are known from previous studies, the level of serum estradiol (E_2) peripheral in patients with the highest endometriosis, especially the proliferative phase, is still unknown.[7]

The biological activity of the estrogen is mediated by estrogen receptors (ERs), including ERα and ERβ therefore, changes in the quantity and the receptor affinity can cause a pathological condition. The two ER subtypes of ERα and ERβ are encoded by two different genes and chromosomes. ERα and ERβ are located in chromosome six locus q25.1 and chromosome 14 locus q22-24, respectively.[8,9] An increased risk of endometriosis is contributed by the *ERα rs2234693* gene polymorphism, especially in the Caucasian group; and the *ERα rs9340799* gene with GG genotype (mutant) contributes four times increasing endometriosis risk [OR: 4.67, confidence interval (CI): 95%: 1.84-11.83] with p=0.001, and 3 times causing the risk of IVF failure with p=0.018 (OR: 3.33, CI 95%: 1.38-8.03).[10] Likewise in Brazil, *ERβ* gene polymorphism rs4986938 showed endometriosis risk and infertility risks.[11] *ER* gene polymorphism shows inconsistent results among countries/ethnicity. However, research on the *ER* gene characteristics, especially in patients with endometriosis in Indonesia, has not been studied yet.

This *ER* gene polymorphism was thought to contribute elevating or lowering the gene expression levels. A previous study reported that expression in ERβ endometriosis tissue increased 100 times compared with normal endometrial tissue. Moreover, ERβ suppressed ERα expression in endometriosis tissue; however, the mechanism is not clearly understood.[12] Therefore, further investigation on *ER* gene polymorphism in patients with endometriosis is required as well.

MATERIALS AND METHODS

Materials

The blood samples in this research were from 83 and 76 women with and without endometriosis, respectively. All samples were obtained from the Polyclinic Immuno-Endocrinology, Department of Obstetrics and Gynecology, RSCM-FKUI, RS Budhi Jaya, and RS Sammeri, and were approved by the Ethical Committee of Universitas Indonesia (no: 165/PT02.FK/ETIK/2010). ERα intron 1 gene polymorphisms rs9340799 and rs2234693 and rs4986938 of ERβ exon 8 were used.

Isolation of DNA from peripheral blood

In amount of 4.5 mL of red blood cell 1x (199 mM EDTA, 100 mM $KHCO_3$, 1.45 NH_4Cl) was mixed into 1.5 mL of peripheral blood. It was then inverted and incubated for 10 min at room temperature. NF 400/NF400R Bench-Top Centrifuge was used to centrifuge the samples at 1500 rotations per minute (rpm) for 10 min at room temperature. The supernatant was slowly discarded, leaving the rest of the sediment in the next tube of leukocyte form. Cell lysis solution of 300 mL, which contained 10 mM Tris-HCl, 0.25 mM EDTA, and 20% sodium dodecyl sulfate, was placed in a tube, pipetted until it became homogeneous, then incubated in a water bath at 37°C for 30-60 min. A 300 mL precipitated protein solution containing 5 M ammonium acetate was added to the solution and homogenized using the Stuart Scientific Autovortex SA6 for 10-20 sec until brown granules were formed. Samples were centrifuged at 3000 rpm for 15 min at 4°C. The brown pellet form (protein) was discarded after centrifugation, and the supernatant containing DNA was collected. The supernatant was transferred in a new tube, which contained 2.3 mL of isopropanol cold solution, then inverted for approximately 25-30 times to get DNA materials. It was centrifuged at 3000 rpm for 5 min at 4°C. The supernatant was discarded, and the pellet was washed with 1.3 mL of ethanol 70% sterile and centrifuged at 3000 rpm for 5 min at 4°C. The supernatant was discarded, and the pellet (DNA) was dried in open air by turning the tube for approximately 2 h at room temperature or 1 h at 37°C. The DNA was rehydrated with 300 mL of TE solution (10 mM Tris-HCl and 0.25 EDTA) and incubated for 2 h at 37°C. It was then transferred to a 1.5 mL sterile tube. NanoDrop (Maestro) was used to measure the DNA's concentration and purity in the case and control groups. The solution is stored at -20°C until further examination.

Amplification of DNA fragments of ER genes

Polymerase chain reaction (PCR) method and specific primers to target gene-based software primer 3 were used for DNA fragment amplification. The primer sequences used for ERα gene intron 1 amplification are 5′-CAG-GGT-TAT-GTG-GCA-AC-ATG-3′ (forward) and 5′-TAC-CTA-TAA-TGA-CAA-AAA-AA-3′ (reverse), whereas for genes ERβ exon 8 are 5′-CGG-CAG-AGG-ACA-GTA-AAA-GC-3′ (forward) and 5′-AGG-CCA-TTG-AGT-GTG-GAA-AC-3′ (reverse). Each reagent has a volume of 25 µL, which consisted of 5 µL genomic DNA, 12.5 µL master mix (Kappa from Bioline), 0.5 µL forward primer, 0.5 µL reverse primer, and 6.5 µL aquabidest (ddH_2O).

At each gene, DNA samples were amplified for 35 cycles. PCR conditions used for *ERα* gene on the region intron 1 had an initial denaturation at 94°C for 6 min, went into a cycle consisting of denaturation at 94°C for 60 sec, annealing at 56°C for 40 sec, and elongation at 72°C for 90 sec. Elongation was at 72°C for 5 min at the end of the cycle. *ERβ* gene amplification stages in exon 8 and PCR *ERα* gene were almost the same; however,

the annealing temperature used was 54˚C. Amplification results were separated by electrophoresis on 2% agarose gel containing ethidium bromide (0.5 mg/mL) in 1x TE buffer (0.04 M Tris-acetate and 0.002 M EDTA; pH 8.0) at 90V for 40 min. Amplicon sizes of *ERα* and *ERβ* genes were 255 bp and 293 bp, respectively.

ER gene polymorphism analysis with restriction fragment length polymorphism for *ERα* gene polymorphism in intron 1 rs9340799 known area by XbaI, rs2234693 with PvuII, and *ERβ* gene in exon 8 rs4986938 area with AluI. DNA cleavage was done by adding 0.5 µL (10U/µL) of enzymes XbaI, PvuII, or AluI (New England Biolabs) into tubes already containing 10.5 µL DNA fragment amplification product, 1 mL of buffer solution of ER 10x, and 9 mL ddH_2O, with a total volume of 21 µL, and incubated in a water bath at 37˚C for 4 h. DNA fragments were analyzed on a 3% agarose gel in 1x TE at 90V for 1 h. Fragment visualization with electrophoresis was observed with ultraviolet (UV) on UV illuminator long live™ Filter spectroline® was used to observe fragment visualization with electrophoresis and photographed with a digital camera.

Statistical analysis

Genotypic polymorphisms distribution and allele frequencies were tested using Thesias 3.0 software program with genetic packages, and continued with SPSS version 21 at p=0.05. Chi-square, Mann-Whitney test, Spearman's correlation (p), t-independent, and two-tailed tests were used to analyze the data.

RESULT

ERα gene polymorphism rs9340799 A/G, ERα gene rs2234693 T/C and ERβ gene rs4986938 G/A

The PCR products of *ERα* genes intron 1 rs9340799 restricted from XbaI enzyme showed A/G nucleotide changes (Figure 1), resulting in a DNA band size of 255 bp for homozygous mutant/GG, two DNA bands with the size of 142 bp and 113 bp for homozygous wild-type/AA, and three DNA band with the sizes of 255 bp, 142 bp, and 113 bp for heterozygous/GA).

The ERα intron 1 *rs2234693* gene PCR products restricted by PvuII showed T/C nucleotide changes (Figure 2), generating a DNA band size of 255 bp for homozygous wild-type/TT, two DNA bands with the size of 158 bp and 97 bp for homozygous mutant/CC, and three DNA bands with the size of 255 bp, 158 bp, and 97 bp for heterozygous/TC.

The ERβ exon 8 *rs4986938* gene PCR products that were cleavage with AluI showed G/A nucleotide changes (Figure 3), which resulted in a DNA band size of 293 bp for homozygous wild-type/AA, two DNA band sizes of 200 bp and 92 bp for homozygous mutant/GG, and three DNA band sizes of 293 bp, 200 bp, and 92 bp for heterozygous/AG.

Genotype distribution and allele frequency ERα gene rs9340799 A/G, ERα gene rs2234693 T/C and ERβ gene rs4986938 G/A of the case and control groups

Table 1 shows the genotype comparison distribution and allele frequency of *ERα* gene rs9340799 with XbaI. It shows that GG genotypes (normal) and heterozygous genotype GA were higher in the endometriosis case group than the control, whereas the AA genotype (wild type) was lower in the endometriosis case group than the control. G allele frequency was higher in the endometriosis case group than controls, whereas the frequency of allele A was lower in the endometriosis case group than in control. The Pearson chi-square test results showed genotype frequencies in the case and control groups were not significant. In contrast, the allele frequencies in endometriosis cases and control groups showed no significant differences with p=0.012, and the control group is G allele (mutant).

Table 2 displays the genotype comparison distribution and allele frequencies of *ERα* gene with PvuII. Table 2 shows

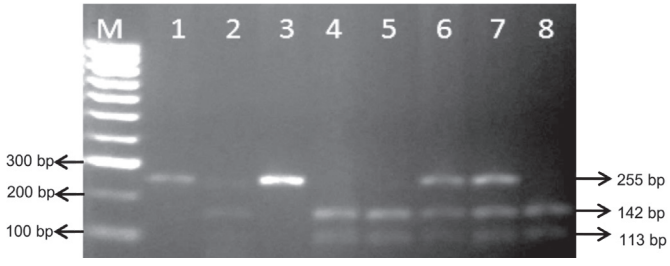

Figure 1. Polymerase chain reaction-restriction fragment length polymorphism results of gene intron 1 rs 9340799 ERα using XbaI. Marker (M), well no: 1 and 3 are the homozygous mutant (GG); well no: 2, 6, and 7 are the heterozygous (AG); and well no: 4 and 5 are the homozygous wild type (AA), ER: Estrogen receptor

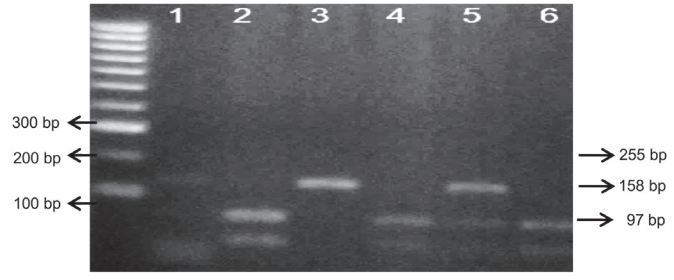

Figure 2. Polymerase chain reaction-restriction fragment length polymorphism of gene intron 1 rs 2234693 ERα using PvuII. Marker (M), well no: 3 is the wild-type genotype (TT); well no: 2, 4, and 6 are the homozygous mutant genotype (CC); and well no: 1 and 5 are the heterozygous genotype (TC), ER: Estrogen receptor

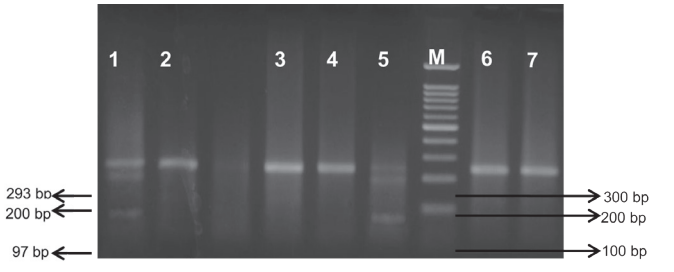

Figure 3. Polymerase chain reaction-restriction fragment length polymorphism of ERβ exon 8 rs4986938 using AluI. Marker (M), well no: 1 and 5 are the heterozygous genotypes (GA); well no. 2, 3, 4, 6, and 7 are the wild-type homozygous genotype (GG). This image does include the mutant genotype (AA), ER: Estrogen receptor

that the normal genotype (TT) and heterozygous genotype (CT) were lower in the case group than in the control group. Meanwhile, homozygous mutant genotype (CC) was higher in the case group than in the control. T allele frequency in the case group was lower than in the control group, whereas the C allele was higher in the case group compared with the control group. The Pearson chi-square test results demonstrated that the genotype distribution in the case and control groups showed no significant difference (p=0.422). Likewise, T and C allele frequency also showed no significant difference (p=0.305).

Table 3 shows the genotype comparison distribution and allele frequency of ERβ with restriction AluI. Table 3 shows that the normal genotype (GG) was lower in the case group than in the control, and heterozygous genotype (GA) was higher in the case group than in the control group. In contrast, homozygous mutant genotype (AA) was not found in the case group, but one was found in control. G allele frequency in the case group was lower compared with the control group, whereas the A allele frequency was higher in the endometriosis case group than in the control group.

Pearson chi-square test showed the genotype distribution and G and A allele frequency in the case and control groups were significantly different (p=0.015 and p=0.034, respectively).

DISCUSSION

This experiment revealed the proportion of genotype GA in endometriosis was more dominant than the other genotypes. This study revealed that the genotype frequencies in the case and control groups showed no difference. The previous study reported that *ERα* gene rs9340799 amplification changes in nucleotides A to G using XbaI restriction in region intron 1.[11] Study from NCBI showed that individuals with genotype AA normal have a lower risk of cases of endometriosis. In contrast, individuals with genotype GG are ten times higher risk of endometriosis.

Paskulin et al.[11] reported that the amplification of the *ERα* gene region intron 1 SNP rs2234693 T nucleotide changes into C using the restriction PvuII. The second difference allele frequency in both groups (case and control) was conducted by chi-square test. It can be concluded that the genotype frequency in the case and control groups were not different, and statistical tests indicated no difference in allele frequency between the two groups with p=0.422 (p>0.05). Hardy-Weinberg balance test also showed no significant difference with p>0.05. Genotype frequencies did not display any difference between the case and control groups. Ayvaz et al.[13] found that *ERα* gene rs2234693

Table 1. Genotype and allele frequency of *ERα rs9340799* gene with XbaI restriction in intron 1 A/G nucleotide change in the case and control groups

	Genotype			X^2	p	Allele frequency		X^2	p	OR
	AA	AG	GG			A	G			(CI: 95%)
Control	32 (42.1%)	28 (36.8%)	16 (21.1%)	-	-	92 (60.5%)	60 (39.5%)	-	-	-
Endometriosis case	22 (26.5%)	33 (39.8%)	28 (33.7%)	5.236	0.073	77 (46.4%)	89 (53.6%)	6.372	0.012	2.54
Total	54	61	44	-	-	167	151	-	-	-

ER: Estrogen receptor, OR: Odds ratio, CI: Confidence interval
Note: The normality test of the ERα (Xba1) genotype distribution in endometriosis and control groups showed that the data were not normally distributed (p<0.05), followed by the chi-square test which showed that the distribution of genotypes in endometriosis and control groups is not significantly different (p>0.05)

Table 2. Genotype and allele frequency of *ERα rs2234693* gene with PvuII restriction in intron 1 T/C nucleotide change in the case and control groups

	Genotype			X^2	p	Allele frequency		X^2	p
	TT	TC	CC			C	T		
Control	18 (23.7%)	46 (60.5%)	12 (15.8%)	-	-	70 (46.1%)	82 (53.9%)	-	-
Endometriosis case	17 (20.5%)	46 (55.4%)	20 (24.1%)	1.724	0.422	86 (51.8%)	80 (48.2%)	1.051	0.305
Total	35	92	32	-	-	156	162	-	-

ER: Estrogen receptor
Note: The normality test of ERα (PvuII) genotype distribution of endometriosis and control groups were not normally distributed (p<0.05) followed by chi-square test which showed genotype frequency was not significantly different with p=0.422 (p>0.05), and allele frequency was also not significantly different with p=0.305 (p>0.05)

Table 3. Genotype and allele frequency of *ERβ rs4986938* gene with AluI restriction in exon 8 G/A nucleotide change in the case and control groups

	Genotype			X^2	p	Allele frequency		X^2	p	OR
	GG	GA	AA			G	A			(CI: 95%)
Control	67 (88.2%)	8 (10.5%)	1 (1.3%)	-	-	142 (93.4%)	10 (6.6%)	-	-	-
Endometriosis case	60 (72.3%)	23 (27.7%)	0 (0.0%)	8.35	0.015-0.31	143 (86.1%)	23 (13.9%)	4.517	0.034	0.44
Total	127	31	1	-	-	287	31	-	-	-

ER: Estrogen receptor, OR: Odds ratio, CI: Confidence interval
Note: The normality test of ERβ (AluI) genotype distribution of endometriosis and control groups were not normally distributed (p<0.05) followed by chi-square test which showed genotype frequency was significantly different (p<0.05) as well as the frequency allele was significantly different p=0.034 (p<0.05)

with PvuII was associated with a decreased male infertility risk, a change in ER polymorphism function, and, in general, is not comprehensible.

The amplification of the *ERβ* gene region of exon 8 rs4986938 nucleotide changes G/A with AluI restriction was done by Paskulin et al.[11] Statistical test results indicated a significant difference in the genotype frequency of ERβ in the case and control groups, with p=0.015 ($p<0.05$).

Allele distribution in ERβ showed no significant difference between the normal allele G and mutant allele A in the case group compared with the control group, which means that normal allele G can reduce endometriosis risk 0.44 times. The distribution of normal allele G seemed to dominate than other alleles, which is similar to a study conducted by Zulli et al.[14] It can be concluded that the presence of a significant difference in genotype frequency and distribution of alleles, the gene polymorphism ERβ with rs4986938 region of exon 8 could contribute to endometriosis risk due to the mutations in this area can affect the changes of amino acid compositions, and may affect the stop codon shift. The transcription keeps working, which causes the increased gene expression; and possible mutations via deletions, which may cause frameshift errors.[15]

CONCLUSION

Polymorphism genotyping, gene allele ERβ rs4986938 G/A and allele frequencies of *ERα* gene rs9340799 A/G may contribute to the occurrence of endometriosis risk.

ACKNOWLEDGMENTS

The authors thank The Ministry of Research, Technology, and Higher Education, Republic of Indonesia (Kemenristekdikti RI) for financial support; Department Biology, the Faculty of Mathematics and Natural Science, Universitas Indonesia; and Department of Medical Biology, Faculty of Medicine, Universitas Indonesia for research facilities.

Conflicts of interest: No conflict of interest was declared by the authors. The authors alone are responsible for the content and writing of the paper.

REFERENCES

1. Burney RO, Giudice LC. Pathogenesis and pathophysiology of endometriosis. Fertil Steril. 2012;98:511-519.
2. Baldi A, Campioni M, Signorile PG. Endometriosis: pathogenesis, diagnosis, therapy and association with cancer (review). Oncol Rep. 2008;19:843-846.
3. Hendarto H. Profil TNF-, GDF-9 dan hyaluronan pada gangguan folikulogenesis sebagai gambaran penurunan kualitas oosit pasien infertil dengan endometriosis. Dissertation. 2007. Universitas Airlangga. Surabaya. Indonesia. http://repository.unair.ac.id/31983/
4. Wiweko B, Puspita CG, Tjandrawinata R, Situmorang H, Harzif AK, Pratama G, Sumapraja K, Natadisastra M, Hestiantoro A. The effectiveness of *Phalleria macrocarpa* bioactive fraction in alleviating endometriosis and/or adenomyosis related pain. eJ Ked Indonesia 2015;3:51-56.
5. Tanbo T, Fedorcsak P. Endometriosis-associated infertility: aspects of pathophysiological mechanisms and treatment options. Acta Obstet Gynecol Scand. 2017;96:659-667.
6. Siva AB, Srivastava P, Shivaji S. Understanding the pathogenesis of endometriosis through proteomics: recent advances and future prospects. Proteomics Clin Appl. 2014;8:86-98.
7. Vercellini P, Viganò P, Somigliana E, Fedele L. Endometriosis: pathogenesis and treatment. Nat Rev Endocrinol. 2014;10:261-275.
8. Cui J, Shen Y, Li R. Estrogen synthesis and signaling pathways during aging: from periphery to brain. Trends Mol Med. 2013;19:197-209.
9. Heldring N, Pike A, Andersson S, Matthews J, Cheng G, Hartman J, Tujague M, Ström A, Treuter E, Warner M, Gustafsson JA. Estrogen receptors: how do they signal and what are their targets. Physiol Rev. 2007;87:905-931.
10. Bulun SE, Cheng YH, Pavone ME, Xue Q, Attar E, Trukhacheva E, Tokunaga H, Utsunomiya H, Yin P, Luo X, Lin Z, Imir G, Thung S, Su EJ, Kim JJ. Estrogen receptor-beta, estrogen receptor-alpha, and progesterone resistance in endometriosis. Semin Reprod Med. 2010;28:36-43.
11. Paskulin DD, Cunha-Filho JS, Paskulin LD, Souza CA, Ashton-Prolla P. ESR1 rs9340799 is associated with endometriosis-related infertility and *in vitro* fertilization failure. Dis Markers. 2013;35:907-913.
12. Bulun SE, Monsavais D, Pavone ME, Dyson M, Xue Q, Attar E, Tokunaga H, Su EJ. Role of estrogen receptor-β in endometriosis. Semin Reprod Med. 2012;30:39-45.
13. Ayvaz OU, Ekmekçi A, Baltaci V, Onen HI, Unsal E. Evaluation of in vitro fertilization parameters and estrogen receptor alpha gene polymorphisms for women with unexplained infertility. J Assist Reprod Genet. 2009;26:503-510.
14. Zulli K, Bianco B, Mafra FA, Teles JS, Christofolini DM, Barbosa CP. Polymorphism of the estrogen receptor β gene is related to infertility and infertility-associated endometriosis. Arq Bras Endocrinol Metabol. 2010;54:567-571.
15. Bebenek K, Garcia-Diaz M, Blanco L, Kunkel TA. The frameshift infidelity of human DNA polymerase lambda. Implications for function. J Biol Chem. 2003;278:34685-34690.

Turk J Pharm Sci 2021;18(1):96-103
DOI: 10.4274/tjps.galenos.2020.21033

ORIGINAL ARTICLE

Fabrication and Evaluation of Transdermal Microneedles for a Recombinant Human Keratinocyte Growth Factor

Rekombinant İnsan Keratinosit Büyüme Faktörü için Transdermal Mikro İğnelerin Üretimi ve Değerlendirilmesi

Melbha Starlin CHELLATHURAI*, Vivien Wang Ting LING, Vijayaraj Kumar PALANIRAJAN

UCSI University, Faculty of Pharmaceutical Sciences, Department of Pharmaceutical Technology, Kuala Lumpur, Malaysia

ABSTRACT

Objectives: Microneedle transdermal patches are a combination of hypodermic needles and transdermal patches used to overcome the individual limitations of both injections and patches. The objective of this study was to design a minimally invasive, biodegradable polymeric recombinant human keratinocyte growth factor (rHuKGF) microneedle array and evaluate the prepared biodegradable microneedles using *in vitro* techniques.

Materials and Methods: Biodegradable polymeric microneedle arrays were fabricated out of poly lactic-co-glycolic acid (PLGA) using the micromolding technique under aseptic conditions, and the morphology of the microneedles was characterized using light microscopy. Sodium dodecyl sulfate-polyacrylamide gel electrophoresis was used to rule out drug-polymer interactions. Standard procedures were used to analyze the prepared microneedle arrays for *in vitro* drug release and to perform a microneedle insertion test. Enzyme-linked immunosorbent assay was used to quantify rHuKGF.

Results: The PLGA polymer was safe for use in the fabrication of rHuKGF microneedles as there was no interaction between the drug and the polymer. The fabricated rHuKGF microneedle arrays had fully formed microneedles with a height of 600 µm and a base of 300 µm. The drug from the microneedle patch was released *in vitro* within 30 minutes. The strength of the microneedles in the patch was good, as they were able to reach a depth of 381±3.56 µm into parafilm without any structural change or fracture.

Conclusion: Microneedle transdermal patches were successfully prepared for rHuKGF, and their evaluation suggested excellent quality and uniformity of patch characteristics. This can have potential applications in the therapeutic arena, offering advantages in terms of reduced dosing frequency, improved patient compliance, and bioavailability.

Key words: Transdermal drug delivery, microneedles, recombinant human keratinocyte growth factor, micromoulding, poly-lactide-co-glycolide

ÖZ

Amaç: Mikro iğne transdermal yamalar, hem enjeksiyonların hem de yamaların bireysel sınırlamalarının üstesinden gelmek için kullanılan hipodermik iğneler ile transdermal yamaların bir kombinasyonudur. Bu çalışmanın amacı, minimal invaziv, biyobozunur polimerik rekombinant insan keratinosit büyüme faktörü (rHuKGF) mikro iğne dizisini tasarlamak; hazırlanan biyolojik olarak parçalanabilir mikro iğneleri *in vitro* teknikler kullanarak değerlendirmektir.

Gereç ve Yöntemler: Biyolojik olarak parçalanabilen polimerik mikro iğne dizileri, aseptik koşullar altında mikro-kalıplama tekniği kullanılarak poli laktik-ko-glikolik asitten (PLGA) üretildi ve mikro iğnelerin morfolojisi ışık mikroskobu kullanılarak karakterize edildi. İlaç-polimer etkileşimlerini belirlemek için sodyum dodesil sülfat-poliakrilamid jel elektroforezi kullanıldı. Hazırlanan mikro iğne dizilerini analiz etmek; *in vitro* ilaç salımı ve mikro iğne yerleştirme testi gerçekleştirmek için standart prosedürler kullanıldı. RHuKGF'yi miktar tayini için enzime bağlı immünosorbent deneyi kullanıldı.

Bulgular: PLGA polimeri, ilaç ve polimer arasında hiçbir etkileşim olmadığından rHuKGF mikro iğnelerinin imalatında kullanım için güvenlidir. Üretilen rHuKGF mikroiğne dizileri, 600 µm yükseklikte ve 300 µm tabanlı mikroiğnelere sahipti. Mikro iğne yamasından ilaç *in vitro* koşullarda 30 dakika içinde salındı. Herhangi bir yapısal değişiklik veya kırılma olmaksızın 381±3,56 µm'lik bir parafilm derinliğine ulaşabildikleri için yamadaki mikro iğnelerin gücü iyi olarak değerlendirildi.

Sonuç: rHuKGF için mikroiğneli transdermal yamalar, başarıyla hazırlandı ve yamanın mükemmel kalitede ve istenen tekdüzelikte olduğu gösterildi. Hazırlanan mikro iğneli transdermal yamanın, terapötik alanda potansiyel uygulamalara sahip olabileceği ve artmış biyoyararlanım, azaltılmış dozlama sıklığı, iyileştirilmiş hasta uyuncu gibi avantajlar sunabileceği belirlendi.

Anahtar kelimeler: Transdermal ilaç taşıma, mikroiğneler, rekombinant insan keratinosit büyüme faktörü, mikro-kalıplama, poli-laktit-ko-glikolid

***Correspondence:** melbha.starlin@gmail.com, **Phone:** +60122309605 **ORCID-ID:** orcid.org/0000-0002-6496-7080

Received: 30.10.2019, **Accepted:** 02.01.2020

INTRODUCTION

Many active drugs cannot be delivered effectively using current drug delivery systems, such as injection and pills.[1] Microneedle transdermal patches consist of a plurality of microprojections, which help to pierce the upper epidermis of the skin far enough to improve the delivery of a broad range of molecules and nanoparticles. Pain-free drug administration is promised, as it is brief enough avoiding the stimulation of nerve fibers.[2] The skin will be restored within one to three days after being treated and no bacterial contamination or long-term irritation occurs. To date, microneedles have been used to deliver drugs of varying molecular weight, bio-therapeutics, vaccines, small molecules, and proteins.[3] They are also used in cosmetology as rollers and pens to facilitate transdermal delivery of peptides and proteins.

Compared with solid microneedles made of silicon or metal, polymeric microneedles have attracted extensive attention because of their excellent biocompatibility, biodegradability, and non-toxic properties.[4] Polymeric microneedles will not leave any sharp biohazard medical waste after use. Polymers with different degradation profiles and swelling properties allow microneedles to be fabricated with different mechanical properties and functions.[5] Poly lactic-co-glycolic acid (PLGA) is one of the most favored Food and Drug Administration (FDA)-approved polymers used in designing biodegradable polymeric microneedles.[6]

Mucositis is one of the main oncological problems caused by high-dose cytotoxic cancer chemotherapy or radiotherapy in patients with hematological malignancies. It is defined as inflammatory or ulcerative lesions on the mucous membranes lining the entire gastrointestinal tract from the mouth to the anus.[7] According to the clinical practice guidelines developed by the Mucositis Study Group of the Multinational Association for Supportive Care in Cancer and the International Society of Oral Oncology, recombinant human keratinocyte growth factor (rHuKGF) is recommended for the prevention and treatment of oral mucositis.[8] The United States FDA also approved the utilization of rHuKGF to treat oral mucositis in patients with hematologic malignancies who are receiving myeloablative radio-chemotherapy with autologous hematopoietic stem cell support.[9]

Endogenous KGF is a 28 kDa protein produced naturally in the body by dermal fibroblasts within the skin, lamina propria cells of the intestines and, most importantly, mesenchymal cells. Its epithelial cell proliferative properties help to maintain epithelial integrity.[10] The specificity of KGF for epithelial cells is due to its exclusive action on KGF receptors, which are present on epithelial cells and absent on cells of hematopoietic origin.[11,12] rHuKGF is a recombinant N-terminal truncated form of human KGF prepared from *Escherichia coli* using recombinant DNA technology. The molecular weight of rHuKGF is only 16.2 kDa, which is smaller than that of endogenous KGF due to the removal of the first 23 N-terminal amino acids with an elimination half-life ($t_{1/2}$) of 4.5 hours.[13] It has similar biological activity to the native protein but higher stability.[14]

Currently, 60 µg/kg/day of rHuKGF is administered intravenously daily for 3 consecutive days before and 3 consecutive days after the patient receives chemotherapy. The drug is commonly dosed in a hospital setting, which means that patients must be hospitalized for a week in order to receive the injection and chemotherapy treatment.[15-17] Because of the inconveniences, pain, and economic burden due to hospital charges, patient compliance will be highly affected, requiring an alternative route of administration. In our previous research, we developed chitosan nanoparticles and β-cyclodextrin-based delivery systems to deliver rHuKGF.[9,10,13] Stability issues due to their complex nature makes proteins difficult drug candidates for transdermal delivery. Therefore, an alternative route, such as transdermal microneedles, is designed to solve the limitations of the current parenteral route.

MATERIALS AND METHODS

Materials

rHuKGF (Sigma-Aldrich, USA), chlorotrimethylsilane, poly (D, L-lactide-co-glycolic acid) in a 75:25 ratio, and polyethylene glycol 400 were purchased from Sigma-Aldrich (M) Sdn. Bhd., Malaysia. A polydimethylsiloxane (PDMS) microneedle mold with 11x11 arrays (Blueacre Technology, Ireland), polyvinyl alcohol (PVA) and polyvinyl pyrrolidone (PVP) [Chemiz (M) Sdn. Bhd., Malaysia], and an ELISA kit ab183362-KGF-FGF-7 (Abcam, USA) were used. Animal studies were not conducted for the prepared microneedles.

Pre-formulation studies

Drug-polymer interaction studies using sodium dodecyl sulfate-polyacrylamide gel electrophoresis (SDS-PAGE)

A Bio-Rad brand SDS-PAGE electrophoresis system was used. Denaturing SDS-PAGE was performed by mixing 10 µL of diluted rHuKGF sample (20 ng of protein) with 10 µL of sample loading buffer and heated in boiling water for 5 to 10 minutes. Samples and Thermo Scientific™ Spectra™ Multicolor Broad Range Protein Ladder were then loaded into precast 12% Tris-Glycine 1.0 mm minigels according to Figure 1. Electrophoresis was then performed at room temperature for approximately 45 minutes with a constant voltage of 120 V in running buffer until the dye front reached the end of the 60 mm gel. Subsequently, the gel was removed and washed three times, 5 minutes each, in ultra-pure water. The gel was then stained using Bio-Safe™ Coomassie Stain for an hour.[18] The de-staining process was completed by agitating the gel in 50 mL of distilled water for a minimum of 30 minutes. Lastly, the gel was imaged using a GS800 calibrated densitometer.[19]

Preparation of the backing membrane

The film casting method was used to fabricate films, and Table 1 shows the formula and composition for the different types of formulated patches.[20] Petri dishes were first treated with 0.2 mL of physically mixed liquid paraffin:dichloromethane (1:10) mixture to facilitate the removal of films from the dishes. Polymer solutions were prepared in distilled water at a concentration of 10% by dissolving dried powder samples of

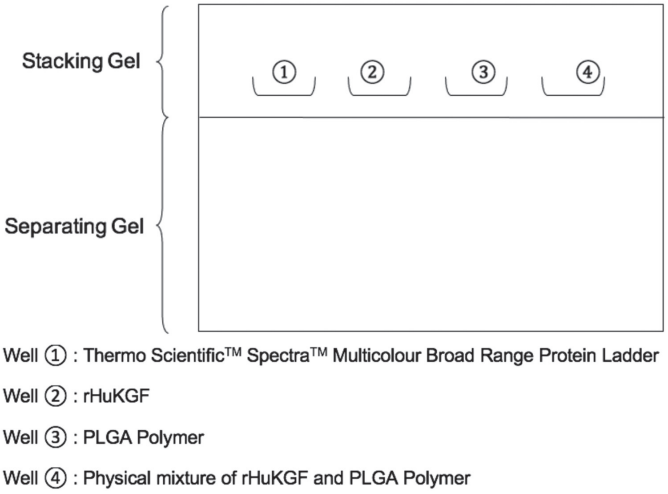

Figure 1. Loading arrangement of marker protein ladder and samples in vertical SDS-PAGE system
rHuKGF: Recombinant human keratinocyte growth factor, PLGA: Poly lactic-co-glycolic acid, SDS-PAGE: Sodium dodecyl sulfate-polyacrylamide gel electrophoresis

Table 1. Composition of backing membrane formulations

Formulation code	Ratio of polymer (10% w/v)	Plasticizer (% w/w of total polymer)	Solvent/patch (mL)
	PVA:PVP	PEG 400	Ultra-pure water
A1	4:6	0	150
A2	1:1	0	150
A3	6:4	0	150
B1	4:6	20	150
B2	4:6	25	150
B3	4:6	30	150

PVA: Polyvinyl alcohol, PVP: Polyvinyl pyrrolidone

PVA and PVP at 100˚ and at room temperature, respectively, followed by vigorous stirring until a clear gel was formed.[21] Varying proportions of PVP and PVA polymer solutions and different percentages of plasticizer were then mixed well to form a final volume of 150 mL. Bubbles were removed by centrifugation. The resultant solutions were poured onto the petri dishes and dried under ambient conditions for 24 hours in a Gelman Sciences microessentials class100 laminar flow work station. The dried cast films were then detached from the petri dish and wrapped in aluminum foil for further use. Evaluation tests were carried out on the next day, and the formulation with the best characteristics was chosen to be used in fabricating microneedle arrays.

Evaluation of the backing membrane

The commercial product Kefentech (ketoprofen plasters) was chosen as the reference.

Physical appearance

All the prepared patches were inspected visually for color and smoothness.

Thickness of the film

The thickness of the films was measured using an electronic digital micrometer screw gauge at three different places.[22] Average and standard deviation (SD) values of the three readings were calculated for each prepared film.

Tensile strength of the film and percentage elongation break test

Three pieces of film strips (4 cm x 2 cm) from each formulation were cut evenly, and the tensile strength and percentage elongation at break were evaluated using a tensiometer. The tensiometer consists of two load cell grips, a lower fixed one and an upper movable one. A film strip was fixed between these cell grips, and the force was gradually applied until the film broke.[23] The tensile strength and percentage elongation at break were read directly from the dial reading.

Preparation of medicated polymeric microneedle arrays

First, the PDMS mold was treated with 0.15 mL of chlorotrimethylsilane and air dried to facilitate the release of replicated PLGA microneedle arrays from the PDMS mold. Different formulations with different concentrations of PLGA polymer solution, as shown in Table 2, were used to fabricate the microneedles.

PLGA was weighed accurately and dissolved fully in acetone. The volume was made up to 1 mL and the solution passed through a 0.22-µm membrane filter to remove contaminants. Subsequently, 1 µL of rHuKGF (5 µg/mL) was pipetted and incorporated into the molten polymer solution. A 300-µL amount of the drug-polymer mixture was then cast into the PDMS microneedle mold using a micropipette. The filled PDMS mold was placed gently in the centrifuge and centrifuged at 2000 rpm for 20 minutes to entrap the drug-polymer mixture into the microneedle array cavity in the PDMS mold. The temperature was fixed at 37˚ during the molding process. The microneedles were then dried for 24 hours under ambient conditions in a controlled air environment in a class 100 laminar flow work station.

After drying of the microneedles, a polymer blend (PVP:PVA) devoid of the drug was cast onto the mold. The best formulation of the polymer blend (PVP:PVA in a 4:6 ratio with 30% plasticizer) that we determined from the previous backing membrane evaluation was used. The polymer solution was poured onto the mold, and the whole device was air-dried at room temperature in a laminar flow hood or freeze-dried overnight. After drying, the replicate PLGA microneedles connected to the polymer blend were released from the PDMS mold. Optical images of the microneedle arrays were obtained using a light microscope.[24,25]

Table 2. Formulation of medicated polymeric microneedles

Formulation code	Polymer (% w/v)	Solvent (mL)
	PLGA (75:25)	Acetone
M1	7	1
M2	9	1
M3	11	1

PLGA: Poly lactic-co-glycolic acid

Evaluation of polymeric microneedles

Morphological characterization of polymeric microneedle arrays

A Zeiss Axio Vert. A1 inverted microscope (Carl Zeiss, Germany) equipped with an HBO 50W mercury vapor lamp and exciter/emitter filter combinations was used for physical characterization of polymeric microneedles. Zen 2012 software (Blue edition) was used for image processing and analysis. Different image sizes were captured and visualized at 5x, 10x, and 20x magnifications with different viewing angles. Observations were carried out from three sides: (A) Top view of the microneedle patch (B) cross section view of the microneedle patch and (C) 70° view of the microneedle patch.[26]

Microneedle insertion test using light microscopy

An eight-layer folded parafilm sheet was used. The thickness of the parafilm sheet was measured at three different places using an electronic digital micrometer screw gauge. The microneedle array was first inserted with 20 N of force into the parafilm sheet for 30 seconds and removed. The parafilm sheets were then unfolded, and the layers containing holes were counted using a light microscope.[27]

In vitro release test in saline

Drug release from microneedles loaded with rHuKGF was determined by using a modified dissolution method. The microneedle array was first pressed against a layer of parafilm in order to expose only the needles. After insertion, the full penetration of microneedles was confirmed by observation under the light microscope. The parafilm with microneedles was then attached to the bottom of a hollow glass tube in which the backing film faced the inside of the tube while the microneedles tips were exposed to the outside. The bottom of the hollow glass tube was immersed in freshly prepared 150 mL pH 6.2 phosphate buffered saline (PBS). The PBS solution was magnetically stirred at 30 rpm and maintained at 37° throughout the test period. Periodically, a 100 µL aliquot of PBS was sampled and immediately replaced with fresh PBS. The concentration of the drug was analyzed using an ELISA kit, and the results were compared with the calibration curve of rHuKGF.

Statistical analysis

The results were expressed as mean ± standard deviation with n=3. Simple regression analysis[26] was performed using GraphPad Prism 7 software.

RESULTS AND DISCUSSION

Drug-polymer interaction studies using SDS-PAGE

Drug-polymer compatibility evaluation was performed using SDS-PAGE for the drug (rHuKGF), PLGA polymer, and their physical mixture (1:1) separately. The results clearly indicate the absence of any chemical interaction between the drug and polymer and thus confirm that rHuKGF is compatible with the PLGA polymer and could be used for the preparation of an rHuKGF-incorporated microneedle transdermal patch. The rHuKGF used in this study was manufactured by Sigma-Aldrich, United States and had a molecular weight of 18.9 kDa which can be proved by Figure 2 as the gel band of rHuKGF located in between the gel band representing 15 kDa and 25 kDa. Figure 2 (A) shows the gel band of the Spectra Multicolor Broad Range Protein Ladder corresponding to its representative molecular weight. The gel band for the PLGA polymer is not prominent, due to the specificity of Coomassie stain, which can only be used to stain and visualize proteins. From the resulting bands, no interaction was observed between the PLGA polymer and rHuKGF, as the band for the drug-polymer physical mixture was located at the same level as that of the drug alone. This means that the gel band shown for the mixture was actually the gel band of rHuKGF, evidencing that the drug had not undergone any structural modification or structural change due to chemical interaction.

Preparation and characterization of the backing membrane

Both PVA and PVP are hydrophilic polymers, and it was found that the thickness of the film increased when the concentration of PVA was increased. Among formulations A1-A3, the thickness of the fabricated films varied from 0.236±0.004 mm to 0.335±0.005 mm as shown in Table 3.

Non-plasticized patches were physically clean, transparent, and had a smooth surface. However, the patches were very fragile, and thus addition of plasticizer was necessary to improve the mechanical properties of the placebo patches.

Formulation A1 with the thinnest film containing a PVA:PVP ratio of 4:6 was chosen as the control formulation. Further

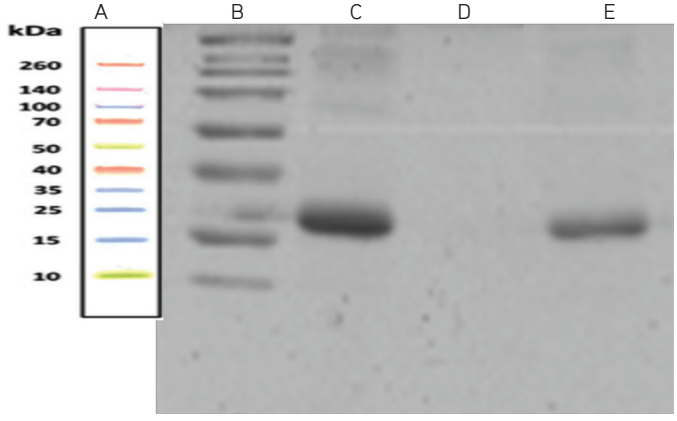

Figure 2. SDS-PAGE gel band of (A) spectra multicolor broad range protein ladder with its molecular weight; (B) spectra broad range protein ladder; (C) rHuKGF; (D) PLGA polymer; and (E) the drug-polymer mixture

SDS-PAGE: Sodium dodecyl sulfate-polyacrylamide gel electrophoresis, rHuKGF: Recombinant human keratinocyte growth factor, PLGA: Poly lactic-co-glycolic acid

Table 3. Thickness of backing membrane without plasticizer

Formulation code	Ratio of polymer (10% w/v)	Mean thickness (mm)
	PVA:PVP	
A 1	4:6	0.236±0.0044
A 2	1:1	0.320±0.0131
A 3	6:4	0.335±0.0045

PVA: Polyvinyl alcohol, PVP: Polyvinyl pyrrolidone

fabrication of films (formulation B1-B3) with a fixed PVA:PVP polymer ratio of 4:6 but different concentration of plasticizer (20%, 25%, and 30% w/w of total polymer) was carried out, and the films were evaluated for physical appearance, thickness of the film, tensile strength, and percentage elongation break of the film.

The results for mechanical properties of the films, including tensile strength and percentage elongation at break, are shown in Table 4. The commercial product Kefentech, chosen as the reference, had a tensile strength of 51.448±8.095 mPa and 266.1% ±7.411% elongation at break. As shown in Table 4, film fabricated from Formulation B3, which contained 30% w/w plasticizer, had the best characteristics as it was the thinnest and had better tensile strength and elongation properties. It had a thickness of 0.117±0.004 mm, tensile strength of 61.362±3.376 mPa, and 288.500% ±11.653% elongation at break. Moreover, the results showed that the patches were of uniform thickness as evidenced by the SD value, which was less than 0.01 mm. Therefore, formulation B3 was chosen as the model backing membrane for further fabrication of microneedle transdermal patches.

Upon addition of plasticizer, the flexibility of polymer macromolecules or macromolecular segments increases as a result of loosening of tightened intermolecular forces.[28] This study indicated that lower concentrations of plasticizer were found to give rigid and brittle patches, whereas higher concentrations gave soft patches. Plasticizer at a concentration of 30% w/v was found to give good flexible patches and was easily removed from the glass surface without any brittle fracture. All the films formed were transparent, flexible, non-sticky, and had a smooth surface. This ensures that the films will maintain a smooth and uniform surface when applied to the skin.

The tensile strength and percentage elongation value of the fabricated formulations depicts that the flexibility increased as the concentration of plasticizer was increased. Sufficient mechanical strength and elongation properties of the backing membrane are important to ease the removal of the microneedle transdermal patch from the skin and to help avoiding tearing of the film during removal.

Preparation and evaluation of medicated microneedle patches

PDMS is commonly used to prepare micro-mold micro-devices because it is chemically inert, non-hygroscopic, thermally stable, and mechanically durable.[29] In this study, PDMS micro-mold was used to fabricate microneedles using the micromolding technique. Preparation of the polymer solution is an important step in the fabrication of microneedles. Each batch of microneedle patches was fabricated using a fresh drug-loaded polymer solution and was stirred well to obtain uniform dispersion of the drug in the solution. However, many bubbles were produced in the long process of stirring and might adversely affect the casting process and microneedle shape. The presence of bubbles also might decrease the mechanical strength of the microneedles, which could be a limitation in some situations. Therefore, an optimal centrifugal force and duration of centrifugation were investigated and were fixed at 2000 rpm and 20 minutes, respectively. Bubbles were successfully removed after centrifugation.

From the results shown in Figure 3, it could be concluded that Formulation M2 with a concentration of 9% w/v PLGA polymer solution was the most suitable for the fabrication of complete and fully formed rHuKGF polymeric microneedles.

The morphology of microneedles was determined at 4x and 10x magnification as shown in Figure 4. Figure 4 (D) shows that each needle was 600 µm in height and 300 µm in base width and was arranged in an 11x11 array with 600 µm tip-to-tip spacing. Microneedles of this size can penetrate the outer skin barrier and deliver drugs to the epidermis and superficial dermis, where drugs can diffuse rapidly for local delivery to the skin or systemic distribution via uptake by dermal capillaries.

Incomplete needle formation by 7% w/v and 11% w/v PLGA polymer solutions could be due to the viscosities of the respective solutions. A solution with low viscosity might be easily spun-off from the opening of the cavity of the micro-mold instead of filling the holes of the micro-mold, while high viscosity might result in difficulty filling in the microneedle mold cavity.

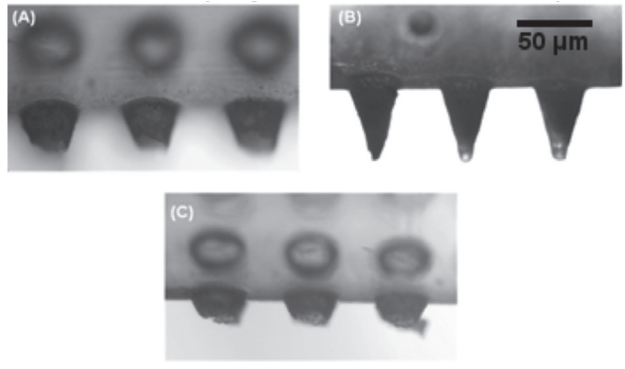

Figure 3. Cross-sectional light microscopy images of a polymeric microneedle array made from (A) 7% w/v PLGA polymer solution; (B) 9% w/v PLGA polymer solution; and (C) 11% w/v PLGA polymer solution
PLGA: Poly lactic-co-glycolic acid

Table 4. Physical characteristics of films fabricated with formulations B1 to B3

Formulation code	Ratio of polymer (10% w/v)	Plasticizer (% w/w of total polymer)	Thickness (mm)	Tensile strength (mPa)	% elongation
	PVA:PVP	PEG 400			
B1	4:6	20	0.140±0.0030	24.800±6.679	244.967±21.170
B2	4:6	25	0.127±0.0015	43.356±6.092	284.767±12.586
B3	4:6	30	0.117±0.0036	61.362±3.376	288.500±11.653

PVA: Polyvinyl alcohol, PVP: Polyvinyl pyrrolidone

Microneedle insertion test using light microscopy

Microneedles should have sufficient mechanical strength to be inserted successfully into the skin without failure during insertion. Results of research carried out by Larrañeta et al.[27] proved that although parafilm presents slightly lower penetration depths than porcine skin, it could still be a promising material to replace biological tissue for insertion studies. The average thickness of a parafilm layer is 127±3.560 µm. The third layer of the parafilm sheet can be reached as shown in Figure 5, but holes did not form in the third layer, which means that the microneedles can correspondingly reach insertion depths between 254±3.560 µm and 381±3.560 µm.

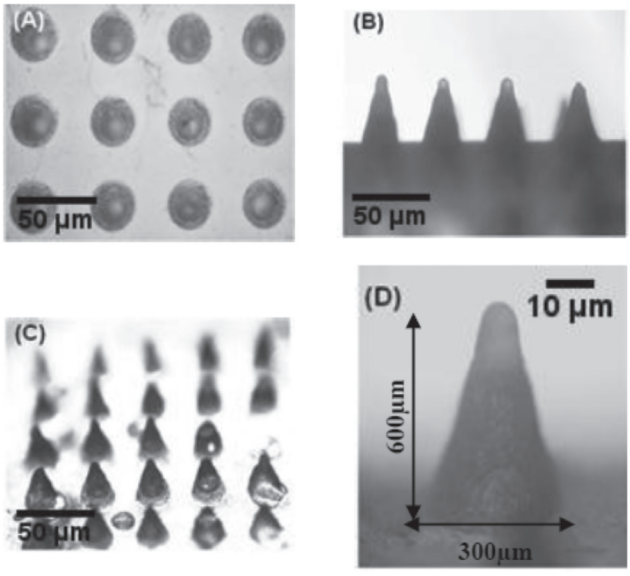

Figure 4. Light microscope images of a section of an 11x11 polymeric microneedle array fabricated using formulation M2: (A) top view at 4x magnification; (B) cross-sectional view at 4x magnification; (C) 70° view at 4x magnification; and (D) cross-sectional view at 10x magnification

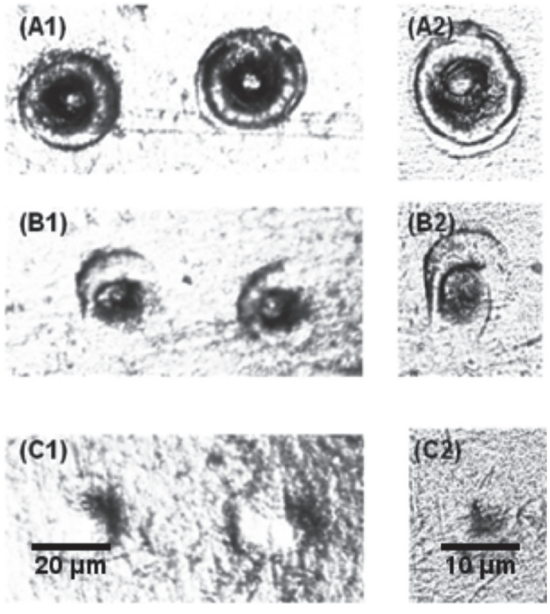

Figure 5. Microscopic observations of holes left on the different layers of a parafilm sheet (A) first layer; (B) second layer; and (C) third layer at (1) 10x magnification and (2) 20x magnification

The average thickness of the stratum corneum and epidermis is between 0.01 and 0.02 mm and 0.1 mm, respectively. Therefore, the results proved that rHuKGF microneedles can successfully overcome the barrier of the stratum corneum and could reach the dermis layer of the skin for drug release. Blood vessels are mostly on the lower part of the dermis and would not be punctured as the needles penetrate only the upper layers of the skin. Besides, the mechanical strength of microneedles was sufficient as it did not undergo structural change or fracture inside the parafilm sheet after insertion test. Thus, the safety of rHuKGF polymeric microneedles is ensured.

In vitro release test

Microneedles loaded with rHuKGF released their contents efficiently within 30 minutes upon incubation in 150 mL PBS solution with pH 6.2. Figure 6 shows that 96.67% of rHuKGF can be successfully released within 15 minutes, and 100% drug release was obtained within 30 minutes. This rapid release might be due to the burst effect of PVP and the solubility of the polymer in the solution. Controlled release was not achieved during the release study, which might have been due to the fabrication methodology.

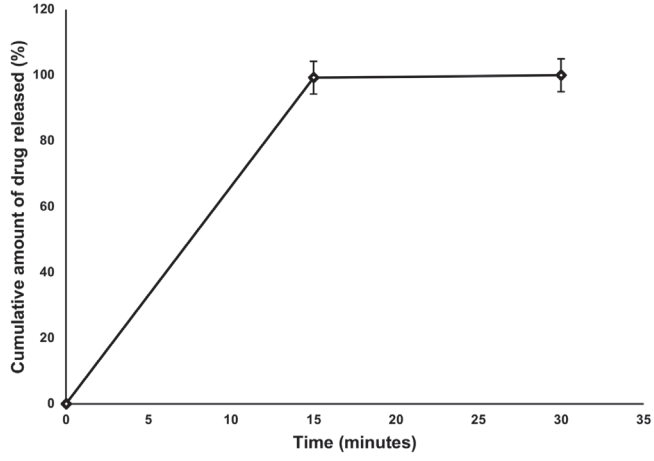

Figure 6. Graph of the cumulative release of rHuKGF into phosphate buffered saline solution over time
rHuKGF: Recombinant human keratinocyte growth factor

As in research performed by Park et al.[30] additional steps were added before direct encapsulation of the drug within microneedles in order to achieve controlled release. The author mentioned that for controlled release, double encapsulation is necessary, in which the drug must first be encapsulated in either carboxymethylcellulose or poly-L-lactide before encapsulation in microneedles. Although controlled release was not achieved, the results could prove that delivery of rHuKGF by using the microneedle technique was successful. Future directions can be focused on the fabrication of controlled release rHuKGF microneedles by using the double encapsulation method in order to solve the frequent administration of drugs before and after chemotherapy.

Theoretically, drug release from microneedles is facilitated either by drug diffusion through the polymer or by degradation

of the polymer. Diffusion is the major pathway of drug release in most controlled release devices and is strongly influenced by the polymer matrix, as the motion of a small molecule is restricted by the three-dimensional network of polymer chains. In diffusion-controlled release, the molecular size and weight play important roles.

However, in the case of dermal application, the surface of the microneedles that pierce the skin will determine how fast small molecules diffuse from the microneedle arrays into the skin. There are several product-related factors that determine the rate of drug delivery. These factors include the solubility and concentration of the drug molecule, the thickness of the back plate, and properties of the microneedle array itself such as length, sharpness, porosity, strength, surface area, and density.[31] However, the rate of drug delivery is also dependent on variables more difficult to control such as the quality of the penetration, the manner of microneedle application and the type of skin. To gain more insight into the usability of polymeric microneedles for drug release into the skin, *in vivo* diffusion studies should be performed.

CONCLUSION

The present study demonstrates that polymeric microneedles for transdermal delivery of rHuKGF can be developed using the PDMS micromolding method. These polymeric microneedle arrays can be fabricated on a large scale at low cost. Polymeric microneedles may provide advantages that overcome the limitations of silicon and metal microneedles. Many polymer materials are inexpensive, mechanically strong, and have been used to fabricate medical devices. PLGA polymer-fabricated microneedles in this research possessed good mechanical strength and could withstand high forces as they were fractured following insertion into a parafilm sheet, which makes these microneedles safe for patients. No interactions were found between rHuKGF and the PLGA polymer, and the drug could be successfully released from microneedles *in vitro*. However, some improvement in the reproduction of small-scale features such as microneedle tips may be possible. Further investigations, such as *in vivo* diffusion studies and fabrication of rHuKGF microneedles for controlled and prolonged release kinetics, can be performed.

ACKNOWLEDGMENTS

This project (reference number: FRGS/2/2014/SKK02/UCSI/02/1) is supported by Department of Higher Education, Ministry of Education Malaysia, under the Fundamental Research Grant Scheme (FRGS) Malaysia and Pioneer Scientists Incentive Fund under Centre of Excellence in Research, Value Innovation and Entrepreneurship (CERVIE), UCSI University, Malaysia (project code: Proj-In-FPS-013).

Conflicts of interest: No conflict of interest was declared by the authors. The authors alone are responsible for the content and writing of the paper.

REFERENCES

1. Larraneta E, Lutton REM, Woolfson AD, Donnelly RF. Microneedle arrays as transdermal and intradermal drug delivery systems: Materials science, manufacture and commercial development. Materials Science and Engineering R: Reports. 2016;104:1-32.
2. Ma G, Wu C. Microneedle, bio-microneedle and bio-inspired microneedle: A review. J Control Release. 2017;251:11-23.
3. Kim YC, Park JH, Prausnitz MR. Microneedles for drug and vaccine delivery. Adv Drug Deliv Rev. 2012;64:1547-1568.
4. Lee JW, Han MR, Park JH. Polymer microneedles for transdermal drug delivery. J Drug Target. 2013;21:211-223.
5. Ye Y, Yu J, Wen D, Kahkoska AR, Gu Z. Polymeric microneedles for transdermal protein delivery. Adv Drug Deliv Rev. 2018;127:106-118.
6. Ulery BD, Nair LS, Laurencin CT. Biomedical applications of biodegradable polymers. J Polym Sci B Polym Phys. 2011;49:832-864.
7. Naidu MU, Ramana GV, Rani PU, Mohan IK, Suman A, Roy P. Chemotherapy-induced and/or radiation therapy-induced oral mucositis-complicating the treatment of cancer. Neoplasia. 2004;6:423-431.
8. Keefe DM, Schubert MM, Elting LS, Sonis ST, Epstein JB, Raber-Durlacher JE, Migliorati CA, McGuire DB, Hutchins RD, Peterson DE; Mucositis Study Section of the Multinational Association of Supportive Care in Cancer and the International Society for Oral Oncology. Updated clinical practice guidelines for the prevention and treatment of mucositis. Cancer. 2007;109:820-831.
9. Kumar PV, Maki MAA, Takahje ML, Wei YS, Tatt LM, Majeed ABBA. Detection of Formation of Recombinant Human Keratinocyte Growth Factor Loaded Chitosan Nanoparticles Based on its Optical Properties. Curr Nanosci. 2018;14:127-135.
10. Maki MAA, Kumar PV, Cheah SC, Siew Wei Y, Al-Nema M, Bayazeid O, Majeed ABBA. Molecular Modeling-Based Delivery System Enhances Everolimus-Induced Apoptosis in Caco-2 Cells. ACS Omega. 2019;4:8767-8777.
11. Rubin JS, Bottaro DP, Chedid M, Miki T, Ron D, Cheon G, Taylor WG, Fortney E, Sakata H, Finch PW, et al. Keratinocyte growth factor. Cell Biol Int. 1995;19:399-411.
12. Stiff PJ, Leinonen M, Kullenberg T, Rudebeck M, de Chateau M, Spielberger R. Long-Term Safety Outcomes in Patients with Hematological Malignancies Undergoing Autologous Hematopoietic Stem Cell Transplantation Treated with Palifermin to Prevent Oral Mucositis. Biol Blood Marrow Transplant. 2016;22:164-169.
13. Kumar PV, Maki MAA, Wei YS, Tatt LM, Elumalai M, Cheah SC, Raghavan B, Majeed ABBA. Rabbit as an Animal Model for Pharmacokinetics Studies of Enteric Capsule Contains Recombinant Human Keratinocyte Growth Factor-Loaded Chitosan Nanoparticles. Curr Clin Pharmacol. 2019;14:132-140.
14. Braun S, Hanselmann C, Gassmann MG, auf dem Keller U, Born-Berclaz C, Chan K, Kan YW, Werner S. Nrf2 Transcription Factor, a Novel Target of Keratinocyte Growth Factor Action Which Regulates Gene Expression and Inflammation in the Healing Skin Wound. Mol Cell Biol. 2002;22:5492-5505.
15. Blijlevens N, Sonis S. Palifermin (recombinant keratinocyte growth factor-1): A pleiotropic growth factor with multiple biological activities in preventing chemotherapy- and radiotherapy-induced mucositis. Ann Oncol. 2007;18:817-826.

16. Niscola P, Scaramucci L, Giovannini M, Ales M, Bondanini F, Cupelli L, Dentamaro T, Lamanda M, Natale G, Palumbo R, Romani C, Tendas A, Tolu B, Violo L, de Fabritiis P. Palifermin in the Management of Mucositis in Hematological Malignancies: Current Evidences and Future Perspectives. Cardiovasc Hematol Agents Med Chem. 2009;7:305-312.

17. McDonnell AM, Lenz KL. Palifermin: role in the prevention of chemotherapy- and radiation-induced mucositis. Ann Pharmacother. 2007;41:86-94.

18. ThermoFisher Scientific. Protein gel electrophoresis technical handbook Comprehensive solutions designed to drive your success. Thermo Fisher Scientific; 2015:63-69. https://assets.thermofisher.com/TFS-Assets/BID/Handbooks/protein-gel-electrophoresis-technical-handbook.pdf

19. Lin EW, Boehnke N, Maynard HD. Protein-polymer conjugation via ligand affinity and photoactivation of glutathione S-transferase. Bioconjug Chem. 2014;25:1902-1909.

20. Jadhav RT, Kasture PV, Gattani SG, Surana SJ. Formulation and evaluation of transdermal films of diclofenac sodium. Int J Pharm Tech Res. 2009;1:1507-1511.

21. Cassu SN,Felisberti MI. Poly(vinyl alcohol) and poly(vinyl pyrrolidone) blends: Miscibility, microheterogeneity and free volume change. Polymer (Guildf). 1997;38:3907-3911.

22. Kumar JA, Pullakandam N, Prabu SL, Gopal V. Transdermal drug delivery system: an overview. Int J Pharm Sci Rev Res. 2010;3:49-54.

23. Prajapati ST, Patel CG, Patel CN. Formulation and evaluation of transdermal patch of repaglinide. ISRN Pharm. 2011;2011:651909.

24. Fredenberg S, Wahlgren M, Reslow M, Axelsson A. The mechanisms of drug release in poly(lactic-co-glycolic acid)-based drug delivery systems--a review. Int J Pharm. 2011;415:34-52.

25. Indermun S, Luttge R, Choonara YE, Kumar P, du Toit LC, Modi G, Pillay V. Current advances in the fabrication of microneedles for transdermal delivery. J Control Release. 2014;185:130-138.

26. Demir YK, Akan Z, Kerimoglu O. Characterization of polymeric microneedle arrays for transdermal drug delivery. PLoS One. 2013;8:e77289.

27. Larrañeta E, Moore J, Vicente-Pérez EM, González-Vázquez P, Lutton R, Woolfson AD, Donnelly RF. A proposed model membrane and test method for microneedle insertion studies. Int J Pharm. 2014;472:65-73.

28. Güngör S, Erdal MS, Özsoy Y. Plasticizers in transdermal drug delivery systems. Unıted Kingdom; IntechOpen; 2012:92-111.

29. Park JH, Allen MG, Prausnitz MR. Biodegradable polymer microneedles: fabrication, mechanics and transdermal drug delivery. J Control Release. 2005;104:51-66.

30. Park JH, Allen MG, Prausnitz MR. Polymer microneedles for controlled-release drug delivery. Pharm Res. 2006;23:1008-1019.

31. van der Maaden K, Sekerdag E, Jiskoot W, Bouwstra J. Impact-insertion applicator improves reliability of skin penetration by solid microneedle arrays. AAPS J. 2014;16:681-684.

Turk J Pharm Sci 2021;18(1):104-110
DOI: 10.4274/tjps.galenos.2020.04379

ORIGINAL ARTICLE

Protective Effect of *Dalbergia sissoo* Extract Against Amyloid-β (1-42)-induced Memory Impairment, Oxidative Stress, and Neuroinflammation in Rats

Dalbergia sissoo Ekstresinin Sıçanlarda Amiloid-β (1-42) ile İndüklenen Hafıza Bozukluğuna, Oksidatif Strese ve Nöroinflamasyona Karşı Koruyucu Etkisi

Shikha RAHEJA[1,2], Amit GIRDHAR[1,2], Anjoo KAMBOJ[3], Viney LATHER[4], Deepti PANDITA[5,6*]

[1]IKG Punjab Technical University, Punjab, India
[2]Jan Nayak Ch. Devi Lal Memorial College of Pharmacy, Haryana, India
[3]Chandigarh College of Pharmacy, Punjab, India
[4]Amity Institute of Pharmacy, Noida, India
[5]Amity Institute of Molecular Medicine and Stem Cell Research, Noida, India
[6]Delhi Pharmaceutical Sciences and Research University, Govt. of NCT Delhi, New Delhi, India

ABSTRACT

Objectives: The ayurvedic literature reports that *Dalbergia sissoo*, a common medicinal plant for gastric and skin problems, has brain-revitalizing effects. However, the neuroprotective effect of this herb on an amyloid-β (Aβ) 1-42 model of Alzheimer's disease (AD) is yet unknown. The current study describes the protective effect of ethanolic extracts of *D. sissoo* leaves (EEDS) against Aβ (1-42)-induced cognitive deficit, oxidative stress, and neuroinflammation in rats.

Materials and Methods: EEDS (300 and 500 mg/kg) was orally administered to rats for 2 weeks prior to intracerebroventricular Aβ (1-42) treatment. The neuroprotective effect of EEDS was assessed by evaluating behavioral, biochemical, and neuroinflammatory parameters in the rat hippocampus. Memory function was assessed via the Morris water maze (MWM) task 2 weeks after Aβ (1-42) administration. After 3 weeks, surgery was performed, all biochemical parameters were evaluated, and histopathological examination of the tissues was carried out.

Results: EEDS improved the cognitive ability of Aβ (1-42)-administered rats in the MWM task. It reduced oxidative stress by significantly decreasing nitrite and malondialdehyde levels and increasing catalase activity and glutathione levels in the rat brain. Moreover, EEDS mitigated neuroinflammation in rats by decreasing the concentration of neuroinflammatory markers in a dose-dependent manner.

Conclusion: *D. sissoo* leaf extract has a beneficial role in alleviating cognitive deficits in AD by modulating cholinergic function, oxidative stress, and neuroinflammation.

Key words: Alzheimer's disease, *Dalbergia sissoo*, cognitive deficit, oxidative stress, amyloid-β (1-42)

ÖZ

Amaç: Ayurveda literatürü, mide ve deri problemleri için yaygın bir tıbbi bitki olan *Dalbergia sissoo*'nun beyni canlandırıcı etkileri olduğunu bildirmektedir. Ancak, bu bitkinin Alzheimer hastalığının (AH) amiloid-β (Aβ) 1-42 modeli üzerindeki nöroprotektif etkisi henüz bilinmemektedir. Bu çalışmada, *D. sissoo* yapraklarının etanol ekstresinin (EEDS) sıçanlarda Aβ (1-42) kaynaklı bilişsel eksikliğe, oksidatif strese ve nöroinflamasyona karşı koruyucu etkisi araştırılmıştır.

Gereç ve Yöntemler: EEDS (300 ve 500 mg/kg) intraserebroventriküler Aβ (1-42) tedavisinden önce sıçanlara 2 hafta süreyle oral olarak uygulandı. EEDS'nin nöroprotektif etkisi, sıçan hipokampusundaki davranışsal, biyokimyasal ve nöroinflamatuvar parametreler değerlendirilerek belirlenmiştir.

*Correspondence: deeptipandita@yahoo.co.uk , Phone: +91 7015976090 ORCID-ID: orcid.org/0000-0002-3644-7045
Received: 09.10.2019, Accepted: 09.01.2020

Bellek işlevi, Aβ (1-42) uygulamasından 2 hafta sonra Morris su labirenti (MWM) testi ile değerlendirildi. Üç hafta sonra cerrahi müdahale yapıldı, tüm biyokimyasal parametreler değerlendirildi ve dokuların histopatolojik incelemesi yapıldı.

Bulgular: EEDS, MWM testinde Aβ (1-42) uygulanmış sıçanların bilişsel yeteneğini geliştirdi. Sıçan beynindeki nitrit ve malondialdehit seviyelerini önemli ölçüde azaltarak ve katalaz aktivitesini ve glutatyon seviyelerini artırarak oksidatif stresi azalttı. Ayrıca, EEDS, nöroinflamatuvar belirteçlerin konsantrasyonunu doz bağımlı bir şekilde azaltarak sıçanlarda nöroinflamasyonu hafifletmiştir.

Sonuç: *D. sissoo* yaprağı ekstresi, kolinerjik fonksiyonu, oksidatif stresi ve nöroinflamasyonu modüle ederek AH'deki bilişsel eksiklikleri azaltmada yararlı bir role sahiptir.

Anahtar kelimeler: Alzheimer hastalığı, *Dalbergia sissoo*, bilişsel eksiklik, oksidatif stres, amiloid-β (1-42)

INTRODUCTION

Dalbergia sissoo Roxb. ex DC., commonly known by the names Indian rosewood, Sheesham, and Shinshapa (Fabaceae), is a perennial tree belonging to the Indian subcontinent and Southern Iran. The leaves and bark of *D. sissoo* are extensively used in traditional medicine for various gastric and skin problems, including dysentery, dyspepsia, and leucoderma.[1,2] The juice of *D. sissoo* leaves is used to treat senility and revitalize brain functions.[3] *D. sissoo* is known to possess diverse phytoconstituents, including biochanin A, tectorigenin, mesoinisitol, isocaviumin, tectorigenin, dalbergin, dalberginone, tannins, fixed oils, and essential oils.[4] A number of studies have reported the antiinflammatory, antioxidant, antispermatogenic, memory-enhancing, cardioprotective, and gastroprotective activities of this plant.[5-10] Extracts of *D. sissoo* leaves were recently shown to have neuroprotective effects against 3-nitropropionic acid-induced neurodegeneration in rats.[11] Biochanin A, the major isoflavone glycoside present in *D. sissoo* leaves, has also been demonstrated to exhibit antioxidant and neuroprotective effects in different studies.[12,13] To date, however, no study has yet evaluated the beneficial effect of *D. sissoo* against amyloid-β (Aβ) 1-42-induced memory impairment, oxidative stress, and neuroinflammation in rats.

Alzheimer's disease (AD), a major neurodegenerative disorder, is a form of dementia that affects approximately 50 million people worldwide; indeed, the disease is recognized as a global public health challenge.[14] AD is characterized by gradual declines in memory function and impaired ability to learn, think, communicate, and make judgments. During the course of the disease, cholinergic neuronal degeneration and dysfunction occur primarily in the cerebral cortex, hippocampus, and amygdala, ultimately resulting in memory impairment. Neuropathological changes in the AD brain are manifested by the deposition of Aβ senile plaques and neurofibrillary tangles.[15] Accumulation of pathogenic Aβ peptides in the aggregated form (i.e., as dimers or oligomers) in specific regions of the brain cause synaptic loss and the breakage of neuronal circuits, which results in neuronal dysfunction.[16] Intracerebroventricular (ICV) administration of aggregated Aβ in rodents mimics the pathological features of AD and induces amnesic effects resulting in memory impairment.[17]

Increased oxidative stress is widely regarded as a crucial factor in the progression of AD.[18] Recent evidence indicates that Aβ-induced neurotoxicity may be associated with increased oxidative stress.[19] Studies have confirmed that antioxidant treatment improves learning ability in Aβ–treated rats and delays the clinical progression of the disease.[20-22] Increased oxidative stress has also been linked with neuronal inflammation and apoptosis.[23] The implication of oxidative stress and neuroinflammation in the pathogenesis of various neurodegenerative diseases, including AD, has rendered treatment with agents possessing antioxidant and antiinflammatory properties a promising approach for managing these diseases.

Various approaches to treat AD, including cholinesterase inhibitors, gene therapy, immunotherapy, modulation of Aβ and tau deposition, and modulation of inflammation and oxidative damage, have been investigated in recent years.[24] Symptomatic treatment with galantamine, donepezil and rivastigmine (cholinesterase inhibitors), and memantine (NMDA receptor antagonist) is currently approved for AD. However, because none of these drugs target the underlying disease mechanism, the search for new drugs that can prevent or delay disease progression remains a crucial undertaking. Plant-based medicines are attractive targets for the treatment of diseases in which the major underlying cause is oxidative stress. Therefore, the current study explores the protective role of *D. sissoo* against Aβ-(1-42)-induced oxidative stress and cognitive dysfunction in rats.

MATERIALS AND METHODS

Drugs and chemicals

Aβ (1-42), donepezil, and commercial kits were obtained from Sigma-Aldrich, USA. Biochanin A was purchased from Clearsynth Labs Ltd., Mumbai, India. All of the reagents used in the experimental work were of analytical grade.

Plant extraction

The green leaves of Indian rosewood were obtained from the medicinal garden of JCDM College of Pharmacy, Sirsa, India. A specimen voucher was submitted to the Raw Materials Herbarium and Museum at the National Institute of Science Communication and Information Resources (NISCAIR), New Delhi, India, and authenticated (ref. no. NISCAIR/RHMD/Consult/2017/3104-53-2). The leaves were properly washed, dried under a shade for 1 week, ground, and defatted with hexane. The powdered leaves were then macerated with ethanol in a beaker and kept at 25˚C±2˚C for 5-6 days. The extract was filtered and evaporated under reduced pressure to remove the solvent completely. The final dried ethanolic extracts of *D. sissoo* leaves [(EEDS), 8 g] was obtained and stored at 2˚C-4˚C in the dark for subsequent experiments.

Extract standardization

EEDS standardization was carried out using high-performance liquid chromatography (HPLC) with biochanin A as the standard compound; this substance is the major constituent of *D. sissoo* leaves.[4,25] The HPLC instrument (Shimadzu) was supplied with an SPD-10AVP ultraviolet-visible detector, reciprocating LC-10 ATVP pumps, a Phenomenex C-18 column (250 mm x 4.6 mm, 5 µm), and a Rheodyne injector. The data were acquired and processed using LC-solution software, version 6.42. Acetonitrile and ammonium acetate (10 Mm) were used as the mobile phase, which was fluxed at a flow rate of 1 mL/min. The corresponding chromatograms were recorded at 200 nm, and the injection volume was 20 µL. The standard calibration curve of biochanin A was prepared using five different concentrations ranging from 1 µg/mL to 5 µg/mL. Stock solutions of the standard and sample were prepared in methanol (10 mg/mL), filtered through 0.22 µm filter paper, and sonicated for 10 min.

Animals

Male Wistar rats (350-400 g) were acquired from Lala Lajpat Rai University of Veterinary and Animal Sciences, Hisar, Haryana, India, housed in an animal house maintained under standard laboratory conditions (temperature: 24˚C±2˚C, relative humidity: 60%-70%, light cycle: 12 h natural light, 12 h dark), and provided water and food as required. The research protocol was approved by the Institutional Animal Ethics Committee (approval date:13.6.2016; approval no: JCDMCOP/IAEC/06/16/36) of JCDM College of Pharmacy. Ethical guidelines were followed during all animal experiments.

Animal groups and drug treatment

The rats were randomly assigned to five groups with eight animals in each group as follows: Group 1; sham control group: Rats were administered the vehicle (4 µL) ICV group 2; Aβ group: Rats were injected with Aβ (1-42) (4 µL) ICV; group 3; Aβ + EEDS (300 mg/kg) group: Aβ model rats were pre-treated with EEDS (300 mg/kg) for 2 weeks; group 4; Aβ + EEDS (500 mg/kg) group: Aβ model rats were pre-treated with EEDS (500 mg/kg) for 2 weeks; group 5; standard group: Aβ model rats were treated with the standard anti AD drug donepezil (5 mg/kg). The doses of *D. sissoo* extract used for treatment were selected on the basis of previous reports.[5,8] The drug treatment schedule is presented in Figure 1.

Intracerebroventricular administration of Aβ (1-42)

Stereotaxic surgery was performed in rats for ICV administration of Aβ (1-42) to induce AD. Anesthesia was induced in rats by intraperitoneal injection of ketamine (100 mg/kg). The scalp was shaved, positioned in a stereotaxic frame, and dissected from the midline to expose the skull. Burr holes were drilled 2 mm posterior to the bregma, 1.5 mm lateral to the midline on either side of the skull, and 1.0 mm below the cortical surface to allow for cannula entry into the hippocampus. Exactly 4 µL of Aβ (1-42) dissolved in saline (1 µg/µL) was slowly infused into the hippocampal region through the installed holes using a Hamilton syringe. The sham group animals were treated with the same surgical procedure and received the same volume (4 µL) of vehicle after surgery. For post-surgical care, the animals were administered gentamycin (5 mg/kg, i.p.) to prevent infection.

Assessment of behavioral parameters

Morris water maze task

Two weeks after induction of AD in rats, memory acquisition and retention were evaluated by the MWM task. The MWM apparatus was equipped with a water tank measuring 130 cm in diameter and 60 cm in height. The tank was filled with water (23˚C±1˚C) to a height of 35 cm. The water was mixed with tempera paint to achieve opacity. The tank was partitioned into four quadrants of the same size, and a platform was installed 2 cm below the water surface in one of the quadrants to allow the animals to escape. The animals were trained for 4 days in succession from day 16 to day 19 (sessions 1-4) with four trials per day. During the training sessions, the animals were left in the pool for 60 s and allowed to locate the platform. Once the platform was correctly located, the rats were guided to and allowed to sit on it for 30 s before the next trial. Escape latency was documented after each trial. On day 20, a probe trial was conducted; here, the platform was removed from the pool, and the animals were randomly released into the tank. The time spent by the animal in the target quadrant was recorded.

Assessment of locomotor activity

On day 21, the motor activity of the rats was measured using a digital actophotometer equipped with infrared light-sensitive photo cells (IMCORP, India). Each animal was placed in the actophotometer for 10 min, and the number of motor counts displayed on the accompanying digital counter was recorded as a measure of motor performance.

Assessment of biochemical parameters

Sample preparation and measurement of total protein

The rats were sacrificed by decapitation for biochemical estimations on day 22 following surgery. The brains were cleaned with ice-cold saline and dissected to isolate the hippocampus. The dissected hippocampal tissue was homogenized with ice-cold phosphate buffer (0.1 mM/L, pH=7.4) and ultracentrifuged (Remi cold centrifuge) at 3000 rpm for 15 min. The clear supernatant obtained was stored at -80˚C and used for further biochemical assays. The amount of protein in each sample was determined using Lowry's method[26] with bovine serum albumin as the standard. Total protein contents are presented in milligrams (mg).

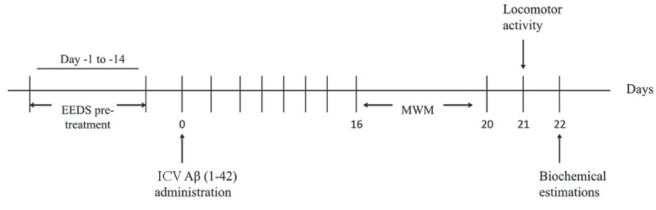

Figure 1. Schematic of the drug treatment schedule
EEDS: Ethanolic extracts of *Dalbergia sissoo* leaves, ICV: Intracerebroventricular, MWM: Morris water maze, Aβ: Amyloid-β

Measurement of oxidative stress markers

Glutathione (GSH) assay was performed by following the method reported by Ellman.[27] GSH concentrations are presented as micromoles per milligram of protein (μmoL/mg protein). Malondialdehyde (MDA) in tissue samples was assessed using the procedure reported by Ohkawa et al.[28] A standard curve was prepared, and the concentration of MDA was estimated and expressed in nanomoles per milligram of protein (nmoL/mg protein). Nitrite in the supernatant was measured via colorimetric assay using Griess reagent.[29] A standard curve of sodium nitrite was plotted, and the amount of nitrite was determined and presented as micromoles per milligram of protein (μmol/mg protein). Catalase activity was measured using the method reported by Aebi, and absorbance was recorded at 240 nm.[30] Enzymatic activity was presented as nanomoles of H_2O_2 consumed per minute per milligram of protein (nmol/min/mg protein).

Measurement of acetylcholinesterase

Acetylcholinesterase (AChE) activity was estimated via the procedure previously demonstrated by Ellman et al.[31] and presented as nanomoles per milligram of protein (nmol/mg protein).

Measurement of neuroinflammatory markers

The concentrations of tumor necrosis factor-alpha (TNF-α) and interleukin-6 (IL-6) in the samples were measured using commercial Quantikine rat assay kits (Becton Dickinson Biosciences, India Pvt. Ltd.)

Histology of brain tissue

The brains of the animals were removed, stored in 10% formalin solution, sliced into thick sections, and then subjected to histopathological examination. The sections were dehydrated, embedded in paraffin blocks, cut into 5-6 μm-thick slices using a microtome, and then stained with hematoxylin-eosin.

Statistical analysis

All of the data were analyzed using Graph Pad Prism software (San Diego, CA, USA). One-Way ANOVA was applied to analyze the biochemical measurements. Tukey's post hoc test was applied for multiple comparisons among groups. Two-Way ANOVA was applied to evaluate the data of escape latency. The results are presented as mean ± standard deviation, and $p<0.05$ was considered significant.

RESULTS

Quantity of biochanin A in EEDS

HPLC analysis revealed that the content of biochanin A, the major constituent of EEDS, was 63.262 μg/mg. The peaks of EEDS (sample) and biochanin A are presented in Figure 2a, b.

Effect of EEDS on reversing Aβ (1-42)-induced memory dysfunction in the MWM task

Two-Way ANOVA showed no significant decrease in escape latencies over four consecutive sessions compared with those at session 1 (day 1) in Aβ (1-42)-lesioned animals. However, in the EEDS pre-treated (300 and 500 mg/kg) groups, escape latencies significantly ($p<0.001$) decreased compared with those at session 1, indicating improvements in cognitive performance. No significant difference in the memory-retaining effects of EEDS (500 mg/kg) and the standard drug donepezil (Figure 3a) was observed. In the probe trial, Aβ (1-42)-injected animals were unable to locate the platform and spent significantly less time in the target quadrant ($p<0.001$, F=593.7, df=39) than the sham-operated animals (Figure 3b).

Effect of EEDS on oxidative stress markers

Compared with sham-operated rats, Aβ (1-42)-injected rats revealed significant increases in MDA and nitrite concentrations, as well as decreases in catalase activity and GSH concentration ($p<0.001$). Compared with the lesioned group, EEDS (300 and

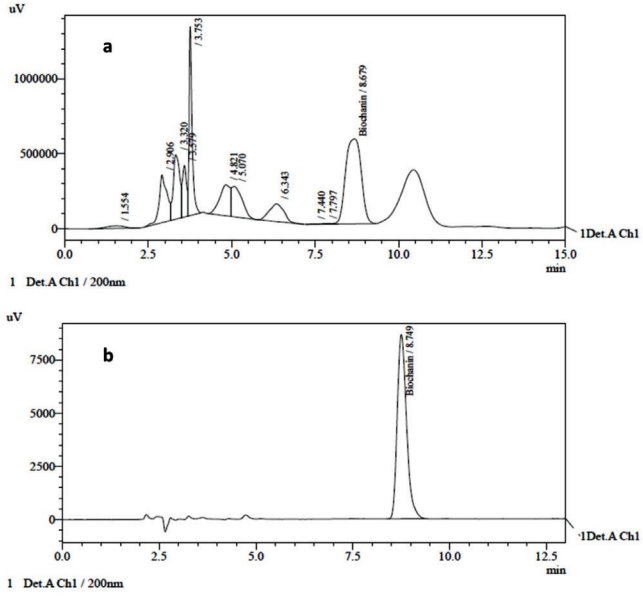

Figure 2. HPLC chromatograms of (a) *Dalbergia sissoo* ethanolic leaf extract and (b) standard biochanin A

HPLC: High-performance liquid chromatography

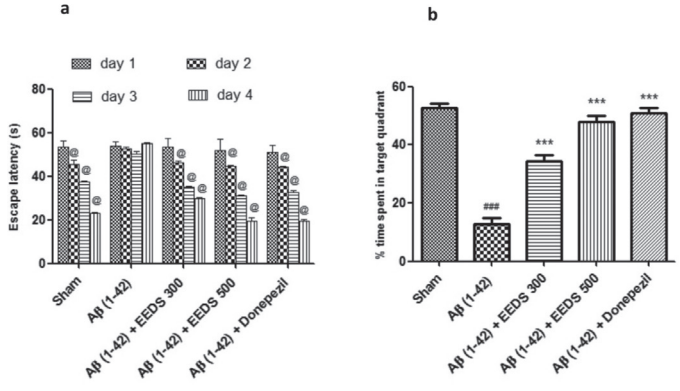

Figure 3. Results of the Morris water maze task. (a) Effects of EEDS (300 and 500 mg/kg) on escape latency in Aβ (1-42)-injected rats. @p<0.001 compared with day 1. (b) % time spent in the target quadrant. ###p<0.001 compared with the sham control, ***p<0.001 compared with the Aβ (1-42) control. Data are expressed as mean ± SD (n=8)

EEDS: Ethanolic extracts of *Dalbergia sissoo* leaves, Aβ: Amyloid-β, SD: Standard deviation

500 mg/kg) administration significantly attenuated oxidative stress by reducing elevated MDA ($p<0.001$, $F=231.9$, $df=29$) and nitrite ($p<0.001$, $F=123.0$, $df=29$) levels and restoring GSH ($p<0.001$, $F=555.5$, $df=29$) and catalase ($p<0.001$, $F=119.1$, $df=29$) levels. Compared with that of donepezil, the effect EEDS (500 mg/kg) on oxidative stress parameters was not significant (Table 1).

Effect of EEDS on AChE activity

AChE activity was significantly augmented in the hippocampus of Aβ (1-42)-injected rats compared with that in sham-operated animals ($p<0.001$). EEDS administration (300 and 500 mg/kg) significantly attenuated the observed increases in AChE activity ($p<0.001$, $F=366.2$, $df=29$) (Table 1).

Effect of EEDS on locomotor activity

EEDS administration (300 and 500 mg/kg) had no significant effect on locomotor activity in all groups ($p>0.05$) (Figure 4).

Effect of EEDS on neuroinflammatory markers

Aβ (1-42) infusion significantly increased TNF-α and IL-6 levels in the hippocampus compared with those in sham-operated rats ($p<0.001$). Pre-treatment with EEDS (300 and 500 mg/kg) significantly attenuated TNF-α ($p<0.001$, $F=990.0$, $df=29$) and IL-6 ($p<0.001$, $F=480.8$, $df=29$) levels in a dose-dependent manner compared with the Aβ (1-42) model group. No significant difference between the effects of EEDS (500 mg/kg) and donepezil (5 mg/kg) was noted (Figure 5a, b).

Histopathological studies

The findings of histopathological studies suggested severe neuronal degeneration in the Aβ (1-42)-treated group. The neurons of Aβ (1-42)-administered brains were reduced in size and had irregular shapes; white patches were also observed (Figure 6). By comparison, the EEDS (300 mg/kg)-treated group showed reduced neurodegeneration and clear nuclei. Moreover, in the EEDS (500 mg/kg)-treated group, neurons retained their original shape and structure, and neuronal degeneration was not visible.

DISCUSSION

AD is accompanied by a progressive decline in memory function, which has been associated with the deposition of hyperphosphorylated tau proteins and senile plaques in neuronal cells. Because Aβ has a pathological role in the progression of AD, the Aβ-injected rat model is regarded as the most reliable model for understanding the pathophysiology and pathogenesis of AD. Previous studies revealed that ICV Aβ (1-42) infusion in rodents causes marked reductions in acetylcholine in the hippocampus and cerebral cortex and dopamine release in the striatum. Administration of Aβ (1-42) in rats also causes impaired learning and memory function.[32] The protein aggravates the production of free radicals, causing oxidative stress and neuronal cell apoptosis. These findings suggest the involvement of multiple neuronal pathways in Aβ (1-42)-induced neurotoxicity. In the current study, we observed declines in memory function after ICV infusion of Aβ (1-42) in rat brain, which is in accordance with previous findings.[22,33]

Plant-derived natural products are of great interest to researchers owing to their versatile applications. Medicinal plants and their phytoconstituents have tremendous potential for development into effective anti-AD drugs. Various plant extracts and bioactive molecules with antioxidant property show protective effects against Aβ (1-42)-induced neurotoxicity.[33-35] The protective effect of *Tetraclinis articulata* essential oil against

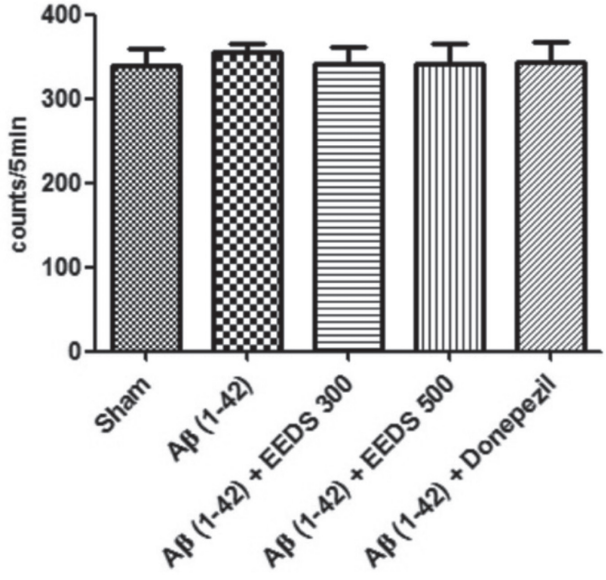

Figure 4. Effect of EEDS (300 and 500 mg/kg) on motor performance
EEDS: Ethanolic extracts of *Dalbergia sissoo* leaves, Aβ: Amyloid-β

Table 1. Effect of EEDS (300 and 500 mg/kg) on various biochemical parameters

Group	GSH (μM/mg protein)	MDA (nmol/mg protein)	Nitrite (μg/mg protein)	Catalase (nmol H_2O_2 consumed/mg protein)	AChE (nmol/min/mg protein)
Sham	11.15±0.4148	4.042±0.6871	21.33±2.805	35.89±3.262	20.77±1.465
Aβ (1-42)	1.528±0.3620#	17.28±0.7286#	47.83±2.927#	11.80±1.795#	62.20±1.819#
Aβ (1-42) + EEDS 300	3.917±0.4286[c]	11.97±0.7575[c]	42.83±2.927[a]	17.24±2.811[b]	57.08±4.524
Aβ (1-42) + EEDS 500	10.25±0.6797[c]	7.892±0.4769[c]	25.67±2.582[c]	32.52±1.951[c]	30.69±1.534
Aβ (1-42) + donepezil	10.88±0.3765[c]	6.733±1.281[c]	22.67±2.338[c]	33.42±2.067[c]	22.42±1.813

#$p<0.001$ compared with the sham control, [a]$p<0.05$ compared with the Aβ (1-42) control, [b]$p<0.01$ compared with the Aβ (1-42) control, [c]$p<0.001$ compared with the Aβ (1-42) control. Data are expressed as mean ± SD
EEDS: Ethanolic extracts of Dalbergia sissoo leaves, GSH: Glutathione, MDA: Malondialdehyde, AChE: Acetylcholinesterase, SD: Standard deviation

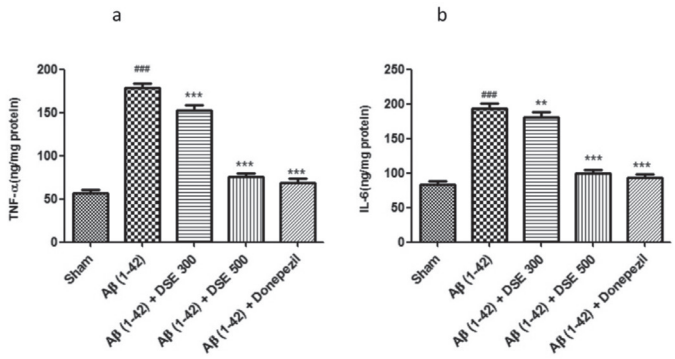

Figure 5. Effect of EEDS (300 and 500 mg/kg) on (a) TNF-α and (b) IL-6 in the Aβ (1-42) model group. ###p<0.001 compared with the sham control, **p<0.01 compared with the Aβ (1-42) control, ***p<0.001 compared with the Aβ (1-42) control. Data are expressed as mean ± SD
EEDS: Ethanolic extracts of *Dalbergia sissoo* leaves, Aβ: Amyloid-β, TNF-α: Tumor necrosis factor-alpha

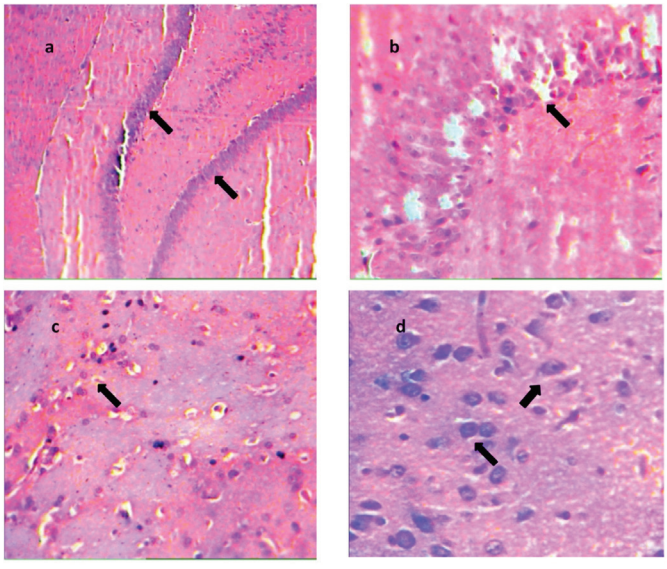

Figure 6. Microscopic sections showing the effects of Aβ (1-42) and EEDS on neuronal degeneration in the hippocampus of rat brain, as determined by hematoxylin-eosin staining. (a) Sham control, (b) Aβ control, (c) Aβ + EEDS 300 mg/kg, and (d) Aβ + EEDS 500 mg/kg
EEDS: Ethanolic extracts of *Dalbergia sissoo* leaves, Aβ: Amyloid-β

Aβ (1-42)-induced oxidative stress and cognitive deficits was recently observed in rats.[36]

Phytochemical studies have revealed the presence of biochanin A as a major phytoconstituent of *D. sissoo* leaves. Biochanin A has been reported to have antioxidant and neuroprotective effects in different studies and is known to attenuate the production of reactive oxygen species, TNF-α, and IL-1β in lipopolysaccharide-treated rats.[37] Biochanin A also shows neuroprotective effects against glutamate-induced cytotoxicity in PC12 cell lines.[38]

The present study examined the protective effect of *D. sissoo* extract against oxidative damage and memory dysfunction in rats. Aβ (1-42) treatment caused memory deficits in the MWM task, as indicated by the observed increase in escape latency. Aβ (1-42) administration in rats also resulted in increased AChE activity, which indicates cholinergic deficits. Moreover, Aβ (1-42)-injected animals showed significant augmentation of nitrite and MDA levels and diminution of GSH levels and catalase activity, resulting in increased lipid peroxidation. These findings support the role of oxidative stress in Aβ-induced neurotoxicity. Finally, Aβ (1-42) infusion in the hippocampus elevated TNF-α and IL-6 levels, thus suggesting that Aβ (1-42)-induced neurotoxicity is associated with neuroinflammation.

EEDS pre-treatment decreased the latency and improved the performance of rats exposed to Aβ in the MWM task in a dose-dependent manner. It also decreased AChE activity and improved cholinergic functions in Aβ (1-42)-treated rat brains. EEDS administration significantly depleted MDA and nitrite levels but increased GSH levels and catalase activity in Aβ (1-42)-lesioned rats. In addition, levels of the neuroinflammatory mediators IL-6 and TNF-α significantly decreased following EEDS pre-treatment, thereby indicating that the extract has ameliorative effects on neuroinflammation.

The outcomes of the present study demonstrated that *D. sissoo* attenuates the oxidative stress and memory dysfunction induced by Aβ (1-42) in rats. In addition, *D. sissoo* reduced AChE activity and neuroinflammation. Therefore, *D. sissoo* may have neuroprotective effects against Aβ (1-42)-induced neurotoxicity. These properties may be attributed to the abundant presence of the phytoconstituent biochanin A in the herb.

CONCLUSION

EEDS ameliorated the effect of Aβ (1-42) on cognitive functions and attenuated oxidative stress and neuroinflammation in rats. The present findings demonstrate that *D. sissoo* may potentially be useful in the prevention or treatment of AD.

ACKNOWLEDGMENTS

The authors sincerely thank JCDM College of Pharmacy, Sirsa, India, and IKG Punjab Technical University, Jalandhar, India, for providing the support and technical assistance necessary to complete this research.

Conflicts of interest: No conflict of interest was declared by the authors. The authors alone are responsible for the content and writing of the paper.

REFERENCES

1. Nadkarni KM. KM Nadkarni's Indian materia medica: with Ayurvedic, Unani-Tibbi, Siddha, allopathic, homeopathic, naturopathic & home remedies, appendices & indexes. India; Popular Prakashan; 1996.
2. Chopra RN, Nayar SL. Glossary of Indian medicinal plants. New Delhi; Council of Scientific and Industrial Research; 1956.
3. Sharma PV. Dravyaguna vijnana (Audbhida aushada dravya). Chaukhamba bharati academy Varanasi; 2003:806-808.
4. Al-Snafi AE. Chemical constituents and pharmacological effects of *Dalbergia sissoo*-A review. IOSR J Pharm. 2017;7:59-71.

5. Hajare SW, Chandra S, Sharma J, Tandan SK, Lal J, Telang AG. Anti-inflammatory activity of *Dalbergia sissoo* leaves. Fitoterapia. 2001;72:131-139.
6. Roy N, Laskar RA, Sk I, Kumari D, Ghosh T, Begum NA. A detailed study on the antioxidant activity of the stem bark of *Dalbergia sissoo* Roxb., an Indian medicinal plant. Food Chem. 2011;126:1115-1121.
7. Vasudeva N, Vats M. Anti-spermatogenic activity of ethanol extract of *Dalbergia sissoo* Roxb. stem bark. J Acupunct Meridian Stud. 2011;4:116-122.
8. Sau S, Handral M. Evaluation of memory enhancing activity of leaf extract of *Dalbergia sissoo* in mice. Int J Pharm Sci Drug Res. 2015;7:263-269.
9. Kasa JK, Singh TU, Parida S, Addison MP, Darzi SA, Choudhury S, Kandasamy K, Singh V, Dash JR, Shanker K, Mishra SK. Assessment of Indian rosewood (*Dalbergia sissoo*) standardized leaf extract on isoproterenol-induced myocardial injury in rats. Cardiovasc Toxicol. 2015;15:250-260.
10. Khan MI, Khan MR. Gastroprotective potential of Dalbergia sissoo roxb. Stem bark against diclofenac-induced gastric damage in rats. Osong Public Health Res Perspect. 2013;4:271-277.
11. Swaroop TVSS, Banerjee S, Handral M. Neuroprotective evaluation of leaf extract of *Dalbergia sissoo* in 3-nitropropionic acid induced neurotoxicity in rats. Int J Pharm Sci Drug Res. 2014;6:41-47.
12. Biradar SM, Joshi H, Chheda TK. Biochanin A ameliorates behavioural and neurochemical derangements in cognitive-deficit mice for the betterment of Alzheimer's disease. Hum Exp Toxicol. 2014;33:369-382.
13. Wang J, Wu WY, Huang H, Li WZ, Chen HQ, Yin YY. Biochanin A protects against lipopolysaccharide-induced damage of dopaminergic neurons both *in vivo* and *in vitro* via inhibition of microglial activation. Neurotox Res. 2016;30:486-498.
14. World Alzheimer Report. The state of the art of dementia research: New frontiers, London: Published by Alzheimer's Disease International; 2018.
15. Singh SK, Srivastav S, Yadav AK, Srikrishna S, Perry G. Overview of Alzheimer's disease and some therapeutic approaches targeting Aβ by using several synthetic and herbal compounds. Oxid Med Cell Longev. 2016;2016:7361613.
16. Palop JJ, Mucke L. Amyloid-β-induced neuronal dysfunction in Alzheimer's disease: from synapses toward neural networks. Nat Neurosci. 2010;13:812-818.
17. Nitta A, Itoh A, Hasegawa T, Nabeshima T. β-Amyloid protein-induced Alzheimer's disease animal model. Neurosci Lett. 1994;170:63-66.
18. Huang WJ, Zhang X, Chen WW. Role of oxidative stress in Alzheimer's disease. Biomed Rep. 2016;4:519-522.
19. Butterfield DA, Swomley AM, Sultana R. Amyloid β-peptide (1-42)-induced oxidative stress in Alzheimer disease: importance in disease pathogenesis and progression. Antioxid Redox Signal. 2013;19:823-835.
20. Bagheri M, Joghataei MT, Mohseni S, Roghani M. Genistein ameliorates learning and memory deficits in amyloid β (1-40) rat model of Alzheimer's disease. Neurobiol Learn Mem. 2011;95:270-276.
21. Wang N, Chen X, Geng D, Huang H, Zhou H. Ginkgo biloba leaf extract improves the cognitive abilities of rats with D-galactose induced dementia. J Biomed Res. 2013;27:29-36.
22. Singh A, Kumar A. Microglial inhibitory mechanism of coenzyme Q10 against Aβ (1-42) induced cognitive dysfunctions: possible behavioral, biochemical, cellular, and histopathological alterations. Front Pharmacol. 2015;6:268.
23. Rosales-Corral S, Reiter RJ, Tan DX, Ortiz GG, Lopez-Armas G. Functional aspects of redox control during neuroinflammation. Antioxid Redox Signal. 2010;13:193-247.
24. Yiannopoulou KG, Papageorgiou SG. Current and future treatments for Alzheimer's disease. Ther Adv Neurol Disord. 2013;6:19-33.
25. Farag SF, Ahmed AS, Terashima K, Takaya Y, Niwa M. Isoflavonoid glycosides from *Dalbergia sissoo*. Phytochemistry. 2001;57:1263-1268.
26. Lowry OH, Rosebrough NJ, Farr AL, Randall RJ. Protein measurement with the Folin phenol reagent. J Biol Chem. 1951;193:265-275.
27. Ellman GL. Tissue sulfhydryl groups. Arch Biochem Biophys. 1959;82:70-77.
28. Ohkawa H, Ohishi N, Yagi K. Assay for lipid peroxides in animal tissues by thiobarbituric acid reaction. Anal Biochem. 1979;95:351-358.
29. Green LC, Wagner DA, Glogowski J, Skipper PL, Wishnok JS, Tannenbaum SR. Analysis of nitrate, nitrite, and [15N] nitrate in biological fluids. Anal Biochem. 1982;126:131-138.
30. Aebi H. Catalase in Methods of Enzymatic Analysis. In: Bergmayer HU, ed. Chemie (2nd ed) FRG, Weinheim; 1974:673-684.
31. Ellman GL, Courtney KD, Andres V Jr, Feather-Stone RM. A new and rapid colorimetric determination of acetylcholinesterase activity. Biochem Pharmacol. 1961;7:88-95.
32. Nabeshima T, Nitta A. Memory impairment and neuronal dysfunction induced by β-amyloid protein in rats. Tohoku J Exp Med. 1994;174:241-249.
33. Ali T, Yoon GH, Shah SA, Lee HY, Kim MO. Osmotin attenuates amyloid beta-induced memory impairment, tau phosphorylation and neurodegeneration in the mouse hippocampus. Sci Rep. 2015;5:11708.
34. Huang SH, Lin CM, Chiang BH. Protective effects of Angelica sinensis extract on amyloid β-peptide-induced neurotoxicity. Phytomedicine. 2008;15:710-721.
35. Shi SH, Zhao X, Liu B, Li H, Liu AJ, Wu B, Bi KS, Jia Y. The effects of sesquiterpenes-rich extract of Alpinia oxyphylla Miq. on amyloid-β-induced cognitive impairment and neuronal abnormalities in the cortex and hippocampus of mice. Oxid Med Cell Longev. 2014;2014:451802.
36. Sadiki FZ, El Idrissi M, Cioanca O, Trifan A, Hancianu M, Hritcu L, Postu PA. *Tetraclinis articulata* essential oil mitigates cognitive deficits and brain oxidative stress in an Alzheimer's disease amyloidosis model. Phytomedicine. 2019;56:57-63.
37. Wu WY, Wu YY, Huang H, He C, Li WZ, Wang HL, Chen HQ, Yin YY. Biochanin A attenuates LPS-induced pro-inflammatory responses and inhibits the activation of the MAPK pathway in BV2 microglial cells. Int J Mol Med. 2015;35:391-398.
38. Tan JW, Tham CL, Israf DA, Lee SH, Kim MK. Neuroprotective effects of biochanin A against glutamate-induced cytotoxicity in PC12 cells via apoptosis inhibition. Neurochem Res. 2013;38:512-518.

Turk J Pharm Sci 2021;18(1):111-121
DOI: 10.4274/tjps.galenos.2020.76390

REVIEW

Current Overview of Oral Thin Films

Oral İnce Filmlere Güncel Bir Bakış

Rukiye SEVİNÇ ÖZAKAR, Emrah ÖZAKAR*

Atatürk University Faculty of Pharmacy, Department of Pharmaceutical Technology, Erzurum, Turkey

ABSTRACT

The pharmaceutical industry is attempting to discover thin films as a new drug delivery system. Thin films have been described as an alternative approach to conventional dosage forms. They are a versatile platform that provides fast, local, or systemic effects. Additionally, these systems can be easily applied by themselves, especially for dysphagia patients, geriatric, pediatric, or bedridden patients, as well as patients who cannot easily access water. These drug delivery systems can be administered in various ways such as orally, buccally, sublingually, ocularly, and transdermally. This review examines oral thin films in all aspects from today's point of view and gives an idea about the growing market share in the world due to the increase in research fields and technological developments. At the same time, it provides an overview of the critical parameters associated with formulation design that affect of thin films, including the design of thin films, anatomical and physiological limitations, the selection of appropriate manufacturing processes, characterization techniques, and the physicochemical properties of polymers and drugs. It also provides insight into the latest thin-film products developed by various pharmaceutical companies.

Key words: Drug delivery dystems, oral thin film (OTF), pharmaceutical industry, polymers

ÖZ

İlaç endüstrisi, yeni bir ilaç taşıyıcı sistem olarak ince filmleri araştırmaktadır. İnce filmler geleneksel dozaj formlarına alternatif bir yaklaşım olarak tanımlanmaktadır. Hızlı, lokal veya sistemik etkiler gösteren çok yönlü platformlardır. Ayrıca, bu sistemler özellikle disfaji hastaları, geriatrik, pediatrik veya yatalak hastalar ile suya kolayca erişilemeyen durumlardaki tüm hastalar tarafından kendi kendilerince kolayca uygulanabilmektedir. Bu ilaç taşıyıcı sistemler oral, bukkal, dil altı, oküler ve transdermal gibi çeşitli şekillerde uygulanabilir. Bu derleme, günümüzün genel bakış açısı ile oral ince filmleri her yönüyle incelemekte, araştırma alanlarındaki ve teknolojik gelişmelerdeki artış nedeniyle dünyada büyüyen pazar payı hakkında fikir vermektedir. Aynı zamanda, ince filmlerin tasarımına, ilaçların ve polimerlerin fizikokimyasal özelliklerine, anatomik ve fizyolojik sınırlamalarına, uygun üretim süreçlerinin seçimine, karakterizasyon tekniklerine ve fizikokimyasal özellikleri de dahil olmak üzere ince filmleri etkileyen formülasyon tasarımı ile ilişkili kritik parametrelere genel bir bakış sağlar. Ayrıca, çeşitli ilaç şirketleri tarafından geliştirilen güncel ince film ürünleri hakkında da fikir vermektedir.

Anahtar kelimeler: İlaç taşıyıcı sistemler, oral ince film (OTF), ilaç endüstrisi, polimerler

INTRODUCTION

The oral mucosal epithelium is a 40-50 cell layer called mucus that is made up of carbohydrates and proteins. The mucosal thickness at the mouth base, tongue, and gums ranges from 100 to 200 μm. The submucosal layer releases a small amount of gel-like fluid known as mucus, consisting of 90%-99% water, 1%-5% water-insoluble glycoprotein, and components such as proteins, enzymes, electrolytes, and nucleic acids. On the other hand, the salivary glands consist of lobules that secrete saliva and parotid from the salivary duct near the sublingual canals and submandibular teeth. Small salivary glands are most often found on the lips and cheek mucosa. The total amount of saliva secreted in 1 min is approximately 1-2 mL. Saliva is composed of mucus, water, amylase (enzyme), lysozyme, mineral salts, immunoglobulins, and blood clotting factors. Mucin and saliva also serve as a barrier for the oral mucosa.[1,2]

The mucosal epithelial structure contains two different areas, the membrane of the stratified epithelium, which is a lipophilic area and space between cells, and a more hydrophilic area.[3] The oral mucosa has a capability between the intestinal mucosa and the epidermis in terms of permeability to substances.It is estimated that the permeability of the buccal mucosa is 4-4000 times better than that of the skin.[2] The mucosal epithelium offers two main drug absorption pathways, the paracellular pathway (intercellular) and the transcellular pathway (intercellular) (Figure 1). The lipophilic structure of the cell membranes facilitates the passage of molecules with a high partition coefficient through the cells, while the polar nature of the intercellular space facilitates the penetration of more hydrophilic molecules. The hydrophobic, hydrophilic, or amphiphilic nature of the drug molecule determines its absorption.[2,3]

*Correspondence: emrahozakar@gmail.com, Phone: +90 442 231 52 17 ORCID-ID: orcid.org/0000-0002-7473-208X
Received: 06.03.2020, Accepted: 05.05.2020

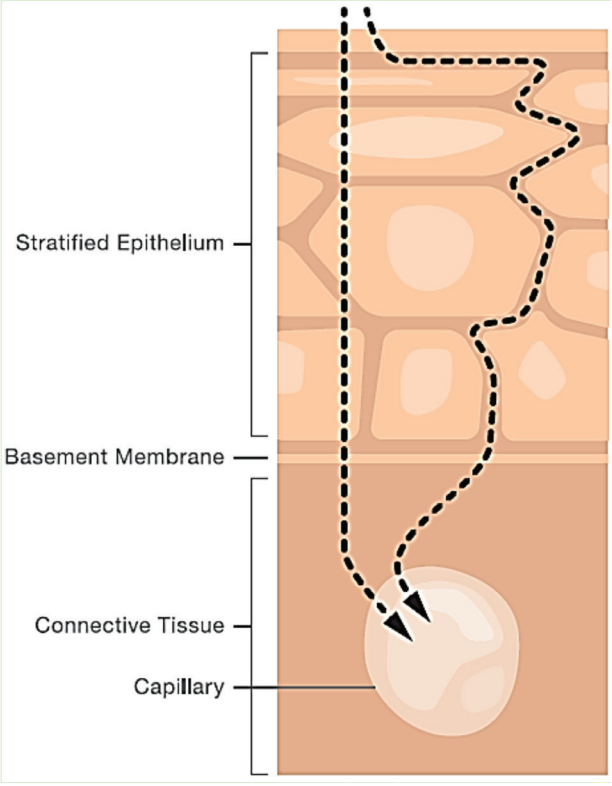

Figure 1. Mucosal pathways-intracellular and intercellular pathways[3]

Many pharmaceutical preparations are applied in tablet, granule, powder, and liquid form. In general, a tablet design is in a form presented to patients to swallow or chew a precise dose of medication. However, especially geriatric and pediatric patients have difficulty chewing or swallowing solid dosage forms.[4] Therefore, many children and elderly people are reluctant to take these solid dosage forms owing to fear of asphyxiation. Orally dissolving tablets (ODTs) have emerged to meet this need. However, for some patient populations, the fear of swallowing the solid dosage form (tablet, capsule), and the risk of asphyxiation remains despite short dissolution/disintegration times. Oral thin film (OTF) drug delivery systems are a preferable alternative under these conditions. The oral bioavailability of many drugs is insufficient due to the enzymes, common first-pass metabolism, and pH of the stomach. Such conventional drugs have been administered parenterally and have shown low patient compliance. Situations like these have paved way for the pharmaceutical industry to develop alternative systems for the transportation of drugs by developing thin dispersible/dissolving films in the mouth.[1,5,6] Fear of drowning, which may be a risk with ODTs, has been associated with these patient groups. Rapid dissolution/disintegration of OTF drug delivery systems is a preferable alternative to ODTs in patients with fear of asphyxiation. When they are placed on the tongue, OTFs are immediately wetted with saliva. As a result, they are dispersed and/or dissolved to release the drug for systemic and/or local absorption. ODTs are fragile and can break during transport. Therefore, oral fast disintegrating/dissolving OTF drug delivery systems are developed as an alternative.[7] Differences between OTFs and ODTs are given in Table 1.[5,8]

Oral disintegrating/dissolving films or strips can be defined as follows: "These are drug delivery systems that they are quickly releasing the drug by dissolving or adhering in the mucosa with saliva within a few seconds due to it contains water-soluble polymers when it placed in the mouth cavity or on the tongue". The sublingual mucosa has high membrane permeability due to its thin membrane structure and high vascularization. Due to this rapid blood supply, it offers very good bioavailability.[4,9] Enhanced systemic bioavailability is owing to skipping the first-pass effect and better permeability is owing to high blood flow and lymphatic circulation. In addition, the oral mucosa is a very effective and selective route of systemic drug delivery because of the large surface area and ease of application for absorption.[6] In general, OTFs are characterized as a thin and flexible polymer layer, with or without plasticizers in their content. They can be said to be less disturbing and more acceptable to patients, as they are thin and flexible in their natural structure. Thin films are polymeric systems that provide many of the requirements expected of a drug delivery system. In studies, thin films have shown their abilities such as improving the initial effect of the drug and duration of this effect, decreasing the frequency of dosing, and increasing the effectiveness of the drug. With thin-film technology, it can be beneficial to eliminate the side effects of drugs and reduce common metabolism procured by proteolytic enzymes. Ideal thin films should possess the desired properties of a drug delivery system, such as a suitable drug loading capacity, rapid dispersion/dissolution, or prolonged application and reasonable formulation stability. Also, they must be nontoxic, biodegradable and biocompatible.[10]

The existence of a variety of biocompatible polymers and variability in production technologies has made it possible to develop a different variety of OTFs. For this reason, OTFs are gaining acceptance and popularity as a new drug carrier dosage form in pharmaceutical technology. A great endeavor has been made to formulate polymeric OTFs that can be delivered via the oral, buccal, sublingual, ocular, and transdermal routes of administration. Among these applications, the use of OTFs for drug delivery across the buccal or sublingual mucosa has gained great attention in recent years. Mechanical strength, related properties, mucoadhesive properties, and drug release rate can also be adjusted by using combinations of polymers, which are the basic structure of thin films, in different proportions. The pharmaceutical industry is affected by the attractive properties of OTFs, and as a result, they are developing thin-film technologies and are currently patenting these formulations.[10]

According to the European Medicines Agency, a thin film that easily dissolves in the oral mucosa is often referred to as an orodispers film. Rapidly dissolving oral films are usually postage stamp-sized OTFs that dissolve/disperse in the oral cavity within 1 min of contact with saliva, resulting in quick absorption and immediate bioavailability of drugs.[1,10] These innovative dosage forms are taken orally but do not require water for ingestion and absorption as do conventional drugs.[11] OTFs should not be confused with buccal films that are designed to remain on the cheek mucosa for a long time.[12]

According to the American Food and Drug Administration (FDA), OTF is defined as "including one or more active pharmaceutical ingredients (APIs), a flexible and non-brittle strip that is placed on the tongue before passing into the gastrointestinal tract, aiming for a quick dissolution or disintegration in the saliva". The first prescribed OTF was Zuplenz (Ondansetron HCl, 4-8 mg) and was approved in 2010. Suboxon (buprenorphine and naloxan) quickly followed as the second approved. Statistics show that four out of five patients choose orally dissolving/disintegrating dosage forms over traditional oral solid dosage forms.[7] At present, in many prescription and over-the-counter product groups, especially in cough, cold, sore throat, erectile dysfunction disorders, allergic reactions, asthma, gastrointestinal disorders, pain, snoring complaints, sleep problems, and multivitamin combinations, etc. OTFs are available and continue to increase.[13] Fast-dissolving oral films have many advantages over other solid dosage forms, such as flexibility and increased efficacy of the API. Also, oral films have dissolution and disintegration with very little saliva fluid in less than one minute compared with ODTs.[1]

An OTF should have the following ideal features[14]

- It should taste good
- Drugs should be very moisture resistant and soluble in the saliva
- It should have appropriate tension resistance
- It should be ionized in the oral cavity pH
- It should be able to penetrate the oral mucosa
- It should be able to have a rapid effect

OTF's advantages over other dosage forms[1,7,10]

- Practical
- Does not require water use
- Can be used safely even when access to water is not possible (such as travel)
- No risk of suffocation
- Improved stability
- Easy to apply
- Easy application to mental and incompatible patients
- There is little or no residue in the mouth after application
- Bypasses the gastrointestinal tract and thus increasing bioavailability
- Low dosage and low side effects
- It provides more accurate dosage when compared to liquid dosage forms
- No need to measure, which is an important disadvantage in liquid dosage forms
- Leaves a good feeling in the mouth
- Provides rapid onset of effects in conditions requiring urgent intervention, for example, allergic attacks such as asthma and intraoral diseases
- Improves the absorption rate and amount of drugs
- Provides enhanced bioavailability for less water-soluble drugs, especially via giving a large surface area while rapidly dissolving
- Does not prevent normal functions such as speaking and drinking
- Offers administration of drugs with a high risk of disruption in the gastrointestinal tract
- Has an expanding market and product variety
- Can be developed and placed on the market within 12-16 months

Disadvantages of OTFs[1,7,10]

- Requires special equipment for packaging
- Is not suitable for drugs that cause irritation in the oral pH and are not durable
- Only a small dose of medication can be administered, but research has shown that the API concentration can be increased by up to 50% by weight (for example, each film strip of Gas-X® of Novartis Consumer Health contains 62.5 mg of Simethicone)
- Is hygroscopic by nature. For this reason, it causes difficulties for long-term protection
- Only drugs absorbed by passive diffusion can be applied in this way
- Since OTFs are resolved rapidly, dose termination is not possible
- OTFs are not registered to any pharmacopoeia
- Preparation method is costly compared with oral dissolving tablets

OTFs are classified in three ways[8,9,15]

1- Flash release (quick release)

2- Mucoadhesive melt away wafers (mucoadhesive wafer)

3- Mucoadhesive sustained-release wafers (mucoadhesive extended-release wafer)

In Table 2 below, the features that distinguish the above OTF types are shown:[8,9,15]

Because of its ease of application and high effectiveness, it is not surprising that drugs in the form of thin-film dosage take a high market share. This technology attracts the attention of both old and newly established pharmaceutical companies. Important sales figures have been reached in the USA and European countries. While the pharmaceutical products market in oral thin-film formulations was $500 million in 2007, it was seen that this rate reached $2 billion by 2010. Also, according to a research report, the global thin-film pharmaceutical products market is expected to increase from $7 billion in 2015 to over $15 billion by the end of 2024. Therefore, it is estimated that there will be an increase of 117% in 10 years (Figure 2).[15]

In Table 3 below are a few examples of OTFs currently used in the world,[16] and auxiliary substances used in OTF formulations are in Table 4.

Table 1. Differences between OTFs and ODTs[5,8]

OTF	ODT
Film	Tablet
More dissolution owing to the larger surface area	Less dissolution owing to the lesser surface area
It is more durable compared to ODTs	It is less durable than OTFs
Patient compliance is high	Patient compliance is low
It may contain a low dose	It may contain a high dose
No risk of asphyxiation	There is a fear of asphyxiation

OTFs: Oral thin films, ODTs: Orally dissolving tablets

Table 2. Features distinguishing OTF types from each other

Features	Quick release	Mucoadhesive wafer	Mucoadhesive extended-release wafer
Area (cm^2)	2-8	2-7	2-4
Thickness (mm)	20-70	50-500	50-250
Structure	Single layer	Multilayer or single	Multilayer
Excipients	Water-soluble polymers	Water-soluble polymers	Low-solubility or insoluble polymers
Pharmaceutical phase	Solid or dissolved/ dispersed	Drug molecules in solid or suspended form	Suspension, solid or dissolved/ dispersed
Application area	Lingual	Buccal or gingival region	Other suitable areas in the gums or oral cavity
Dissolution	60 s	Gel consists in minutes	8-10 h maximum
Effect	Local or systemic	Local or systemic	Local or systemic

OTF: Oral thin film

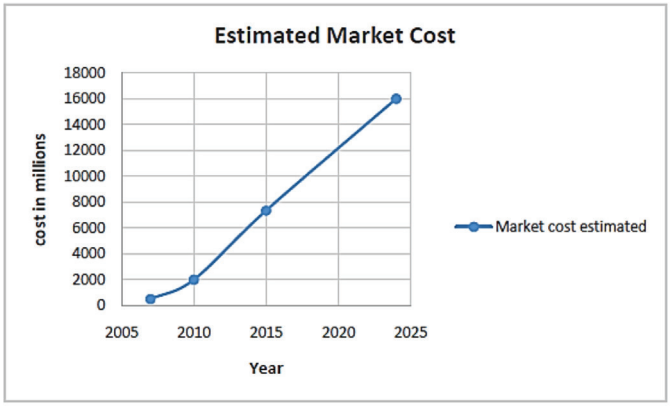

Figure 2. Estimated market share of OTFs by year[15]
OTFs: Oral thin films

Active ingredients used in OTFs

The API must be dissolved for absorption to occur. If the active substance is very lipophilic, it is insoluble in the aqueous medium, and absorption may not be at the desired level. Therefore, there is a delicate balance between the lipophilicity and solubility of the drug. The primary mechanism of drug absorption is passive diffusion. As a result, the partition coefficient, degree of ionization, and molecular weight have a major influence on the transport of drugs across the oral mucosal membranes. The API's pKa and the degree of ionization at ambient pH must be taken into account when considering bioavailability. The degree of absorption is generally proportional to the lipophilicity or partition coefficient of the API. However, the solubility of the drug also plays a significant role. The nonionized form of the drug shows more lipid-soluble properties and therefore penetrates by diffusion through biological membranes.[3,14,17]

There is no uniformity problem in the distribution of water-soluble APIs. However, water-insoluble APIs must be distributed homogeneously to have acceptable content uniformity.[7]

APIs to be used in OTFs[7]

- Should be used in a low dosage
- The feeling and taste left in the mouth should be appropriate
- Must have low molecular weight
- Must be stable and soluble in saliva

Its potential and therapeutic effectiveness are also important in the selection of the API. The most suitable APIs for OTFs are anticancer drugs, antiasthmatic, antitussives, antihistamines, antiepileptics, antianginal drugs, antiemetics, cardiovascular drugs, neuroleptics, analgesics, anxiolytics, antiallergic drugs, hypnotics, sedatives, antibacterial drugs, anti-Alzheimer's drugs, and diuretics, and expectorants.[1,14]

Film-forming polymers used in OTFs

The selection of polymers is one of the most critical and important parameters in the successful preparation of oral films due to their tensile strength, which depends on the type and amount of films used. According to the total weight of the dry film, at least 45% polymer by weight must be present, but 60%-65% by weight of the polymer is chosen to achieve the desired properties. Polymers can be utilized alone or in combination to achieve the desired film properties. Because OTFs are rapidly dispersed and dissolved in the oral cavity, the film-forming polymers utilized must be water-soluble. At the same time, the films obtained must be durable, which will not cause any damage during transport and storage (Table 5).[1,7,14]

Properties of an ideal polymer for OTFs are the following[1,7,14]

- The polymer used must be nontoxic and non-irritating
- There should not be impurities
- It must have enough wetting and spreading properties
- It must have sufficient stress and tensile strength
- It should be accessible and not too expensive
- The shelf life should be reasonable

Table 3. OTC and prescription OTF examples used in the world[16,17]

Trade name	Year	Drug	Polymer	Plasticizer
OTC products				
Listerine, PocketPaks® oral care strips (Johnson & Johnson)	2001	Menthol	Pullulan	Glyceryl oleate Macrogol
Sudafed® PE (Johnson & Johnson)	2005	Phenylephrine	Maltodextrin Pullulan Carrageen	Glycerin
Theraflu® Day Time Thin Strips (Novartis Consumer Healthcare)	2004	Dextromethorphan Diphenhydramine Phenylephrine	Hypromellose (HPMC) Maltodextrin	Propylene Glycol Macrogol
Gas-X Thin Strips® (Novartis Consumer Healthcare)	2006	Simethicone	Maltodextrin HPMC	Polyethylene glycol Sorbitol
Chloraseptic® Sore Throat Relief Strips (InnoZen)	2004	Benzocaine	Corn starch	Erythritol Macrogol
Suppress Cough Strips® (InnoZen)	2005	Menthol	Carrageen Pectin Sodium alginate	Glycerin
Pedia-Lax™ Quick Dissolve Strip (C. B. Fleet)	2008	Sennoside	HPMC	Glycerin
SpotScent Oral Care Strips® (Spotscent)	2003	Parsley seed oil	Modified cellulose	Glycerin
Orajel™ Kids Sore Throat Relief Strips (Church & Dwight Co.)	2007	Benzocaine	Pectin	Glycerin
Day Time Triaminic Thin Strips® Cough & Cold (Novartis Consumer Healthcare)	2004	Phenylephrine Dextromethorphan	HPMC	Polyethylene glycol
IvyFilm®, IvyFilm Kiddies® Extract (Lamar-Forrester Pharma)	2016	Hedera Helix	Pullulan	Glycerin
Benadryl® Allergy Quick Dissolve Strips (McNeill-PPC)	2006	Diphenhydramine	Carrageen Pullulan	Glycerin
Prescribed products				
Sildenafil Sandoz Orodispersible Film® (Sandoz)	2014	Sildenafil	HHPMC	Glycerin
Sildenafil Orodispersible Film (IBSA Farmaceutici Italia Srl)	2016	Sildenafil	Maltodextrin	Glycerin polisorbat Propylene glycol Monocaprylate
Zuplenz® (Vestiq Pharmaceuticals)	2012	Ondansetron	HHPMC	Polyethylene oxide Colloidal silicon Dioxide
Risperidone HEXAL® SF Schmelzfilm	2010	Risperidone	HHPMC Maltodextrin	Glycerin

OTC: Over-the-counter, OTF: Oral thin film, HPMC: Hydroxypropyl methylcellulose

- It should not cause secondary infections in the dental areas or oral mucosa
- It should have a good feeling in the oral cavity
- It must not be an impediment to the disintegration time

The combined use of different polymers provides specific properties to OTFs. For example, gelatins have different molecular weights, so high-molecular-weight glossy and highly attractive films can be obtained using gelatins. Pullulan is often used to prepare a thin film with high mechanical strength and dissolution; it is also stable at a wide range of temperatures. The mixture of high-methoxy pectin and chitosan or low-methoxy pectin results in a thin film that shows perfect mechanical strength. Film-forming polymers such as methylcellulose, hydroxypropyl cellulose, and carboxymethyl cellulose form a thin film that disperses and/or swells due to its hydrophilic structures that help to absorb water. The use of combined polymers and the properties of the obtained OTFs are given in Table 6.[10]

Plasticizers used in OTFs

Plasticizers help to increase the flexibility and lower the Tg of the polymer, reducing the friability of the film. Plasticizers

Table 4. Formulation components of OTFs[1,7]

Component	Amount	Examples
Active substance	5%-30%	Montelukast sodium, ropinirole hydrochloride, triclosan, sertraline, metoclopramide hydrochloride, telmisartan, dicyclomine hydrochloride, tianeptine sodium, amlodipine besylate, and livocyrazine dihydrochloride, etc.
Film-forming polymer	40%-50%	Carbohydrates, proteins, and cellulose derivatives
Plasticizer	0%-20%	Glycerin, PEG-400, 300, propylene glycol, malic acid, sorbitol, castor oil, triethyl citrate, tributyl citrate, and triacetin, etc.
Saliva stimulants	2%-6%	Ascorbic acid, citric acid, lactic acid, tartaric acid, and malic acid
Sweeteners	3%-6%	Natural (sucrose, mannitol, sorbitol, dextrose, glucose, liquid glucose, fructose, and isomaltose, etc.), synthetic (aspartame, saccharin, sucralose, acesulfame-K, cyclamate, alitam, and neotame, etc.)
Superdisintegrant	0%-8%	Sodium starch glycollate, crosspovidone, and polacrilin potassium
Flavoring agents	Quantum satis	Peppermint, cinnamon, clove, lemon, orange, vanilla, and chocolate, etc.
Surfactants	Quantum satis	Sodium lauryl sulfate, benzalkonium chloride, polysorbate, and poloxamer 407, etc.
Coloring agents	Quantum satis	Titanium oxide, silicon dioxide, and zinc dioxide, etc.

OTFs: Oral thin films

also increase tensile strength. Plasticizers must be compatible with the drug, solvent, and polymer used. Sorbitol, mannitol, glycerin, diethyl phthalate, triethyl citrate, tributyl citrate, macrogol, propylene glycol, and citric acid esters are the most commonly used (Table 7).[1,7,14,16]

Surfactants used in OTFs

Surfactants as dispersing or wetting agents helping the film to dissolve in a short time and release the API quickly. It is preferable to use poloxamer 407, sodium lauryl sulfate, and polysorbate.[14,16]

Sweeteners used in OTFs

Natural and artificial sweeteners are used to increase the flavor of OTFs. Polyhydric alcohols such as mannitol, sorbitol, maltitol, and isomalt are the most frequently used. In addition, polyhydric alcohols can be used in combination to provide a good feeling and coldness in the mouth. Also, polyhydric alcohols do not leave a bitter aftertaste in the mouth and are less carcinogenic. The sweetening feature of most polyols, except xylitol and maltitol, is less than half that of sucrose (both have a similar sweetness to sucrose). The use of natural sugars in these preparations is restrained in diabetic patients. For that reason, artificial sweeteners are most popular in pharmaceutical preparations and foods. In OTFs, aspartame and saccharin are commonly used as artificial sweeteners.[7,14,16]

Saliva stimulants used in OTFs

Saliva stimulating agents increase the saliva production rate and help break down formulations faster. Also, acids generally used in food production could be utilized as saliva stimulating agents. Ascorbic acid, malic acid, citric acid, tartaric acid, and lactic acid are some of the saliva stimulating agents.[7,16]

Superdisintegrants used in OTFs

Superdisintegrants, when added to OTF formulations, provide rapid disintegration as a result of the combined effect of both water absorption and swelling. Superdisintegrants accelerate disintegration and dissolution by providing absorption and swelling owing to their excessive water absorption. Powerful interaction with saliva is very important for disintegration. Some of the commonly used superdisintegrants and their concentrations are shown in Table 8.[7,14]

Coloring agents used in OTFs

FD and C approved colorants, EU approved colorants, natural coloring agents, or pigments can be included in formulations up to 1% by weight.[7]

Flavoring agents used in OTFs

The choice of a pleasant flavor depends on the type of API to be used. The acceptance of the dosage form by the patient as a result of oral disintegration or dissolution depends on the taste perceived within the first few seconds after the consumption of the OTF and subsequently at least 10 min in the mouth. Therefore, the choice of flavoring agent is extremely important. Flavoring agents that are frequently used in formulations are given in Table 9.[7,17]

Preparation methods of OTFs[1,7,10,17]

One of the following methods or combinations could be utilized in the preparation of oral dissolving/disintegrating thin films:

Solvent and semisolid casting method

The solvent casting method is the most generally utilized method to prepare OTFs because of its simple preparation, low processing cost, and ease of application.[10,19] In brief, water-soluble components are prepared by mixing in a heated

Table 5. Common polymers utilized in OTFs[1,7,14,18]

Component	Class	Examples
Natural	Carbohydrate	Pectin, pullulan, maltodextrin, sodium alginate, and sodium starch glycollate
	Protein	Gelatin
	Resin	Polymerized resin (new film-forming)
Synthetic	Cellulose derivatives	Hydroxy propyl methylcellulose (K50, K3, K15, E5, E3, and E15), carboxy methylcellulose, methylcellulose (A3, A15, and A6), sodium carboxymethyl cellulose, croscarmellose sodium, and microcrystalline cellulose
	Vinyl polymer	Polyvinylpyrrolidone (K90 and K30), polyvinyl alcohol, and polyethylene oxide
	Acrylic polymer	Eudragit (RL-100, 9, 10, 11, 12, and RD-100)

OTFs: Oral thin films

Table 6. Combined polymers and the properties of the obtained OTFs[9]

Combined polymers	Dispersion Time (s)	Appearance	Film-forming capacity
HPMC E-15 + PEG 400	120	Transparent	Well
HPMC E-15 + Glycerin	92	Transparent	Well
HPMC K4M	-	-	Very low
HPMC E-15 + Pullulan	-	-	Low
HPMC E-15 + PVA	78	Transparent	Medium
HPMC E-15 + PVP	67	Transparent	Medium
HPMC E-15 + PVA + MCC	-	-	Low
HPMC E-15 + MCC	42	Semi-transparent	Best
PVA	52	Transparent	Medium
PVA + PVP + Glycerin	64	Transparent	Medium
PVA + PVP + PEG 400	52	Transparent	Medium
PVP	-	-	Very low
Pullulan + PVA	-	-	Very low
Gelatin	-	-	Very low
Eudragite RL-100	-	-	Very low
Pullulan + Guar gum + Xanthan gum + Carrageenan	19	Transparent	Very well

OTFs: Oral thin films, HPMC: Hydroxypropyl methylcellulose, PVA: Polyvinyl alcohol, PVP: Polyvinylpyrrolidone, MCC: Microcrystalline cellulose

magnetic stirrer. Then, drug and other excipients are added to this mixture to obtain a viscous solution. The solution prepared by this method is poured into a petri dish and the solvents allowed to evaporate. Depending on the solvent system used, these are kept for 20-25 or 24-48 h at room temperature or 40°C-50°C in the oven for a shorter period of time. The films obtained after evaporation of the solvents are 15-20 mm in diameter, 0.2-0.3 mm thick, and carefully separated from the petri dishes. Depending on the amount of active substance they contain, they are cut into pieces of the desired size.[1,7] In the semisolid technique, the semisolid gel mass is poured into suitable molds and dried using gel-forming polymers. Then they are prepared by cutting into the desired sizes.[9,19]

Advantages and disadvantages of the solvent casting method[1,7,10]

- Films are of uniform thicknesses
- Films are clear and bright
- Films are quite flexible
- Prepared films are quite thin (12-100 µm)
- Offers better physical properties
- The method cost is suitable
- Compared to the "hot melt extrusion" method, APIs are not exposed to high temperatures and do not have stability problems
- The polymer selected should be soluble in water or in a volatile solvent
- It should have a suitable viscosity

Hot melt extrusion method

The hot melt extrusion method is a widely utilized method to formulate sustained-release tablets, granules, transmucosal, and transdermal drug delivery systems. The mixture containing the formulation components is mixed and melted by means of an extruder with heaters. As a result, the liquid mixture is turned into film form through molds.[9,19]

Table 7. Plasticizers used in OTFs and their ratios[7]

Polymer	Plasticizers	Concentration (w/w %)
HPMC PVA	Glycerin	15 14-15
Maltodextrin	Propylene glycol	7-8
Lycoat NG 73, PVA, and HPMC	Polyethylene glycol 400	25 7-8
Pullulan	Polyethylene glycol 4000	20-25

OTFs: Oral thin films, HPMC: Hydroxypropyl methylcellulose, PVA: Polyvinyl alcohol

Table 8. Superdisintegrants used in OTFs and their concentrations

Superdisintegrants	Commercial name	Concentration (w/w %)	Disintegration mechanism
Sodium starch glycollate	Explotab, primogel	2-8	Fast water absorption and subsequent fast swelling
Crosspovidone	PolyplasdoneXL10	2-5	Absorption and swelling go together
Polacrilin potassium	Amberlite IRP 88 Indion 294	0.5-5	Fast water absorption and subsequent fast swelling

OTFs: Oral thin films

Table 9. Flavoring agents used to mask the dominant tastes in OTFs[7]

Dominant taste	Flavoring agents
Salty	Peach, butterscotch, maple, vanilla, and apricot
Sour	Citrus, raspberry, and licorice root
Sweet	Fruit or vanilla
Bitter	Chocolate, anise, mint, walnut, and wild cherry

OTFs: Oral thin films

Solid dispersion extrusion

In this method, the solid dispersion is prepared by extruding the formulation components with the drug and then made into a thin film with molds.[19]

Rolling method

The solvents commonly used in this method are water and/or water/alcohol mixtures. Through the high shear processor, the active compound and other components are solved in a small amount of aqueous solvent. The viscous mixture is transferred onto the carrier roller and rolled. The resulting films are prepared by cutting to the desired sizes and then dried in a controlled manner.[9,19]

Characterization of OTFs

Within the scope of characterization studies of the prepared OTFs, various analyses and measurements are carried out. Among these, organoleptic and morphological control, moisture absorption, swelling ability, flexibility (elongation), folding ability, pH determination, weight variability, thickness, flavor, content uniformity, dispersion, dissolution rate, release kinetics, degree of transparency, scanning electron microscope (SEM), X-ray powder diffraction (XRD), fourier transform infrared spectroscopy (FT-IR), and differential scanning calorimetry (DSC) analyses and measurements are located.[20-22]

It is difficult to distinguish in OTFs due to the short periods of disintegration and dissolution processes. The American Association of Pharmaceutical Scientists/International Pharmacy Federation for OTFs has stated that the disintegration test can be utilized in place of the dissolution test utilized for ODTs. If the API is molecularly dissolved in OTF, the rate of API released is dependent only on the film's disintegration time. At the same time, if the API is dispersed in a particulate form in the film matrix, both the dissolution rate and disintegration time tests are recommended. While the European Pharmacopoeia has given a disintegration time of up to 3 minutes for ODTs, a time of 30 s or less is recommended according to the FDA and USP (American Pharmacopoeia) guidelines. Since the saliva volume in the mouth is less than 2 mL, these tests are generally recommended in a small environment for disintegration testing in 2-7 mL of fluid under similar conditions prevailing in the oral cavity. OTF can be placed on the surface of the liquid in a petri dish, and the disintegration time can be determined utilizing a chronometer. In the meantime, the petri dish can be shaken continuously to mimic the tongue's mouth movement. This method is simple and offers ease of application. Otherwise, it creates some difficulties, and the process is very difficult to apply to automation.[16]

Drug release from OTFs is usually carried out in an environment set at 37°C (artificial saliva fluid or a pH 6.8 phosphate buffer) according to the pharmacopoeia requirements for solid oral dosage forms utilizing a pallet or basket apparatus. However, the dissolution apparatus has some disadvantages for OTFs. While using the basket apparatus, it may result in sticking to the edges and clogging of the basket pores, whereas in the use of the pallet apparatus, OTFs are probably stuck to the bottom or remain on the surface of the container in dissolution medium. Platinums and double-sided tapes are used to simulate adhesion *in vivo* and prevent swimming. Each film is placed on a rectangular glass plate and fixed to the bottom of the dissolution medium. As a consequence of fast disintegration, the drug is released very rapidly, and specimens of the analyzed medium are taken in a short time.[16]

In evaluating the taste-masking properties of OTFs, it can be determined *in vitro* using a dissolution test apparatus. *In vivo* testing with volunteers is the safest; however, it is ethically problematic. Before the experiment, four standard materials are used for volunteers, and sensory sensitivity thresholds are assessed against flavors. These flavors are quinine (bitter), sodium chloride (salty), tartaric acid (sour), and sucrose (sweet). Volunteers start by washing their mouths with distilled water. Then, they place an amount of pure drug and then a film

specimen containing the same amount of drug to their tongue for 30 s. Then, the volunteers spit and rinse their mouths with water. They are then subjected to a rating process numbered 0 to 3 for taste evaluation: 0-tasteless, 1-slightly bitter taste, 2-moderately bitter taste, and 3-very bitter taste.[16]

There are many studies in the literature of OTFs used as alternatives to conventional drugs available on the market in the treatment of a wide range of diseases. Among the APIs used in these studies are tramadol HCl, chlorpromazine, metoclopramide HCl, lovastatin, diclofenac sodium, palonosetron HCl, zolpidem tartrate, bufotenine, etoricoxib, levocetirizine dihydrochloride, leukotriene receptor antagonist, cinitapride hydrogen tartarate, meloxicam, escitalopram, phenylephrine HCl ondansetron HCl, fluticasone propionate, ergotamine, and caffeine.[4,11-13,23-36]

Evaluation of OTFs

- ***Morphological and organoleptic control:*** The color, homogeneity, transparency, smell, and texture of the OTFs are examined visually and sensually.[23,32] They should be evaluated especially in terms of taste and flavor characteristics.[28,31]

- ***Moisture absorption capacity:*** This test is carried out under high humidity conditions to control the physical stability and integrity of the films. After weighing the samples individually, they are placed in desiccators containing aluminum chloride solution and exposed to moisture for 3 d. Then, the films are weighed and their % moisture absorption capacities are calculated with the formula below.[1]

$$\% \text{ Moisture absorption capacities} = \frac{(\text{Initial Weight - Final Weight})}{\text{Initial Weight}} \times 100$$

- ***Tensile strength:*** Tensile strength is the maximum tensile force applied until the thin-film specimen breaks. It is obtained by dividing the applied force by the cross-sectional area of the film and multiplying by a hundred:[2]

$$\% \text{ Tensile Strength} = \frac{(\text{Load at Failure })}{(\text{Film Thickness} \times \text{Film Width})} \times 100$$

- ***Percentage elongation:*** When a pulling force is applied, the tensile increases. This tensile continues until the integrity of the film form deteriorates. The percentage of elongation can be determined by measuring the final size of the film before its integrity deteriorates. This rate increases as the amount of plasticizer is enhanced. Elongation percentages of OTF formulations are calculated by the formula below:[1,2]

$$\% \text{ Tensile Strength} = \frac{(\text{Load at Failure})}{(\text{Film Thickness} \times \text{Film Width})} \times 100$$

- ***Weight variability:*** 1x1-cm^2 films are cut from each formulation, and weight variability is calculated by weighing them individually on a sensitive scale.[31]

- ***Thickness:*** The thickness measurement is required as it is directly related to the quantity of drug in the OTF. At the same time, a suitable thickness is necessary for the comfortable application of the films. For example, the ideal thickness of buccal thin films should be between 50 and 1000 µm.[10] For this purpose, at least five films from each formulation are measured from five different points, and the results are given as mean and standard deviation (x^- and SS).[7]

- ***Flexibility (folding endurance):*** The flexibility of thin films is determined by folding a film repeatedly at the same place at an angle of 180˚ until it breaks. The number of folds made before breaking is noted. The film that exhibits 300 times or more folding endurance is considered to have excellent flexibility.[7,10,34]

- ***Determination of pH value:*** Determining the pH of OTFs is important in terms of their solubility/dispersion in the oral cavity, taste properties, and rapid release of the drugs. For this purpose, 1.5%-2% (w/v) agar is added to the isotonic solution and dissolved. Then this solution is poured into a petri dish and incubated until it forms a gel at room temperature. Thin-film samples are placed on it. Subsequently, pH papers with a pH range of 1-11 are touched to OTFs, and their pH is determined according to the change in the color of the paper.[7,31]

- ***Determination of swelling degrees:*** The swelling of the polymeric film is important in terms of measuring the water absorption capacities of OTFs and obtaining information about their resistance to water. Randomly selected OTFs are weighed individually and kept in simulated physiological fluid in a petri dish within the specified period. Then, each film is weighed and measured at different time intervals until the increase in weight reaches a constant level. The degree of swelling is calculated using the equation below:[10]

$$\% \text{ Swelling Degree} = \frac{(\text{Final Weight - Initial Weight})}{(\text{Initial Weight})} \text{ x } 100$$

- ***Content uniformity:*** For content uniformity, each film is filtered after being dissolved in a suitable solvent, and the drug content in each film is measured by the appropriate quantification method. It is expected that the relative standard deviation % is not more than 6%.[7,12]

- ***Disintegration test:*** The disintegration time is described as the time (seconds) that a film disperses when it comes into contact with saliva or water. Disintegration time is when the thin film begins to disintegrate or disperse. The weight and thickness of the film play a significant role in determining the physical properties of water-soluble films.[5]

- The disintegration test apparatus specified in pharmacopoeias can also be used to determine the disintegration times of OTFs. Normally, the disintegration time of the film composition is usually 5-30 s, and this is a phenomenon that varies according to the formulation content. There is no official guide to detecting the disintegration times of films that break down fast.[22]

- ***Dissolution rate test:*** In the literature, many studies used Franz diffusion cells to test drug release from polymeric films while some improvizations were made on the apparatus to be used for dissolution rate testing.[37] The greatest obstacle in the dissolution rate assay is the placement of film specimens. In addition, various methods have been applied in the literature in which the dissolution rate of the film is adhered to the bottom of the glass container or the mixing apparatus using a double-sided adhesive band (Figure 3).[7]

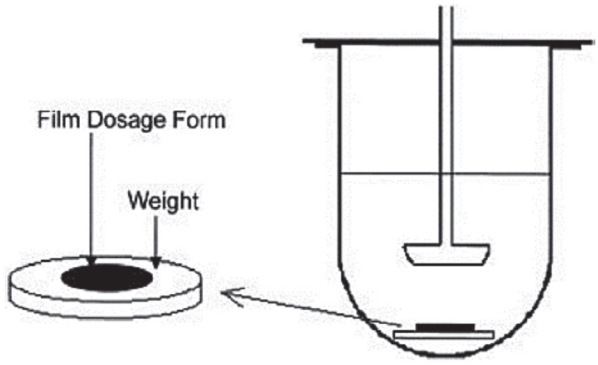

Figure 3. Modification of the disintegration test apparatus used in the evaluation of OTFs
OTFs: Oral thin films

- ***Determination of release kinetics:*** The dissolution results of all film formulations containing API in the pH 6.8 artificial saliva or pure water are applied to the computer program in order to determine the appropriate kinetic model. It is determined by mathematical programs and formulas that the formulations are compatible with 0. degree, 1. degree, Korsmeyer-Peppas or Higuchi models or not.[26,38]

- ***Transparency:*** The transparency of OTFs could be measured utilizing a ultraviolet (UV) spectrophotometer. OTF formulation specimens are cut rectangularly and placed inside the UV spectrophotometer cuvette. The permeability of the film is made at a wavelength of 600 nm. The following equation is used for the results obtained:[22]

$$\text{Transparency} = \log T600 / b$$

[T600= Transmittance at 600 nm, *b* = film thickness (mm)]

- ***Packaging:*** Fast-dissolving film systems can be packaged in single packages, multiple blister packages and using a variety of options such as multi-unit rolls. There are some patented packaging systems for OTFs in the pharmaceutical market at present.[2]

- ***FT-IR:*** Using FT-IR (ATR) spectrophotometer is measured and examined infrared spectra that all components entering the formulations to detect unwanted interactions between formulation components and the pure API.[32]

- ***Surface and structural morphology:*** Surface and structural morphology are examined using a SEM. In this way, the presence of smoothness, surface roughness or pores and particle distribution can be determined.[7,28]

- ***XRD:*** The X-ray diffraction analysis helps to determine the crystal or amorphous nature of the drugs included in the films. In this way, it can be checked whether the drugs in the OTFs have undergone any changes in the preparation process of their conformational sequences and whether they have turned into its polymorphs, if any exist.[7,28]

- ***DSC:*** DSC analysis is performed to demonstrate the compatibility of the drug with other auxiliary substances. The reference and sample are brought to the same temperature, and the interactions in the sample are examined depending on the heat exchange.[7] For this purpose, a certain amount of OTF sample is cut, placed in the alumina pan, and analyzed under a certain flow of atmospheric nitrogen (mL/min).[28,34]

OTF stability

According to the International Council on Harmonisation guidelines, the stability of OTFs is maintained under controlled conditions (25˚C temperature/60% relative humidity and 40˚C temperature/75% relative humidity) for 12 months. During storage, OTFs must be controlled for weight uniformity, morphological properties, film thickness, tensile properties, water content, and dissolution tests at certain time intervals.[9,23,27]

CONCLUSION

OTFs have emerged as a revolutionary trend, and most pharmaceutical companies in this field continue their research and development activities to adapt their drugs in various categories to this technology. This technology is an innovative drug delivery system for all patient groups who have swallowing problems, especially pediatric and geriatric patients. It also offers many advantages over the other dosage forms, such as improved bioavailability and faster effects. It is one of the most important dosage forms that can be used orally in cases of emergency and when an immediate-onset effect is desired. Therefore, it can be concluded that OTFs with excellent patient compliance and many advantages have innovative futuristic opportunities.

Conflicts of interest: No conflict of interest was declared by the authors. The authors alone are responsible for the content and writing of this article.

REFERENCES

1. Sharma D, Kaur D, Verma S, Singh D, Singh M, Singh G, Garg R. Fast dissolving oral films technology: A recent trend for an innovative oral drug delivery system. Int. J. Drug Deliv. 2015;7:60-75.
2. Siddiqui MDN, Garg G, Sharma PK. A Short Review on "A Novel Approach in Oral Fast Dissolving Drug Delivery System and Their Patents". Advan Biol Res. 2011;5:291-303.
3. Chan R. Oral thin films: Realms of Possibility. Frederick Furness Publishing Ltd. 2016;12-17.
4. Hussain MW, Kushwaha P, Rahman MA, Akhtar J. Development and Evaluation of Fast Dissolving Film for Oro-Buccal Drug Delivery of Chlorpromazine. Indian Journal of Pharmaceutical Education and Research. 2017;51:S539-S547.
5. Malke S, Shidhaye S, Desai J, Kadam V. Oral films: Patient compliant dosage form for pediatrics. The Internet Journal of Pediatrics and Neonatology. 2009;11:1-7.
6. Ghodake PP, Karande MK, Osmani RA, Bhosale RR, Harkare RB, Kale BB. Mouth dissolving films: Innovative vehicle for oral drug delivery. International Journal of Pharma Research & Review. 2013;2:41-47.
7. Kathpalia H, Gupte A. An Introduction to Fast Dissolving Oral Thin Film Drug Delivery Systems: A Review. Current Drug Delivery. 2013;10:667-684.
8. Niyaz USH, Elango K. Oral fast dissolving films: An innovative drug delivery system. World Journal of Pharmacy and Pharmaceutical Sciences. 2018;7:881-907.

9. Mahboob MBH, Riaz T, Jamshaid M, Bashir I, Zulfiqar S. Oral Films: A Comprehensive Review. International Current Pharmaceutical Journal. 2016;5:111-117.
10. Karki S, Kim H, Na SJ, Shin D, Jo K, Lee J. Thin films as an emerging platform for drug delivery. Asian Journal of Pharmaceutical Sciences. 2016;11:559-574.
11. Khadra I, Obeid MA, Dunn C, Watts S, Halbert G, Ford S, Mullen A. Characterisation and optimisation of diclofenac sodium orodispersible thin film formulation. International Journal of Pharmaceutics. 2019;561:43-46.
12. Koland M, Charyulu RN, Vijayanarayana K, Prabhu P. In vitro and in vivo evaluation of chitosan buccal films of ondansetron hydrochloride. Int J Pharm Investig. 2011;1:164-171.
13. Alam M, Tasneem F, Pathan SI. Formulation and evaluation of swellable oral thin film of metoclopramide hydrochloride. Bangladesh Pharmaceutical Journal. 2014;17:102-112.
14. Saini P, Kumar A, Sharma P, Visht S. Fast disintegrating oral films: A recent trend of drug delivery. Int J Drug Dev Res. 2012;4:80-94.
15. Godbole A, Joshi R, Sontakke M. Oral thin film technology: Current challenges and future scope. International Journal of Advanced Research in Engineering and Applied Sciences. 2018;7:1-14.
16. Wasilewska K, Winnicka K. How to assess orodispersible film quality? A review of applied methods and their modifications. Acta Pharmaceutica. 2019;69:155-176.
17. Hoffmann EM, Breitenbach A, Breitkreutz J. Advances in orodispersible films for drug delivery. Expert Opin Drug Deliv. 2011;8:299-316.
18. Akeuchi H, Yamakawa R, Nishimatsu T, Takeuchi Y, Hayakawa K, Maruyama N. Design of rapidly disintegrating drug delivery films for oral doses with hydoxypropyl methylcellulose. Journal of Drug Delivery Science and Technology. 2013;23:471-475.
19. Reza KH, Chakraborty P. Recent industrial development in Oral Thin Film Technology: An Overview. PharmaTutor. 2016;4:17-22.
20. Patil P, Shrivastava SK. Fast Dissolving Oral Films: An Innovative Drug Delivery System. International Journal of Science and Research. 2014;3:2088-2093.
21. Joshua JM, Hari R, Jyothish FK, Surendran SA. Fast dissolving oral thin films: An effective dosage form for quick releases. Int J Pharm Sci Rev Res. 2016;38:282-289.
22. Irfan M, Rabel S, Bukhtar Q, Qadir MI, Jabeen F, Khan A. Orally disintegrating films: A modern expansion in drug delivery system. Saudi Pharm J. 2016; 24:537–546.
23. Murthy AV, Ayalasomayajula LU, Earle RR, Jyotsna P. Formulation and Evaluation of Tramadol Hydrochloride Oral Thin Films. Int. J. Pharm. Sci. 2018;9:1692-1698.
24. Pragathi P, Vishnu P, Abbulu K. Formulation and evaluation of lovastatin oral disintegration thin films. GSC Biological and Pharmaceutical Sciences. 2018;3:35-42.
25. Bhowmik SC, Alam M, Pathan SI. Preparation and evaluation of palonosetron hydrochloride oral thin film. Bangladesh Pharmaceutical Journal. 2019;22:228-234.
26. Rani TN. Formulation development and optimization of oral thin films of zolpidem tartarate. Medical Science & Healthcare Practice. 2017;1:26-41. https://core.ac.uk/download/pdf/268085974.pdf
27. Venkateswarlu K. Preparation and evaluation of fast dissolving buccal thin films of bufotenin. Journal of In Silico & In Vitro Pharmacology. 2016;2:1-5.
28. Senthilkumar K, Vijaya C. Formulation development of mouth dissolving film of etoricoxib for pain management. Advances in Pharmaceutics. 2015;1-11.
29. Lakshmi PK, Sreekanth J, Sridharan A. Formulation development of fast releasing oral thin films of levocetrizine dihydrochloride with Eudragit® Epo and optimization through Taguchi orthogonal experimental design. Asian Journal of Pharmaceutics. 2011;5:84-92.
30. Kapoor D, Vyas RB, Lad C, Patel M, Tyagi BL. Fabrication and characterization of oral thin films of leukotrine receptor antagonist. Journal of Drug Delivery and Therapeutics. 2015;5:77-82.
31. Jelvehgari M, Montazam SH, Soltani S, Mohammadi R, Azar K, Montazam SA. Fast dissolving oral thin film drug delivery systems consist of ergotamine tartrate and caffeine anhydrous. Pharmaceutical Sciences. 2015;21:102-110.
32. Chinnala KM, Vodithala S. Formulation and evaluation of fast disintegrating oral thin films of cinitapride hydrogen tartarate. International Journal of Current Advanced Research. 2017;6:4737-4740.
33. Zaman M, Hanif M, Qaiser AA. Effect of Polymer and Plasticizer on Thin Polymeric Buccal Films of Meloxicam Designed by Using Central Composite Rotatable Design. Acta Pol Pharm. 2016;73:1351-1360.
34. Ammar HO, Ghorab MM, Mahmoud AA, Shahin HI. Design and In Vitro/In Vivo Evaluation of Ultra-Thin Mucoadhesive Buccal Film Containing Fluticasone Propionate. AAPS PharmSciTech. 2017;18:93-103.
35. Mushtaque M, Muhammad IN, Fareed Hassan SM, Ali A, Masood R. Development and pharmaceutical evaluation of oral fast dissolving thin film of escitalopram: A patient friendly dosage form. Pak J Pharm Sci. 2020;33:183-189.
36. Bonde M, Sapkal N, Daud A. Full factorial design, physicochemical characterization of phenylephrine HCl loaded oral thin film. Asian Journal of Pharmaceutics. 2015;9:137-145.
37. Adrover A, Pedacchia A, Petralito S, Spera R. In vitro dissolution testing of oral thin films: A comparison between USP 1, USP 2 apparatuses and a new millifluidic flow-through device. Chemical Engineering Research Design. 2015;95:173-178.
38. Kumar MK, Nagaraju K, Bhanja S, Sudhakar M. Formulation and evaluation of sublingual tablets of terazosin hydrochloride. International Journal of Pharmaceutical Sciences and Research. 2014;5:417-427.